The development of advanced smart polymer formulations for potential biomedical applications

A thesis submitted for the degree of

Doctor of Philosophy

By

Shane C. Halligan B.Eng.

Based on research carried out under the supervision of

Dr Luke M. Geever, Dr John G. Lyons

& Prof Clement L. Higginbotham

Materials Research Institute,

Athlone Institute of Technology,

Dublin Road, Athlone, Co. Westmeath, Ireland. *October* *2020*

List of Contents

List of Figures

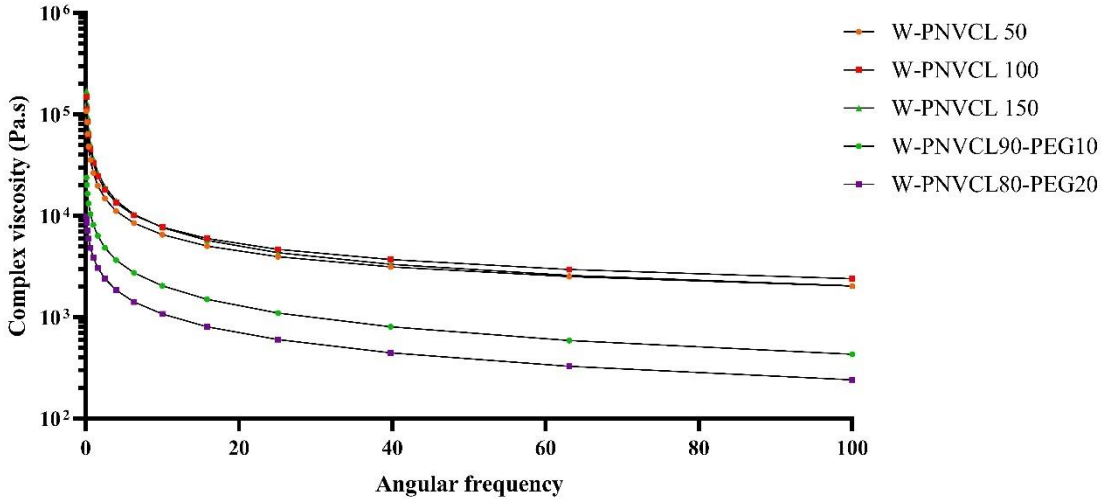

List of Tables

List of Equations

Declaration

I Shane Halligan hereby declare that this thesis submitted to the Higher Education and Training Awards Council for the degree of Doctor of Philosophy is a result of my own work and has not in the same or altered form, been presented to this institute or any other institute in support for any degree other than for which I am now a candidate.

Signed: _____ (Shane Halligan)

Date: _____

Acknowledgements

Firstly, I would like to express my sincere gratitude to my advisor Dr Luke Geever, for the continuous support of my PhD study and related research, for his patience, motivation, and immense knowledge. His guidance helped me during my time in research and writing of this thesis.

A very special thanks to Dr Sean Lyons for all of his guidance, support, and technical help. Also, I would like to thank Sean for trading me to the caretakers within the first few weeks.

Prof. Clement Higginbotham for giving me your invaluable input, positive attitude, support, numerous Christmas parties and of course, our social gathering and for boosting morale in the workplace.

Special thanks to Kieran Murray, Alan Mannion and Alan Murphy for their kind assistance with the training and testing of the equipment during my time here and also for the very insightful chats.

Many thanks to all the postgraduates in the Research Hub whom I have met over the last few years. Special thanks to Megan (FRIEND) and her replacement MEGAN 2.0 for all her help in nutrition advice and for putting up with me over the last few years. As the only other hard-core food enthusiast in AIT, I will never be skinny without her☺. A big thanks to Maurice and Shane Brennan, for their scientific advice. Also other big thanks to Brian Mullarney, Gavin Burke, Conor Coffey, Romina Pezzoli *"acetaminophen,"* Laura christmaskellsh, Sarah Jane Devaney, Nico Barbolosi and Maya Frost.

I have met a lot of exciting people in Athlone IT; there have been some unique/unusual characters to work with. Thanks for all the craic and banter (especially the canteen discussions) which has made my time here very enjoyable. You are a great bunch of people to work and socialize with! Long may it continue!

On a more personal note, I would like to thank my girlfriend, Cécile Jacquot, for her patience and support. This certainly would not be possible without you.

Last but not least a huge thank you to all my family; my two wonderful sisters Karen and Elaine and my parents Maureen and Johnny for their guidance and support.

Dissemination of results

Publications to scientific journals

HALLIGAN, S.C., DALTON, M., MURRAY, K.A., DONG, Y., WANG, W., LYONS, J.G. & GEEVER, L.M. 2017. Synthesis, characterisation and phase transition behaviour of temperature-responsive physically cross-linked poly (*N*-vinylcaprolactam) based polymers for biomedical applications. Materials Science and Engineering: C (Impact Factor 5.08), 79, 130–139, 10.1016/j.msec.2017.03.241. (Awarded best paper MRI, 2017)

HALLIGAN, S.C, MURRAY, K.A, VRAIN V, J.G. J. G. LYONS. GEEVER, L.M, Controlling the Thermosensitivity of Poly (*N*-vinylcaprolactam) for Smart Glass Applications *via* Electron Beam Irradiation, Mater. Today Proc. 10 (2019) 430–435. doi:10.1016/J.MATPR.2019.03.006. (Cite Score: 1.09)

HALLIGAN, S.C, MURRAY, K.A, M. HOPKINS, I, ROGERS. J. G. LYONS, VRAIN V, GEEVER, L.M, Enhancing and controlling the key attributes of Poly (*N*-vinylcaprolactam) through electron beam irradiation for biomedical applications (manuscript submitted to Journal of Applied Polymer Science) (Impact Factor of 2.188)

HALLIGAN, S.C, MURPHY A., BRENNAN S, ROGERS I, LYONS J,G., GEEVER, L.M, Hot-melt extrusion of temperature-responsive hydrogel Poly (*N*-vinylcaprolactam) (manuscript in preparation)

Additional Peer-reviewed articles

DALTON, M.B. & HALLIGAN, S.C., MURRAY, K.A., DONG, Y., WANG, W., LYONS, J.G. & GEEVER, L.M 2017. The Effect Acetic Acid has on Poly (*N*-Vinylcaprolactam) LCST for Biomedical Applications, Polym. Plast. Technol. Eng. (Impact Factor 1.705) 57 (2018) 1165–1174. doi:10.1080/03602559.2017.1373400.

DALTON, M.B., HALLIGAN, S., KILLION, J., MURRAY, K.A. & GEEVER, L.M. 2014. Smart Thermosensitive Poly (*N*- vinylcaprolactam) Based Hydrogels for Biomedical Applications; Advances in Environmental Biology 8 (24) (2014):1-6

E. KENNY , A. MURPHY , M. FROST , HALLIGAN, S.C, GEEVER, L.M, Effect of incorporating micro-sized hydroxyapatite and milled hydroxyapatite by hot-melt extrusion. *International Conference on Material Science & Smart Materials:* Proceedings *2018*

FALLON, M; PEZZOLI, R; HALLIGAN, S.C, GEEVER, L.M & HIGGINBOTHAM, C., Synthesis and characterisation of novel temperature and pH-sensitive physically cross-linked hydrogels of poly (*N*-vinylcaprolactam) containing itaconic acid. (manuscript under review for Gels)

Book Chapters

LIMA, G.G. DE, HALLIGAN, S.C., GEEVER, L.M., NUGENT, M.J.D., DALTON, M. & MC CONVILLE, C. 2017. Controlled Release of Poorly Soluble Active Ingredients from Bioresorbable Polymers. *In* Devine, D., *ed. Controlled Release of Poorly Soluble Active Ingredients from Bioresorbable Polymers*. Smithers Rapra, pp.77-111.

Conference Presentations

HALLIGAN, S.C., DALTON, M.B., MURRAY, K.A., DONG, Y., WANG, W., LYONS, J.G. & GEEVER, L.M. synthesis and characterisation of poly *(N*-vinylcaprolactam) based polymers for biomedical applications. BINI 2017. *Proceedings of the Royal Academy of Medicine in Ireland Section of Bioengineering 2017 pp 55*

HALLIGAN, S.C., MURRAY, K.A., DONG, Y., WANG, W., LYONS, J.G. & GEEVER, L.M., Controlling the Thermo-sensitivity of Poly (*N*-vinylcaprolactam) Injectable Hydrogels *via* electron beam Irradiation. *Advanced Energy Materials 2017*

HALLIGAN, S.C., FROST M., LYONS, J.G. & GEEVER, L.M., Exploiting the use of Melt Processing Technology to develop novel Poly (*N*-vinylcaprolactam) formulations., *Advanced Materials for Biomedical Applications 2017*

FALLON, M; PEZZOLI, R; HALLIGAN, S.C, GEEVER, L.M & HIGGINBOTHAM, C., Synthesis and characterisation of novel temperature and pH-sensitive physically cross-linked hydrogels of poly (*N*-vinylcaprolactam) containing itaconic acid. BINI 2018 *Proceedings of the Royal Academy of Medicine in Ireland Section of Bioengineering 2018*

E. KENNY , A. MURPHY , M. FROST, HALLIGAN, S.C, GEEVER, L.M, Effect of incorporating micro-sized hydroxyapatite and milled hydroxyapatite. *International Conference on Material Science & Smart Materials 2018 pp 299*

Abstract

In the past twenty years, a theme in the pharmaceutical industry is to move towards more efficient use of active pharmaceutical ingredients and the need for improved delivery systems. Smart polymers throughout the literature have been suggested for several different biomedical applications such as *in-situ* forming gels. Fundamentally, this work focuses on the application of temperature responsive polymers as a platforms for improved drug delivery systems.

Poly (*N*-vinylcaprolactam) (PNVCL) is a biocompatible smart polymer that offers superior characteristics for various medical device applications. PNVCL phase transitions can be tailored in order to suit the requirements of current and next-generation devices.. Physically cross-linked Poly (*N*-vinylcaprolactam)-Vinyl acetate (PNVCL-VAc) copolymers were initially prepared by photopolymerisation. The structure of the polymers was established by Fourier transform infrared spectroscopy, nuclear magnetic resonance and gel permeation chromatography. A determination of the lower critical solution temperature (LCST) of the polymers in aqueous solution was achieved by employing four techniques: cloud point analysis, UV- spectroscopy, differential scanning calorimetry and rheometry. The sol-gel transition was established by the tube inversion method and by rheological analysis. The characteristics of PNVCL with the addition of VAc were determined and the effects on the phase transition were established. The PNVCL based polymers exhibited a decrease in the LCST as the composition of VAc increased. The sol-gel transition was found to be affected by the composition and concentration of the material.

Sterilisation of PNVCL was investigated using an industrial scale electron beam sterilisation process. Physically cross-linked Poly (*N*-vinylcaprolactam)-Vinyl acetate (PNVCL-VAc) copolymers were prepared by photopolymerisation and were subsequently exposed to ionising radiation *via* electron beam technology. The mechanical characteristics and phase transitions of the physically cross-linked PNVCL samples were tailored by controlling the electron beam irradiation dose. Importantly PNVCL and PNVCL-VAc samples (5 wt% in solution) underwent a phase transition between 33-27 °C, following electron beam irradiation. Furthermore, all samples displayed a Young's Modulus between 1024-1517 MPa depending on the addition of copolymer and electron beam irradiation dose. The electron beam sterilisation process proved successful in enhancing/modifying many fundamental polymer properties, and this ability to formulate and sterilise in one step could prove a very attractive approach for many biomedical applications.

Combining a smart polymer system with hot-melt extrusion (HME) could allow for a targeted hybrid drug delivery system. Initial melt processing trials were conducted to determine suitable parameters such as temperature, screw speed, drying time and particle size. PNVCL based smart polymers were successfully extruded; this was achieved through the use of the incorporation of PEG as a plasticiser. PNVCL based samples were subsequently melt processed on a pharmaceutical-grade extruder leading to modified mechanical and phase transition properties. It was observed *via* FTIR and GPC analysis that the chain length of the polymer increased and that chemical changes were occurring. Therefore, a washing step was developed to remove any unreacted monomers in the smart polymer matrix. This reactive processing approach was found to be extraordinarily efficient and easily adjustable to alter PNVCL properties. Melt processing of PNVCL opens new avenues and potential applications for modifications, such as polymerisation and the blending of different materials within the smart polymer matrix.

PNVCL was subsequently used as a smart polymer carrier for Acetaminophen (APAP); Physically cross-linked PNVCL based polymers were prepared by photopolymerisation. Hot-melt extrusion was used as a fabrication technique to incorporate APAP into PNVCL matrix, in an attempt to develop smart drug delivery carriers. FTIR established the structure of the

extrudates. Determination of the drug release profile was achieved by employing HPLC. The findings suggest that interactions between PNVCL and APAP varied, according to the drug-polymer ratios. This study is the first of its kind to report the use of temperature-responsive polymers *via* a melt processing approach.

Abbreviation

5-FU	5-fluorouracil
AA	Acrylic acid
AAm	Acrylic amide
AIBN	4,4′-azobis(isobutyronitrile)
AMA	Allyl methacrylate
ANOVA	Analysis of variance
APAP	Acetaminophen
API	Active pharmaceutical ingredient
AR	Advanced Rheometer
ASD	Amorphous solid dispersions
ATBC	Acetyl tributyl citrate
ATR	Attenuated total reflection
ATR-FTIR	Attenuated total reflectance Fourier transform infrared
BCS	Biopharmaceutical classification system
BE	Backscattering electrons
BSE	Back scattering electrons
Bq	Becquerel.
CA MH	Citric acid monohydrate
CMRP	Cobalt-mediated radical polymerisation
CTA's	Chain transfer agents
Ci	Curie
DDS	Drug delivery system
DMA	Dynamic mechanical analysis
DMAEMA	2-(Dimethylamino)ethyl methacrylate
DMF	N, N′-dimethylformamide
DMSO	Dimethylsulfoxide
DOM	Domperidone
DOX	Doxorubicin
DSC	Differential scanning calorimetry
EC	Ethylcelulose
EGDMA	Ethylene glycol dimethylacrylate
EMA	European Medicine Agency

ES	Electrostatic spinning
EtO	Ethylene oxide
Eudragit® E	Vinylprrolidoneethyl methacrylate copolymer
EVA	Ethylene vinyl acetate
FA	Folic acid
FDA	Food and Drug Administration
FMEA	Failure mode and effects analysis
FRP	Free-radical polymerisation
FTIR	Fourier transform infrared spectroscopy
G′	Elastic component
G″	Loss modulus
GBE	Ginkgo biloba extract
GPC	Gel permeation chromatography
HCl (DPD)	Diphenhydramine
HCl (PRP)	Propranolol
HGC	Hexanoyl glycol chitosan
HME	Hot-melt extrusion
HPC	Hydroxypropyl cellulose
HPLC	High-performance liquid chromatography
HPMC	Hydroxypropyl methylcellulose
IPN	Interpenetrating polymer network
IPN-NGs	Interpenetrating Polymeric Network Nanogels
Kollidon®VA	Vinylpyrrolidone/vinyl acetate copolymer
LCST	Lower critical solution temperature
LDPE	Low-density polyethylene
LGTT	Lower gel transition temperature
MFI	Melt flow index
MMA	Methyl methacrylate
M_n	Molecular number
MP	Methylparaben
M_w	Molecular weight
NIPAM	*N*-isopropylacrylamide
NMR	Nuclear magnetic resonance

NVCL	*N*-vinylcaprolactam
PAT	Process analytical technology
PCLA	Poly (ε-caprolactone-lactide)
PCLDMA	Poly (ε-caprolactone) dimethacrylate
PDI	Poly dispersity index
PDMPO	Poly dimethyl phenylene oxide
PE	Polyethene
PEBA	Polyether-block-amide
PEG	Poly (ethylene glycol)
PEGDMA	Poly (ethylene glycol) dimethacrylate
PEG–PLGA	Poly (ethylene glycol)–poly (lactide-co-glycolide)
PEO	Poly (ethylene oxide)
PET	Polyethene terephthalate
PS	Polystyrene
PLA	Poly (L-actic acid)
PLGA	Poly (lactic-co-glycolic acid)
PMMA	Poly (methyl methacrylate)
PMOL	Paracetamol
PNIPAm	Poly (*N*-isopropylacrylamide)
PNVCL	Poly (*N*-vinylcaprolactam)
PNVCL-co-PNIPAm	Poly (*N*-vinylcaprolactam-co-*N*-isopropylacrylamide)
PP	Polypropylene
PRP	Propranolol
PS	Polystyrene
PVA	Polyvinyl acetate
PVAC	Poly (vinyl acetate)
PVC	Poly (vinyl chloride)
PVE	Poly vinyl ether
PVP	Poly (vinyl pyrrolidone)
PVPVA	Poly (vinyl pyrrolidone co (vinyl acetate)
QbD	Quality by design
RAFT	Reversible addition fragmentation chain transfer
RPM	Revolutions per minute

RDS	Relative standard deviation (%)
SAL	Sterility assurance level
SD	Standard deviation
SE	Secondary electrons
SEM	Scanning electron microscopy
SI	International System of Units
SOTA	State of the art
Soluplus	PEG6000/vinyl caprolactam/vinyl acetate copolymer
T_{deg}	Degradation temperature
TCPS	Tissue culture polystyrene
TEC	Triethyl citrate
T_g	Glass transition temperature
THF	Tetrahydrofuran
T_m	Melting temperature
TSE	Twin screw extrusion
UCST	Upper critical solution temperature
UGTT	Upper gel transition temperature
USD	United States dollar
USP	United States Pharmacopeia
UV	Ultra-violet
UW-PNVCL	Unwashed Poly (*N*-vinylcaprolactam)
VAc	Vinyl acetate monomer
W-PNVCL	Washed Poly (*N*-vinylcaprolactam)
Wt%	Weight percent

Chapter 1:

Introduction

1. Literature Review

1.1. Problem statement

The development of novel drug delivery systems is an extremely active area for development in the pharmaceutical industry, and there are obvious economic and therapeutic advantages to improving how drugs are administered [1]. However, the limitations of traditional drug delivery techniques such as the ingested tablet and injection, routes, have been recognised for some time now. Historically, these types of delivery systems have not incorporated a means of controlled release. With these types of dosage forms, high peak blood concentrations may be reached soon after administration with possible adverse effects related to the transiently high concentration. This can cause problems, as with each dose of a non-controlled release drug, the concentration of drug available to the body immediately peaks and then declines rapidly [2]. For some ailments, it is desirable to release drugs at a constant rate, thereby maintaining drug concentration within the therapeutic range and eliminating the need for frequent dosages. The goal in such cases is to maintain therapeutic blood dosage tissue levels of the drug for an extended period of time and have a 'zero order' release pattern (the amount of drug released is independent of the amount of drug in the system) [3].

Such systems exist in the form of modified-release (MR) dosage forms, which in many cases have improved upon traditional immediate-release dosage formulations with regards therapeutic effect and improved patient compliance [4]. There are many different types of modified-release drug delivery products, including delayed-release (e.g., enteric-coated), extended-release, and orally disintegrating tablets [5]. Alternatively, injectable delivery systems have been developed for long-acting injectable antipsychotics (LAIs) which address nonadherence through biweekly/monthly injections [6].

Providing control over drug delivery can be the most important factor at times when conventional methods, such as ingested tablet and injection cannot be used. These include situations requiring the slow release of water-soluble drugs, the fast release of low solubility drugs, drug delivery of two or more agents with the same formulation, and systems based on carriers that can dissolve or degrade and be readily eliminated [1,7]. The common themes underlying newer delivery modes, including delayed-release, extended-release and on-off release systems, is increased therapeutic efficiency as well as

increased patient compliance, and often, the common key ingredient of all these technologies is a polymeric material [8]. Current technology has developed to such a level that delivery of drugs at a constant rate for a certain period of time, ranging from days to years is not a major challenge anymore. For example, Implanon, an FDA-approved contraceptive drug delivery system, comprised of a single-rod implant, releases the drug over 3 years [9].

Although significant progress has been made in the controlled drug delivery area, more advances are yet to be made for treating many clinical disorders, such as diabetes and rhythmic heart disorders. In these cases, the drug has to be delivered in response to fluctuating metabolic requirements or the presence of certain biomolecules in the body [10]. In such cases, it would be most desirable if the drugs could be administered in a manner that precisely matches physiological needs at proper times (temporal modulation) and/or at the proper site (site-specific targeting) [3]. It would be highly beneficial if the active agents were delivered by a system that sensed the signal caused by disease, judged the magnitude of the signal and then acted to release the right amount of drug in response. Such a system would require coupling of the drug delivery rate with the physiological needs by means of some feedback mechanism [11]. The promise of these types of systems known as stimuli-responsive or environmentally sensitive materials have been reported in the literature since as early as the 1980's [12]. Environmentally sensitive "smart" polymers have become one of the materials of choice when designing such smart drug delivery systems. A smart polymer can be tailored to release an active pharmaceutical ingredient (API) under specified conditions for a given application, for example, programming a smart polymer system to have an on-off release when the system reaches the target area [13,14].

While smart polymers show great promise and have been researched widely in recent years, several drawbacks present themselves, which prevents them from achieving their true potential. Following an extensive review of the most up-to-date literature, the fabrication methods used (normally beaker scale experiments), limited data on the effect of industrial-scale sterilisation on smart polymers, and the methods of drug entrapment are amongst the key problems to be addressed. The proposed study will entail large scale melt processing research utilising the incorporation of smart temperature-sensitive polymers while attempting to overcome the aforementioned weaknesses. Interestingly in the literature, there have been no reports of melt processing of smart temperature-sensitive polymers to date.

1.2. Aims of the project

The primary goal of this study is the development of hybrid smart polymer systems that when combined with hot melt extrusion technology, could be used for mass manufacture of stimuli-responsive drug delivery platforms. The aims of the programme of research are as follows:

(1) To develop and optimise a reproducible and controllable polymerisation procedure to obtain temperature-responsive polymers.
(2) To examine the effect of an industrial scale sterilisation process on the smart temperature-sensitive polymers developed.
(3) To investigate if melt processing of the smart temperature-sensitive polymers was possible and if the resultant extrudate could be utilised for biomedical applications.
(4) To incorporate an active pharmaceutical ingredient into the smart temperature-sensitive polymer materials *via* a melt processing step, and assess the resultant hybrid platforms for potential as delivery vehicles utilising drug release testing.

1.3. Background

Polymers are one of the most important materials used in both medical and pharmaceutical practice - Modern day healthcare would simply not be possible without the use of plastics. Advancements in polymer technology have enabled plastics to be used in healthcare applications that demand high consistency, performance, precision and regulatory compliance. Innovations in the field of plastics have contributed to the advancement of medicine, including improvements in surgical equipment and techniques, critical care and life support hardware. The application of plastic technology to medicine has also contributed to decreasing rates of infection and medication-related error.

Drug delivery is the technology behind the transport of an active pharmaceutical ingredient to target tissue where it can safely achieve the desired therapeutic effect. In recent years, different approaches to enhance the therapeutic effect of the API has become a significant development. Current trends are indicating movement away from conventional drug delivery systems to targeted drug delivery systems.

Conventional drug delivery systems are still widely used today; however, they do have many drawbacks, including poor patient compliance and peak and valley release rates. These disadvantages, combined with an improved and predetermined release rate of drugs over a long period, are behind the rationale to develop a drug delivery system that can target a specific site in the body whereby enhancing the therapeutic effect of the drug [1,4].

Table 1-2 presents a summary of the history of drug delivery systems. The first-generation, also known as the conventional drug-delivery system, was developed between the 1950s and the 1980s. This generation relied on four drug release mechanisms, that ultimately led to oral and transdermal controlled release systems, with the oral system being the most promising due to its convenience [15–17].

Table 1-1: Past, present and future of drug delivery technology [15,16].

Year **1940 to 1980**	**1980 to 2010**	**2010 onwards**
First-generation	**Second-generation**	**Third-generation**
Basics of controlled release	Smart delivery systems	Modulated delivery systems
Oral delivery • Twice a day, once a day	Zero-order release • First-order vs zero order	Drug delivery technologies • Non-toxic excipients
Transdermal delivery • Once a day, once a week	Peptide and protein delivery • long-term depot using biodegradable polymers	Peptide and protein delivery's • Delivery for greater for 6 months • Controlled release kinetics • Non-invasive delivery
Drug release mechanics • Dissolution • Diffusion • Ion exchange • Osmosis	Smart polymer and hydrogels • Environment sensitive	Smart polymer and hydrogels • Single specificity and sensitivity • Fast, responsive kinetics
	Nanoparticle • Tumour-targeted delivery • Gene delivery	Targeted drug delivery • Non-toxic to nontarget cells • Overcoming blood-brain barrier
Successful control of physicochemical properties of the delivery	Inability to overcome biological barriers	Need to overcome both physicochemical and biological barriers

The second-generation was introduced in the 1980s and differentiated itself by relying on more difficult formulations. One such formulation was stimuli-responsive polymers, which attracted a great deal of attention at the time, for its use in drug delivery

applications [15,18]. Besides their ability to be used in various locations (ocular, nasal, rectal, transdermal and intramuscular) these stimuli-responsive polymers showed enormous potential in the treatment of cancer, pain, diabetes and deep vein thrombosis [15,19]. However, this drug generation enjoyed limited success, due to the risk of toxicity of the materials, the possible dose dumping and the increased potential of hepatic first-pass metabolism. The necessity of surgical procedures to insert or remove the system, along with poor drug loading decreased their market potential. Moreover, due to high manufacturing costs and poor system availability, limited success was achieved.

An example of a drug delivery system from the second-generation that was unsuccessful due to difficulties in formulations and dose dumping was poly (lactic-co-glycolic acid) (PLGA). PLGA is a biodegradable polymer that was designed to deliver APIs for several months *via* injections. However, the PLGA had difficulty controlling the initial burst release of the API, which resulted in only 50 percent of the drug being released in the first day or two [16]. During the second-generation, insulin delivery systems were developed. Exubera is an example of a delivery system that at the time offered a lower bioavailability of insulin, which resulted in several times more drug release than what was required by the conventional injection methods. This, in turn, resulted in unexpected side effects that, along with other factors, caused the withdrawal of the product from the market [15–17,20]. In the 1990's the first drug delivery system approved by the Food and Drug Administration (FDA) was an injection of Liposomal amphotericin B. At that time there were only 10 polymer-based drug delivery systems on the market that were commercially available to treat diseases ranging from cancer to fungal infection, as well as muscular degeneration

Synthesisable biodegradable and biocompatible polymers with tunable molecular weights of stimuli-responsive polymers are the next stages in drug delivery technologies. These third-generation systems should be able to target site-specific tissues with a fast release profile in response to a predetermined stimulus. They should also contain high loading efficiency and content, as well as improved gelling capabilities at tumour sites [21,22].

In the future, stimuli-responsive polymer drug delivery systems are expected to cure a large number of diseases safely and efficiently, including cancer. In order to do so, it is essential to understand how molecular weight, chemical composition and solution concentration can have an impact on the way different stimuli-responsive polymers

undergo a phase transition which makes them attractive compared to conventional polymers. Although several improvements have been made in this area, by controlled polymerisation methods, there is still a demand to continue investigating stimuli-responsive polymer formulations and focus more on cost-efficient production methods [23,24].

This thesis aims to investigate polymer based, targeted drug delivery platforms, for two potential administration routes; namely the oral and subcutaneous routes. Overall a smart solid dosage form and a thermo-gelling system; based on a stimuli-responsive polymer will be investigate. Despite being of conventional form, smart solid dosage forms are made up of stimuli-responsive polymers, which places them amongst third-generation drug delivery technologies. Thermo-gelling polymers have become an attractive material in recent years due to their ability to provide sustained and prolonged drug release. They have been shown to improve patient compliance compared to conventional drug delivery systems.

Currently, a standard method used for the polymerisation of stimuli-responsive polymers is by photopolymerisation. This is mainly due to its ability to control the concentration, intensity and wavelength of the initiating light, temperature and monomer structure. This straightforward production of stimuli-responsive polymers offers modification to the polymer network that can benefit the physical and chemical properties of the material. Although photopolymerisation was successfully applied in the second generation to synthesise and altered stimuli-responsive polymers, the product has broad molecular weight distribution and the removal of any unreacted monomer is difficult. Currently, there is still a lack of availability on the market of stimuli-responsive polymers [25,26].

Some photopolymerisation products would benefit from secondary processes such as radiation. Currently, radiation is being used as a secondary process to sterilise and to enhance the material's properties. Irradiation can be used to sterilise and formulate in a one-step process to inactivate most pathogens and to improve the performance of the final product of polymer-based biomedical devices [27,28]. Advantages of radiation sterilisation include short sterilisation times, especially for electron beam and minimal effect on the three-dimensional structure of the polymer. This method is very efficient, reliable and relatively inexpensive. Irradiation may improve the physical and chemical properties by reinforcing the cross-links formed between polymer chains [29].

Sterilisation of stimuli-responsive polymers has not been fully explored in the literature to date, so the effect of radiation on these polymers is relatively unknown. Photopolymerisation and radiation technology might be useful to modify the final product characteristics, such as the phase transition of polymers. For the third- generation of stimuli-responsive polymers, the drug loading remains a challenging process.

One technology that has been proven to be efficient to load drugs into the polymer matrix is hot-melt extrusion (HME). HME is a powerful processing technology for the production of pharmaceutical solid dosage forms in which it can load a polymer by dispersing an API into the polymer matrix [30–32]. It has been investigated that using HME can provide time-controlled, conventional, targeted drug delivery and improved bioavailability of poorly soluble drugs. However, there is a lack of literature on the processing of stimuli-responsive polymers and the potential effects it has on the final polymer characteristics. If successful, stimuli-responsive polymers can gain many of the advantages of melt processing, which would allow for a new platform for third-generation drug delivery.

1.3.1. History of drug formulation

Drug formulation has changed dramatically over the last few decades with more significant change expected in the future. The history of drug discovery dates back to the 1900s, when a shift occurred, from using traditional herbal remedies, to a more modern approach based on synthetic chemistry. During this period, oral ingestion such as the compound Aspirin was the traditional preferred route of drug administration. Aspirin has grown in popularity and has become one of the most researched drugs in the world [33,34].

In the following decades, drug discovery was needed to treat injured soldiers, which resulted in antibiotics being produced. In the 1940s, methods for industrialised penicillin production were developed. Penicillin antibiotics were among the first medications used to fight against bacterial infections. However, after the discovery of penicillin, researchers found that some disease-causing pathogens were resistant to antibiotic penicillin [35].

During the 1950s, drugs were formulated with the aim to achieve a sustained and controlled therapeutic effect. Throughout the 1960s, controlled and targeted systems were suggested. However, these techniques would not see mass implemention until the 1980s.

During this period, a number of approaches were proposed to meet the growing demand, examples of investigated technologies included:

- drug carrier systems,
- implants,
- coatings,
- micelles,
- liposomes

The goal of the proposed approaches was to attain maximum therapeutic efficiency, with minimal risk of harmful side effects [36–38]. With all the progress, many drug formulations, even those created using the most advanced strategies, have unexpected side effects due to the drug interacting with healthy tissues that are not the target location. Hence, more advanced drug delivery systems are crucial to controlling the rate at which the drug is released as well as the precise location where the drug is released in the body.

1.4. Hydrogels

Hydrogels are a 3-dimensional cross-linked polymer network that has the ability to swell and absorb large quantities of water. The ability to absorb large volumes of water is due to the hydrophilic segment of the polymer. A polymer with low hydrophilicity can swell in water; nevertheless, with a further increase in hydrophilicity, the polymer can become water-soluble [39–41].

Natural and synthetic polymers can be physically or chemically cross-linked to produce hydrogels; this gives them physical characteristics like soft tissue. Hydrogels are used in biomedical applications due to their high water content, making the hydrogel biocompatible with similar physical properties to human tissues [42–44]. Hydrogel-based drug delivery systems have been an active research area of the biomedical industry and the number of published studies has exponentially increased since the 1970s. Certain hydrogels display a response to stimuli from the surrounding environment such as volume, viscosity, pH, temperature or mechanical stress [39,45,46].

These hydrogels are called stimuli-responsive hydrogels or smart hydrogels. Due to their popularity, hydrogels have set a significant research trend in this field. However, it is essential to note that the number of smart hydrogel drug delivery systems approved by the FDA is still minimal, as this is a relatively new field of study. A comprehensive

analysis of hydrogels in clinical trials is displayed below in Figure 1-1. In total, there are 425 clinical trials involving hydrogel materials.

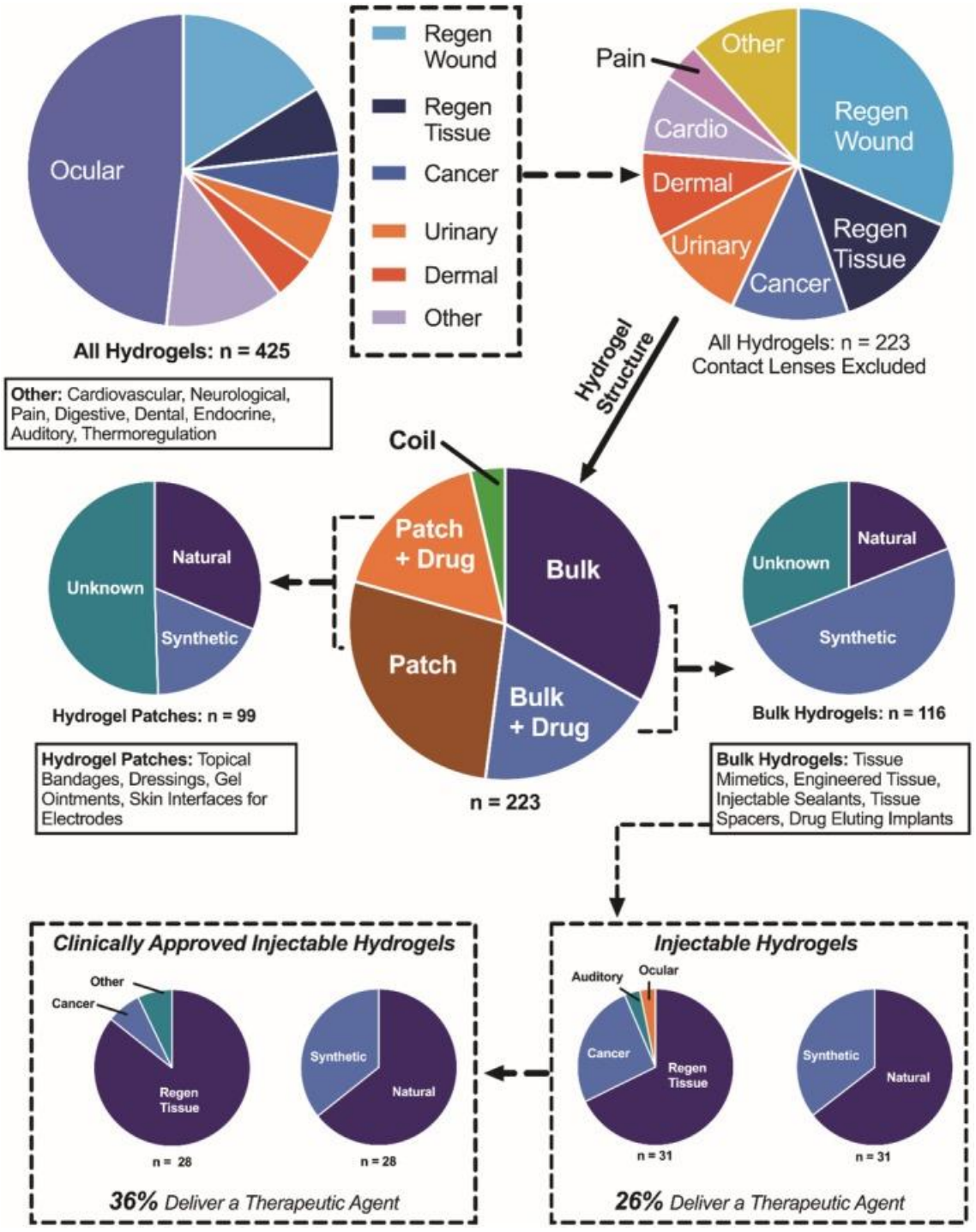

Figure 1-1: Clinical landscape of hydrogels[47] .

The primary clinical application of hydrogel materials was for soft contact lenses (202 unique clinical trials). With contact lenses excluded from further analysis, there were 223 clinical trials, spanning diverse medical applications. Trials which used the hydrogel

as a tissue substitute, or a mechanical support to augment existing tissues (Regen Tissue) were analysed separately from those which used hydrogels as a dressing or barrier to facilitate healing of an abrasion, burn, or ulcer (Regen wound). Of the 223 non-lens hydrogel clinical trials, 8 used a hydrogel coil (cardiovascular application), 99 used a hydrogel patch, and 116 used a bulk hydrogel. Of the 116 bulk hydrogels, 31 were delivered via injection. Within the domain of injectable hydrogels, there are 28 approved clinical products and 31 devices in clinical trial. Within each hydrogel grouping (i.e., patch, bulk, injectable), we also stratified clinical trials by material origin (i.e., natural, synthetic, or unknown). Material origin was determined from either the clinical trial description or the device's U.S. patent. Solid lines denote categorization or clarification of a group, while dotted lines represent extraction of a particular subset [47].

Improving the controlled delivery of therapeutic agents would lead to improved methods of drug administration. Stimuli-responsive hydrogels are the candidates that are the most promising in designing drug delivery systems based on polymers [48].

Hydrogel structures are dependent on the cross-links present within their network. There are two main types of cross-linking found in hydrogels: chemical cross-links and physical cross-links (Figure 1-1).

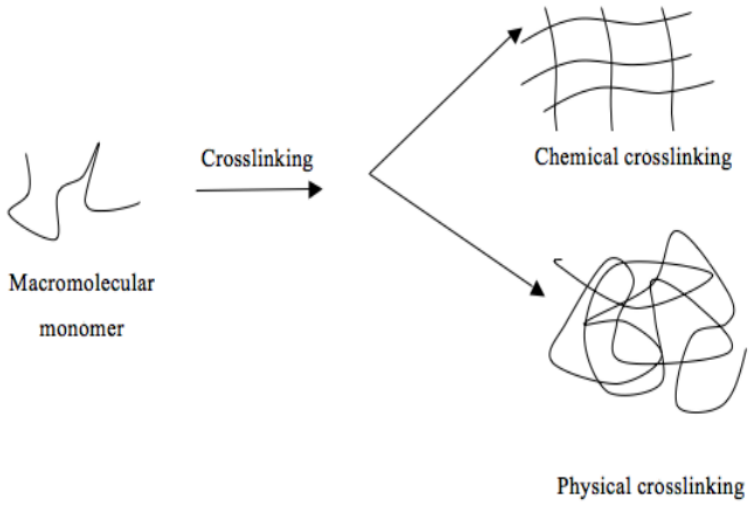

Figure 1-2: Schematic of chemical and physical cross-linked polymers [49].

Chemical cross-linking is a procedure of connecting two or more molecules by covalent bonds. The chemical cross-linking of natural and synthetic polymers can be achieved by the reaction of the functional groups such as hydroxyl group (OH), carboxyl group (COOH) and amino group (NH_2) with cross-linking agents [50]. Cross-linking

agents are molecules that contain two or more reactive groups capable of chemically attaching to specific functional groups. Chemical cross-linking can alter the properties of a polymer. One such feature is the swelling and erosive behaviour, which varies with the amount of cross-linking agents added to the polymer [51]. The strength of cross-linked hydrogels is associated with chemical bonds [52]. For example, the conventional hydrogels cross-linked by chemical bonds are very brittle due to intrinsic structural inhomogeneity and lacking an effective energy dissipation mechanism [53].

Currently, there is significant interest in physically cross-linking polymers due to the absence of the chemical cross-link agent during the polymerisation process, leading to lower toxicity [51]. Physical cross-linking of hydrogel chains can be achieved using a variety of environmental triggers, for example [52];

- pH,
- temperature
- ionic strength

Physically cross-linked hydrogels are held together by molecular entanglement [54]. Argin *et al*. (2014) demonstrated physically cross-linked xanthan gum and chitosan, which can be used to entrap probiotic bacteria in the controlled delivery to the gastrointestinal tract [55]. Currently, chemical cross-linked hydrogels are used for manufacturing contact lenses, hygiene products, tissue engineering, wound dressings and drug delivery systems [56].

Chemical and physical cross-links can coexist in a hydrogel network; these types of hydrogels are called interpenetrating polymer networks (IPN). Hydrogels with interpenetrating networks have emerged as innovative biomaterials for drug delivery, due to the ability of the network to act as two independent networks or as one single network [57]. The network cannot be separated unless chemical bonds are broken. IPN show excellent performance over conventional polymers, specifically in areas of controlled drug release and drug targeting. This is due to IPN superior properties of swelling, stability, biocompatibility, nontoxicity and biodegradability, which has appealed to pharmaceutical companies. In recent years, numerous research reports on the IPN based delivery systems have shown that these chemical and physical cross-links have emerged as a novel method in controlled drug delivery [58,59]. Madhusudana *et al*. (2013) has reported on Interpenetrating Polymeric Network Nanogels (IPN-NG) composed of natural gelatine, with the results suggesting that these new type of IPN-NG will be useful carriers for treatment for conditions such as colorectal cancer [60].

1.5. Stimuli-responsive hydrogels

During the 1970s, hydrogel research shifted from water-swollen networks to systems that can respond to changes in the external environment [61]. These stimuli-responsive hydrogels have been receiving increased attention in biomedical applications, such as drug delivery systems and tissue engineering due to their unique abilities to respond to environmental conditions [62,63]. Thus, stimuli-responsive hydrogels have been suggested as being a superior drug delivery system to conventional hydrogels [64]. One of the most promising applications for a stimuli-responsive hydrogel is drug delivery. This type of delivery allows the drug to increase the concentration in one specific organ or tissue, which can improve the efficiency and safety of medicines that are already on the market. The successful development of targeted drug delivery systems will enable novel strategies such as anticancer drug delivery and gene therapy [65,66]. This will primarily help with the efficiency of the drug and reduce the side-effects by targeting the specific site. Cancer and most chronic conditions require active, safe targeting drug-delivery systems [67]. Stimuli-responsive hydrogels can react differently to environmental conditions. These can be classified into three main categories biological, physical and chemical stimuli (Figure 1-2) [63,68–70].

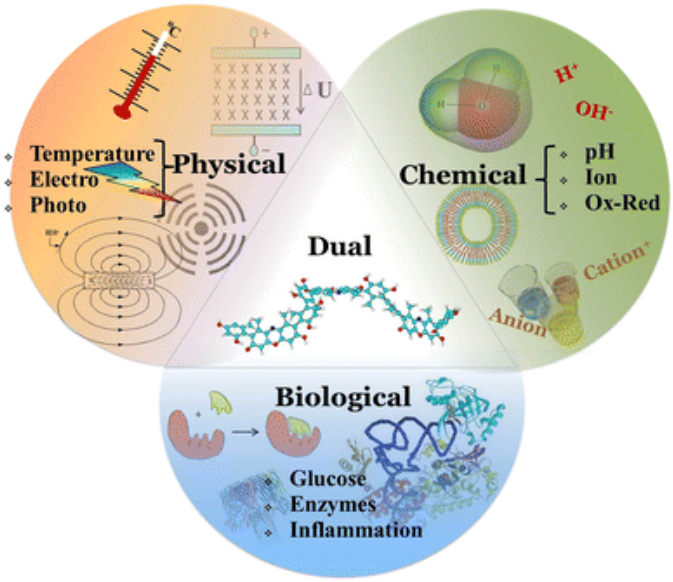

Figure 1-3: Environmental stimuli that trigger the phase transition [71].

Dual-responsive hydrogels can also co-exist; this is where two stimuli-responsive monomers are bonded together to create a hydrogel that can respond to both stimuli. For example, combining pH and temperature-responsive monomers will result in pH-

temperature-responsive hydrogels, where the phase separation temperature will depend on the pH of the medium. Combining a pH based monomer into temperature-responsive hydrogel benefits the system as an oral drug delivery system, where the pH hydrogel will protect the drug in the presence of acid pH, such as the stomach and deliver it to the alkaline pH region in the small intestine. This field of drug delivery technology is in its early stages of development, and a variety of stimuli-responsive systems are constantly being developed. Researchers face a wealth of challenges when manufacturing such systems, including processability and phase separation difficulties, the required use of solvents, the shrinkage and brittleness of the polymers that comes with the high degree of cross-linking, the lack of toxicity data, the precise temperature of the gelation, the burst effect and the irreproducible drug release kinetics [72]. Additionally, many of these systems lack standardised manufacturing methods and toxicity assessments, which hinders their regulatory and ethical approval, and ultimately limits their clinical translation. However, stimuli-responsive polymers have one major advantage over conventional drug delivery systems: their ability to target a specific site for improved therapeutic effect. Accordingly, those systems have grown in popularity in the field of drug-delivery technologies and a small number of formulations have been recently introduced on the market as listed in Table 1-2.

Table 1-2: Smart polymers products that are on the market [72].

Brand	Drug	Excipients	Stimuli	Route	Company
TimopticXE	Timolol maleate	Gellan gum	pH	Ophthalmic	Merck and Co., Inc.
Oncogel Regel depot technology	Paclitaxel	Poly (lactide co-glycolide)-poly (ethylene glycol)-polylactide co-glycolide)	Thermal	Parenteral	Macromed, Inc.
hGHD1 Regel depottechnology	Human growth hormone				
Cytoryn	Interleukin-2				
Azasite	Azithromycin	Poloxamer 407, polycarbophil	pH	Ophthalmic	Oak Pharms, Inc
Akten	Lidocaine HCl	Hypromellose	pH	Ophthalmic	Akron Inc.
Pilopine	Pilocarpine HCl	Carbopol 940	pH	Ophthalmic	Alcon Laboratories, Inc
Virgan	Ganciclovir	Carbomer 974P	pH	Ophthalmic	Thea Pharmaceuticals, Ltd.

1.5.1. Hydrogels that are temperature-responsive

Temperature-responsive hydrogels are the most commonly studied due to their physiological significance. Temperature-responsive hydrogels contain hydrophilic and hydrophobic segments. When the temperature is within the range of the phase transition, the balance between the hydrophilic and hydrophobic segments is altered, and the phase separation or sol-gel transition can follow [73]. Hydrogel solutions that can be injected into any tissue, organ or body cavity in a minimally invasive manner prior to sol-gel transition [61,74].

A temperature-responsive hydrogel shows a thermally induced phase transition in solution. The phase behaviour of temperature-sensitive hydrogels is governed by the Gibbs free energy of mixing, which is displayed in Equation 1-1:

$$\Delta G_m = \Delta H_m - T\Delta S \qquad \text{Equation 1-1}$$

ΔH_m and $T\Delta S$ are the enthalpy and the entropy of mixing. Two components will only mix if the Gibbs free energy of mixing is negative: $\Delta G_m < 0$. Upon heating, the entropy of mixing can dominate and lead to decreasing miscibility, with increasing temperature. A typical phase diagram consists of two-phase boundaries; the lower boundary corresponds to thermally induced mixing known as an upper critical solution temperature (UCST), while the upper boundary corresponds to thermally induced demixing known as a lower critical solution temperature (LCST), which is illustrated in Figure 1-4. Temperature-responsive hydrogels, which become insoluble upon heating, have a LCST where the hydrophilic and hydrophobic balance changes. Hydrogel systems that exhibit LCST behaviour have gained significant attention in biomedical applications in recent years [63]. The change in temperature affects the hydrogen bonding of the polymer molecules, which results in the volume phase transition [75].

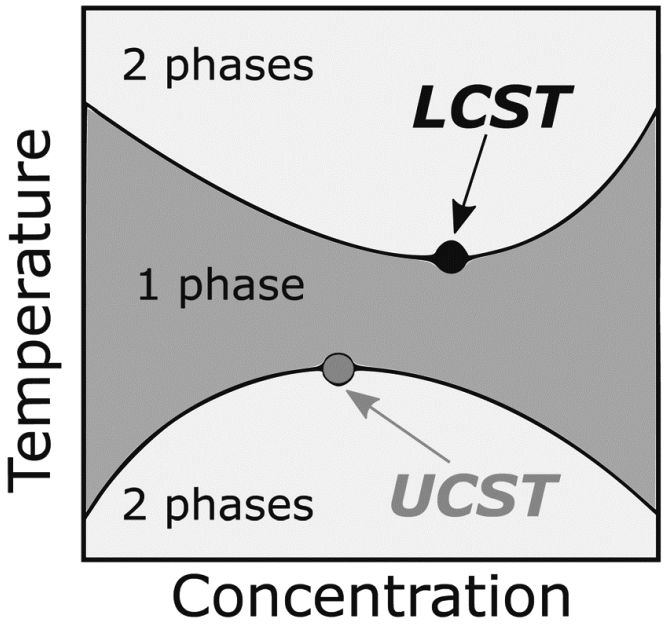

Figure 1-4: A typical phase diagram displaying the UCST and LCST points for a stimuli-responsive hydrogel [76].

One of the most renowned temperature-responsive hydrogels is Poly (*N*-isopropylacrylamide) (PNIPAm), which exhibits a phase transition at around 32 °C in aqueous solution. The aim of researching temperature as a release trigger is to achieve a controlled drug release by precisely matching the temperature sensitivity of the hydrogel to the target site. Temperature-responsive hydrogels have become an attractive candidate for designing nano-vehicles for targeting specific tissues. The temperature range at which these nano-vehicles should release is between 37 °C and 42 °C [77].

PNIPAm is considered the gold standard of temperature-responsive polymers; however, it is challenging to synthesise in bulk. To purchase PNIPAm is prohibitively expensive in an academic context, with 1Kg currently costing in excess of $50,000. An alternative to PNIPAm is Poly (*N*-vinylcaprolactam) (PNVCL) which is acknowledged for its superior characteristics, with regards to biocompatibility, solubility and having non-ionic and non-toxic features. However, limited suppliers of PNVCL currently exist worldwide with quantities being produced in small scale batches at high cost. This may be due to a limited commercial market for PNVCL when compared to PNIPAm.

Moreover, PNVCL has a similar LCST range, compared to PNIPAm, which is between the physiological range of 32 °C and 38 °C [78]. The LCST behaviour of PNVCL is sensitive to alterations in the polymer concentration, the molecular weight of the polymer and also the composition of the solution [79]. PNVCL sensitivity to these

alterations allows for a tuned LCST behaviour. Those who have carried out studies on the effect of salts on thermosensitive polymers have found that the LCST may be increased (known as the 'salting-in' effect) or decreased (known as the 'salting-out' effect) depending on the chemical structure of the added salt [80–82].

1.5.2. pH-responsive hydrogels

Hydrogels that are pH-responsive are becoming popular; the pH sensitivity of hydrogels is due to the presence of a weak acid or base on the polymer backbone, which accepts or releases protons depending upon external conditions [83]. Thus, at specific pH values, they can dissociate in aqueous solutions, forming polyelectrolytes. The pH at which hydrogels show volume change depends on the type of weak acid or base used.

Some hydrogels can contain weak acid functionality; they will swell as the pH of the medium increases. Hydrogels that are pH-responsive are commonly used to develop controlled release formulations for oral administration [84]. Specific body organs have a different pH, such as the stomach, which is entirely different from the neutral pH in the intestine tissues. Chronic wounds can have a pH range between 5.4 and 7.4. Cancer tissues have been reported to be acidic extracellularly [75].

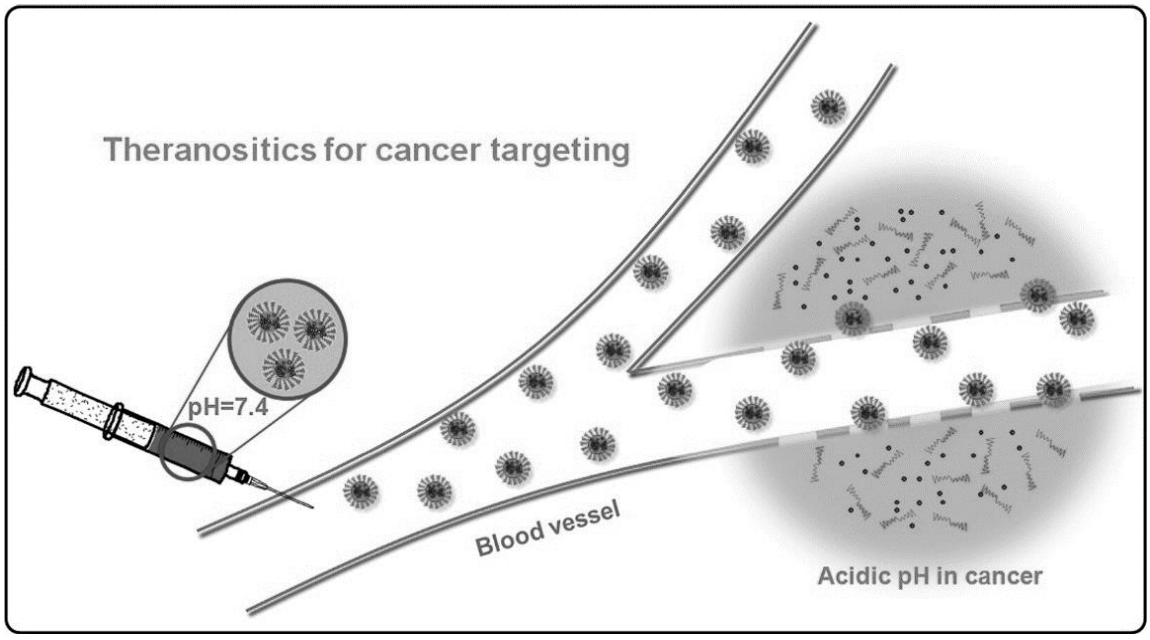

Figure 1-5: Example of cancer-targeting research [85].

Cancer tissue usually has a pH below 7 and healthy body tissue is between pH 7.2-7.4. Tumours with low pH primarily result from a high glycolysis rate, which can

produce lactic acid. This low pH benefits the tumour cells and promotes invasive cell growth. The low pH of a tumour provides a tissue-specific stimulus that may be exploited for targeting applications. pH-sensitive hydrogels can be tailored to carry, deliver and control the release of a therapeutic agent in cancer tissue, as displayed in Figure 1-5 [85].

1.5.3. Combining pH and temperature-responsive hydrogels

Hydrogels can be sensitive to both pH and temperature. The presence of pH-sensitive comonomers, which are charged, increases the LCST of the temperature-responsive comonomers due to the increase in hydrophilicity of the polymer. pH and temperature-responsive hydrogels can undergo volume changes in response to changes in temperature and pH. The magnitude and location of temperature-induced gel collapse can be altered significantly by changing the solution pH. This allows tailoring of a temperature-responsive hydrogel to meet specific process or system needs. These unique characteristics are of great interest in drug delivery [86] and cell encapsulation [87].

An injectable pH-and temperature-responsive biodegradable hydrogel poly (β-amino ester urethane) and triblock poly (ε-caprolactone-lactide)-poly (ethylene glycol)-poly-(ε-caprolactone-lactide) (PCLA-PEG-PCLA) was used to enhance sustained release by dual ionic interactions. The injectable hydrogels suppressed the initial burst release and extended the release period for 13 days *in-vitro* and 5 days *in vivo* [88].

1.6. Drug release mechanism

Controlled drug release occurs when a polymer, whether natural or synthetic, is carefully combined with an API in such a way that the API is released from the material in a predetermined manner [89]. The mechanism that determines the release of polymers can occur as diffusion through a rate-controlling membrane, osmosis, ion exchange or degradation.

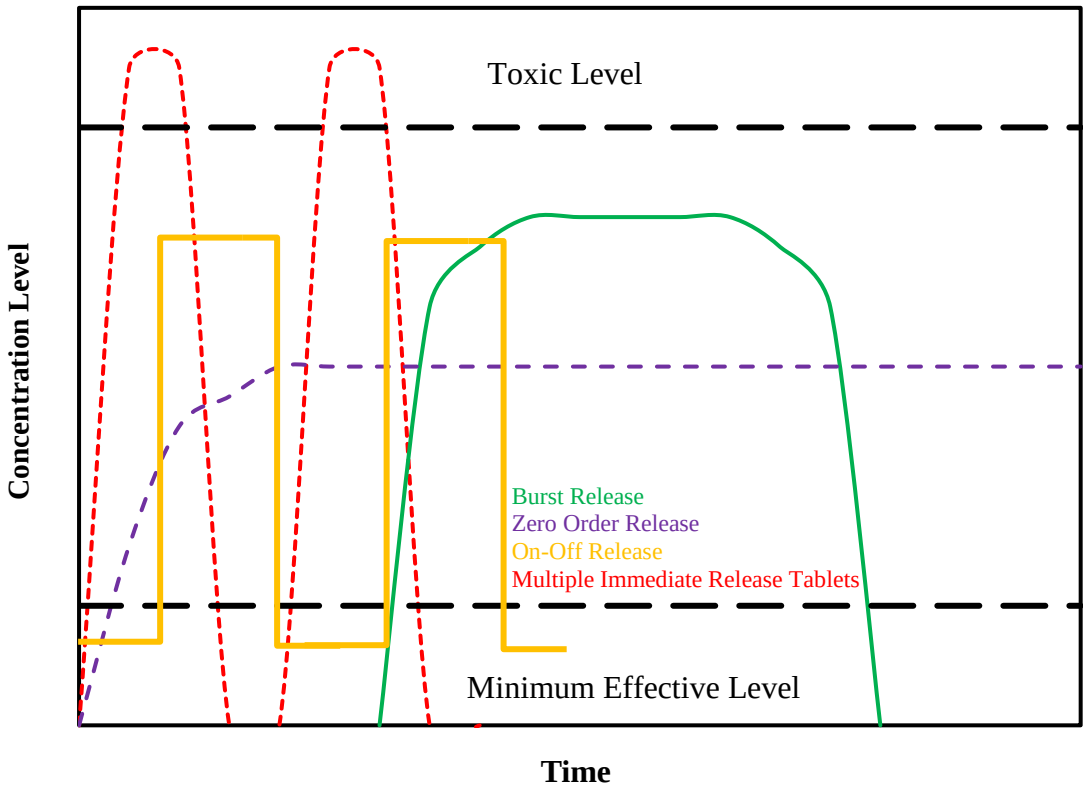

Figure 1-6: Examples of different types of drug release of active therapeutic agents over time.

The advantage of using biodegradable polymers to deliver the API is that these materials do not need to be removed from the body after the drug delivery is completed. Traditionally, drug delivery is *via* conventional treatments, which require repeated administration. Repeated administration of drugs can result in inconsistent (peak and valley) drug concentrations, meaning that high levels of the drug are administered to reach therapeutic levels for a sufficient period as illustrated in Figure 1-6.

Such methods have two distinct disadvantages; the risk of reaching toxic levels and low compliance by the patient. The mechanism of drug release from polymers and their release kinetics are dependent on the choice of polymer and the fabrication technique used [90,91]. The hydrophilic segment of the polymer chains results in erosion of the polymer matrix, with two primary mechanisms of degradation: bulk and surface degradation [92,93].

When the rate of penetration of water is considerably higher, compared to the rate of polymer hydrolysis, bulk degradation will be the principal mechanism. This is due to the degradation of the polymer backbone, resulting in fast penetrating water before surface degradation can take place. The surface degradation will be the leading

mechanism when the degradation of the polymer matrix is faster than the rate of water diffusion into the polymer [94]. When the surface degradation process is evenly spread and confined to the surface of the device or formulation; then, the drug release process will be controlled by surface degradation and exhibit zero-order release kinetics [95]. The drug release rate may deviate from zero-order release kinetics, as it is dependent on a number of factors including chemistry, molecular weight, crystallinity, porosity and glass transition temperature of the polymer [96].

Furthermore, drug release profiles can also be controlled by a change in temperature. Several smart drug delivery carriers have been designed for a number of applications such as cancer therapy. On-off switching capability of a smart polymer can release APIs ranging from 6 months to a year [97–99]. Additionally, their adjustable properties can also be used in smart devices technology such as sensors where stimuli sensitive "on-off" properties are desirable. Smart polymer on-off switching capability allows the release of API, reflecting the "on" state at higher temperatures and the "off" state at lower temperatures. A positive thermosensitive drug-release microcapsule (MC) was designed by Ichikawa *et al*. (2000). This microcapsule demonstrated a positive thermosensitive on-off pulsatile drug release around 32 ºC [100].

1.7. Swelling-controlled release systems

In hydrogel systems the absorption of water from the environment changes the dimensions and/or physical properties of the system and thus the drug release kinetics. Examples of systems that exhibit swelling controlled release are physically and chemically cross-linked hydrogels [101]. It should be noted that erosion and diffusion are also involved in the release of active agents from physically cross-linked gels, while diffusion also has a significant role to play in the release of drug from chemically cross-linked gels. In spite of this, it is accepted that the swelling step remains the rate-controlling mechanism in the release of drug from both of these types of hydrogels.

Information on the degradation kinetics of physically cross-linked hydrogels is rather limited at this time. This is because the degradation and release characteristics of most degradable hydrogels depend on a complex, interrelated set of events. On contact with water the physically cross-linked component swells to form a hydrated matrix layer (gel layer). This then controls the further diffusion of water into the matrix. Diffusion of the drug through the gel layer controls its rate of release. The outer gel layer will erode as it becomes

more dilute and the rate of erosion depends on the nature of the gel. The classic description of the events following immersion of a physically cross-linked gel in aqueous media is as follows:

- Surface drug (if water-soluble) dissolves and gives a 'burst effect'.
- The hydrophilic polymer hydrates and an outer layer forms.
- The gel layer becomes a barrier to uptake of further water and to the transfer of drug.
- Drug (if soluble) release occurs by diffusion through the gel layer; insoluble drug is released by erosion followed by dissolution.
- Following erosion the new surface becomes hydrated and forms a new gel layer.

The relative importance of each release mechanism will depend on the physiochemical properties of the gel layer, the aqueous solubility of the drug and the mechanical attrition of the matrix in the aqueous environment [102]. Drug dissolution and polymer relaxation also have an effect on the drug release kinetics from physically cross-linked polymers [103].

Chemically cross-linked hydrogels, however, do not dissolve in aqueous media. Following submersion of the hydrogel in water, the following three zones may be identified in the swelling process as illustrated in Figure 1-7: (zone 1) a matrix of unswollen, completely dried, rigid polymer, (zone 2) a fairly thin layer in which the polymer chains are slowly hydrating and relaxing, and (zone 3) adjacent to the bulk water is a layer of completely swollen gel. The diffusion coefficient of a drug in the dried hydrogel is very low initially, but it increases significantly as the gel absorbs water. Thus, the drug release from the device is a function of the rate of water uptake from the environment as well as the drug diffusion. For such a device, it would be difficult to predict the effect of the water uptake rate on the rate of drug release.

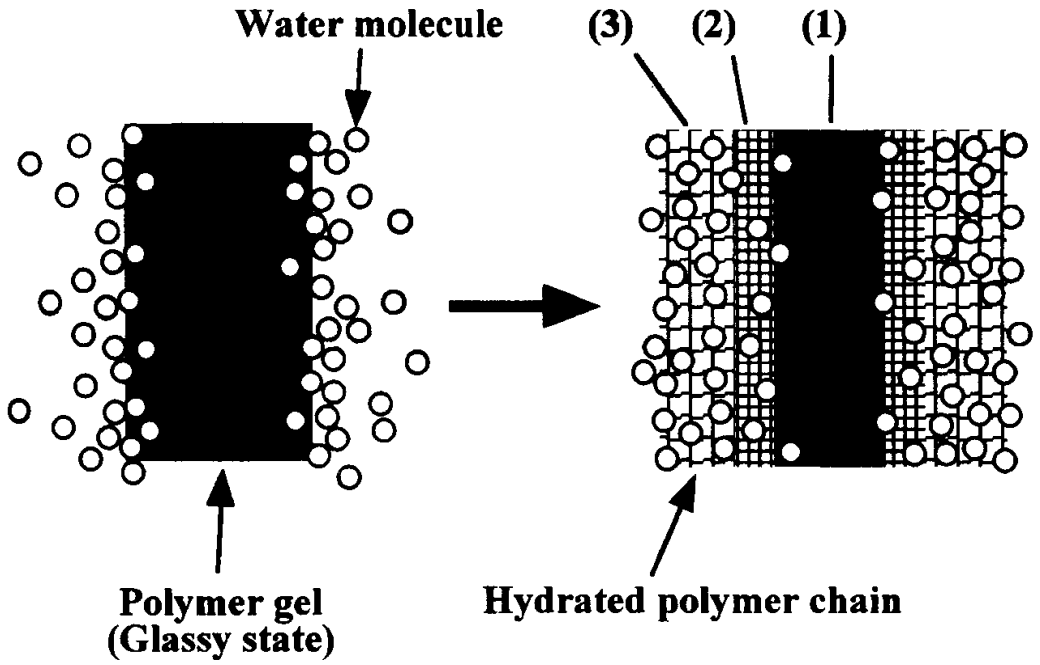

Figure 1-7: Water uptake process for chemically cross-linked hydrogels from an initially glassy dry state [104].

The barrier to diffusion can therefore be decreased by swelling of the hydrogel, which creates voids or pores in the gel structure. Hydrogels permit the transfer of water and low molecular weight solutes. Such hydrogels have been used widely in various applications, especially in the controlled drug delivery area where limited diffusional characteristics are required [105]. Swelling of temperature-sensitive hydrogels in pure water is a common preliminary test procedure that is widely conducted in other published works for these types of hydrogels [106–108].

1.8. Implantable drug delivery systems

Implantable drug delivery systems are desirable for several reasons to deliver drugs, particularly those that cannot be delivered *via* the oral route, are irregularly absorbed *via* the gastrointestinal tract, or that benefit from site-specific delivery. Implantable systems are typically cylindrical. Implantation is typically carried out in a variety of ways , such as;

- Subcutaneously (under the skin),
- Intramuscularly (in a muscle),
- Intravenously (in a vein)
- Intrathecally (around the spinal cord),

With the aid of implantation devices, needles, or the use of surgery [109]. Intramuscular tissue is an ideal location for implantation of drug-depot devices, due to high-fat content that facilitates slow drug absorption, minimal innervation, and a lower possibility of localised inflammation [110]. The most common implantable devices and drug/device combination products are drug-eluting stents, artificial organs, biosensors, scaffolds for tissue engineering, and heart valves [111]. Implants can be used as delivery systems for either systemic or local therapeutic effects. For systemic therapeutic effects, implants are typically administered intramuscularly, or intravenously, whereby the incorporated drug is delivered from the implant and absorbed into the blood circulation. Implants for local effects are placed into specific body sites, where the drug acts locally [112].

Implants are typically designed to release drug in a controlled manner, allowing the adjustment of release rates over extended periods, ranging from several days to years. Implantable drug delivery systems should be designed to substantially reduce the need for frequent drug administration over the treatment period. As such, they should be environmentally stable, biocompatible, sterile, and be readily implantable and retrievable by medical personnel to initiate or terminate therapy. Also they must enable controlled drug release at an optimal dose, be easy to manufacture and provide cost-effective therapy over the treatment duration.

One of the most widely known subdermal implants is Implanon, which is a contraceptive drug delivery system. Implanon is FDA-approved. Implanon consists of a single-rod implant (length 4 cm, width 2 mm) and has a polyethylene vinyl acetate core that encapsulates 68 mg of etonogestrel and releases the drug over 3 years. The rate of drug release is controlled by a polyethylene vinyl acetate membrane covering the rod. Protection from pregnancy can be extended beyond the initial 3 years upon removal and immediate replacement with a new implant. Designed for easier subcutaneous insertion and removal than Norplant, Implanon has found high acceptance by patients [9].

While systems such as Implanon are typically robust and structurally resilient over their intended lifetime, their obvious drawback is these are nonbiodegradable polymers and as such need extraction after depletion of the drug. While their biocompatibility is typically proven for the duration of the proposed use, the risk of infection at the site of subcutaneous implantation following long-term *in situ* placement is undesirable.

To overcome these drawbacks of nonbiodegradable implants, biodegradable systems, based on polymers such as poly(lactic acid) (PLA), poly(lactic-co-glycolic acid) (PLGA), poly(caprolactone) (PCL) or their block copolymer variants with other polymers have been developed. A significant advantage of biodegradable systems is that the biocompatible polymers used for fabricating these delivery systems are eventually broken down into safe metabolites and absorbed or excreted by the body. Complete degradation of the post drug implant makes surgical removal of the implant after the conclusion of therapy unnecessary, thereby reducing potential complications with explantation and increasing patient acceptance and compliance. Among the many biodegradable polymers that have been explored as a component of an implantable drug delivery system, polyesters are perhaps the most widely investigated. An additional benefit is that they have been approved by the FDA for use in several pharmaceutical products. In general, the ease of fabrication by several techniques is an additional reason why these polyesters have been adopted substantially more than other polymers. For example, polymers such as PCL lend themselves to injectable formulations that subsequently form depot-like implants *in situ* at the location in tissue [113]. Melt extrusion processing techniques, solvent evaporation, and compression moulding are reported methods for implant fabrication [110]. An example of a biodegradable implant is Zoladex, containing goserelin acetate, which is a decapeptide analogue of lutinizing hormone-releasing hormone. It uses PLGA or PLA as a carrier, in which the drug is dispersed in the polymer matrix using the hot-melt extrusion method. For commercial use, the implant is distributed in the form of a prefilled syringe that is administered subcutaneously. The drug is continuously released for 1 or 3 months [110]. Hydrogels can also be implanted surgically into the body for the treatment of various conditions. INFUSE, for instance, is a type I collagen gel that releases recombinant human bone morphogenetic protein-2, and is used for the treatment of long bone fractures and spinal fusion [3]. Implantable drug delivery systems are finding increasing applications in areas such as;

- women's health,
- chronic disease therapies,
- oncology,
- pain management,
- neurology.

Implants continue to make a significant contribution to therapy and disease management.

1.8.1. Injectable hydrogels in drug delivery

Drug delivery is of vital importance to healthcare sectors. It is a broad term that covers issues such as the formulation, technology and systems for transporting API in the body [114]. The primary goal of any drug delivery device is to achieve the desired therapeutic result, with minimum side effects, as safely as possible. However, in some cases, such as chemotherapy for cancer, the current treatment methods primarily rely on the use of conventional cytotoxic drugs that have an adverse side effect, with only limited effectiveness. Many studies have indicated that these problems could be attributed to the lack of target specificity of the current state of anti-tumour drugs. The most substantial drug delivery device is expected to be produced by oral medications or injectables [114].

Controlled drug delivery has many advantages, such as improved bioavailability by preventing premature degradation and enhancing uptake by controlling drug release rates and reducing side effects by targeting the diseases [38]. Polymers show improved pharmacokinetics, more extended circulation and more efficient tissue targeting, in comparison to small molecule drugs. They can be used as the polymeric drug, as a drug carrier, or can be combined with small molecules.

The development and success of a targeted drug delivery system will allow new therapeutic strategies such as in anticancer drug delivery, protein delivery and gene therapy [115]. This primarily helps the efficiency of the drug by reducing the side-effects of high loading. Cancer and other conditions require effective, safe targeting drug-delivery systems [116]. The criteria for targeted drug-delivery systems are:

- Modulation of drug release
- Maximisation of drug precision
- Reduced drug toxicity

The most promising future for controlled released drugs is those that are polymer-based, due to the extensive processability and the physical and chemical properties that allow for detailed modulation of dosage to suit specific applications [116].

In-situ forming hydrogels can take the form of clear polymer solutions before administration, which undergoes sol-gel in response to changes in stimuli in the solution, an overview can be seen below in Figure 1-8. Some appealing biomedical applications have been proposed for *in-situ* forming hydrogels, particularly in areas of drug delivery and cell therapies. This is due to their unique advantages, such as minimal invasion, lack of organic solvent and photo-initiator, site-specific delivery and ability to deliver

hydrophobic/hydrophilic drugs. For example, drugs or cells can be encapsulated *in-situ*, forming hydrogel solutions at low temperature and the mixed solutions rapidly undergo sol-gel transition after injection into the body [18]. This substantial entropy gain is caused by the release of bound water molecules from the hydrophobic segments at the sol-gel transition [63].

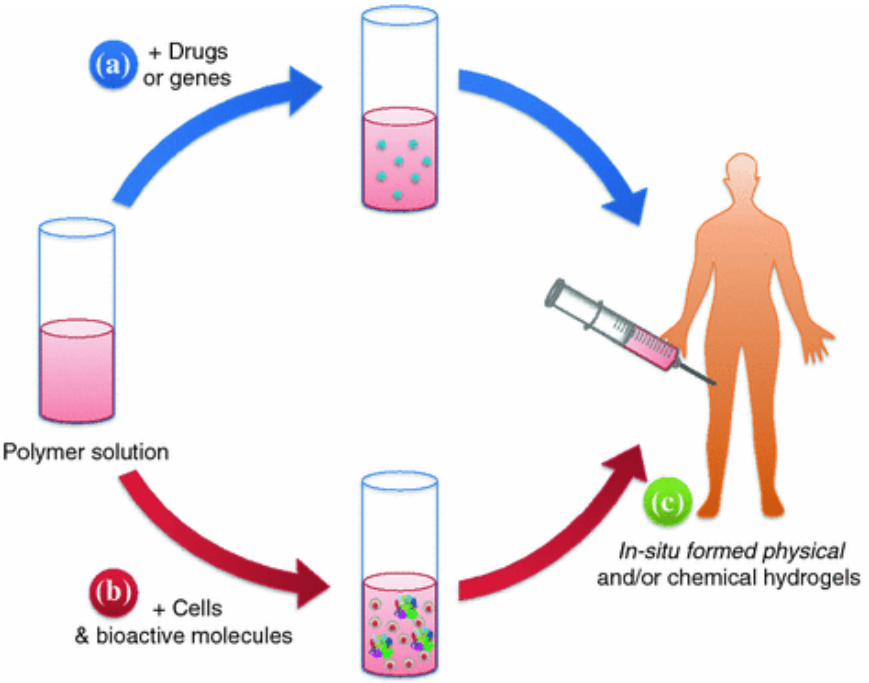

Figure 1-8: Overview of *in-situ* forming hydrogels systems [117].

One significant disadvantage of some temperature-responsive hydrogels based on PNIPAm and PNVCL is that they are not biodegradable. Biodegradable polymers refer to a category of polymers that can be cleaved into small polymer fragments *in-vivo*. The biodegradability allows these polymers to be used in many applications, particularly in drug delivery and tissue engineering [118]. Thus, recent research has been focused on the development of the biodegradable ability of temperature-responsive hydrogels. In order for a hydrogel to be biodegradable, the presence of either hydrolytically or proteolytically labile bonds in their backbone is essential to allow it to be degradable. Therefore a number of research groups have attempted to incorporate a degradable backbone to allow PNVCL to be biodegradable [119].

Rejinold *et al.* (2011) developed curcumin-loaded chitosan-g-PNVCL nanoparticles for cancer therapy. This hydrogel system had biodegradable, biocompatible and temperature-responsive properties, which was extremely efficient on cancer cells, with minimal toxicity to healthy cells *in-vitro* [120]. Gan *et al.* (2016) synthesised novel

temperature-responsive biodegradable hydrogels, prepared from *N*-isopropylacrylamide (NIPAM) and two biodegradable cross-linkers, poly (ε-caprolactone) dimethacrylate (PCLDMA) and bisacryloylcystamine. In a physiological pH, the hydrogels could be biodegraded slowly in glutathione solution at 37 °C [121].

Prabaharan *et al*. (2009) entrapped self-assembled stable micelles of PNVCL-b-PEG block copolymers combined with folic acid (FA) for anti-cancer drug systems. The release profile at 37 °C showed PNVCL-b-PEG-FA micelles had a slower and more controlled release of the entrapped 5-fluorouracil (5-FU) compared to release profiles at 25 °C. PNVCL-b-PEG-FA micelles loaded with 5-FU did not induce remarkable cytotoxicity; however, these micelles displayed a cytotoxicity effect against mouse mammary carcinoma cells due to the availability of loaded anti-cancer drugs delivered to the inside of the cancer cells [122,123].

In another study, Venkatareddy *et al*. (2010) prepared poly (NVCL-co-VAc) microspheres by free-radical emulsion polymerisation in the presence of 5-FU [124]. The authors reported high drug release rates of 5-FU from the formulations prepared with higher amounts of NVCL than those formulations prepared using lower quantities of NVCL. Slower drug release is observed from formulations prepared with a lesser amount of NVCL, attributed to the hydrophilic nature of both the drug and the NVCL in the copolymer [124].

Prabaharan *et al*. (2008) used biodegradable chitosan-g-PNVCL for the controlled release of the hydrophobic drug ketoprofen. The release rate was influenced by both the pH and temperature of the medium. At pH 7.4 and 37 °C, the chitosan-g-PNVCL showed a compact structure with reduced pore size and strong hydrophobic interactions with the drug molecules, resulting in a slow and steady release of the drug from the system [125].

Additionally, Thermo-gelling hydrogels are becoming popular in eye treatment as conventional eye drops move quickly away from the surface of the eye, resulting in poor bioavailability. To improve on this poor bioavailability, Cho *et al.* (2016) developed a temperature-responsive biodegradable hexanoyl glycol chitosan (HGC) as a carrier for topical drug delivery to the eye. By controlling the concentration of *N*-hexanoylation, the thermo-gelling behaviour could be controlled for glaucoma therapy. In *vivo* experiments demonstrated that HGC is maintained on the periocular surface for a more extended period due to its increased viscosity at body temperature [126].

1.9. Fabrication techniques for polymeric drug delivery systems

A vast number of fabrication techniques may be utilised to produce polymer platforms for drug delivery applications. The fabrication techniques which are used to synthesise a drug formulation can significantly affect the material's chemical and physical properties. Each technique is, therefore utilised for drug delivery applications in order to create a material with optimum properties. Three of the main fabrication techniques used include electrospinning, spray drying and HME.

The electrospinning technique produces nonwoven fabrics consisting of extremely fine polymer fibres. The method involves applying a high electrostatic field to a capillary connected to a syringe containing a polymer solution. One electrode is placed in the collector and the other in the polymer solution [127]. Electrospinning can produce fibres of varying lengths: from a few nanometers to hundreds of microns [128]. The main advantage of electrospinning is that it can provide drug delivery systems that are appropriate for tissue and cell growth by controlling the pore size and fibre length.

Spray drying is a conventional technique used in pharmaceuticals to produce a dry powder from a liquid phase. It has been successfully used in the pharmaceutical industry to prepare polymers for controlled drug delivery systems. Spray drying is a rapid, reproducible and easy to scale-up method, as it is a one stage process, which needs ambient temperature. The method is mildly dependent on drug solubility and its interactions with the polymer [129].

HME is possibly the most attractive technique, as it is utilised for a wide variety of applications. It was established in the early 1930s and has rapidly become one of the most applied processing technologies in the plastic, rubber and food industries, producing items ranging from pipes, sheets and bags. Today, more than half of all plastic products are produced by HME [130]. The principle of HME is to transfer raw material at an elevated temperature to a product that has a uniform shape. During the HME process, it is very common for two or more raw materials to produce a novel composite with different chemical and physical properties.

1.9.1. Hot-melt extrusion

There are three main types of extruders, single; twin and planetary. Single screw extruders consist of a barrel and a rotating screw. The more advanced twin-screw extruder consists of two screws inside a barrel. Throughout the barrel, heaters are placed to control the barrel temperature, which is monitored by thermocouples. During the HME process, several tasks are performed such as feeding, melting, mixing, venting and developing localised pressure at the die. The HME process has a few control parameters that include screw speed (RPM), feed rate, process-section temperatures and vacuum level for venting. To monitor the HME process, the key parameters are the melt pressure, melt temperature and motor amperage. Also, downstream processing is required, such as cooling, cutting and collecting the final product [131].

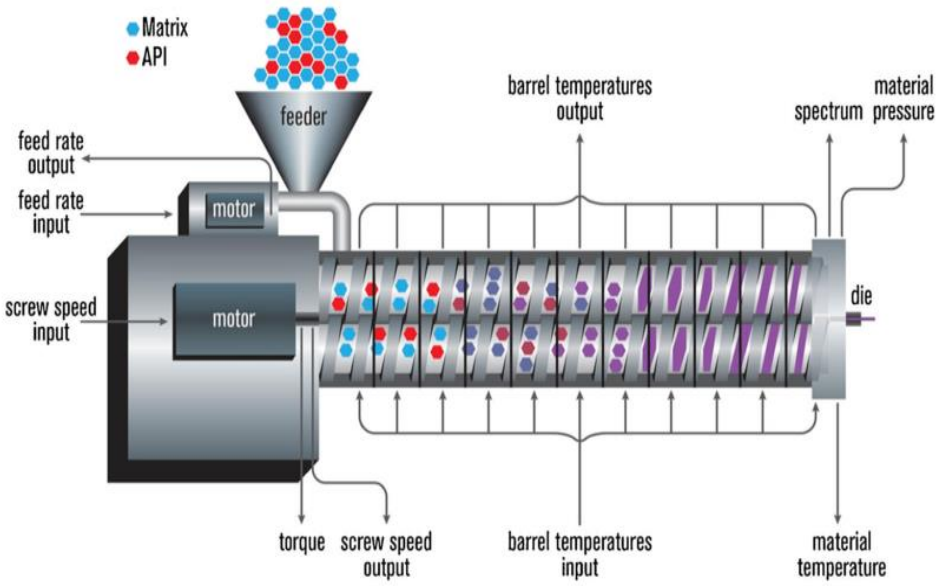

Figure 1-9: Schematic diagram of a small-scale extruder [132].

The polymer is heated above the glass transition or melting temperature, screws then turn, which blends the polymers. This forces the polymer melt through a die located at the end of the barrel. Extrudates produced using this technique assume the shape of the die [133]. The primary aim of utilising HME in drug delivery technology is to improve the dissolution rate, solubility enhancement, solid dispersions and bioavailability. The first record of HME being applied to pharmaceutical applications with polymer and high glass transition temperature was in the 1980s by the BASF Company for enhancing the

solubility of poorly soluble actives [134,135]. Figure 1-9 displays a typical HME process diagram and the various components.

To optimise the extrusion process, plasticisers and stabilisers may be added to allow the material to be processable. To date there are a limited number of products on the market that are produced by HME, one such product is Nexplanon®. Nexplanon® is a long-term birth control implant. This contraceptive arm implant allows a steady and slow release of API into the bloodstream to prevent pregnancy. Nexplanon® can provide up to 3 years of pregnancy prevention [136,137].

The miscibility of polymer blends is an essential aspect in defining the chemical and physical properties of the material. The most popular method for the determination of polymer miscibility is differential scanning calorimetry (DSC), which is a thermo-analytical technique. The DSC method can be used to investigate whether or not polymer blend systems are miscible or immiscible, provided that each of the homopolymer transition temperatures are sufficiently well separated. DSC can evaluate the glass transition temperature characteristics of a copolymer blend. For example, copolymer blends of polystyrene (PS) (Tg = 100 °C) and poly dimethyl phenylene oxide (PDMPO) (Tg = 210 °C) are miscible in every weight percentage (wt%). The DSC thermogram of PS/PDMPO copolymer should thus show one single glass transition temperature, located between 100 °C and 210 °C, dependent upon the different wt% of the homopolymer components within the blend.

On the other hand, copolymer blends based on polystyrene and polyisoprene (Tg = -70 °C) are immiscible. The PS/PI copolymer blends should thus exhibit two distinct glass transition temperatures in the same temperature ranges as their respective homopolymers. In summary, polymer blend systems which show two Tg's by DSC are recognised as being immiscible; those which show only a single Tg may or may not be miscible [138–140].

Fourier transform infrared (FTIR) spectroscopy is another widely used technique that examines molecular bonding interactions in polymer blends. The presence of different chemical groups in co-polymer blends often leads to several types of repulsive and attractive interactions. FTIR spectroscopy is often used to explore these types of interactions. It is particularly suitable for the detection of specific interactions when hydrogen bonding is present. However, it has been suggested that the hydrogen bonding interactions can occur in any system containing a proton donor group and a proton

acceptor. The strength of the hydrogen bond may affect the characteristics of the covalent bonds on interactive species; hence, a frequency shift can be observed. The stretching frequency of the acceptor group, such as the carbonyl group C=O, is also moved to lower frequencies (longer wavelengths), usually with an increased intensity of hydrogen bonding. However, a hydroxyl group of the phenol ring (H–O) bending vibration usually shifts to a shorter wavelength when bonding occurs; this shift is less pronounced than that of the stretching frequency. The IR carbonyl-hydroxyl stretching range or flexion mode hydroxyl-hydroxyl interactions are also sensitive to the hydrogen bonding formation [141].

It is well-known that in most miscible polymer blends, specific interactions such as dipole-dipole forces, hydrogen bonding and charge transfer complexes are drivers for the miscibility.

Materials that are immiscible, often have low thermal and mechanical properties, which are less attractive for industrial applications. However, in some specific applications, partially miscible blends have been used [142].

1.9.2. Pharmaceutical applications of melt processing

HME is one of the most favourable processing techniques of solid compounds which exposes the compounds to pressure, temperature and shear deformation. HME technology is used today in pharmaceutical and manufacturing applications. Currently, more than 40% of API today have poor water-solubility [132]. The bioavailability of an orally administered drug depends on solubility and permeability. Enhancement of oral bioavailability and improving water-soluble drugs remains one of the most challenging aspects of drug development today. Solid dispersion by HME allows unique drug delivery systems to be developed.

Table 1-3 shows products that have been developed to enhance poorly water-soluble drugs by solid dispersions [143]. The amorphous conversion and molecular dispersion of polymer compounds can be achieved using both hot-melt and solvent methods. HME is preferred due to the environmental and economic limitations associated with the solvent methods. A typical HME process includes the heating and softening of a mixture of a drug and a thermoplastic polymer, followed by extrusion of the molten mass through a die in the shape of cylinders or films.

Table 1-3: Table of products on the market which contain immediate release amorphous solid dispersions [143].

Product	Drug	Preparation method	Carrier polymer	Indication
Kaletra®	Lopinavir, Ritonavir	Melt extrusion	PVPVA64	HIV
Norvir®	Ritonavir	Melt extrusion	PVPVA64	HIV
Gris-PEG®	Griseofulvin	Melt technology	PEG	Dermatophytosis
Fenoglide®	Fenofibrate	Melt spraying	PEG	High cholesterol level

The high shear mixing of the molten mass may cause dispersion of a drug into the polymer matrix at a molecular level, along with the possibility of drug-polymer interactions. However, such amorphous solid dispersions of poorly water-soluble drugs are known to exhibit physical and chemical instability because of higher molecular mobility. Moreover, polymers with a higher glass transition (T_g) are usually preferred in the solid dispersion to improve the shelf life of the final formulation of amorphous compounds [144]. During processing and storage, evaluation of the physicochemical stability of these amorphous solids is essential [145]. Table 1-5 displays a list of polymers that are commonly used for drug delivery. Amorphous polymer materials may be processed above their T_g. The aim is to achieve a homogenous mixture of drug and polymer. The importance of a homogeneous mixture of drug and polymer is to allow the material to deform inside the extruder, which is fundamental in the HME process [136,146].

Selecting a suitable polymer is based on two criteria: drug-polymer miscibility and drug-polymer stability. Polymers with a lower T_g than the drug offers the advantage of not exposing the drug to high processing temperatures and possible degradation. The use of plasticiser plays a significant part in the HME process. Plasticiser reduces the chain-chain interaction and reduces the frictional forces along the polymer chains, resulting in lower processing temperatures for HME [134].

Table 1-4: Polymers commonly used for immediate release *via* HME [137].

Immediate release
Polyethene oxide (PEO)
Polyethene glycol (PEG)
Polyvinylpyrrolidone (PVP)
Vinylpyrrolidone/vinyl acetate copolymer (Kollidon)
Vinylprrolidoneethyl methacrylate copolymer (Eudragit)
PEG6000/vinyl caprolactam/vinyl acetate copolymer(Soluplus)

Melt processing has some disadvantages. The main drawbacks of HME include thermal processing (drug/polymer stability), the use of a limited range of polymers, high flow properties of polymers and it is not suitable for relatively high heat-sensitive polymers such as proteins [130].

Mixing, melting, homogenising and shaping is continuously performed as a one-step process on a single machine, while it also has advantages over conventional techniques to manufacture controlled-release products [147]. In controlled-release, HME offers promising formulations where a drug is homogeneously embedded in the polymer matrix [32]. Ma *et al.* (2013) studied the development of hydroxypropyl methylcellulose (HPMC) based controlled release formulations *via* HME with an API (Theophylline) embedded in the polymer phase. HPMC is a problematic polymer for the use in melt processing due to its high glass transition temperature, low degradation temperature and high viscosity. These problems were partially overcome by plasticising the HPMC with up to 40% PEG. The authors found that the dissolution results showed sustained release profiles without burst release for the HPMC formulations [148].

Additionally, Palem *et al.* (2013) prepared domperidone (DOM) immediate release films produced *via* HME, confirmed by *in-vitro* and *in-vivo* techniques. The HME film formulations contained a combination of PEO and HPMC and Eudragit as polymeric carriers and PEG as a plasticiser. The extruded films demonstrated no drug excipient interaction and showed excellent content uniformity. The selected HME film formulation exhibited *in vivo* residence time (120 min) and *in-vitro* drug release of 84.8% in 2 hours. Bioavailability from the optimised HME films was 1.5 times higher than the oral dosage. The results indicated that HME is a viable technique for the preparation of DOM films, with improved bioavailability characteristics [149].

HME has emerged as an FDA approved method, whereby regulatory tests must be complied with [30–32]. The FDA, along with other global regulatory agencies such as

the European Medicine Agency (EMA), defines the quality of a drug product through the concept of quality by design (QbD), from its development cycle to its commercial production. As an FDA approved method, QbD ensures transparency, efficiency and quality at any stage of the development cycle of HME, including process improvement, scale-up, optimisation, and control [91,106], and throughout its commercial production. Similarly, QbD is a guarantee that the products remain consistently and reliably free of contaminants [132,150]. An example of this approach can be seen in Figure 1-10.

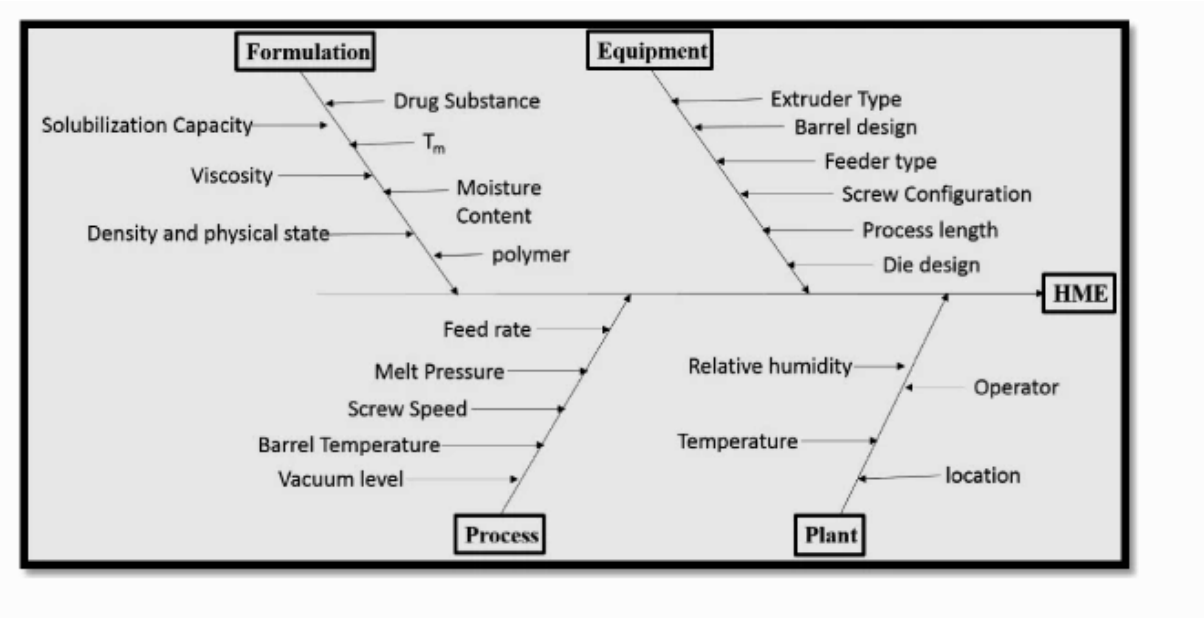

Figure 1-10: Ishikawa diagram of the melt processing [132].

Process analytical technology (PAT) is an important component of QbD. Its goal is to design, analyse, and control the pharmaceutical manufacturing processes of a drug product, through a series of pre-defined parameters that are linked to its critical quality attributes. This framework ensures the consistent quality of both the manufacturing chain and the end product. The FDA guidelines divide PAT into the four steps below [132,150]:

1. Identify and measure critical materials and process attributes that relate to the product quality.
2. Design a process measurement system that allows real-time or near-real monitoring of all critical attributes. There are different measurements available for monitoring:
    - At-line: measurement where the sample is removed, isolated, and analysed in close proximity to the process stream;

- In-line: measurement where the sample is not removed from the process stream. It can be invasive or non-invasive;
- On-line: measurement where the sample is diverted from the manufacturing process and may be returned to the process stream;
- Off-line: measurement that is disconnected in a timely and local manner from the manufacturing process.

3. Design a process control that provides adjustments to ensure control of all critical attributes.
4. Develop mathematical relationships between product quality attributes and measurements of critical materials and process attributes.

1.9.2.1. Plasticisers

The use of plasticisers in HME allows for the lowering of the processing temperature. Plasticisers occupy sites along the polymer chain, which prevents chain to chain interactions, enabling the reduction of the chain's stiffness. This also provides a decrease in the risk of thermal degradation. Plasticisers can be divided into three different classes such as traditional, non-traditional and unique plasticisers. The most commonly used conventional plasticisers are triacetin, citrate ester, vitamin E D-alpha tocopheryl and low molecular weight polyethene glycols. Non-traditional plasticisers are included in formulations to serve other critical functions and are often low-molecular-weight materials such as the active substance itself [132,135].

1.10. Drug loading of smart temperature-responsive polymers

There are three primary methods of loading drugs into a hydrogel matrix, with each method having its advantages and disadvantages [151]:

- Permeation is one of the easiest ways of loading a hydrogel. This is where the drug will diffuse into the hydrogel, depending on the porosity of the hydrogel and the size of the drug. This is beneficial for small molecules; however, it releases the drug very quickly and takes some time for the drug to diffuse into the hydrogel.

- Entrapment is when the drug is mixed with the polymer before cross-linking. After forming an aqueous solution of the polymer, diffusion allows the drug to be released out of the polymer matrix.
- Covalent bonding is when the drug is bonded to the polymer carrier. This method limits tissue exposure to the agent but only when the hydrogel breaks down or when the molecular tether is broken [49].

The success of an efficient drug delivery device hinges upon its ability to construct biocompatible carriers that allows high loading of drug molecules without any premature release of drug cargo before reaching the target organ [152]. A Hydrogel drug delivery device is used to enhance the theraputic efficiency via encapsulation of active molecules in a polymer matrix. The encapsulation enhances the stability of drug molecules, improves the targeting properties and prolongs the pharmacological activity *via* the continuous local release of active molecules [153].

Permeation is the most common method of incorporation of a drug into a hydrogel. This is where a drug is dissolved in a solution, and the hydrogel is placed into the solution and allowed to swell. The main advantage is the lack of complexity and fewer washing steps. The main disadvantage of this method is that it has a reduced drug-loading capacity for hydrophobic drugs and a rapid burst drug release during hydrogel swelling. To overcome many of these disadvantages, a second approach is used, which is called the entrapment method. During the polymerisation process, the drug is added into the monomer mixture. One of the main disadvantages of this approach is that the drug may interfere with the polymerisation process resulting in higher than average unreacted monomer, also exposing the drug to toxic monomer and initiators with a high level of toxicity may compromise the hydrogel safety. As consequences, it is required that hydrogel-drug systems undergo several washing steps.

Therefore, it is suggested in this study that loading a smart polymer such as PNVCL by melt processing would offer significant advantages over the traditional smart polymer-drug loading methods. Table 1-5 summarises the advantages and disadvantages of the most common methods of loading a drug into a hydrogel matrix. The other method that is explored in this section is the use of HME, which is based uponincorporating a drug into conventional polymers.

Some examples of the loading efficiency of a drug into a hydrogel would be as follows. Yadavalli et al. (2015) developed a dual stimuli-responsive polymer for targeted cancer treatment. These temperature-responsive polymers were based on a poly (N-isopropylacrylamide) matrix with pH-responsive chitosan. These drug delivery systems were successfully loaded with curcumin using the solvent evaporation method which is based on the entrapment method as previously described, with a drug loading of 86% by weight. However, achieving such a high drug loading efficiency is uncommon using the aforementioned approach in the majority of cases. One such example of lower loading levels is presented by Eswaramma et al. (2017) where guar gum was modified by grafted copolymerisation using *N*-vinylcaprolactam, Zidovudine, and the subsequent anti-HIV drug with only 68% encapsulation efficiency [154]. Another study with a low release profile from a PNVCL system was developed by Rejinold et al. (2011), chitosan-*g*-poly (*N*-vinylcaprolactam) hydrogels were prepared by free radical polymerisation. The 5-FU drug was incorporated into the carrier by entrapping the drug during cross-linking reaction. This novel system presented the release profiles at above and below the LCST of the carrier system. After 3 days, 40% curcumin had been released at above the LCST range of the system, while at below LCST, only a 5% drug release is observed which confirms the drug release mechanism is based on the LCST of the polymeric carrier system [120].

Table 1-5: List of advantages and disadvantages of using the different methods of incorporation of a drug into a hydrogel matrix [155–157].

Method	Advantages	Disadvantages
Permeation	Suitable for physical, chemical cross-linked and IPN hydrogels	Difficulty in scale-up
	Relatively high loading efficiencies for hydrophilic drugs	High possibility of burst release
		Limited hydrophobic drug delivery via hydrogels and non-homogenous dispersion of hydrophobic drugs within the hydrogel
		Only can be used with small molecules
Entrapment by conventional methods	Can load small molecules, peptides and nanospheres	A rapid burst drug release during hydrogel swelling and fast drug release from large porous hydrogel
	Suitable for physical, chemical cross-linked and IPN hydrogels	Possibility of drug deactivation in entrapment method
	Release duration days to weeks	
	Suitable for loading of hydrophilic and hydrophobic drugs	
Hot-melt extrusion	Sustained drug release	Materials must be relatively moisture-free
	Incorporation of hydrophilic and hydrophobic drugs	Drugs are exposed to heat and mechanical shear
	Tuneable physical properties	
	Increasing solubility of highly hydrophilic drugs	
	Continuous process and easy to scale up	

* The information relating to the hot-melt extrusion method above is based upon the advantages and disadvantages of using conventional polymer drug delivery systems.

1.11. Photopolymerisation

Free-radical polymerisation (FRP) is an important method widely used in the plastic industry since the 1940s. It remains one of the most heavily used organic processes and millions of tons of polymers including polyethene (PE), polypropylene (PP), polystyrene (PS), poly (vinyl chloride) (PVC), poly (vinyl acetate) (PVAC) and poly (methyl methacrylate) (PMMA) are produced by this route every year. The FRP technique involves photochemical initiated polymerisation reactions.

FRP is based on the continuous addition of vinyl monomers to a free-radical, which is a molecule with an unpaired electron. The process begins with initiator decomposition, which can release radicals. A vinyl monomer unit is added to the free-radicals of the growing chains. The chain growth is finally terminated by the combination, disproportionation, or chain transfer of the propagating radicals to form polymer molecules [158]. Thus, upon exposure to ultraviolet (UV) or visible light, a suitable liquid monomer formulation is converted into a solid polymer. If the monomer contains more than one reactive function, a cross-linked polymer network is readily produced. Initiating polymerisation by radiation curing is beneficial, as it reduces the need for volatile organic solvents. An overview of the FRP process is displayed in Figure 1-11.

Furthermore, it allows for temporal control of initiation and proceeds more rapidly than thermal polymerisation. Most monomers commonly employed in photopolymerisation do not readily produce sufficient initiating species upon light exposure. Therefore, it is usually necessary to incorporate a photoinitiator that will begin the polymerisation process. As the photoinitiator absorbs UV light energy, it fragments into free-radicals. The free-radical class of initiators represent greater than 90% of commercially used initiator chemistry due to their availability, high quantum yields of radical generation and monomer radical formations. Free-radicals initiate the polymerisation process, attacking reactive double bonds on monomer molecules.

Although the use of photoinitiator offers high efficiency, homogeneity, greater porosity and cross-linking density of hydrogels, the presence of photoinitiator could have a detrimental effect on cells. Williams *et al*. (2005) evaluated the cellular toxicity of Irgacure® 164, 657 and 2959 ultraviolet sensitive photoinitiator on six different cell populations used for engineering various tissues. Williams found photoinitiator 2-

hydroxy-1-[4-(hydroxyethoxy) phenyl]-2-methyl-1-propanone (Irgacure® 2959) caused minimal toxicity [159].

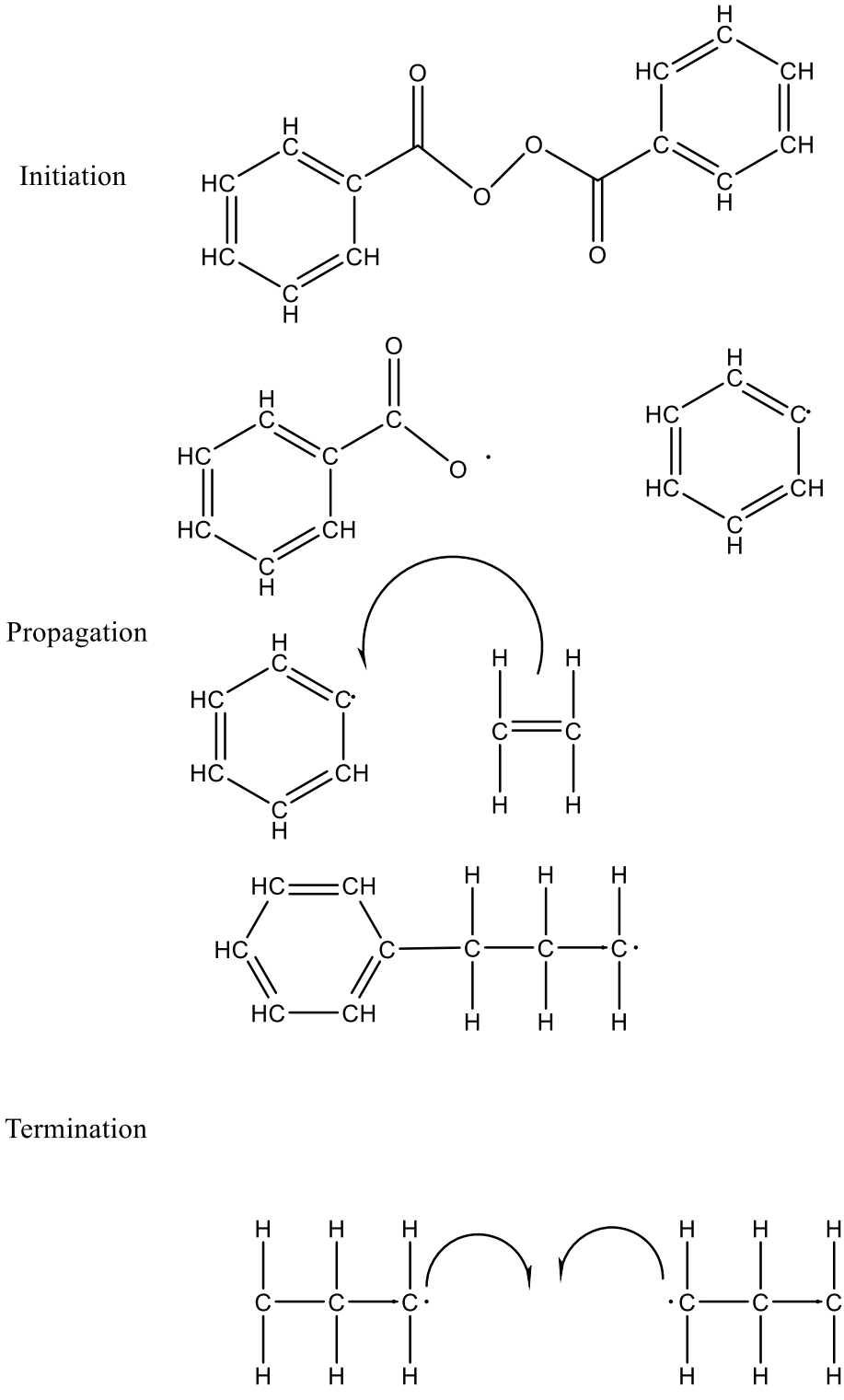

Figure 1-11: A summary of photo-induced polymerisation reaction which occurs when a photochemical event produces a reaction's initiation step.

1.12. Introduction to sterilisation

Sterilisation is one of the fundamental processes implemented during the production of all medical devices. The rationale for this particular process is to render the products free of microbial contamination. Organisms can be removed *via* filtration, whereas the destruction or inactivation of viable organisms can be accomplished by exposing them to dangerous conditions or by destroying the cell structures that are essential for life. However, it is not possible to directly measure the sterility of a material or product, but if the conditions of the sterilisation process are defined, then validations can be carried out with indicators, or they can be performed physically [160]. Sterilisation has become increasingly complicated due to the requirements of preventing patients from being exposed to infections caused by viable organisms on the implantable materials during their care. The three primary methods of sterilisation are autoclaving, ethylene oxide (EtO) and radiation, each having their advantages and disadvantages.

Autoclaving is a method that involves exposing the materials to saturated steam under high pressure at 121 °C for 15-20 minutes. The benefits of this system are efficiency, speed and low cost. However, most implants that are non-metallic, such as polymers, are limited due to their melt temperature. Therefore, they cannot be sterilised by this method.

A more common process to sterilise implantable materials is EtO, which is sensitive to temperatures higher than 60 °C. These low temperatures make it an appealing process for polymer-based systems. EtO is a process that lasts for at least 3 hours and involves temperatures between 30 °C and 60 °C. EtO can eliminate all known fungi, bacteria, viruses and spores and is compatible with most medical devices. EtO is only recommended when it is pharmaceutically necessary due to the known potential of EtO for genotoxic carcinogenicity. However, EtO is still the most common sterilisation method, used for over 70% of total sterilisations [161]. Radiation sterilisation involves ionising radiation, which is divided into gamma and electron-beam radiation. Gamma radiation uses Cobalt (60) and Cesium (127) radioisotopes, while electron-beam radiation uses high-energy electrons. In recent years, electron-beam radiation has become popular mainly due to the enhancement of accelerator technology, which brought with it a lower cost per kilowatt, advances in radiation chemistry and the availability of polymer formulations designed for the process [161].

1.12.1. Electron beam processing

Electron beam processing was first established in the 1950s. Electron beam processing is commonly used in radiation chemistry and it can be used to improve polymer formulations [162]. Currently, radiation processed products are being used in healthcare, food preservation and polymer-based industries. Electron beam radiation is a form of ionising energy that is usually classified by its low penetration and high dosage rates. The beam consists of a highly charged, concentrated stream of electrons generated by the acceleration and conversion of electricity. Electrons are produced by equipment referred to as accelerators [162]. There are two methods to measure the radiation, depending on whether the radiation is coming from a radioactive source or the radiation dose is absorbed by an object. A different unit of measure is used depending on what method is being measured. For example, the amount of radiation being given off, or emitted, by a radioactive material is measured using the conventional unit curie (Ci), named after Marie Curie, or the alternative SI unit becquerel (Bq). In contrast, the radiation dose absorbed by an object is measured using the conventional unit rad or the SI unit gray (Gy). Dose rate is the term used for the amount of ionising radiation delivered per unit time during an irradiation process.

The interaction of high energy electrons with condensed materials is dependent on both the kinetic energy of the electrons and the atomic composition of the irradiated materials. An atom emits radioactivity when the nucleus is breaking down to reach a nonradioactive (stable) state. This happens when the nucleus has too many particles, too much energy, or too much mass to be stable. When an object is exposed to radiation, energy is deposited in the material. This energy is called the absorbed dose and is measured using the conventional rad or the SI Gy. The rad, which stands for radiation absorbed dose, used to be the conventional unit of measurement, but the kilogray (kGy) has replaced it [163].

1.12.1.1. Electron beam irradiation effects on polymers

Exposing a polymer to electron beam irradiation can result in some physical and chemical modifications. The process of interaction for high-energy electrons with the material can be divided into three primary events:

1. *Ionisation:* The electron transfers its energy to the bonding electron in the absorbing polymer, after that the electron is knocked out. This event only takes place when the transferred energy during the interaction is higher than the bonding energy of the bonding electron. The ionised molecule separates into a free-radical ion at approximately the same time.
2. *Excitation:* This causes the movement of electrons from the ground state to the excited state. Eventually, the excited molecule dissociates into free-radicals.
3. *Capture of Electron:* This is also an ionisation process where the molecules can capture electrons with lower energy. As a result, the ion can dissociate into a free-radical and a radical ion.

Apart from the primary reactions, some secondary reactions occur in which ions, or excited molecules take part. The primary and secondary fragmentations, radicals are produced that can initiate a free-radical process leading to polymerisation, cross-linking, backbone or side-chain scissions, structural rearrangements and so on. These molecular changes within the polymer matrix can result in the following changes: embrittlement, loss of elongation, recrystallisation, increased free-radical content and peroxide levels, acid formation or pH shifts, consumption of radiation stabilising additives, generation of volatiles and extractable changes in hardness, colour, density, molecular weight, flexural properties, modulus and tensile strength [164]. The three fundamental responses of polymeric materials to the electron beam are:

1. Cross-linking – the formation of an insoluble material.
2. Neutral – little to no effects on mechanical properties.
3. Scissoring – the lowering of the molecular weight of a material.

1.12.1.2. Cross-linking and chain scission

Polymers exposed to electron beam irradiation experience chain scission and cross-linking. However, only one or the other can predominate, which is illustrated below in Figure 1-12. The structure of polymers often decides the preponderance of one process over another. Cross-linking is where intermolecular bonds link one polymer chain to another, which results in the formation of 3-dimensional networks. The degree of cross-linking is proportional to the radiation dose. Cross-linking can enhance the mechanical, thermal and chemical properties, environmental and radiation stabilities.

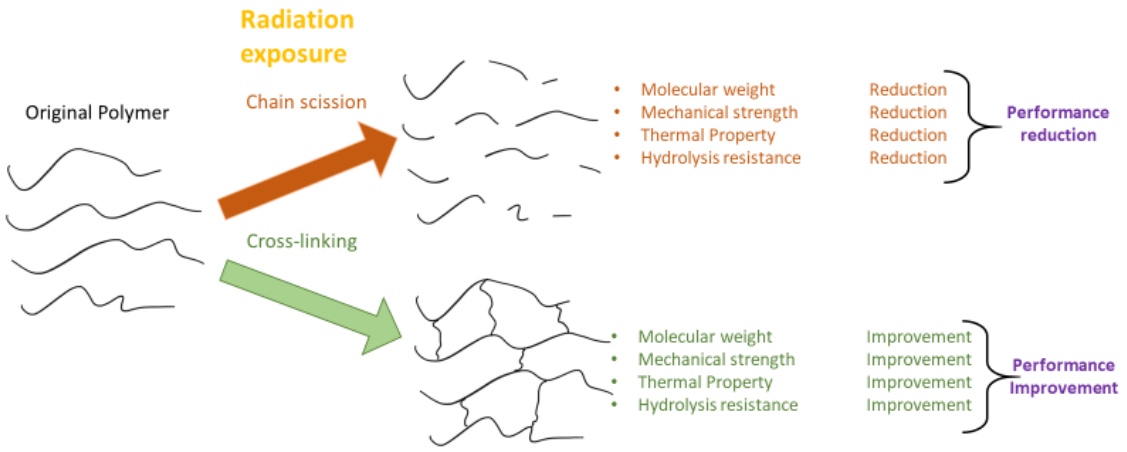

Figure 1-12: Overview of cross-linking and chain scission due to electron beam processing [165,166].

Chain scission is usually an undesirable effect, especially for medical polymers, as it can reduce polymer molecular weight and mechanical properties. In addition, the chain scission process minimises both strength and stiffness, lowers fatigue and the ability to elongate and weaken adhesive bonds. This process is initiated when polymer radicals react with oxygen to form peroxy radicals, which subsequently chain propagate, chain branch and eventually terminate the chain reaction [167].

1.13. Polymers used in this study

1.13.1. *N*-Vinylcaprolactam

N-Vinylcaprolactam (NVCL) is a monomer that has the ability to change its hydrophilic and hydrophobic behaviour. This is due to the carboxylic and amide group (ring-like structure). The amide group is connected to a vinyl group, which allows the monomer to be hydrophobic. The polymerisation occurs through the vinyl group, which indicates that the backbone of the polymer is a vinyl type [168,169]. PNVCL polymer is soluble both in polar and non-polar solvents, such as water (below 31 °C), alcohols, DMF, DMSO, tetrahydrofuran (THF), p-dioxane, chloroform and dichloromethane.

1.13.2. Poly (*N*-Vinylcaprolactam)

The corresponding polymer of NVCL is poly (*N*-vinylcaprolactam) (PNVCL). The first published research of the monomer was reported in 1968 [170]. In reviewing the literature, research into the use of PNVCL remains low, compared to poly *N*-isopropylacrylamide [60]. PNIPAm and PNVCL both have the LCST in the physiological range [171]. PNVCL is a temperature stimulus polymer that makes the transition from the hydrophilic to a hydrophobic state, with increasing temperature [168]. PNVCL is considered advantageous over PNIPAm due to its low toxicity levels, allowing PNVCL to be biocompatible and suitable for *in vivo* applications [60,170].

PNVCL has a broad LCST range (31-38 °C), which is primarily because this parameter is dependent on polymer concentration and molecular weight which would explain the slight variation in the literature [172,173]. One of the main areas of research is the development of PNVCL based systems for drug delivery. A number of PNVCL based systems for drug delivery have been developed over the past decade, such as micelles, nanoparticles, micro/nanogels, hydrogels, microspheres and beads.

1.13.3. Vinyl acetate

Vinyl acetate monomer (VAc) and its corresponding polymer polyvinyl acetate (PVAc) is a biocompatible and biodegradable polymer that is widely used in pharmaceutical and biotechnical applications, including drug carriers and tissue engineering. PVAc is a ductile material that can be synthesised *via* free-radical polymerisation. PVAc polymers that contain functional groups such as carboxylic acid (COOH) usually show excellent biocompatibility in contact with blood, body fluids and tissues. Several research studies have shown that PVAc improves the blood compatibility of some polymers [174].

Alhusein *et al.* (2013) reported that the incorporation of VAc encourages the controlled release of the antibiotic tetracycline. This has proved useful for potential applications in wound healing and especially useful in complicated skin and skin-structure infections [175]. Kermagoret *et al.* (2014) successfully copolymerised NVCL for the first time in a controlled manner with hydrophilic *N*-vinyl amide or hydrophobic vinyl ester monomers to precisely tune up and down the LCST of the resulting copolymers [176].

1.13.4. Poly (ethylene glycol)/poly (ethene oxide)

Poly (ethylene glycol) (PEG), otherwise known as poly (oxyethylene) (PEO), was first approved over two decades ago for the use of therapeutic products. The first PEG-protein products are now on the market (Adagen®, Oncospar®, Pegasys and PEG-Intron®) [177]. Peg-Intron is used to treat chronic hepatitis C in adults. PEG is a highly investigated polymer for the alteration of biological macromolecules for various pharmaceutical and biotechnical applications [177]. The properties that account for the success of PEG in biomedical applications are its non-ionic properties, hydrophilicity, decreased interaction with blood and high biocompatibility [178]. The success of PEG in applications such as drug delivery has led to other uses in the medical field, such as cardiovascular devices [179]. PEG is a polyether compound with hydroxyl groups and which is available over a wide range of molecular weights. PEG is also available with different geometries such as branched and star [177].

1.14. Reviewing Poly (*N*-vinylcaprolactam)

Polymerisation in bulk of PNVCL results in high molecular weight polymers. However, to achieve a lower molecular weight of PNVCL, chain transfer agents (CTA's) are simply added to the mixture. Allylbenzene and Mercaptopropionic acid have been used to alter the molecular weight of PNVCL from 24,000 to 59,000 g/mol. Until recently, controlled free-radical polymerisation of NVCL was only reported by reversible addition-fragmentation chain transfer (RAFT) polymerisation achieving for PNVCL, which resulted in M_n from 18,000 to 150,000 g/mol. The importance of controlling molecular weight for PNVCL relies on the fact that the phase transition properties of PNVCL is reported to be molecular weight dependent [23].

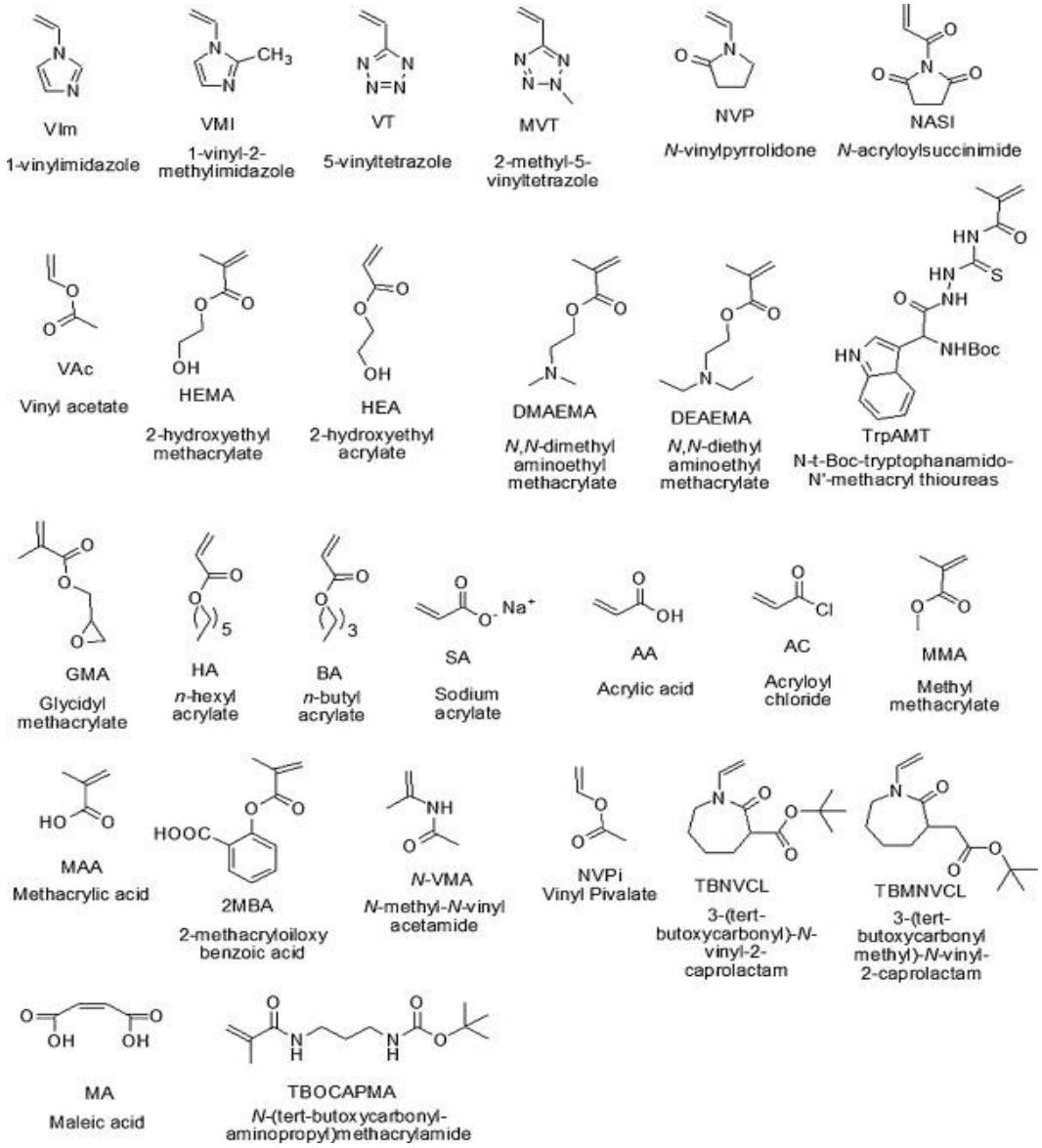

Figure 1-13: Chemical structures of monomers that were copolymerised with NVCL [23].

In the 2000s the phase transition of PNVCL was further studied. It was established that PNVCL displayed a Type I behaviour which represented the "classical" Flory–Huggins miscibility behaviour: by increasing the molecular weight of the polymer, the position of the phase transition temperature shifts toward lower polymer concentration. In the case of infinite molecular weight, the phase transition temperature is characterised by a limiting polymer concentration [23,180,181]. PNVCL phase transition can also be altered by introducing hydrophilic or hydrophobic segments to the polymer chain while adding new properties to the polymer. Figure 1-13 illustrates all current monomers that are copolymerised with PNVCL. Copolymers have the ability to change the phase transition temperature of PNVCL. Generally adding a hydrophobic segment to the

polymer chain can decrease the overall hydrophilicity and shift the PNVCL phase transition towards lower temperatures. Likewise, the incorporation of the hydrophilic segment to the polymer chain can increase the overall copolymer hydrophilicity and its phase transition. For example, for PNVCL-*b*-PEG copolymers, the LCST was increased from 33 to 39 °C when the hydrophilic block length was increased.

In 1996 the first report of a covalently cross-linked hydrogel, based on PNVCL was published where all other previous reports were on physical gels of PNVCL. Different methods were used to synthesise these types of hydrogels, including free radical polymerisation, free radical cross-linking and photopolymerisation. The most common type of initiators used to react the NVCL chains are 4,4′-azobis(isobutyronitrile) (AIBN), aliquat persulfate, azobis-4-cyanovaleric acid, photo-initiator Irgacure® 2959 and photo-initiator Irgacure® 184 [23].

Gaballa *et al*. (2013) prepared a number of copolymers by photopolymerisation: NVCL/AA, NVCL/MAA, NVCL/AA/DMAEMA and NVCL/MAA/DMAEMA. All copolymers form physically cross-linked hydrogels. NVCL/AA and NVCL/MAA exhibited a similar phase transition in water; however; at pH 1.2 and pH 6.8 the phase transition changed to 25.6 °C and 29.2 °C respectively [182].

Çakal *et al*. (2012) prepared chemically cross-linked NVCL copolymeric hydrogels with both basic DEAEMA and acidic itaconic acid (IA) comonomers. Conventional free radical cross-linking polymerisation at 60 °C using AIBN as an initiator for 24 hours was used. In the case of DEAEMA containing hydrogels, the cross-linker was varied from EGDMA to allyl methacrylate (AMA) to test their effect in hydrogel properties. The highest equilibrium swelling and lowest percent gelation were observed for the hydrogel without DEAEMA. While in the case of the IA containing hydrogels, the incorporation of IA will reduce the gelation of the hydrogels [183].

Many types of PNVCL based carriers for drugs have been developed over the past number of years, such as micelles, nanoparticles, hydrogels, microspheres and beads. In Table 1-6 shows examples of preparation methods for PNVCL-based systems developed for drug delivery.

Poly (MMA-*co*-NVCL) copolymeric nanoparticles were loaded with the lipophilic drug etoposide. The addition of the high molecular weight drug to the copolymeric nanoparticles proved to be successful with a 35–67 wt% drug entrapment concerning the copolymer. It was observed that, as the PNVCL content in the copolymer

increases, there was an increase in particle size, accompanied by a decrease in molecular weight and encapsulation efficiency of etoposide [184].

Table 1-6: Preparation methods and examples of drug molecules incorporated into PNVCL systems using different polymerisation techniques [23].

Copolymer	Method of synthesis	Drug-loaded
Poly (chitosan-*g*-NVCL)	Graft polymerisation	Ketoprofen
PNVCL-*b*-PEG	Free radical polymerisation	5-Fluorouracil
Poly (NVCL-*co*-itaconate)	Free radical polymerisation	Farmazin
Poly (NVCL-*co*-VAc)	Free radical emulsion polymerisation	5-Fluorouracil
Poly (NVCL-*co*-NIPAAm)	Free radical emulsion polymerisation	Ciproflaxin
Poly (NVCL-*co*-MAA)	Free radical polymerisation	Insulin
PDEAEMA-*b*-PNVCL-*b*-PDMAEMA)	RAFT polymerisation	Metronidazole

1.14.1. Outlook and perspectives for poly (*N*-vinylcaprolactam)

PNVCL was selected for study based upon its known biocompatibility, phase transition properties and price. Over the past decade, PNVCL has been suggested for use in some biomedical applications such as drug delivery and tissue engineering. However, for a material to be deemed suitable for these applications, the material must be sterilised; however, there is no information on sterilisation of PNVCL on commercial-scale equipment. To date, much research has been carried out on the synthesis and characterisation of novel temperature-responsive polymers to alter the LCST in the physiological range. However, no research has focused on the effect of melt processing and how this process may affect LCST behaviour. The ability to melt process a smart material for use in drug delivery may lead to the development of novel drug carrier systems.

PNVCL is a versatile polymer whereby the phase transition can be modulated by tuning its molecular weight, chemical composition and solution concentration. With current research developing a controlled polymerisation method, PNVCL based materials are chosen to control the phase transition and allow for the development of complex drug delivery systems with loading and release of functional molecules triggered by temperature. Moreover, several papers demonstrate that PNVCL is not toxic. Although PNVCL is not yet FDA approved, the increasing number of reports showing its

applicability in drug delivery (e.g., cancer treatment) and tissue-engineering precludes, suggesting that its approval is a matter of time [23].

There are also some limitations of PNVCL based materials that need to be studied and overcome. For example, PNVCL polymers are currently being reported mainly as potential drug delivery systems. However, numerous drugs are introduced in the presence of the toxic monomer before free radical polymerisation. Although PNVCL is reported as non-toxic, NVCL is toxic and exposing a drug to toxic monomers and a free radical process is not ideal for a drug delivery system. One way to overcome this is by HME, whereby introducing the drug during the melt process step which is a widely accepted method to incorporate drugs into a polymer.

Overall, advancing methods of PNVCL polymer synthesis and characterisation will help achieve a much more in-depth understanding of PNVCL based materials and enrich the pool of potential applications in the future.

Chapter 2:

Materials and methods

2. Materials and Methods

2.1. Material selection

Previous work performed in our laboratory involved the synthesis of novel temperature-responsive polymers and pH-sensitive hydrogels with a controllable response [182,185]. The primary material in this study is a temperature-responsive monomer, *N*-Vinylcaprolactam (NVCL). *N*-Vinylcaprolactam was obtained from Sigma-Aldrich, Ireland, with a molecular weight of 139.19 g/mol and a storage temperature of 2-8 °C. Figure 2-1 below illustrates the chemical structure of NVCL.

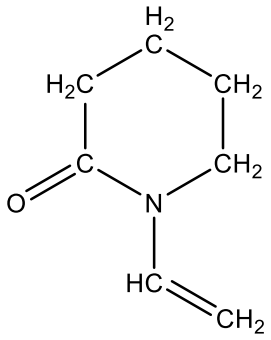

Figure 2-1: Chemical structure of *N*-vinylcaprolactam.

The second material investigated in this study was vinyl acetate (VAc), which was chosen because it is a hydrophobic monomer. It is a biocompatible and biodegradable compound that is widely used in pharmaceutical and biotechnical applications. Vinyl acetate-based polymers have been used in applications such as adhesives, paints and concrete additives to pharmaceuticals [186]. Vinyl acetate used in this study was obtained from Sigma-Aldrich, Ireland, with a molecular weight of 86.09 g/mol. In Figure 2-2, the chemical structure of vinyl acetate is shown.

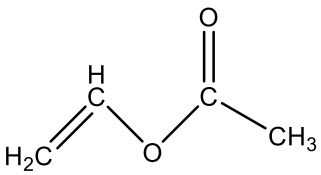

Figure 2-2: Chemical structure of vinyl acetate.

1-hydroxycyclohexyl phenyl ketone (Irgacure® 184) is a highly efficient non-yellowing photoinitiator which is used to initiate the photopolymerisation of polymers.

Irgacure® 184.was used to initiate the reaction of free-radical polymerisation, as illustrated in Figure 2-3.

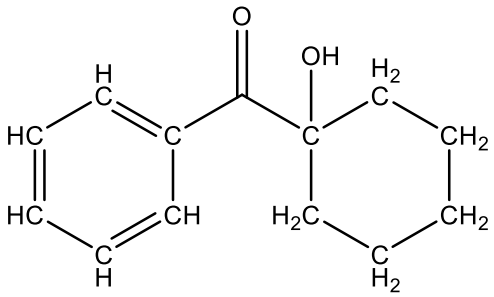

Figure 2-3: Chemical structure of 1-hydroxycyclohexyl phenyl ketone (Irgacure® 184).

Polyethylene glycol (PEG) was also selected for investigation in this study. Polyethylene glycol was obtained from Sigma-Aldrich, Ireland, with molecular weights of 600, 1,000, 2,000, 10,000 and 35,000 g/mol. Figure 2-4 shows the typical chemical structure of polyethylene glycol.

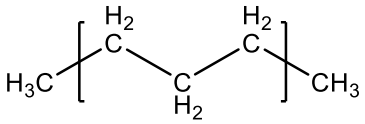

Figure 2-4: Chemical structure of polyethylene glycol.

Acetaminophen (APAP) was selected as a model drug. APAP is widely used as an analgesic pain reliever drug [187,188]. APAP is useful as a model drug candidate to examine the effects of the manufacturing processes, due to its different polymorphic forms, which may result in significant changes in the solubility and drug release rates [187]. Acetaminophen was obtained from Sigma-Aldrich, Ireland, with a molecular weight of 151.16 g/mol and has a high solubility in water (4.15 mg/mL). Figure 2-5 below exhibits the chemical structure of APAP.

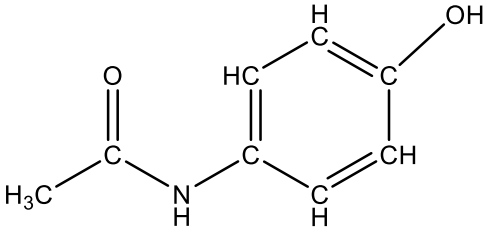

Figure 2-5: Chemical structure of Acetaminophen.

Detailed below in Figure 2-6 is a summary of the testing carried out in order to achieve the key objectives of this study.

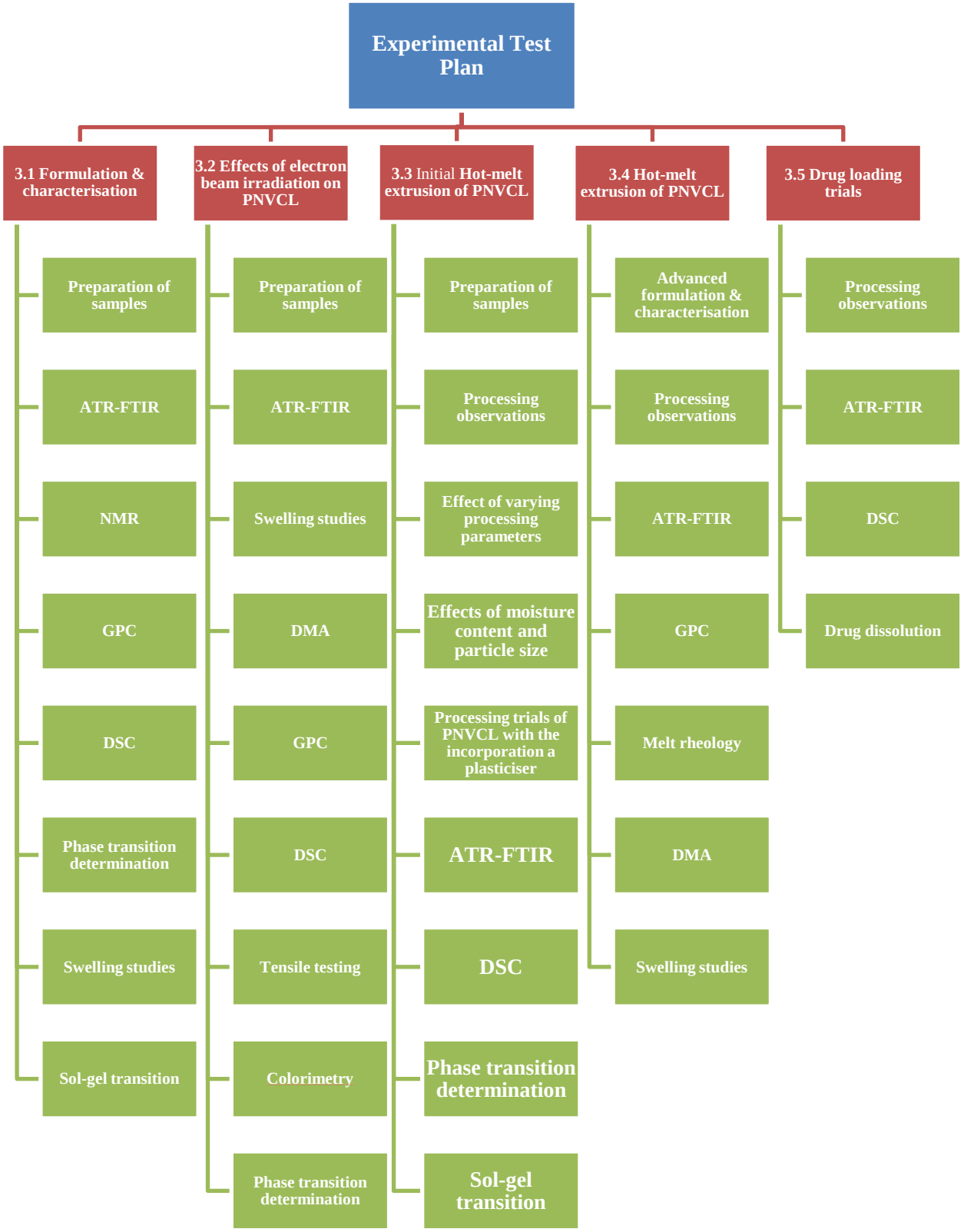

Figure 2-6: Overview of the various testing methods carried out in this study.

2.2. Photopolymerisation of samples

The polymers investigated in this study were prepared by free-radical polymerisation using ultra-violet (UV) light. These polymers were synthesised *via* physical cross-linking using a UV curing system (Dr Gröbel UV- Elektronik GmbH) (Figure 2-7). This particular irradiation chamber is a controlled radiation source, with 20 UV-tubes that provide a spectral range of between 315-400 nm, at an average intensity of 10–13.5 mW/cm^2. The prepolymerised mixtures were prepared by combining desired amounts of the monomers and 0.001, 0.05, 0.1, 1 and 5 wt% photoinitiator. The batches were placed in a 50 ml beaker and mixed using a magnetic stirrer for 20 minutes until a homogeneous mixture was achieved. The solutions were pipetted into silicone moulds that contained disc and dumbbell specimen impressions. Photopolymerisation was carried out at 15 minute intervals, where the samples were turned to ensure gels got the same level of UV exposure during the polymerisation process.

Figure 2-7: Dr Gröbel UV- Elektronik GmbH used in this study.

2.2.1. Photopolymerisation 1

Initial studies were carried out to determine the effect on the phase transition temperature of incorporating VAc monomer into NVCL, in an attempt to alter the phase transition temperature behaviour. Listed in Table 2-1 are different monomeric

compositions, which were photopolymerised using a UV chamber (Dr Gröbel UV-Electronik GmbH).

Table 2-1: Physically cross-linked samples containing 0.1 wt% of Irgacure®184 and 5, 10 and 20 wt% of VAc.

Polymer code	NVCL	VAc (wt%)	Irgacure®184 (wt%)
P(NVCL90-PEG10-1000)	100	0	0.1
P(NVCL90-PEG10-600)	95	5	0.1
P(NVCL80-PEG20-1000)	90	10	0.1
P(NVCL80-PEG20-600)	80	20	0.1

2.2.2. Photopolymerisation 2

This research was carried out to investigate the effect of HME on stimuli-responsive polymers. After extensive analysis, PEG was selected to incorporate with NVCL at different molecular weights and concentrations to enhance melt processability (Table 2-2).

Table 2-2: Physically cross-linked samples containing 0.1 wt% of Irgacure®184 and 10 and 20 wt% of PEG

Polymer code	NVCL (wt%)	PEG (M_w 1,000)	PEG (M_w 600)
P(NVCL90-PEG10-1000)	90	10	0
P(NVCL90-PEG10-600)	90	0	10
P(NVCL80-PEG20-1000)	80	20	0
P(NVCL80-PEG20-600)	80	0	20

2.2.3. Photopolymerisation 3

The polymers were prepared to determine the effects of drying and washing the polymers. Below in Table 2-3 are different monomeric compositions, which were photopolymerised.

Table 2-3: Physically cross-linked samples containing 0.01, 0.05, 0.1, 1 and 5 wt% of Irgacure®184.

Polymer Code	NVCL (wt%)	VAc (wt%)	Irgacure®184 (wt%)
PNVCL 0.01 wt%	100	0	0.01
PNVCL 0.01 wt%	100	0	0.05
PNVCL 0.1 wt%	100	0	0.1
PNVCL 1 wt%	99	0	1
PNVCL 5 wt%	95	0	5

2.2.3.1. Washing step

PNVCL samples were soaked in *N*-pentane or xylene for 3 hours after the 3 hours mark the solvent was removed and replaced with fresh solvent 3 times, followed by drying under a vacuum oven at 60 °C to constant weight, in order to extract residual monomer and other low molecular weight residues.

2.3. Processing and characterisation

2.3.1. Hot-melt extrusion conditions

2.3.1.1. Initial hot-melt extrusion conditions

Preliminary melt compounding, detailed herein, was carried out using an MP 19 TC 25 laboratory-scale co-rotating twin-screw extruder (APV Baker, Newcastle-under-Lyme, UK) having 16mm diameter screws and a length-to-diameter ratio of 35/1. All samples were dried in an oven for 3 hours at 90 °C before extruding. Screws were used in the co-rotating intermeshing mode with a long continuous mixing section made up of 30°, 60° and 90° bilobal kneading elements, to ensure a gradual change from conveying to high shear mixing throughout the study, unless otherwise stated.

Table 2-4: Profile of temperature zones used in hot melt extrusion of PNVCL during this study.

Temperature profile (°C)	Die	Zone 6	Zone 5	Zone 4	Zone 3	Zone 2	Zone 1
Profile 1	180	170	160	150	120	110	90
Profile 2	170	160	150	140	110	100	80
Profile 3	160	150	140	130	120	110	80

The mixing sections were positioned towards the die end of the extruder. The compounding temperature profile was established on the APV extruder using six temperature controllers placed along the length of the barrel. A seventh temperature controller was used to regulate the temperature at the die (Table 2-4). The RPM of the screws was maintained at such a rate to ensure that the materials were starved-fed into the feed zone of the extruder. Sample codes and screw speed used in this study are outlined in Table 2-5. The resultant melt was extruded through a die to form a strand. The extrudates were collected every 10 minutes after the start of the process to allow the extruder to purge.

Table 2-5: Sample codes for PNVCL based materials used in the initial extrusion trials.

Polymer code	NVCL (wt%)	PEG (M_w 10,000) (wt%)	PEG (M_w 35,000) (wt%)	Screw speed (RPM)
I-PNVCL 20	100	0	0	20
I-PNVCL 30	100	0	0	30
I-PNVCL 40	100	0	0	40
I-PNVCL 60	100	0	0	60
P(NVCL90-PEG10-10000)	90	10	0	20
P(NVCL80-PEG20-10000)	80	20	0	20
P(NVCL90-PEG10-35000)	90	0	10	20
P(NVCL80-PEG20-35000)	80	0	20	20

2.3.1.2. Hot-melt extrusion conditions for PNVCL

A bench-top Prism TSE, 16 mm twin-screw extruder (Figure 2-8), with intermeshing co-rotating screws, was used to prepare samples (Table 2-6). Following processing, optimised samples were extruded, with a dual temperature profile of 150 °C, in the extruder feeding area and 200 °C in the rest of the barrel and die.

Figure 2-8: Bench-top Prism twin-screw extruder used in this study.

Table 2-6: Sample codes for PNVCL based materials used in the extrusion trials.

HME Formulation	Pre-treated	PNVCL (wt%)	PEG (M_w 2,000) (wt%)	Screw speed (RPM)
W-PNVCL 50	Washed (W)	100	0	50
W-PNVCL 100	Washed (W)	100	0	100
W-PNVCL 150	Washed (W)	100	0	150
UW-PNVCL 50	Unwashed (UW)	100	0	50
UW-PNVCL 100	Unwashed (UW)	100	0	100
UW-PNVCL 150	Unwashed (UW)	100	0	150
W-PNVCL90-PEG10	Washed (W)	90	10	100
W-PNVCL80-PEG20	Washed (W)	80	20	100
UW-PNVCL90-PEG10	Unwashed (UW)	90	10	100
UW-PNVCL80-PEG20	Unwashed (UW)	80	20	100

2.3.1.3. The incorporation of a model drug

The melt processability of PNVCL and a model drug was investigated on a Prism TSE, 16 twin-screw extruder. Samples used for this study were dried for 3 hours at 90 °C and contained PEG (Table 2-7).

Table 2-7: Sample code of PNVCL and APAP.

HME Formulation	PNVCL (wt%)	PNVCL80/PEG20 (wt%)	APAP (wt%)	Screw speed (RPM)

PNVCL	100	0	0	100
PNVCL 90-APAP10	90	0	10	100
PNVCL 80-APAP 20	80	0	20	100
PNVCL 70-APAP 30	70	0	30	100
PNVCL/PEG	0	100	0	100
90(0.8PNVCL/0.2PEG)-10APAP	0	90	10	100
80(0.8PNVCL/0.2PEG)-20APAP	0	80	20	100
70(0.8PNVCL/0.2PEG)-30APAP	0	70	30	100

2.3.2. Vacuum packing

Vacuum packing was conducted on unprocessed PNVCL and P(90 NVCL-10VAc). In this work, only the tensile specimens, disc and granules were vacuum packed. Vacuum packing was performed to ensure the samples were contained in a controlled environment at room temperature. The sample size, weight and orientation remained the same for all samples to facilitate consistency during the electron beam irradiation process.

2.3.3. Electron beam irradiation

Electron beam irradiation was carried out in STERIS Applied Sterilization Technologies by Mr Olivier Vrain, the work was supported by Dr Kieran Murray form CelgenTek part of the Zimmer Biomet Group. A MEVEX high energy electron beam irradiator was used to irradiate vacuum-packed PNVCL and P(90 NVCL-10VAc) ASTM testing specimens, disc and granules, at doses of 5, 25 and 50 kGy. The dose rate was approximately half of the total kGy per pass on each side to accomplish a uniform irradiation dose at room temperature. All samples were exposed for approximately 5 s per pass. The period between the first and second pass was between 250 and 260 s. Each of the aforementioned times was calculated and evaluated by STERIS Applied Sterilization Technologies personnel. All samples were irradiated at room temperature at the STERIS facility (Tullamore, Ireland). The non-irradiated samples served as a baseline for each of the results.

2.3.4. Preparation of aqueous solutions

Homogeneous solutions of the samples were prepared by weighing appropriate amounts of the PNVCL based samples and distilled water, leaving these mixtures at room temperature until completely dissolved. These aqueous solutions were produced for subsequent use in LCST measurements.

2.3.5. Particle size analysis

The particle size of the PNVCL based samples was measured using mechanical sieving. Approximately 100 g of granulated extrudates for each sample were loaded on a stack of sieves with 9 aperture sizes: 3350, 2000, 1000, 850, 420, 220, 125, 63 and 32 µm (Endecott test sieve shaker, Endecotts Ltd.). Each of the samples were subjected to agitation for 5 min.

2.4. Characterisation methods

2.4.1. Differential scanning calorimetry

2.4.1.1. Thermal analysis of polymers

Differential scanning calorimetry studies were performed using a differential scanning calorimeter (TA Instrument DSC 2920) (Figure 2-9). The DSC was calibrated with indium as standard. The samples had a dry weight of between 8-12 mg and sealed aluminium pans were used to contain them for the DSC experiment. All samples were examined under a pure nitrogen atmosphere, and each one of them was ramped from 20 °C to 200 °C at a rate of 10 °C/min.

2.4.1.2. Thermal analysis of aqueous polymer solutions

Aqueous polymer solutions were examined under a pure nitrogen atmosphere. All samples were ramped from 10 °C to 60 °C, at a rate of 1 °C/min using a similar technique as described in the previous section. The results were plotted as a function of heat flow (W/g) against temperature (°C).

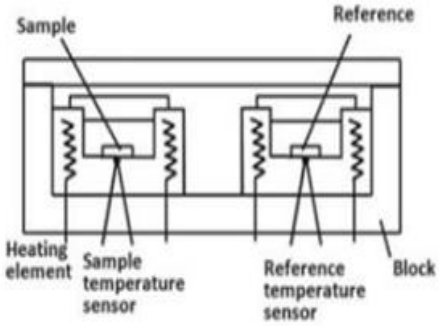

Figure 2-9: TA DSC 2920 used in this study (left-hand side) and schematic diagram of DSC (right-hand side).

2.4.2. Attenuated total reflectance Fourier transform infrared spectroscopy

Attenuated total reflectance Fourier transform infrared spectroscopy (ATR-FTIR) was carried out on a Perkin Elmer Spectrum One (Figure 2-10), fitted with a universal ATR sampling accessory. All data was recorded at room temperature (< 20 °C), in the spectral range of 4000-650 cm^{-1}, utilising a 10 scan per sample cycle and a fixed universal compression force of 80 N. Subsequent analysis was performed using Perkin Elmer Spectrum software. The procedure used to treat the spectra was baseline correction and smoothing of the spectra. For spectra normalisation OriginPro 7.5 software was used.

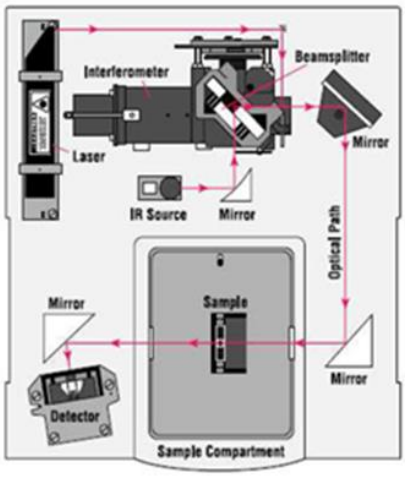

Figure 2-10: Perkin Elmer Spectrum One ATR-FTIR used in this study (left-hand side) and schematic diagram of FTIR (right-hand side).

2.4.3. Nuclear magnetic resonance

Nuclear magnetic resonance (NMR) was carried out in the Conway Institute, University College Dublin by Professor Wenxin Wang. 1H NMR was conducted on a 300 MHz Bruker NMR with the MestReNova processing software. The chemical shifts were referenced to the lock chloroform (CDCl3, 7.26 p.p.m.).

2.4.4. Swelling studies

After photopolymerisation, the samples were placed in a vacuum oven for 24 hours, at 40 °C and the apparent dry weights (Wd) were measured. The samples were tested at temperature (< 20 °C) and (40 °C), below and above the LCST. Samples were placed in 50 ml of distilled water to determine the swelling ratio of the samples. The percentage of gel swelling was calculated using Equation 2-1. All reported swelling studies were measured in distilled water. Tests were carried out in triplicate below and above LCST and the data was presented as mean ± SD.

Swelling Ratio (%) = ((Wt-Wd)/Wd)*100 Equation 2-1

Where Wt and Wd are the weights of the gels in the swelled state and the dry state, respectively.

2.4.5. Rheology

2.4.5.1. Melt Rheology

The rheological properties of PNVCL samples were studied using the Discovery Hybrid Rheometer 2, with an oven heating assembly (DHR-2, TA Instruments) (Figure 2-11). The samples were placed in between two flat plates of 25 mm diameter after calibration of the zero gap. For the analysis of pure polymer, a frequency sweep was conducted at 180-200 °C in increments of 10 °C and the plots of resultant viscosity versus angular frequency were generated. Controlled strain at 2 %, was used for melt rheology, which was within the linear viscoelastic region of all the samples as obtained following an amplitude sweep. All measurements were carried out in duplicate

Figure 2-11: Discovery Hybrid Rheometer 2, with oven heating assembly.

2.4.5.2. Rheological testing for phase transition

Dynamic rheological tests were conducted on aqueous polymer solutions, with an Advanced rheometer AR 1000 (TA Instruments) fitted with a Peltier temperature control (Figure 2-12). The instrument was calibrated for inertia and mapped before use in all cases. The geometry used in this analysis was a 4 cm diameter cone steel plate. Aqueous polymer solutions of 1.5 mL were pipetted onto the Peltier plate. The sample gap was set at 0.5 mm for the studies carried out. To determine the phase transition temperature of the selected sample solutions, temperature ramp tests were performed. In this study, the storage modulus (G′) and loss modulus (G″) were examined with a change in temperature from 20-50 ºC at the rate of 1 ºC/min. Tests were conducted at 0.5 %, control strain, which was within the linear viscoelastic region of the samples. All measurements were carried out in duplicate.

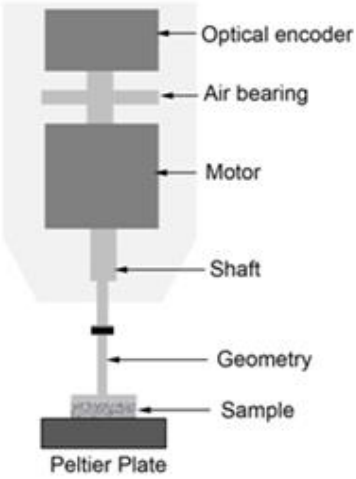

Figure 2-12: Advanced Rheometer AR 1000 (left) used in this study and schematic diagram typical for rheometry (right).

2.4.6. Gel Permeation Chromatography

Gel permeation chromatography was carried out using a PL GPC-120 system with a refractive index detector and a PLgel 5 μm MIXED-D columns (300 × 7.5 mm) with a guard column fitted. The GPC was set to a flow rate of 0.5 ml per minute. The system was allowed to equilibrate at 40 °C for 24 hours, with chloroform circulating before the test took place. Agilent Polystyrene standards were used as reference standards, with a range from 3,000,000 g/mol to 162 g/mol.

2.4.7. Dynamic mechanical analysis

Dynamic mechanical analysis (DMA) measurements were performed on PNVCL samples with a TA Instruments DMA Q800. Samples with dimensions of 35×6×3 mm were clamped in the instrument using a dual cantilever. Each of the samples was heated from 20 °C to 160 °C at a rate of 3 °C/min while using the multifrequency strain mode. A constant frequency of 1Hz was applied, while a strain rate of 0.1 % was used to calculate the viscoelastic behaviour of the samples regarding the storage modulus (E′), loss modulus (E″) and tan delta (tan δ). All measurements were carried out in duplicate.

2.4.8. Particle size

Two different methods were used to reduce PNVCL particle size, the first was with the aid of a Colortronic granulator and a planetary mono mill Fritsch PULVERISETTE 6. The granulator was used to turn PNVCL dices into granules. To turn the PNVCL granules into powder, samples were placed inside an egg-shaped stainless steel vial using a Fritsch Pulverisette 6 mixer with zirconia balls as the milling media for 5 minutes at 600 RPM.

2.4.9. Hardness testing

A type D shore durometer was employed to test 6 disc samples of equal thickness from each batch on a flat anti-vibration bench. Each of the samples was stored at room temperature for 24 hours before testing while the experiment was performed at room temperature conditions also. This experimental procedure involved raising the stage that contained the sample up to the indenter for a period of 30 seconds. After this time elapsed the result from the digital readout was recorded. Each result was noted (D scale) and the average was calculated for each batch. Ten tests were carried out for each sample, with the mean calculated from each of the ten results. The results provided information on the hardness of the samples before and after irradiation.

2.4.10. Tensile testing

Tensile testing of the non-irradiated and irradiated PNVCL and P(90 NVCL-10VAc) ASTM dumbbell specimens was performed to measure the tensile strength, Young's modulus and percentage elongation at break. The samples were synthesised to dimensions of 33 mm (length of the narrow section) × 6 mm (width of the narrow section) × 3mm (overall thickness) and had an overall length of 115 mm. The experiment was carried out per ASTM D638-03 while implementing a crosshead speed of 50 mm/min. An Instron 3365 (Instron Ltd, UK) (Figure 2-13) universal testing machine was employed to conduct each experiment, where a 5kN load cell was applied during the experiments, with a gripper distance of 40 mm from each other. Five tests were executed for each dose range, with the mean calculated from each of the five results.

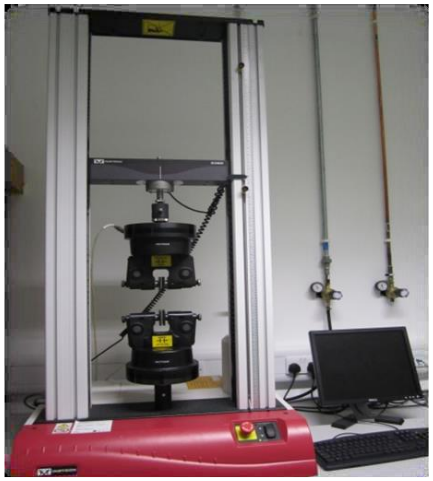

Figure 2-13: Instron tensile tester used in this study.

2.4.11. Moisture Analysis

In accordance with ISO/DIS 12418-2 standards, a known quantity of sample was placed into a Mettler Toledo moisture analyser. Once the sample was evenly spread across the aluminium pan, the test was started. The moisture analyser heated the sample to a pre-set temperature of 130 °C. As the samples were being heated, the water present was evaporated and the moisture content was determined by the mass loss from the sample. All measurements were carried out in triplicate. The Mettler Toledo moisture analyser used in this research is displayed in Figure 2-14.

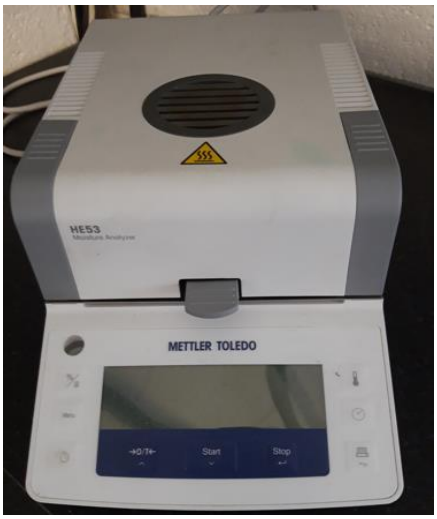

Figure 2-14: Mettler Toledo moisture analyser used in this study.

2.4.12. Colourimetry

Colour measurements were performed according to ASTM D 1925 using a Lovibond RT600 sphere spectrophotometric colourimeter (Figure 2-15). Calibration was conducted on the instrument before testing using a calibration unit that was provided with the equipment (L = 94.91, a = −1.01, b = +0.09). All samples were stored in a dark area at room temperature for one week following irradiation before being tested. Five tests were performed on each sample from the different materials. Each test provided values for Hunter L (black (0) to white (100)), Hunter a (green (−) to red (+)) and Hunter b (blue (−) to yellow (+)). The overall colour difference (ΔE) was established by implementing a statistical analysis of the ΔE values for L, a, and b. ΔE was calculated by using the following equation:

$$\Delta E = \sqrt{(\Delta L)^2 + (\Delta a)^2 + (\Delta b)^2} \qquad \text{Equation 2-2}$$

ΔE is expressed as the difference between the control sample and the irradiated sample colour values. Ten tests were carried out for each sample, with the mean calculated from each of the ten results.

Figure 2-15: Lovibond RT600 sphere spectrophotometric colourimeter used to quantify the colour difference in this study.

2.4.13. Cloud point measurement

The LCST of polymer solutions can be determined by using a visual cloud point method. A sealed glass test tube, with a 75 mm path length, was filled with selected polymer solutions and placed in a thermo-stable bath. The temperature was increased manually, at a rate of less than 1 °C per 2 minutes, after the temperature reached a few degrees below the pre-estimated cloud point temperature. The LCST was recorded at the temperature at which the sample began to show initial signs of becoming turbid. All measurements were carried out in triplicate.

2.4.14. High-performance liquid chromatography

The concentration of APAP was determined using high-performance liquid chromatography (HPLC). HPLC analysis was carried out using a system consisting of a Waters Alliance e2695 separations module combined with a Waters 2487 dual λ absorbance detector. A 150 mm × 4.6 mm Thermo Scientific ODS Hypersil column with a particle size of 5 µm was used for separation and quantitation of the APAP content. The mobile phase was prepared according to the USP method by using HPLC grade methanol, water and glacial acetic acid in the ratio of 69:28:3. All solvents were obtained from Sigma Aldrich. The mobile phase was filtered through 0.20 µm nylon filters and degassed under vacuum. A flow rate of 2 ml/min was maintained during the procedure, the detector was set at 275 nm, and the samples injection volume was 20 µL. A filtered solution of acetonitrile and water 1:1 was used to wash the needle between injections. A calibration graph for acetaminophen was obtained by plotting the peak area versus concentration and the corresponding regression equation was used to calculate the concentration of the unknown. The release profile was then observed from a plot of time versus cumulative release (%). The extrudate weight was maintained consistently at 1.00g, with the sample dimensions approximately 3.5cm length, by 2mm wide and a thickness of 4mm.

2.4.15. UV-spectroscopy

The LCST behaviour of samples was also investigated using a UV-spectroscopy synergy HT BioTek plate reader (Figure 2-16). The transmittance of samples in aqueous polymer solutions was measured at 500 nm, at intervals of 1 ºC in the range of 25-44 ºC.

The solution was allowed to equilibrate at each temperature for 20 minutes before the transmittance was measured. All measurements were carried out in triplicate.

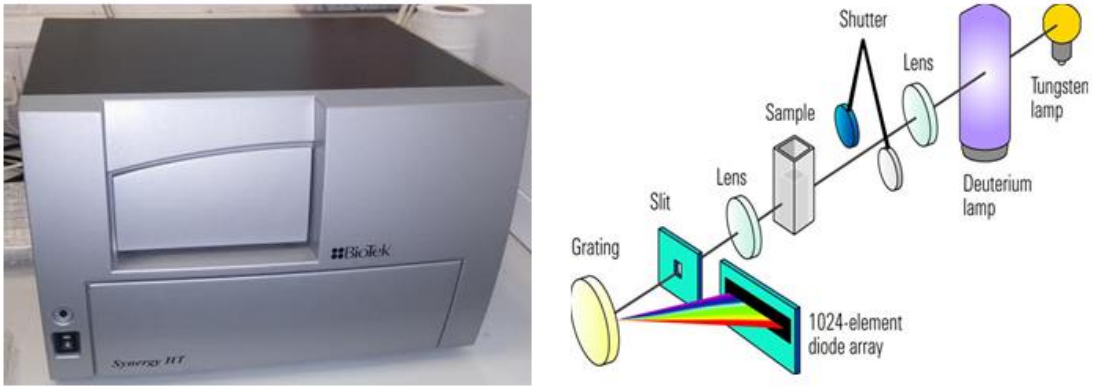

Figure 2-16: UV-spectroscopy Synergy HT BioTek plate reader used in this study (left-hand side) and schematic diagram (right-hand side).

2.4.16. Tube inversion method

Aqueous polymer solutions (1 mL) of all samples were placed in 10 mm diameter glass tubes. Samples were kept at a constant temperature for 10 minutes in a thermostable bath, before inverting the tube at intervals of 1 °C. Before switching to the next temperature, the samples were cooled in an ice-water bath until the polymer solution became homogeneous. Gelation temperature was seen as the temperature at which the polymer solution did not flow by inverting the tube. All measurements were carried out in triplicate.

2.4.17. Statistical analysis

Statistical analysis was performed using GraphPad Prism 8. All data is presented as means ± standard deviation (SD). Data was analysed by one-way analysis of variance (ANOVA) followed by the Tukey post hoc test. P-values < 0.05 were deemed significant. Where sample size was limited to less than 3, a range of observed values are reported. Data is presented as mean± relative standard deviation (RSD) for the mechanical testing of PNVCL based samples.

Chapter 3:

Results and discussion

3. Results and discussion

3.1. Synthesis, formulation development and characterisation of temperature-responsive physically cross-linked Poly (*N*-vinylcaprolactam) based polymers

3.1.1. Preface

Stimuli-responsive polymers are known as polymers that experience moderately large and abrupt, physical or chemical changes in response to small external changes in environmental conditions [189]. Chemical stimuli, such as pH, ionic factors and chemical agents, will change the interactions between polymer chains or solvents, at the molecular level. The physical stimuli, such as temperature, electric or magnetic fields and mechanical stress, will affect the level of various energy sources and alter molecular interactions at critical onset points [190,191].

Among all stimuli-responsive polymers investigated, temperature-responsive polymer systems have received significant interest, due to the fact that temperature is a vital physiological factor in the body; some diseases manifest themselves by a change in temperature [191]. Temperature-responsive polymers have allowed for novel developments in tissue engineering [42] and drug delivery carriers [168]. Drug delivery carriers, which are based on temperature-responsive polymers, have unique characteristics such as controlling drug release rate and lowering toxicity, which results in a controlled drug delivery system [192]. Common sources of toxicity include photoinitiators and organic solvents [193]. However, improvements can be made by an optimum selection of photoinitiators as well as photoinitiator concentration, as discussed previously in Section 1.10. Stimuli-responsive polymers are useful for controlling drug release profiles and interactions with cells. Stimuli-responsive drug carriers are constructed by introducing stimuli-responsive polymers into conventional drug carrier systems.

Temperature-responsive injectable polymers are also attractive for the use of controlled drug delivery systems, where the aqueous solution of these polymers can undergo a sol-gel transition in response to a change in temperature [18]. The LCST behaviour of PNVCL can be altered by polymer concentration, the molecular weight of

the polymer and also the composition of the solution, as previously discussed in Section 1.13. [60]. In a comprehensive review, PNVCL was found to have been used in several biomedical applications, such as a matrix for microbial cell entrapment. Results showed that enzymatic activities of microorganisms decreased after cell entrapment in the PNVCL gel. Another application for PNVCL was found as a cell culture scaffold. The large pore size and high surface area of PNVCL provide excellent support for cell growth and the interconnected porosity provides better nutrient transfer for cell growth and proliferation [23].

Kermagoret *et al.* (2013) successfully copolymerised NVCL in a controlled manner with *N*-vinyl pivalate (NVPi) and VAc, which allowed the authors to precisely tune the LCST [176]. The copolymers were prepared by cobalt-mediated radical polymerisation (CMRP) using the bis-(acetylacetnato) cobalt (II) complex as a controlling agent. Wan *et al.* (2010) reported the synthesis of NVCL and vinyl acetate (VAc) block copolymers using controlled radical polymerisation *via* macromolecular design by the interchange of xanthate, *via* reversible addition-fragmentation chain transfer (RAFT) [194]. Vinyl acetate (VAc) was selected due to its hydrophobic nature and its applications, ranging from drug delivery and pharmaceuticals [186,195,196].

Although the homopolymer had been synthesised by various methods of free-radical polymerisation, this is the first study to report on the synthesis of PNVCL-VAc by free-radical photopolymerisation, using 1-hydroxycyclohexyl phenyl ketone (Irgacure® 184) to initiate the reaction [23]. An overview of the test methodologies applied are illustrated in Figure 3-1. Altering the composition of VAc has the potential to affect the phase transition, swelling, dissolution and sol-gel transition behaviour of the copolymers, which offers great possibilities for use in drug delivery systems.

The aim of this section is to synthesise smart temperature-sensitive polymers utilising a bulk polymerisation method. Processing of novel smart polymer formulations on a large scale may offer many benefits including the potential to produce smart polymers with tuneable properties.

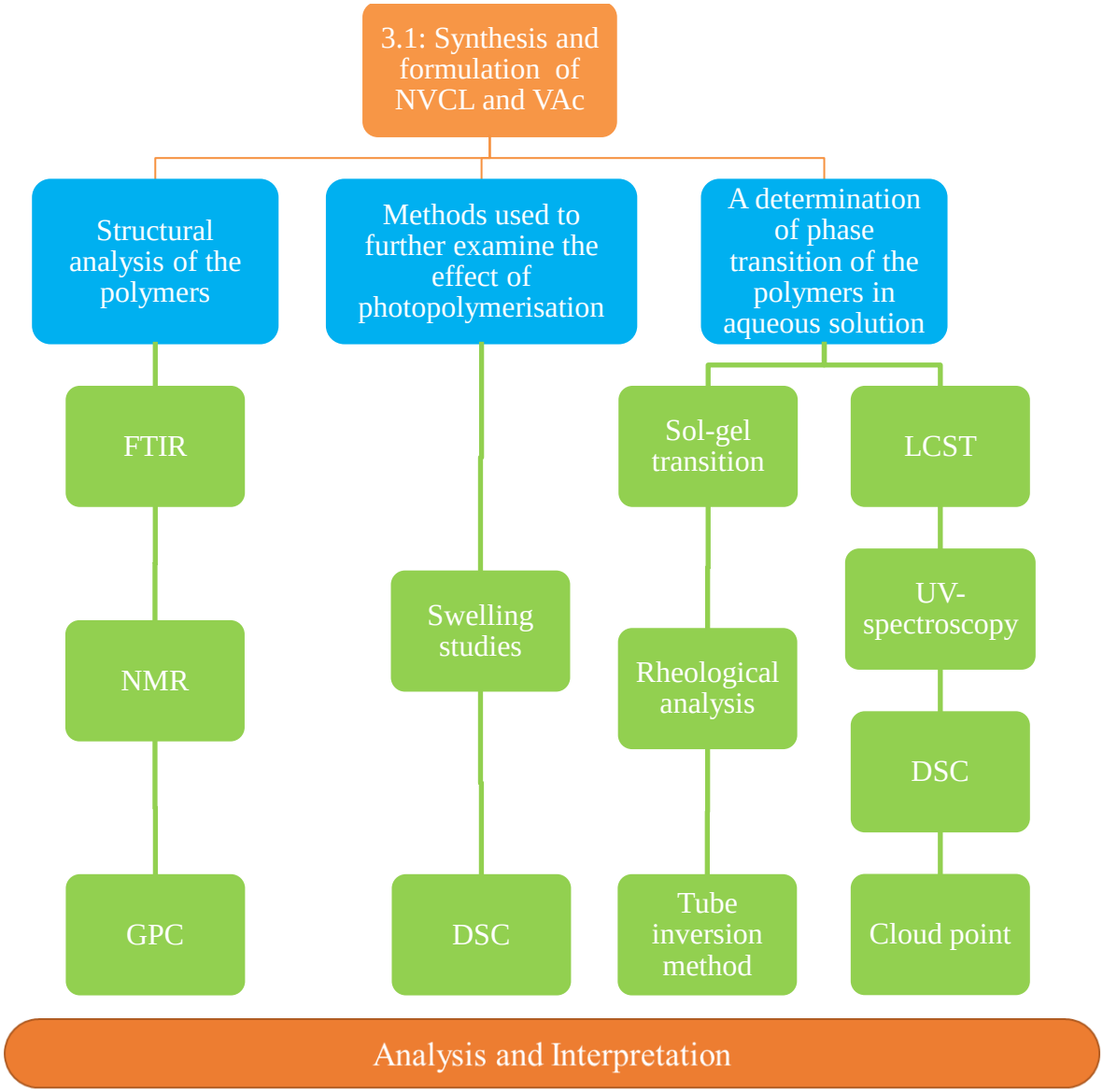

Figure 3-1: Workflow chart of work carried out in Section 3.1 of this study.

3.1.2. Preparation of samples

Smart polymers have enormous potential in various applications. In particular, smart polymeric drug delivery systems have been explored as "smart" delivery systems able to release, at the appropriate time and site of action, entrapped drugs in response to specific physiological triggers. The responses vary widely from swelling/contraction to disintegration. Synthesis of new polymers with greater biocompatibility and better biodegradability would increase and enhance current applications. The most attractive features of smart polymers arise from their versatility and tunable sensitivity. The most significant weakness of all these external stimuli-sensitive polymers is slow response

time. The versatility of polymer sources and their combinatorial synthesis makes it possible to tune polymer sensitivity to a given stimulus within a narrow range [197].

Accompanying the accelerated growth of biomedical technology, polymers that have the ability to be prepared under bio-friendly conditions are urgently needed. Ko *et al.* (2013) reported that considering biomedical applications, polymerisation involving high temperature or toxic metals should be avoided [198]. Therefore, a more appealing method of polymer synthesis, namely photopolymerisation, is considered in this study. One of the most advantageous and straightforward approaches to photopolymerisation is the bulk polymerisation method, which is used to synthesise PNVCL during a one-step process. If successful, this method could potentially produce a significant quantity of material for subsequent melt processing trials. Physically cross-linked polymers based on NVCL were synthesised *via* photopolymerisation by incorporating VAc at 5, 10 and 20 wt%, along with 0.1 wt% Irgacure® 184 photoinitiator. Concentration levels of the photoinitiator were kept at 0.1 wt%, as previous studies have shown that minimising photoinitiator concentration levels enhances the biocompatibility of the polymer [199]. All samples were optically transparent, indicating that the polymers are amorphous and the chains sorted in a random fashion (Figure 3-2) [200].

The structure of a polymer is commonly defined in terms of crystallinity. This might also be thought of as the degree of order or regularity in how the molecules are packed together. A well-ordered polymer is considered crystalline. The opposite is an amorphous polymer. Generally, amorphous polymers provide transparency while crystalline polymers do not, particularly in thicker products such as injection-moulded end products. Crystallinity causes refraction of the light ray. For the crystalline polymer to get clarity, the end product should be very thin, like film, and oriented so that the size of the crystals becomes smaller, hence preventing them from refracting the light rays [201,202].

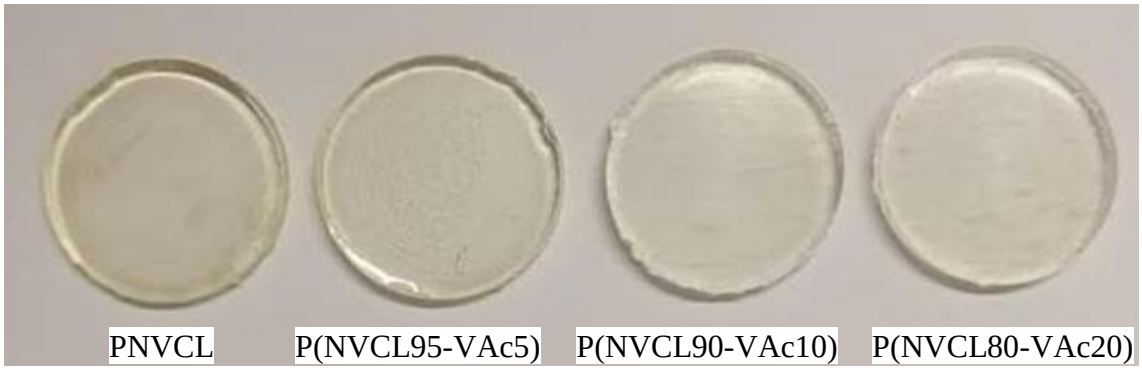

Figure 3-2: PNVCL based samples were optically transparent while increasing the concentration of VAc slightly increased the transparency of the polymers.

3.1.3. ATR-FTIR

Characterisation of polymers includes vibrational spectroscopic infrared (IR) analysis, which provides information about the polymer molecules. IR energy is a small portion of the electromagnetic spectrum. Wavelengths in IR spectroscopy are normally measured in wavenumbers which are the reciprocal units of the IR wavelength (cm^{-1}). The IR spectrum can be divided into three frequency regions which are:

- Near-infrared (13000-4000 cm^{-1})
- Mid-infrared (4000-200 cm^{-1})
- Far infrared (200-10 cm^{-1})

The most common IR frequency used in polymer characterisation is the Mid-infrared (4000-200 cm^{-1}). The infrared spectrum of a substance is recorded by passing a beam of IR light through the sample. When a chemical substance is subjected to such energy, transitions between molecular vibrational and rotational energy levels cause the absorption of IR energy and gives rise to absorption bands at characteristic frequencies.

The light not absorbed by the sample is then detected by a spectrometer which reveals how much energy is absorbed at each wavelength by producing a characteristic spectrum for the substance. A spectrum consists of a sequence of absorption peaks/bands as a function of the wavelength. Each IR-active bond during the molecular vibration will absorb IR energy at a particular/specific vibrational frequency. The resulting IR spectrum comprises a series of peaks each corresponding to specific functional groups included in the molecular structure, which is useful for identifying the substance [203].

NVCL monomer and NVCL-VAc based copolymers were analysed using ATR-FTIR to determine if polymerisation had occurred. Attenuated total reflection (ATR) is a

sampling technique commonly used with vibrational spectroscopy which allows the samples to be directly analysed with minimum preparation. In ATR a beam of infrared light passes through the sample in such a way that it reflects at least once off the internal surface in contact with the sample. Before analysis, all samples were dried in a vacuum oven at 40 °C for 24 hours. In the NVCL monomer spectrum, Figure 3-3, a band at 1655 cm^{-1} was attributed to the C=C group. Further characteristic peaks for NVCL were detected for the amide group (C=O) at 1622 cm^{-1}, while the CH_2 in the caprolactam ring was observed at 1438 cm^{-1}, in accordance with the literature [42]. The stretching and bending vibrational bands of the C–H bond in the vinyl group (=CH and $=CH_2$) were observed at 3108 cm^{-1} and 989 cm^{-1}, respectively.

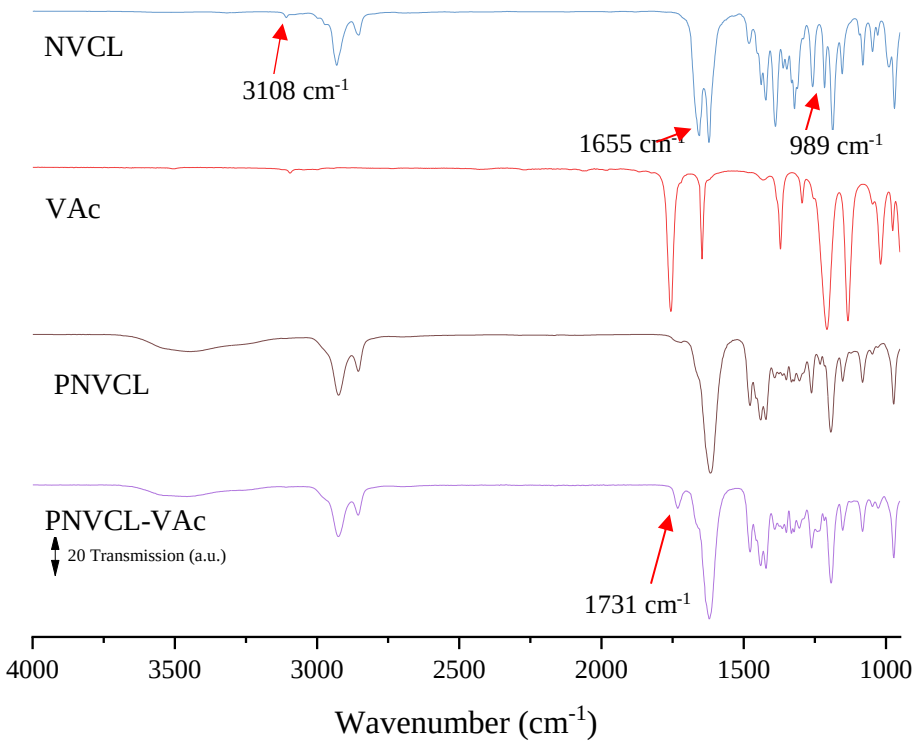

Figure 3-3. FTIR spectra of NVCL, VAc, PNVCL and PNVCL-VAc copolymer (P(NVCL80-VAc20)). Arrows mark the characteristic bands of NVCL and VAc in samples P(NVCL80-VAc20).

For successful polymerisation of NVCL, the bands corresponding to the C=C bond in the vinyl group of the NVCL monomer should disappear, as was the case in this study. PNVCL absorbs moisture which corresponds to the broad band at ~3400 cm^{-1} which relates to the O–H stretching; this is associated with the polymer's hydrophilic

character. These findings correspond with other studies that involved successful polymerisation of PNVCL [42,60].

The PNVCL-VAc spectra exhibited new bands not typically associated with PNVCL, which indicates that the copolymer reaction successfully took place, as represented in Figure 3-3. One such band occurred at 1731 cm^{-1} which corresponds to the C=O stretching of the aliphatic ester group of VAc [204]. The C=O of the aliphatic ester group increased in intensity as the concentration of VAc increased in the samples. The wavelength at ~3400 cm^{-1} (O–H groups) exhibited a decrease in intensity at higher VAc loadings, due to the more hydrophobic nature of VAc. Table 3-1 presents a summary of the bands obtained for NVCL and the copolymers synthesised.

The characteristic bands of PNVCL were also observed in the spectra of the copolymers. However, there was no significant shift in the characteristic bands for samples P(NVCL100) and P(NVCL80-VAc20). For example, PNVCL C–N and –CH2 functional groups displayed no shift in position when compared with the addition of VAc. A similar finding was reported by Kozanoğlu *et al.* (2011) when comparing NVCL and PNVCL, where there were changes in the conformation of the molecules and interaction of molecules upon polymerisation [73].

Below in Figure 3-4 displays the suggested polymerisation step involved in the synthesis of PNVCL. The double bond vinyl groups present in the NVCL segment is what enables the polymer to undergo free-radical polymerisation in the presence of the Irgacure ® 184 photoinitiator resulting in the formation of PNVCL. The decomposing of Irgacure ® 184, results in the generation of two radicals. The free radicals are then available to react with the NVCL monomer in the photopolymer solution resulting in the opening of the C=C bond present in the vinyl segment, thus allowing a polymer network to be formed.

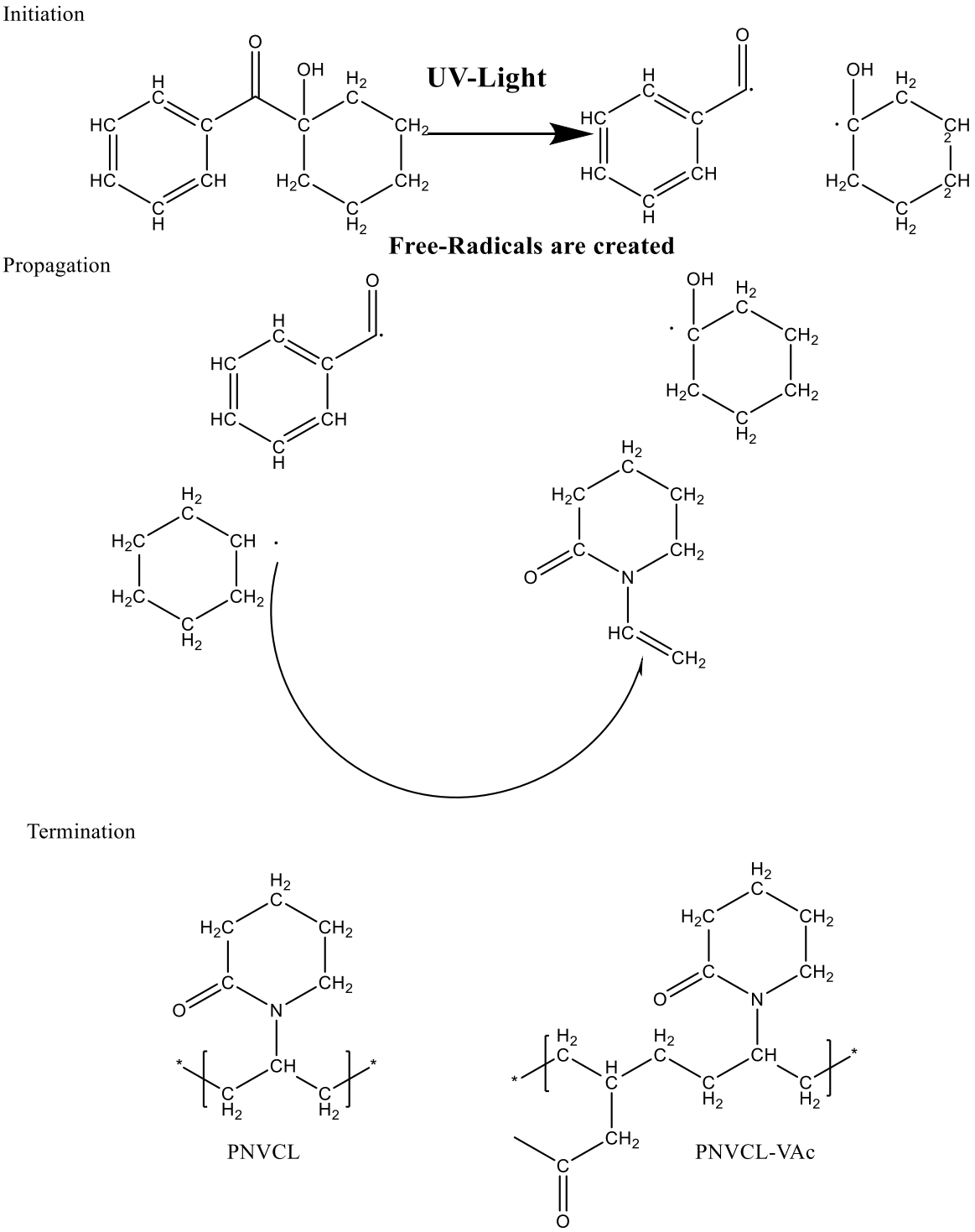

Figure 3-4: A proposed mechanism for polymerisation of PNVCL polymer.

Table 3-1: FTIR bands for NVCL and PNVCL based samples.

Functional group	Polymer code				
	NVCL	**P(NVCL100)**	**P(NVCL95-VAc5)**	**P(NVCL90-VAc10)**	**P(NVCL80-VAc20)**
Aliphatic C–H	2930, 2853	2924, 2854	2924, 2855	2924, 2856	2924, 2857
Ketone C=O	1622	1617	1619	1620	1620
C–N	1481	1477	1477	1477	1477
$–CH_2$	1438	1440	1440	1440	1440
C=C	1655	-	-	-	-
=CH & CH_2	3108, 989	-	-	-	-
O–H	-	3443	3432	3464	3457
Ester C=O	-	-	1731	1732	1732

3.1.4. Nuclear magnetic resonance

Nuclear magnetic resonance was performed to further validate the findings of the FTIR analysis. As Figure 3-5 shows, the polymer structures were characterised by ^{1}H NMR. The copolymer composition can be calculated from the integral data e, h and n assigned, as indicated in Figure 3-5. The following equations (Equations 3-1 to 3-4) demonstrate the calculation:

$$m = e/3 \quad \text{(Equation 3-1)}$$

$$n = h/2 \quad \text{(Equation 3-2)}$$

$$VAc\% = m/(m+n) \times 100\% \quad \text{(Equation 3-3)}$$

$$PNVCL\% = n/(m+n) \times 100\% \quad \text{(Equation 3-4)}$$

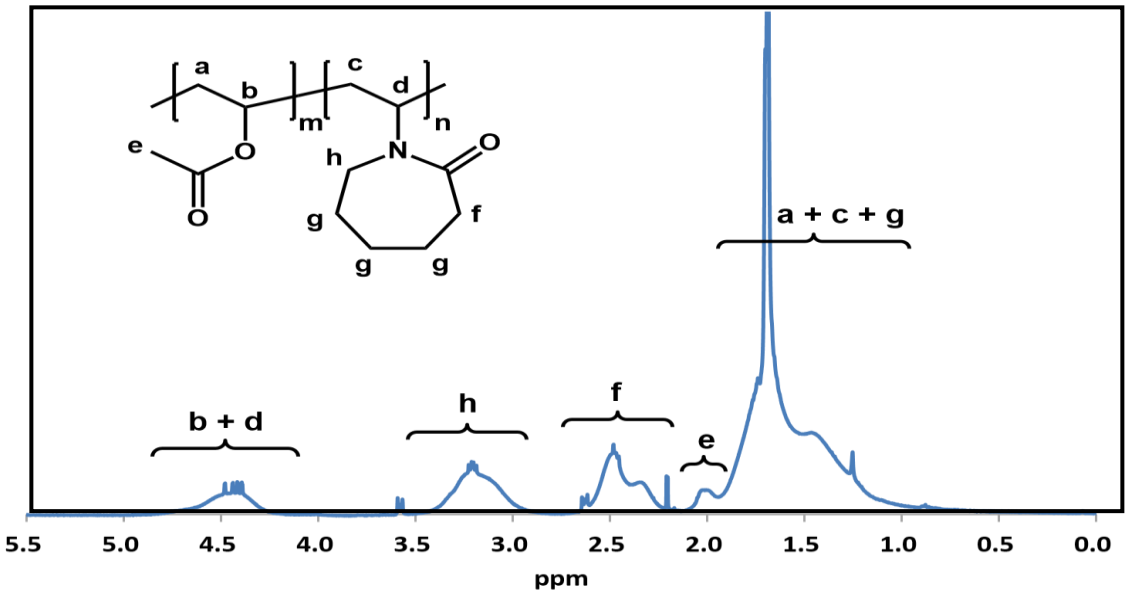

Figure 3-5:^{1}H NMR spectrum for the PNVCL-VAc copolymer in $CDCl_3$.

The ^{1}H NMR spectrum of copolymer samples seen in Figure 3-6 shows that the VAc% increased from P(NVCL100) to P(NVCL95-VAc5), to approximately 10 wt%, and P(NVCL90-VAc10) to approximately 16 wt%. Qian *et al.* (2014) examined the chemical structure of PNVCL and copolymers by ^{1}H NMR, which found new resonance

signals attributed to the protons on the addition of copolymers [205]. This further confirms that polymerisation occurred [191,205,206].

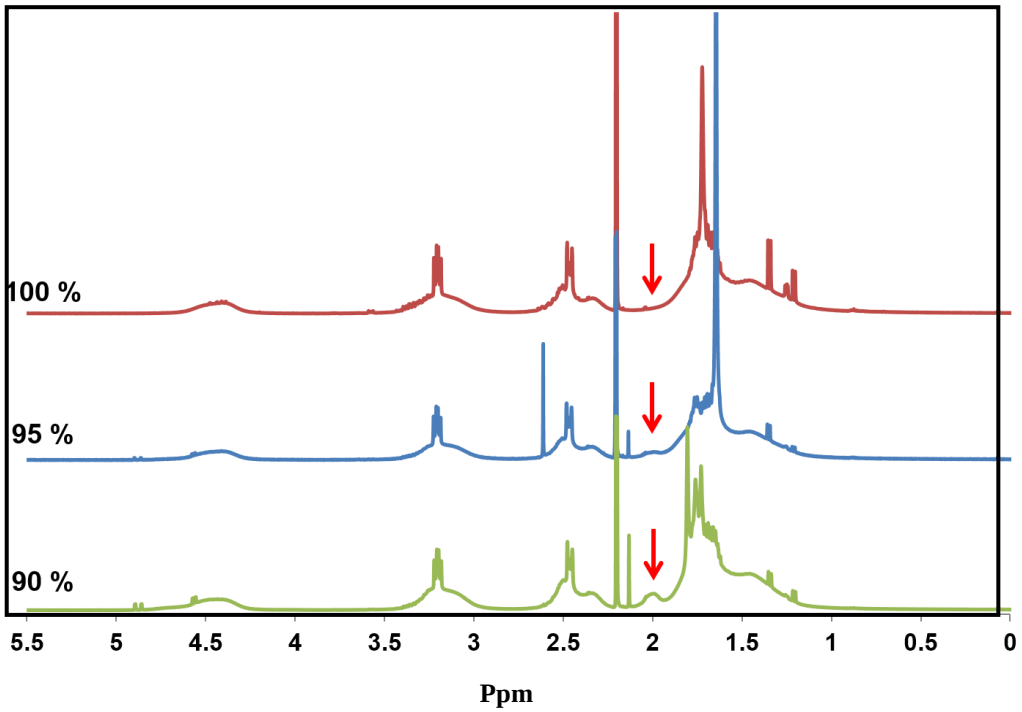

Figure 3-6: ^{1}H NMR spectrum of different PNVCL-VAc copolymers. The arrows highlight the characteristic peak attributed to the VAc.

3.1.5. Gel Permeation Chromatography

The release characteristics of polymer drug delivery systems is an important aspect, and one such factor affecting the release rate of an entrapped drug is particle size. It is well-known that it is possible to change the release rate of a drug by changing the copolymer composition, as well as the molecular weights of the polymer [207]. Altering the molecular weight of hydrogel delivery systems has a major impact on the drug release, mainly due to the hydrogel breakdown rate being dependent on the length of the chains for physically cross-linked samples. However, for chemically cross-linked samples, the mesh size is the main factor for a drug to be released from its hydrogel matrix. The results obtained for the molecular number (M_n), molecular weight (M_w), and polydispersity (PDI) of the samples will be discussed further in Section 3.2.9.

Altering the composition of NVCL and VAc during photopolymerisation resulted in an increase in the M_w and M_n, providing further evidence that a copolymerisation reaction has taken place. The LCST behaviour of PNVCL is known to be influenced by

the M_w [170,208]. Following GPC analysis, a M_w of 167,974 g/mol was recorded for PNVCL, and a M_w of 239,484 g/mol was found for P(NVCL90-VAc10).

As previously mentioned, the release rate of a drug can be affected by the M_w and composition of the polymer. The molecular weight of PNVCL based polymer is probably the most critical factor in controlling the LCST and the swelling of the hydrogel. An increase in the M_w of a polymer often contributes to a decrease in drug released. Thus, by adjusting the M_w of a polymer, it is possible to control the release rate of a drug. Mittal *et al*. (2007) studied the effects of adjusting the M_w on the release behaviour of PLGA. Results showed that drug release *in-vitro* decreased with the increase in M_w of poly (lactide-co-glycolide (PLGA) [209].

Controlling the composition of polymer and copolymer is another possible way to control the release rate of a drug. Li *et al.* (2013) studied poly (ethylene glycol)–poly (lactide-co-glycolide) (PEG–PLGA) copolymers doxorubicin (DOX), loaded into micelles through nanoprecipitation. It was found that the *in-vitro* release behaviour could be adjusted by regulating the composition percentage of the copolymer [210].

3.1.6. Differential Scanning Calorimetry

Studies of PNVCL have focused almost entirely on its behaviour in aqueous media, with fewer studies done on the polymer in the solid-state. Differential scanning calorimetry (DSC) measurements were conducted over the temperature range of 20-200 ºC for all samples. One broad transition was observed between 60-150 ºC for all the NVCL based polymers; this transition was identified as the glass transition temperature (T_g).

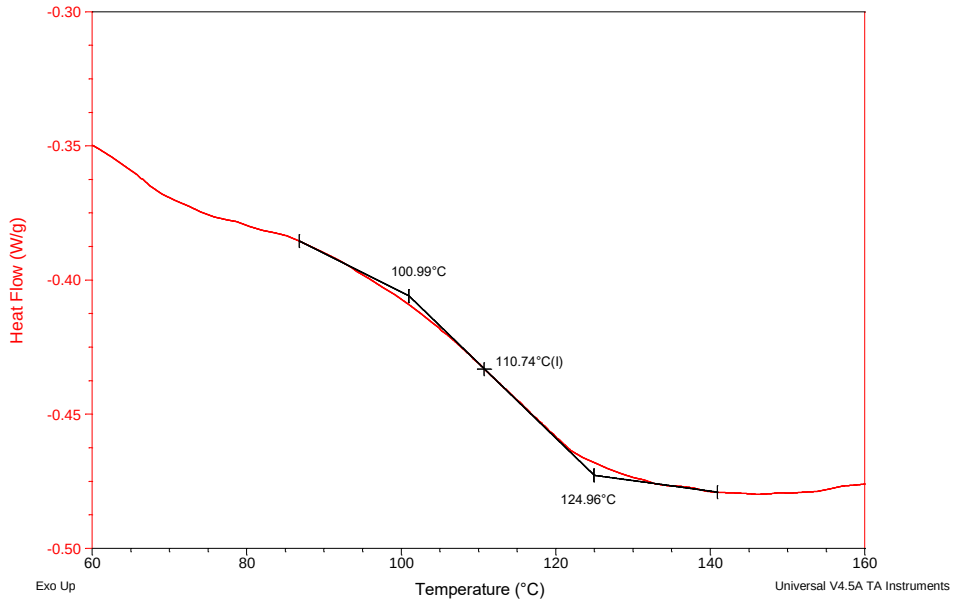

Figure 3-7. A representative thermogram illustrating the glass transition of PNVCL homopolymer.

Table 3-2 summarises the glass transition results for each of the samples analysed. The T_g of a polymer is a distinguishing aspect in the design of a controlled drug delivery system. Lebedev *et al.* (2013) reported a T_g for PNVCL at 147 °C, while Meeussen *et al.* (2010) reported a T_g of 145 °C [211,212]. For the PNVCL homopolymer developed in this study, the T_g was determined to be approximately 110.7 °C (Figure 3-7). The difference in T_g compared to the literature can be associated with various factors, though molecular weight is often cited as one of the major contributors [213].

The T_g of NVCL based copolymers was found to be dependent on the incorporation level of Vac Table 3-2), whereby increasing the composition led to a decrease in the glass transition value. This indicates that the incorporation of VAc has a plasticising effect on PNVCL. This is likely due to the VAc's low molecular weight (86.09 g/mol), allowing for greater flexibility in the polymer's chains, resulting in lowered T_g values.

Table 3-2: Glass transition temperatures recorded for NVCL based samples.

Sample code	**P(NVCL 100)**	**P(NVCL95 -VAc5)**	**P(NVCL90-VAc10)**	**P(NVCL80-VAc20)**
T_g Value range (°C)	109.3-112.1	102.0-104.6	97.0-101.4	73.2-78.0

3.1.7. Phase transition determination

The LCST of temperature-responsive polymers plays a crucial role in designing a targeted drug delivery system, as the phase transition temperature is the point at which the drug can be released [214]. The most critical factors affecting the phase transition of PNVCL are $M_{w,}$ copolymer composition, and concentration in aqueous media. The LCST is expected to decrease with increasing polymer molecular weight based on the changes in the polymer-solvent interaction. In this section, the phase transition was measured by employing four techniques to determine the LCST (Table 3-3). By utilising each of these techniques, common trends were established, for example, the LCST was found to be influenced by the monomeric ratio and the polymer concentration in solution at a fixed molecular weight of PNVCL.

The incorporation of a more hydrophobic monomer (VAc) to NVCL resulted in a decrease in the LCST, whereby the polymers developed in this study have LCST's in the range of 26.2-34.5 °C (Table 3-3), which would be very favourable for potential biomedical thermo-gelling applications.

Table 3-3: LCST of NVCL based samples which was established using cloud point (n=5), UV- spectroscopy (n=3), DSC (n=2) and rheological analysis (n=2).

Sample code	**LCST range determined using Cloud point (°C)**	**LCST range determined using UV-Spectroscopy (°C)**	**LCST range determined using DSC (°C)**	**LCST range determined using Rheological analysis (°C)**
P(NVCL100) (3 wt%)	31.2-32.2	32.0-32.8	31.0-34.0	30.3-33.1
P(NVCL100) (5 wt%)	31.1-32.3	32.2-32.8	30.9-34.4	31.4-33.2
P(NVCL100) (10 wt%)	33.033.6	32.9-33.9	33.5-35.4	32.2-34.8
P(NVCL95-VAc5) (10 wt%)	31.4-32.2	31.0-31.8	30.0-33.8	31.6- 34.2
P(NVCL90-VAc10) (10 wt%)	29.4-30.6	29.1-29.7	28.2-33.4	27.1-31.2
P(NVCL80-VAc20) (10 wt%)	26.1-27.9	26.0-26.8	23.9-28.6	23.8-28.5

3.1.7.1. Cloud point measurements

Visual observation of LCST was initially employed to establish the phase transition behaviour. This testing was carried out to ascertain the range of LCST's for PNVCL based copolymers before more sophisticated phase transition testing. Cloud point was defined as the temperature at which the first sign of turbidity occurred in the solution [215]. Cloud point measurement results can be seen in Figure 3-8. Samples showed a reversible phase transition in water, which was in agreement with the literature [191]. The opaque solution slowly changed back to the transparent, colourless solution as the temperature reduced. It has been suggested that, at a certain temperature, water becomes a poor solvent to the polymer, possibly due to the new and less polar polymer conformation, causing the prevalence of the polymer-polymer interaction, leading to phase separation [216]. In Table 3-3, the cloud point analysis of copolymer samples resulted in a decrease in LCST, with increased VAc incorporation during photopolymerisation.

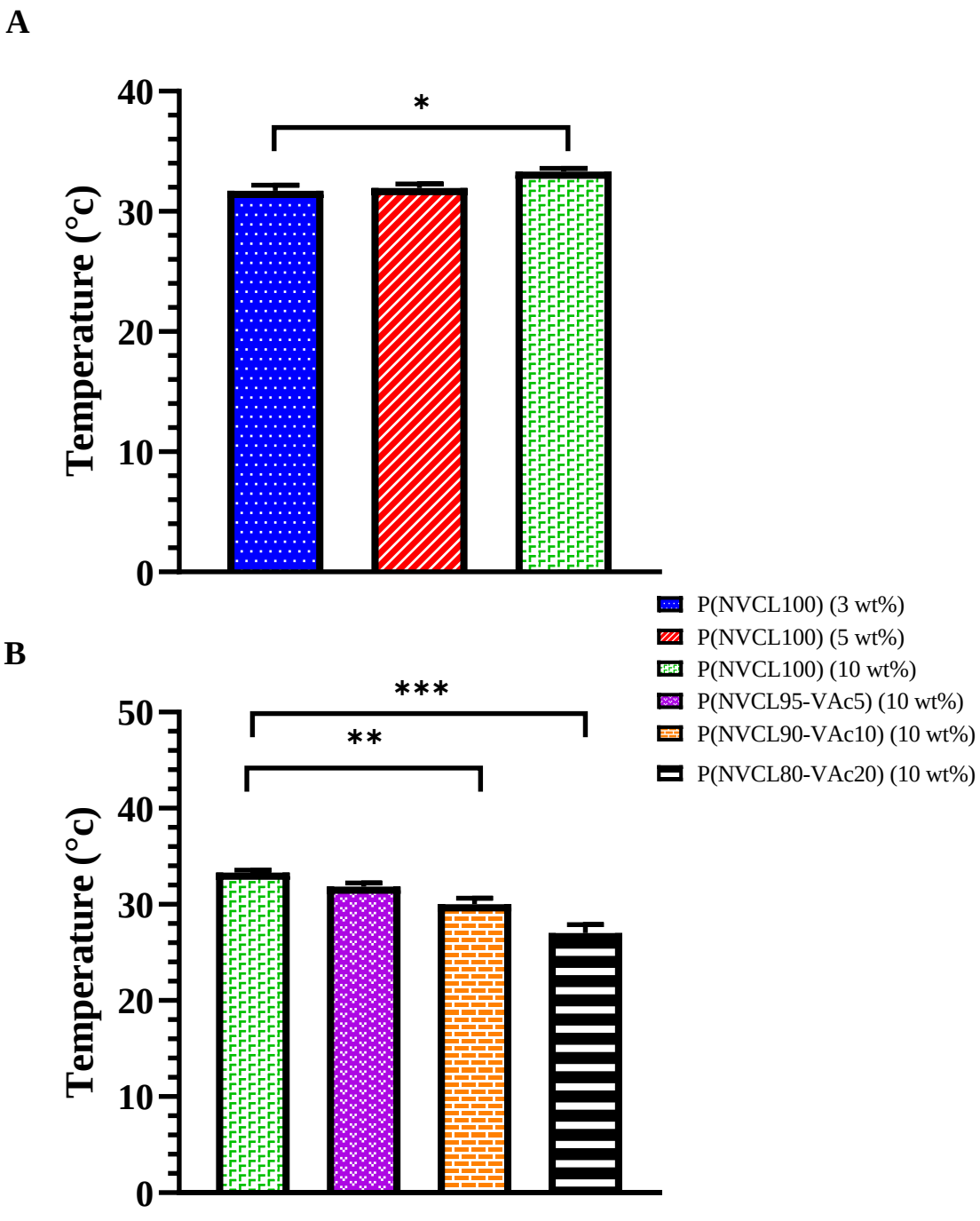

Figure 3-8: Statistical analysis of the interaction of PNVCL with VAc at different weight percent (a) concentration and (b) composition of VAc measured by cloud point measurement. The LCST (ºC) data are presented as mean±SD (n = 3). One-way ANOVA followed by Tukey multiple comparison test. Significantly different * $p < 0.05$; ** $p < 0.01$ and *** $p < 0.001$ vs. control.

3.1.7.2. Differential scanning calorimetry

DSC was also used to analyse LCST behaviour. For PNVCL, Ferraz *et al*. (2014) reported an LCST of 33-36 °C, while Shi & Zhang (2006) reported an LCST of around 32 °C. In this study, one transition was identified during the heating scan between 32-35 °C for all homopolymer samples. This transition was related to the LCST, which is in accordance with the values achieved by previous authors [217,218]. In all cases, the onset value of the endothermal peak was used to establish the LCST value. The relatively strong hydrogen bonds formed between water molecules and N–H or C=O groups in dilute solutions became weaker and broke as the temperature was raised, resulting in the endothermic heat of phase separation [219].

Illustrated in Figure 3-9 is a thermogram for PNVCL homopolymer (10 wt%) in aqueous solution, where the onset value recorded was 34.5 °C. However, in some cases, it was found there was a difference of over 2 °C between the calorimetric peak and onset values. It is understood that a small portion of the gel starts to undergo its phase transition at the onset temperature, while the majority experience the transition at the peak value [215,220]. The incorporation of VAc during polymerisation resulted in a decrease in the LCST.

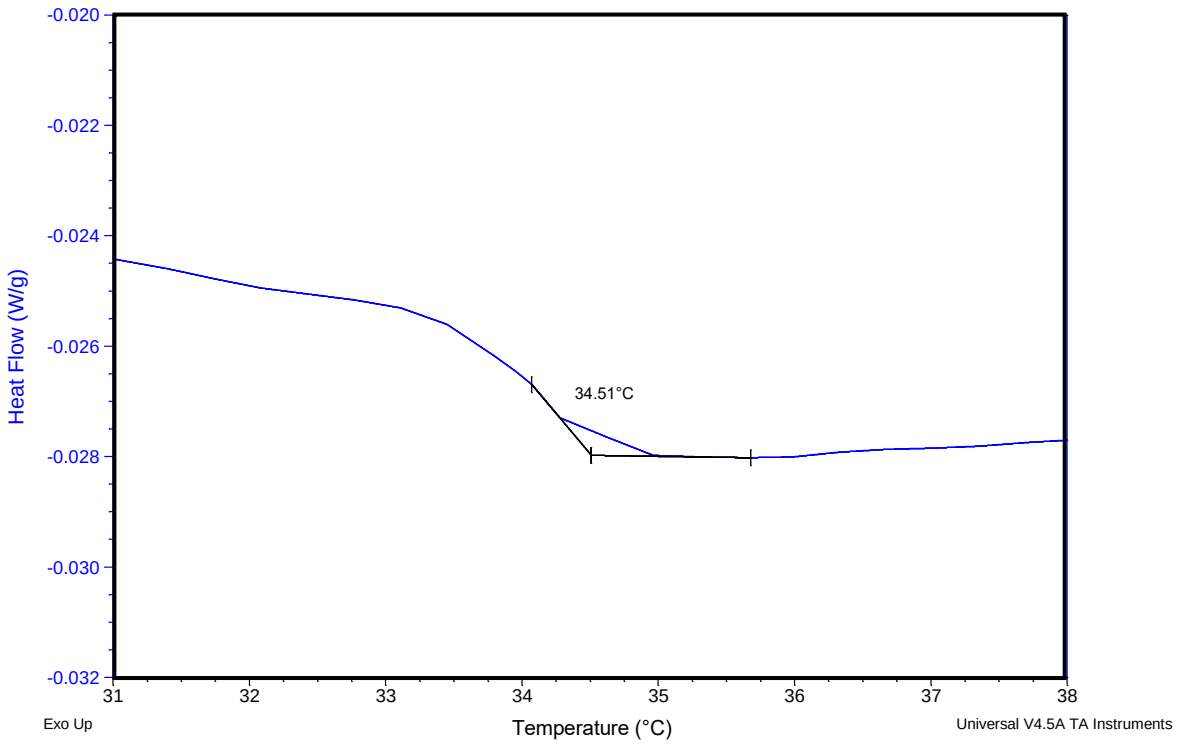

Figure 3-9. A representative thermogram illustrating the LCST of PNVCL homopolymer (10 wt%) aqueous solution.

3.1.7.3. UV-spectrometry

Aqueous solutions of PNVCL homopolymer (3 wt%) and (10 wt%) were also investigated using UV-spectrometry. All samples were analysed over a temperature range of 25-44 °C. Figure 3-10, illustrates the phase transition behaviour of PNVCL. This was noticeable by the change in its optical transparency below (left) and above (right) the LCST. At temperatures below the LCST, PNVCL solution is transparent and colourless; above the LCST, the solution is opaque.

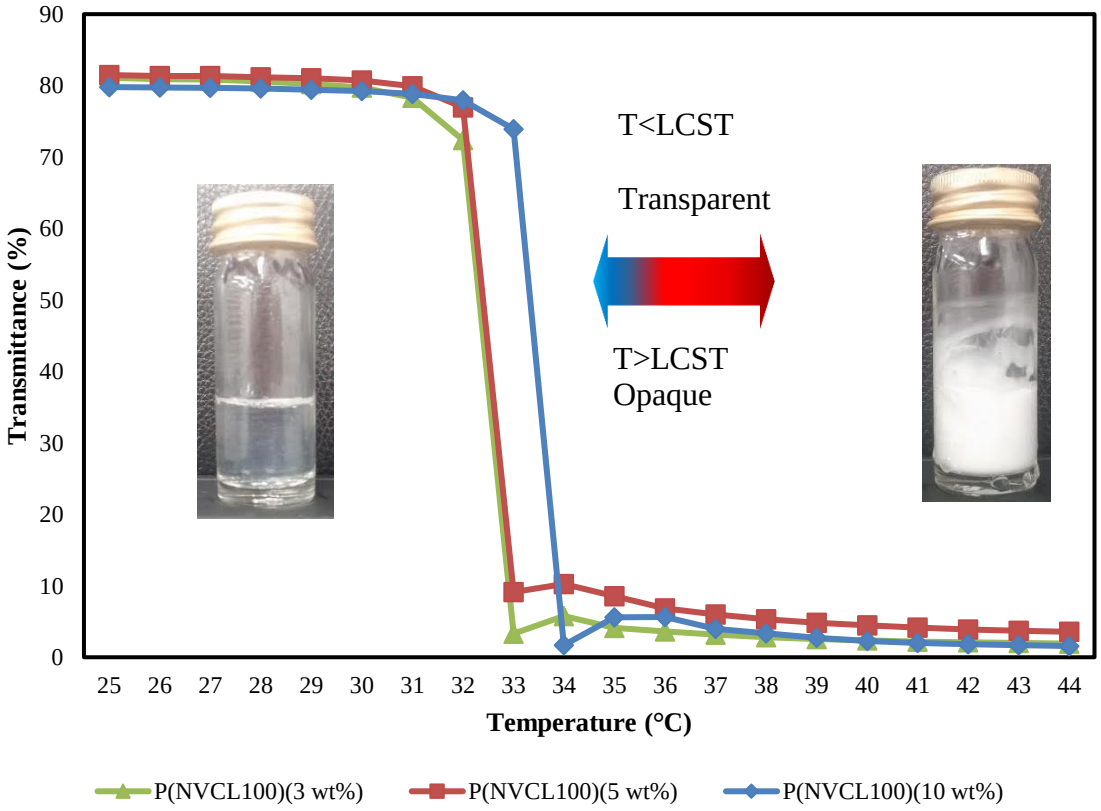

Figure 3-10. The UV-spectrometry analysis, which illustrates the LCST of PNVCL homopolymer at different aqueous solution concentrations. UV-spectroscopy data are presented as mean±SD (n = 3).

The phase transition temperature obtained for PNVCL was within the range reported in previous observations [42,217,218]. Concentration affects the LCST as the water content increases the hydrogen bond interactions amongst the water and the polymer, this requires more thermal energy to break the water structure, resulting in increased LCST. Furthermore, phase transitions of all NVCL-VAc copolymers were measured, with the LCST found to decrease almost linearly, with an increasing

concentration of VAc. Overall, the findings from cloud point measurement, DSC and UV-spectrometry correlate very well as all results displayed similar trends.

3.1.8. Swelling studies

Temperature-responsive polymers have been proposed as smart, solid dosage forms, whereby the active agent can be incorporated directly during polymerisation. Swelling is one of the most important factors in controlling the release mechanisms for drug delivery systems [213]. As a hydrogel swells, the mesh size increases. The degree of swelling of a hydrogel is a balance between forces that constrain network deformation and the osmosis that leads to water absorption [3]. Swelling studies were carried out on all samples, above and below the LCST in distilled water, as was determined by previous phase transition experiments. Samples were tested in distilled water to determine the swelling. At 1 hour time intervals, samples were removed from the distilled water and blotted with filter paper to absorb excess water on the surface and then the samples were weighed.

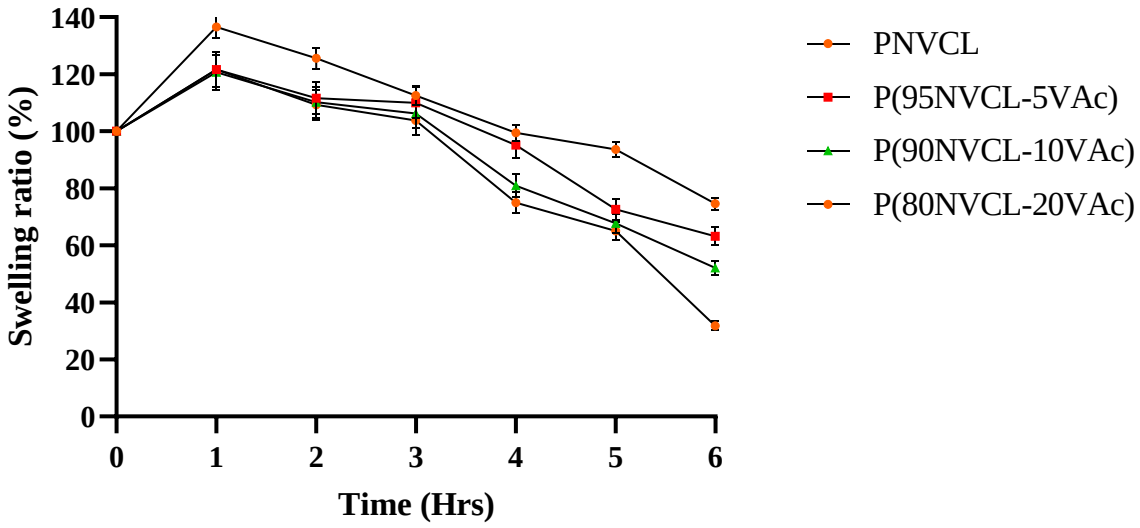

Figure 3-11. Swelling behaviour of PNVCL based samples tested below LCST at 20 °C. Swelling ratio (%) data are presented as mean±SD (n = 3).

Distilled water was preheated to the required temperature before submerging the samples. Graphical results are shown in Figure 3-11 and Figure 3-12, which display the polymer swelling behaviour below and above LCST. For samples below LCST, the

maximum swollen weight had been reached after 1 hour for all samples. Subsequent to the maximum swollen weight being achieved, the polymer started to break down. After 6 hours, the polymers had lost their structure and could not be weighed.

Contrasting swelling behaviour was observed for the PNVCL samples above LCST; within 6-24 hours, the peak swelling was achieved. Swelling studies were performed until the maximum swollen weight of the sample was achieved. When the temperature is below LCST, the hydrogen-bonding of the hydrophilic segments dominates the interaction between water and the polymer chains. Thus, the polymer absorbs water which leads to the breakdown of polymer chains.

When the temperature increases above the LCST, the polymer chains shrink and repel the water molecules through hydrophobic segments, which results in the precipitation of polymer and a globular state appears [192]. Controlled swelling is required for tissue engineering and drug delivery, which is influenced by the dissolution behaviour of the polymer [193,221].

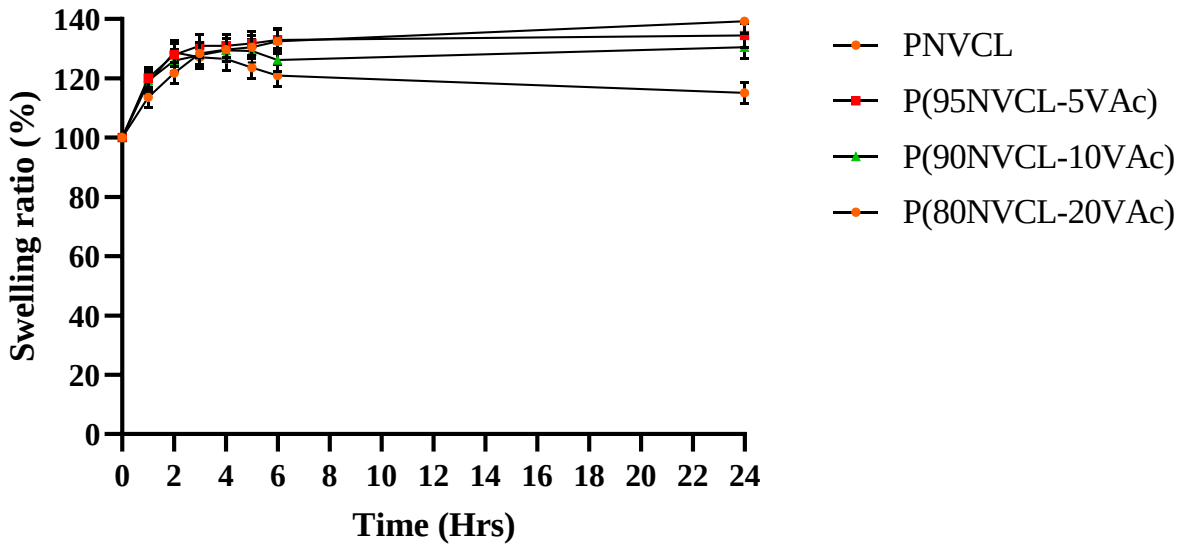

Figure 3-12. Swelling behaviour of PNVCL based samples tested above LCST at 40 °C. Swelling ratio (%) data are presented as mean±SD (n = 3).

3.1.9. Sol-gel transition

Thermo-gelling polymers that undergo sol-gel transition have proven to be appealing in biomedical fields, particularly in potential drug delivery and injectable tissue engineering applications [222–224]. Injectable, *in-situ* setting semi-solid drug depots, are

being established as alternative delivery systems [225]. Polymers, with a sol-gel transition between room temperature and body temperature, are predicted to be the most beneficial [226]. Thermo-gelling systems can comprise of drugs or cells and such systems aid in delivery to the desired site. During the sol-gel transition, all of the ingredients in the system form a matrix, whereby drugs can be released in a controlled manner [198]. Singh *et al.* (2014) highlighted that in order for the design of an injectable hydrogel for drug delivery applications to be successful, some essential requirements were needed, for example, the hydrogel must be biocompatible and biodegradable. Furthermore, efficient drug loading and controlled drug release over a range of time scales are required [18].

In this section, the sol-gel transition was measured using the tube inversion method and rheological analysis. Samples synthesised in this study had sol-gel transitions within the range 33.6-47.1 °C (Table 3-4). These novel copolymers could potentially be used as thermo-gelling systems, which should have a LCST below 37 °C so that the materials could undergo gelation when injected into the body [198,227]. These results followed similar trends as reported in Section 3.1.7 with regard to PNVCL phase transition.

Table 3-4: Sol-gel transition temperatures for PNVCL based samples which was established using tube inversion method (n=3) and rheological analysis (n=2).

Sample code	Sol-gel range determined using Tube inversion method (°C)	Sol-gel range determined using Rheological analysis (°C)
P(NVCL100) (3 wt%)	46.6-57.6	45.2-46.4
P(NVCL100) (5 wt%)	41.8-43.8	42.3-43.1
P(NVCL100) (10 wt%)	36.7-37.9	36.7-38.5
P(NVCL95-VAc5) (10 wt%)	34.8-35.8	35.1-36.7
P(NVCL90-VAc10) (10 wt%)	33.7-34.7	33.1-35.3
P(NVCL80-VAc20) (10 wt%)	32.8-34.6	32.5-34.7

3.1.9.1. Tube inversion method

The tube inversion technique was used in determining the sol-gel transition of all samples (3 wt% and 10 wt% aqueous solutions), within the range of 20-50 °C. At temperatures below the sol-gel transition, PNVCL remained as a colourless solution, while above the sol-gel transition, the polymer transformed into a gel. Concentration affected the sol-gel transition, whereby increasing the concentration resulted in a decrease

in the sol-gel transition temperature as displayed in Figure 3-13. Incorporating VAc during photopolymerisation also resulted in a decrease in the temperature of the thermo-gelling transition.

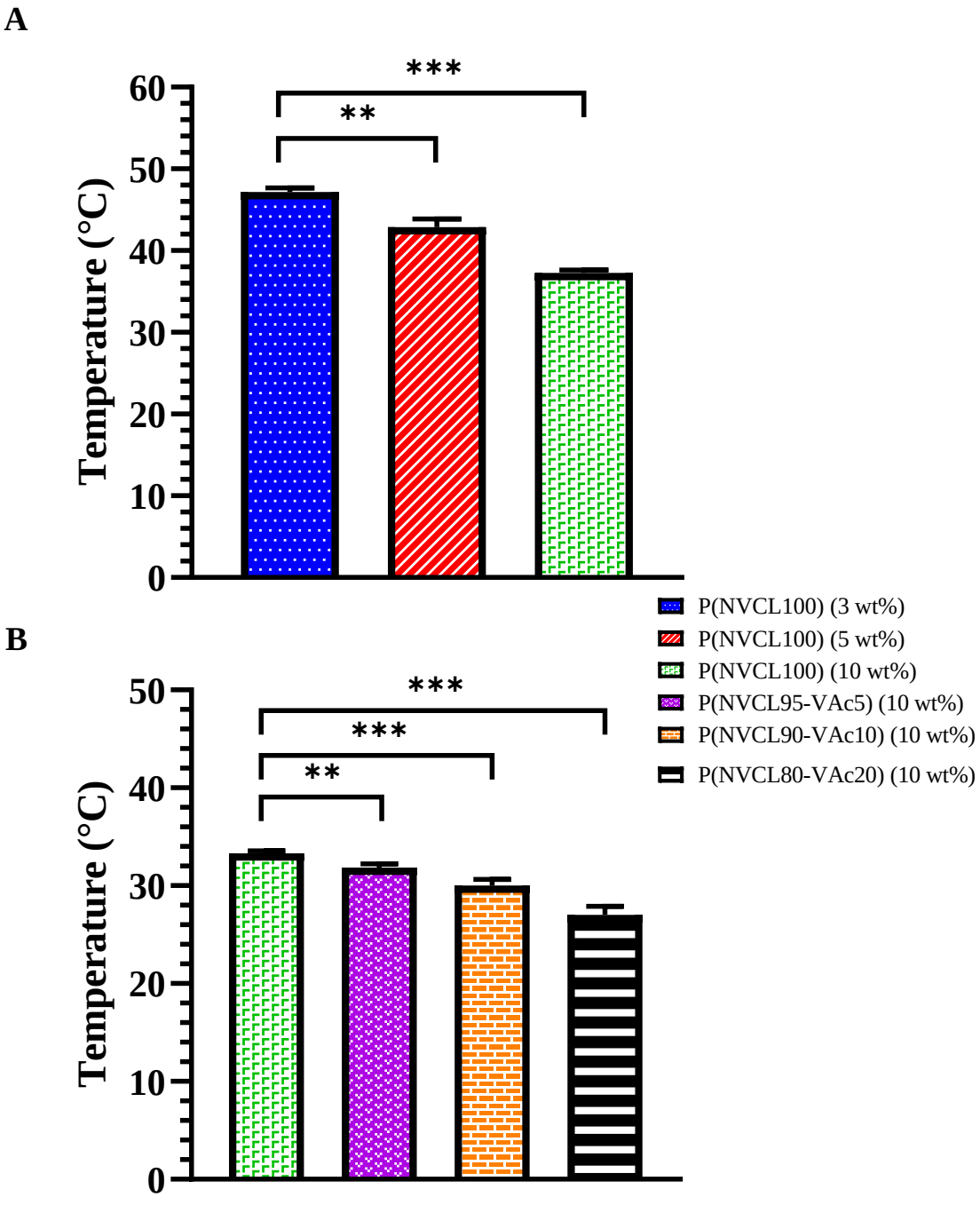

Figure 3-13: Statistical analysis of the interaction of PNVCL with VAc at different weight percent (a) concentration and (b) composition of VAc measured by tube inversion method. The LCST (ºC) data are presented as mean±SD (n = 3). One-way ANOVA followed by Tukey multiple comparison test. Significantly different * $p < 0.05$; ** $p < 0.01$ and *** $p < 0.001$.

3.1.9.2. Rheological analysis

Dynamic temperature ramp tests were performed on all samples (3 wt% and 10 wt% aqueous solutions), where G′ and G″ were measured as a function of the temperature within the range 20-50 °C (Figure 3-14). For the samples analysed in this work, the onset temperature for the LCST is marked with the arrow (↓) [228]. It is known that the elastic component, (G′), dominates the LCST when it first responds and is more sensitive to temperature change than the loss modulus (G″) [229]. As the LCST is approached, the values for G′ (●) and G″ (○) increased, until G′ and G″ were equal; this point is known as the sol-gel transition temperature [230,231].

The sol-gel transition temperature has a tendency to decrease when the concentration of polymer in the solution is increased [231]. According to Figure 3-14, marked with the arrow (↑), the sol-gel transition temperature for PNVCL homopolymer P(NVCL100) (3 wt%) was 47 °C. Figure 3-14 illustrates the sol-gel transition behaviour for PNVCL; the LCST is the point at which the polymer changes colour, but it is still in solution (middle) (Figure 3-14), and above the sol-gel transition (right) (Figure 3-14) the sample has solidified. While reviewing the results for PNVCL homopolymer, increasing the concentration led to a decrease in the gelling temperature, while the incorporation of VAc also resulted in a decrease in the LCST. The systems developed have the potential to gel at approximately 3-7 °C above the LCST, depending on VAc incorporation level during photopolymerisation. The gelling point of the homopolymer (3-10 wt% in solution) was above 37 °C. Importantly, all copolymers (10 wt% in solution) gelled between 33.6-35.9 °C.

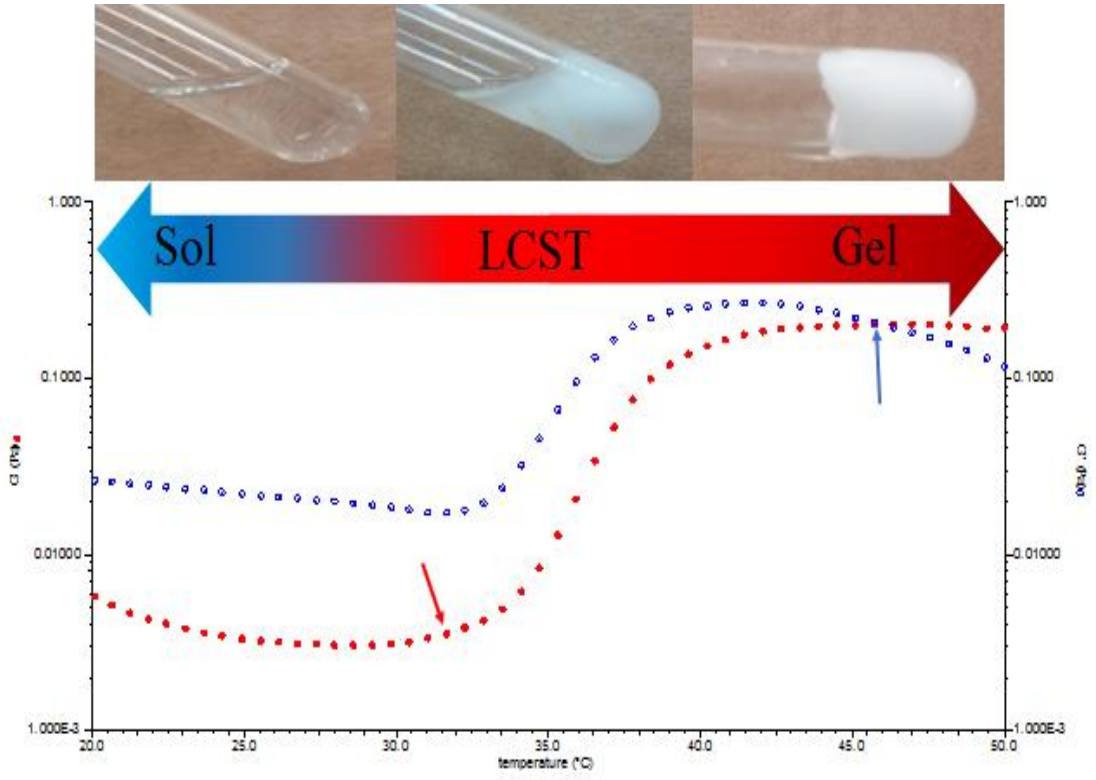

Figure 3-14. A representative graph of G′ (●) and G″ (○) for PNVCL homopolymer (3 wt% aqueous solution). The onset temperature for the LCST is marked as the arrow (↓). The sol-gel transition temperature is marked as the arrow (↑) where G′ and G″ are equal.

3.1.10. Summary

The main aim of this section was to synthesise a smart polymer, PNVCL, *via* photopolymerisation. This was successfully achieved with the smart polymer samples developed found to have tuneable properties depending upon the chosen formulation. In summary, successful polymerisation of NVCL-VAc was achieved, resulting in physically cross-linked polymers. This was confirmed by data *via* FTIR, NMR, and GPC. The LCST was determined by employing four different approaches: optical cloud point, UV-spectroscopy, DSC and rheometry. This study allows for a much greater understanding of the LCST phase and the sol-gel transition of novel PNVCL based copolymer systems, which were influenced by the concentration and monomeric feed ratio. The LCST of PNVCL was determined to be within the range of 31.6-34.5 °C, depending upon the polymer concentration in aqueous media. Also, copolymers exhibited a decrease in a phase transition within the range of 26.2-32.9 °C. The sol-gel transition was determined to be within the range of 33.6-47.1 °C.

Overall findings indicated that the use of this polymerisation method worked well, and had potential for drug delivery applications. However, any medical device that will be implanted into the body must first be sterilised, with the following section focusing on this area.

3.2. Effects of electron beam irradiation processing conditions on the property behaviour of Poly (*N*-vinylcaprolactam)

3.2.1. Preface

Sterilisation of smart polymer materials is often overlooked until later in the technology development phase of medical devices or controlled drug delivery systems. However given that sterilisation has been reported to have a considerable effect on smart polymer properties, it is critically important to consider its effects sooner rather than later in the research and development phase. This body of work involved collaboration with STERIS Applied Sterilization Technologies, who carried out all sterilisation trials free of cost on their commercial-scale electron beam equipment.

Ionising radiation is energy in the form of waves or particles that have the potential to remove bound electrons from the orbit of an atom, causing the atom to become charged or ionised [232]. Additionally, they are also able to break chemical bonds and cause harm in living matter which is why it is popular in the sterilisation of materials. Radio waves, microwaves, infrared radiation, visible light, ultraviolet radiation, X-rays and gamma rays are all classified as electromagnetic radiations, with the difference being the frequency and wavelength. Figure 3-15 illustrates frequency and wavelength for the spectrum of electromagnetic radiation [164].

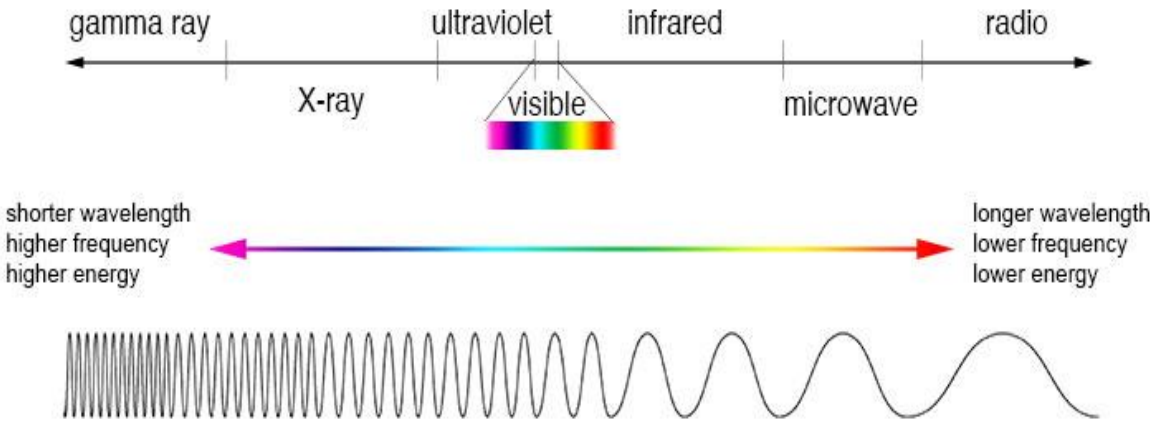

Figure 3-15: The Electromagnetic Spectrum [233].

Sterilisation is essential for any medical device to be used in the body. It prevents against any microorganisms infringing on the body's defence mechanisms [234]. Commonly employed sterilisation techniques include steam, ethanol immersion, dry heat, ethylene oxide and radiation sterilisation. There are many physical and chemical methods of sterilisation. Chemical sterilisation avoids increased temperatures but has the disadvantages of lengthy degassing times, potentially toxic residues and geometric changes in the materials. An efficient and appealing alternative to these techniques is radiation sterilisation. Radiation-induced chemical alterations, cross-linking and/or chain shortening are dependent on the dose and compositional ratios of the incorporated polymers [235]. Electron beam irradiation is currently being used in commercial applications which provides many companies with an effective and efficient means of sterilisation, and also of enhancing the properties and performance of polymers and other materials.

Table 3-5 lists the advantages and disadvantages of the primary radiation sources; however, the key radiation source that is important for this study is electron beam radiation. Electron beam radiation consists of a highly charged stream of electrons, which are produced by the acceleration and conversion of electricity. Heated filaments such as tungsten are used in the process to generate the electrons. This process uses no radioactive materials [236].

Table 3-5: Key advantages and disadvantages of the primary radiation sources

Method	Advantages	Disadvantages
X-Ray	Full pallet processing	Longer processing time than electron beam
	Can power off the source	Inefficient
	High penetration	Material degradation - stable radiation materials required
	Excellent dose uniformity ratio	
	Very labour efficient	
	Powered by electricity	
	Faster treatment than gamma irradiation	
Gamma-ray	It is a cold method; increase in temperature is so slight – suitable for heat-sensitive materials	Long processing time
	Control of the method is straightforward that can be made only by the parameter of the applied dose	Material degradation - stable radiation materials required
	High-density materials can be processed	Dose rate is lower than electron beams
	Flexible batch size	It has no dose rate flexibility
	No quarantine period	
	Good penetration	
	Non-uniform packing	
Electron beam	Provide short exposure times	Limited penetration
	Faster cycle time - Time is money	Uniform packing required
	Flexible batch size	Material degradation - stable radiation materials required
	Simplifies validations	
	Can power off the source	
	Eliminates operator dependencies	
	Enable real-time monitoring	
	Control of the method is effortless that can be made only by the parameter of the applied dose	
	More material compatibility than gamma-ray	

Although there are many studies on the use of electron beam technology to enhance the properties and performance of conventional polymers [237–239], far fewer studies focus on the use of sterilisation methods on stimuli-responsive polymers. One such polymer which has the potential to benefit from electron beam technology is PNVCL as the polymer molecular weight strongly influences the LCST behaviour. This is due to PNVCL having a Type I Flory–Huggins miscibility behaviour, which contends that increasing the chain length of the polymer, the position of the LCST shifts towards lower temperature [23]. Therefore, an understanding of the changes induced by irradiation sterilisation is essential in the design of temperature-responsive polymers. Electron beam is by far the fastest and most cost-effective sterilisation technology in commercial use today. The ability to enhance polymer properties *via* irradiation processes has gained increased attention in the biomedical industry recently [23,240].

Currently, there are a number of studies centred on altering the phase transition of PNVCL by the incorporation of hydrophilic and hydrophobic segments into PNVCL polymer matrix [170,241]. However, it is important to note that little information exists on the electron beam irradiation of PNVCL [185,239,242], and current studies focus only on relatively low radiation doses. The current study focuses on PNVCL based samples utilising electron beam doses ranging from 0 to 50 kGy. The workflow is displayed in Figure 3-16. By accurately controlling the electron beam dose rate, it is hoped that properties such as phase transition, mechanical properties and swelling behaviour can be manipulated and controlled. As electron beam sterilisation has the potential to enhance many key smart polymer properties, the ability to formulate and sterilise in one step could prove a very attractive approach for many biomedical applications.

The aim of this section is to examine the effect of an industrial scale sterilisation method on novel smart temperature-sensitive polymers, to investigate the potential to formulate and sterilise in one step and the ability to enhance the physical and chemical characteristics of novel smart polymer formulations.

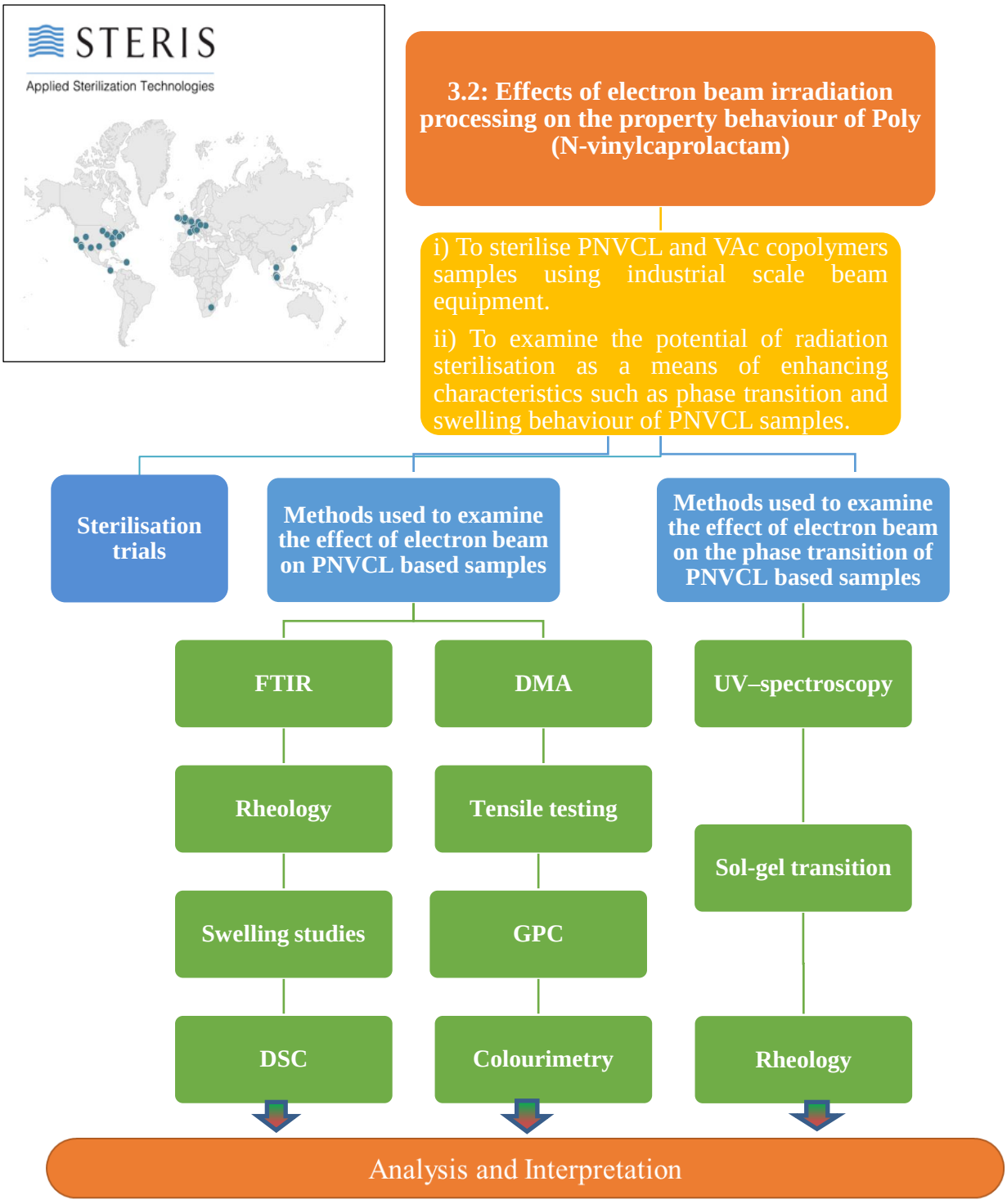

Figure 3-16: Work breakdown structure for the evaluation of the effect of the electron beam processing on PNVCL.

3.2.2. Preparation of samples

All sterilisation processes require validation of the efficiency and reproducibility of the process. Depending on the type of sterilisation involved, it may be accomplished by partial, sub-lethal, or repetitive processing, using the representative product and biological challenges. The entire validation must be documented to provide evidence for a high degree of assurance that the specified process will consistently produce a product meeting the predetermined conditions and quality attribute [243]. Process variables are used to describe the irradiation process so that the variables can be identified in order to control the process and make it predictable and reproducible. These process variables are used to define the process framework. The numerical values of process variables are called the process parameters [244]. Some of the process variables remain the same from product to product while others change. The main variables for modelling the irradiation process are:

- Distance to product (challenging to control for large packages)
- Beam energy
- Beam geometry
- Scan width and scan distribution

With electron beam irradiation, the objective of the validation process is to demonstrate that the required dose is delivered to the entire batch of material or product by the use of calibrated dosimeters. A radiation dosimeter is a device that measures dose uptake of external ionizing radiation. Dosimeters are used to measure radiation at laboratories, which are calibrated against a national standard to ensure that measurement results are consistent with the International System of Units (SI). At the initial stages, it is necessary to identify the effects that electron beam irradiation will have on the materials used in the products, their components and packaging. As each polymer reacts differently to ionising radiation, it is essential to confirm that the maximum dose likely to be administered during the process will not adversely affect the quality, safety or performance of the product throughout its shelf life. Experimental samples of the product should be irradiated to at least the highest dose to be encountered during routine processing. For example, a product that is to receive a dose of 25 to 40 kGy should be tested by irradiating samples to at least 40 kGy [245,246].

When selecting a suitable dose, it is intended that the minimum permissible dose necessary to provide the required sterility assurance level (SAL) is chosen. This is dependent upon the intended end use of the product. For example, a medical device such as an artificial joint implant which must receive a sterilisation dose high enough to ensure that the probability of an organism surviving the dosage is no higher than one in one million units tested (10^{-6}). From there, it is essential to determine the product loading pattern which takes into consideration a description of the packaged product, the orientation of the product with respect to the conveyor flow and electron beam, unit count within the package, package dimensions and mass, the orientation of product within the package, and acceptance variations in these parameters [236,247].

To assess the sterilisation, indicators and dosimeter were used. Overall, industry associations have prescribed and adopted a minimum irradiation dose of 25 kGy, to sterilise medical devices to ensure that there is a probability of less than one in a million of any articles having a bioburden on them [248]. For this reason, PNVCL samples were irradiated to and above 5, 25 and 50 kGy so that it would be possible to meet regulatory compliances for sterilisation.

Physically cross-linked polymers, based on NVCL, were synthesised *via* photopolymerisation. The copolymers were synthesised by incorporating VAc 10 wt%, along with 0.1 wt% Irgacure® 184 photoinitiators. Vacuum packing leads to depleted oxygen content during the irradiation procedure, which would minimise oxidative degradation, as there is no oxygen to react with the free radicals generated during the process [249]. Figure 3-17 illustrates the colour change of each sample, before and after irradiation (i.e. 0, 5, 25 and 50 kGy). As the irradiation dose increased from 5 to 50 kGy, a notable discolouration was observed; in particular, the 50 kGy samples turned a dark yellowish colour.

Figure 3-17: PNVCL based samples were optically transparent and increasing the irradiation dose of the electron beam from 0-50 kGy led to a colour change in the samples.

3.2.3. ATR-FTIR

Electron beam irradiation can alter the physical and chemical properties of polymers. This can occur through main-chain scission (degradation) or cross-linking, which are reliant on the electron beam dose and copolymer ratios [240]. ATR-FTIR analysis was carried out on the irradiated and non-irradiated PNVCL based samples, to ensure if electron beam irradiation led to undesirable changes in the material. For example, it is essential to ensure that the caprolactam ring is present within the PNVCL structure. ATR-FTIR analysis confirmed that the caprolactam ring was detected in all PNVCL samples (Figure 3-18). All samples displayed the aliphatic (C–H) band of the caprolactam ring at 2924 cm^{-1}, in accordance with the literature [42,250,251]. The retention of caprolactam functionality in the PNVCL samples demonstrated that electron beam irradiation did not affect the overall structure of the material [42,60]. PNVCL absorbs moisture which corresponds to the broad band at ∼3400 cm^{-1} which relates to the O–H stretching; this is associated with the polymers hydrophilic character. It was observed that increasing the irradiation dose lead to a decrease in this broad band. Additionally, other characteristic bands of PNVCL are the peaks corresponding to the C=O and the C-N bonds which are found at 1620 and 1453 cm^{-1} respectively. The retention of these bands gives further evidence that the PNVCL structure was not greatly affected during the electron beam process. There was very little change in the irradiated PNVCL when compared to the non-irradiated PNVCL. However, transmittances corresponding to 1453 cm^{-1} are decreased in irradiated compared to non-irradiated PNVCL samples. This indicates that those functional groups in the samples absorb less energy due to the restriction of vibration aroused from the interaction. 3D networks are formed, which again restrict the motion of those functional groups and therefore, absorption intensities are reduced

The PNVCL-VAc spectra exhibited a band at 1731 cm^{-1}, which corresponds to the C=O (Figure 3-19) stretching of the aliphatic ester group of VAc [204,252]. As illustrated in Figure 3-19, it was noted that there is a decrease in the intensity of the C=O. This reduction in the intensity of the aliphatic ester group of VAc resulted from an increased irradiation dose. The reduction of intensity in the non-hydrogen-bonded C=O may be due to hydrolysis of the aliphatic ester group segment.

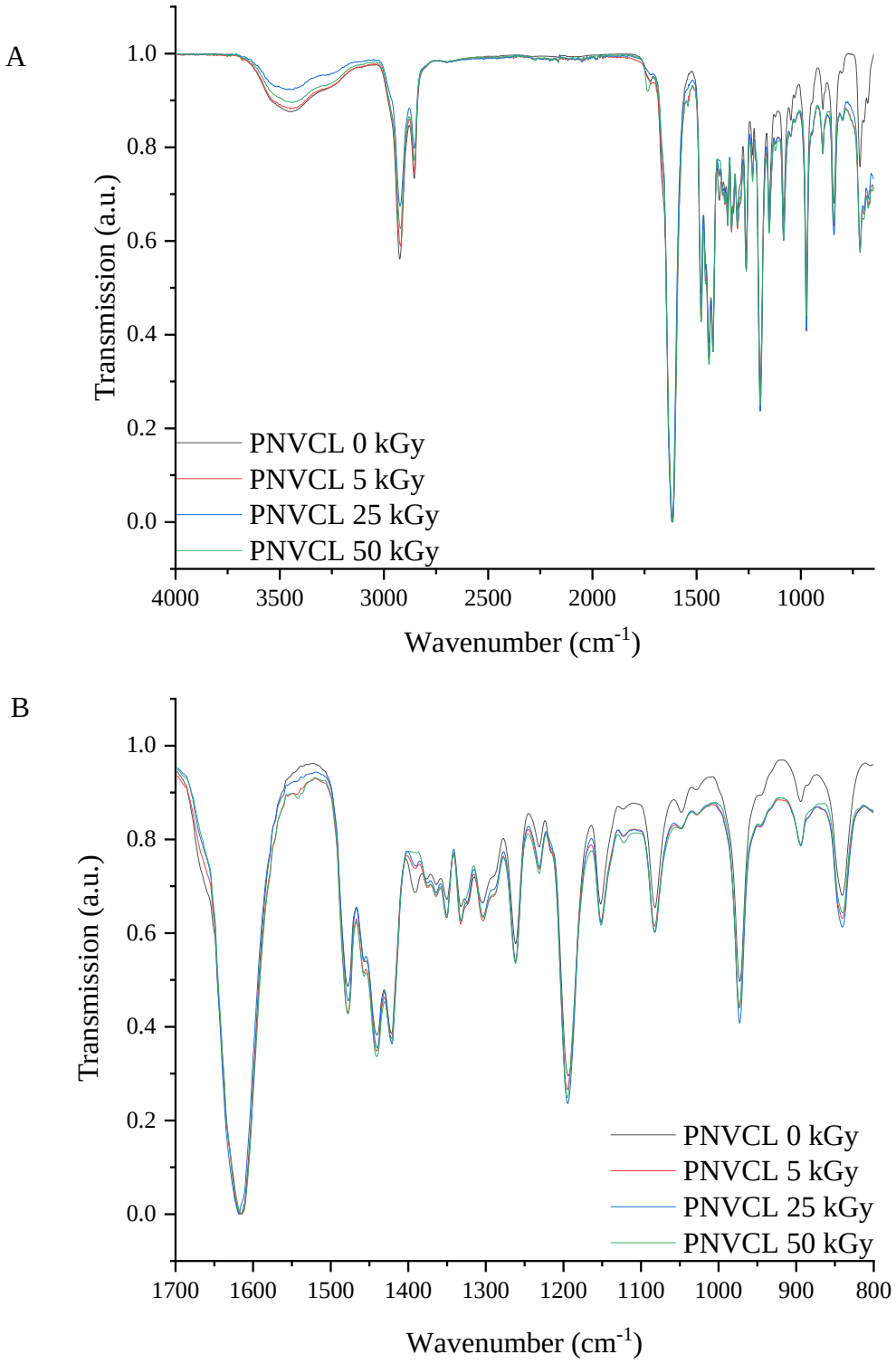

Figure 3-18: Normalised FTIR Spectra normalisation of PNVCL before and after electron beam irradiation at 5, 25 and 50 kGy. A) FTIR spectra of PNVCL B) zoomed section of PNVCL

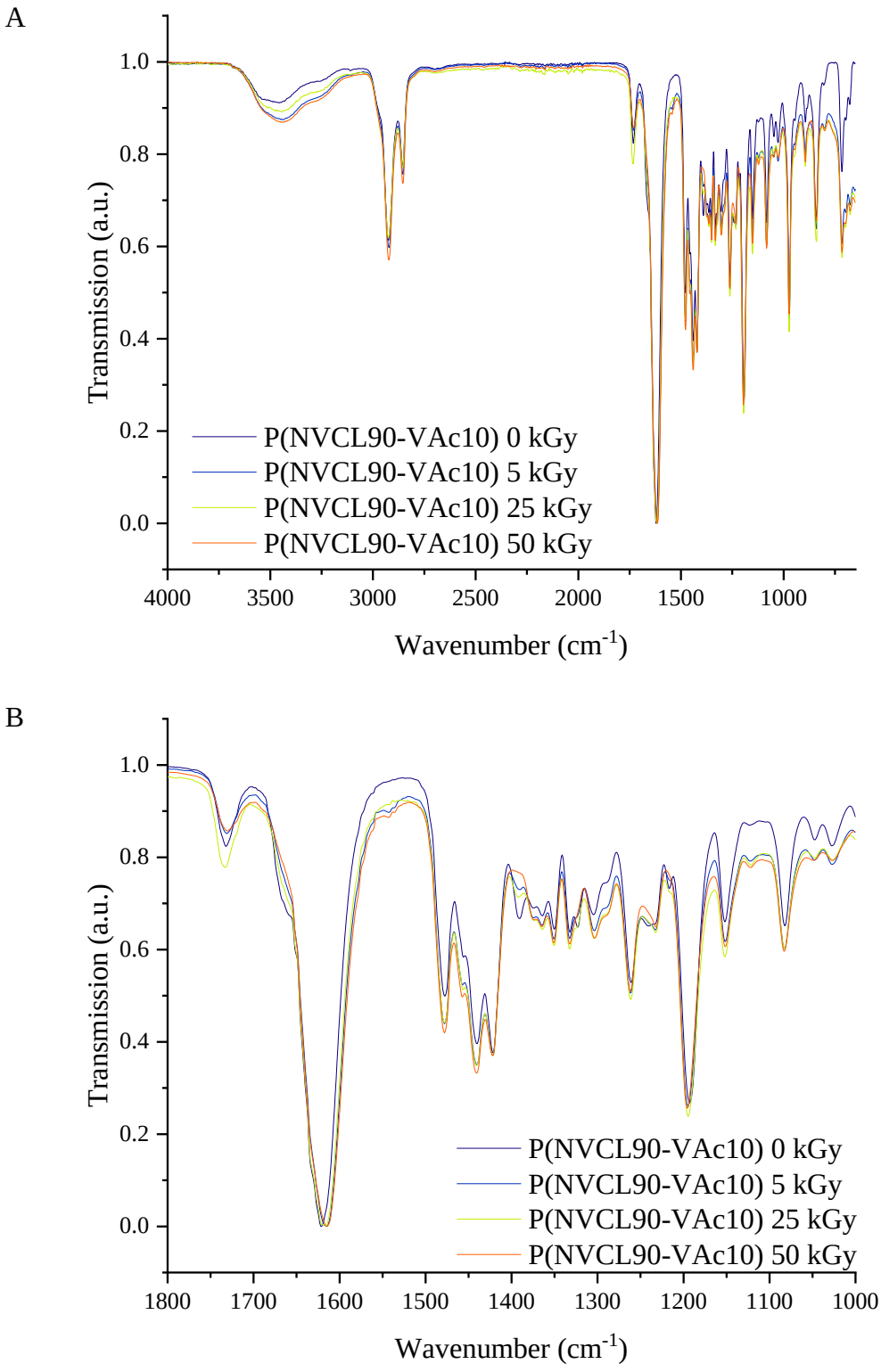

Figure 3-19: Normalised FTIR Spectra normalisation of P(NVCL90-VAc10) copolymer before and after electron beam irradiation at 5, 25 and 50 kGy. A) FTIR spectra of P(NVCL90-VAc10) B) zoomed section of P(NVCL90-VAc10)

Figure 3-20 is the proposed mechanism for cross-linking of irradiated PNVCL polymer. It is assumed that the cross-linking occurs in the vinyl segment of PNVCL. The proposed mechanism of cross-linking for irradiated PNVCL polymer. More advanced techniques such as NMR would be necessary to quantify this further. Overall, electron beam processing samples exhibited a similar reduction in the absorption of the above-mentioned functional groups. These chemical changes, indicate that alteration of the materials mechanical performance may have occurred (crosslinking of polymer materials generally leads to increased stiffness and altered mechanical properties). Therefore, mechanical testing were conducted to determine if changes had occurred and to what extent the material behaviour had been altered [29,238].

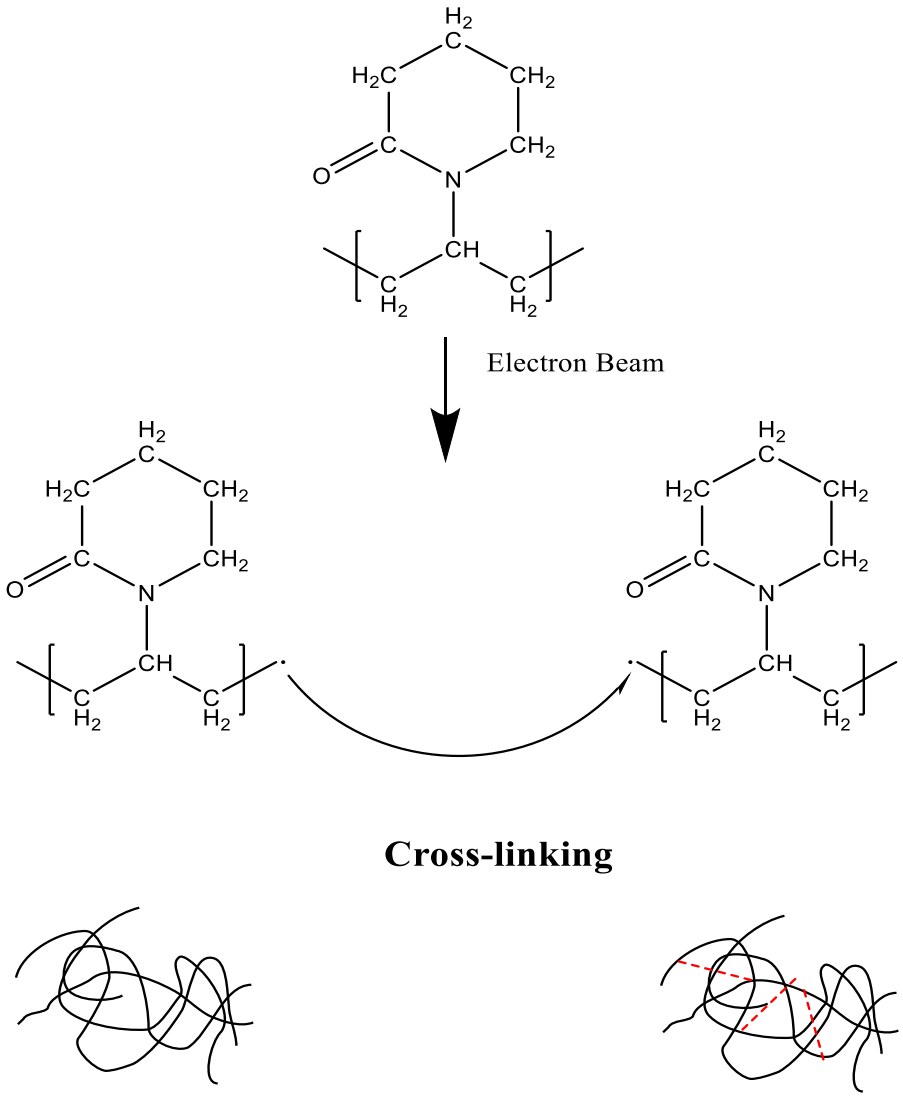

Figure 3-20: Proposed mechanism for cross-linking of irradiated PNVCL polymer.

3.2.4. Dynamic mechanical analysis

PNVCL testing in literature mainly includes several chemical analyses and its behaviour in aqueous solution. However, far fewer studies report the mechanical properties of PNVCL. The mechanical properties of the dry polymer should be taken into account to determine the effect of the electron beam irradiation. Also, this knowledge of PNVCL in a dry state could be useful for transportation and handing purposes for future biomedical applications. Dynamic mechanical analysis (DMA) measurements were conducted over a temperature range of 30-160 ºC for selected samples (0-25 kGy), as 50 kGy samples were too brittle which will be discussed later in the tensile testing analysis (Section 3.2.6.), to examine the effect that electron beam irradiation had on the mechanical properties.

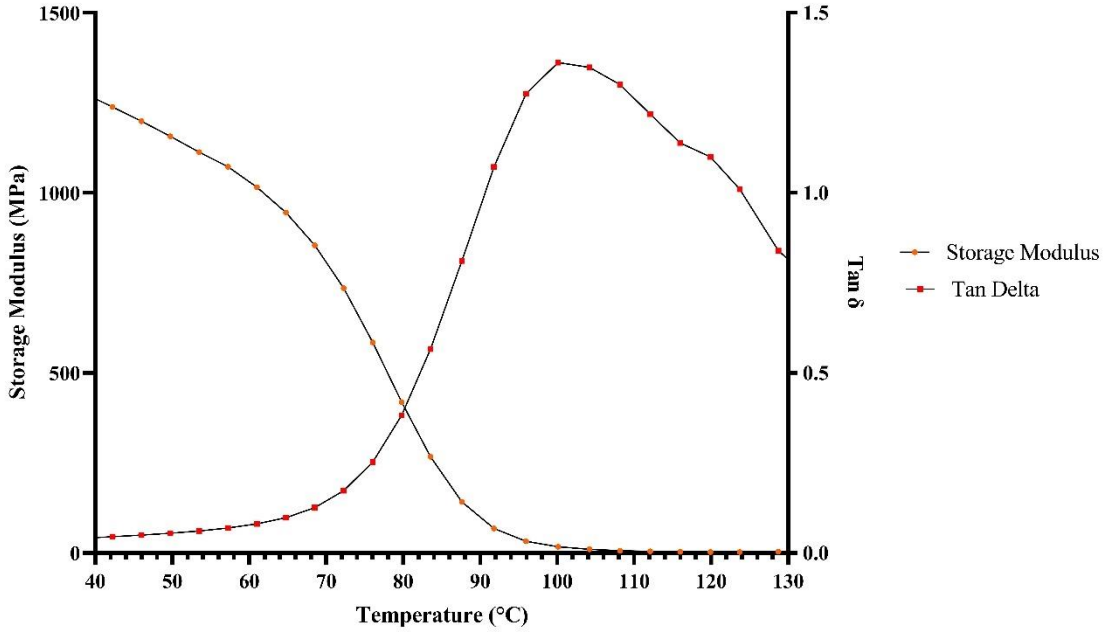

Figure 3-21: The collected data of E′ and tan δ for PNVCL homopolymer. Mean DMA data is presented (n = 2).

All samples tested exhibited a broad transition, which was identified as the linear viscosity-elastic region. DMA measurements for PNVCL, which are presented in Figure 3-21, displays a graph representing the collected data for E′ and Tan δ. The dynamic glass transition temperature (Tg) found that using DMA can be interpreted in three ways. The first is at the temperature of the middle point of storage modulus vs temperature curve.

The second measurement is the maximum temperature which loss modulus occurs, and finally, third is the maximum peak of Tan δ. The glass transition temperature can be described as the temperature range where a polymer changes from a "glassy" rigid or hard state to a more compliant, pliable or a "rubbery" state [253].

Figure 3-22 displays the Storage Modulus (E′) vs temperature for selected samples analysed. Table 3-6 is a summary of the results, it can be observed that, as the temperature increased, the E′ decreased. This is due to a reduction in stiffness, which is the material undergoing a transition from a glassy to a rubbery state. Samples that were irradiated at higher doses resulted in a greater E′, compared to those exposed to lower doses, this is similar to other reports in literature [254]. In the case of PNVCL pre-irradiation (0 kGy), the storage modulus amounted to ~1450 MPa, which increased to ~1550 MPa for a dose of 25 kGy at room temperature.

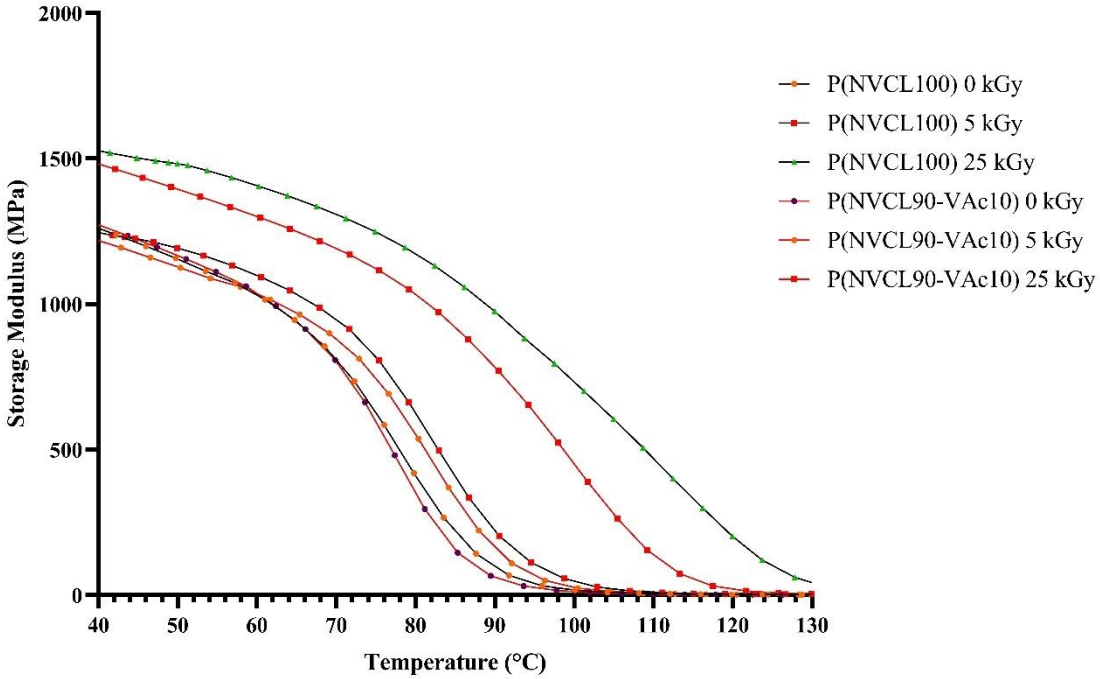

Figure 3-22: Storage Modulus (MPa) reported using DMA measurement. Mean DMA data is presented (n = 2).

The Loss Modulus (E″) vs temperature is displayed in Figure 3-23. E″ relates to energy dissipation within the PNVCL matrix. Therefore, increasing the temperature within the T_g range will result in an increase in the E″. This is a measurement of molecular friction that dissipates most of the force. As the temperature reaches the T_g, there is a

reduction in the molecular friction, resulting in a peak in E″. The increases in E″ for the PNVCL based samples is likely a result of radiation-induced cross-linking, reducing the molecular friction, and causing a slight shift of transition temperature to higher values.

Similar findings were reported by Mansouri *et al.* (2016) who examined the effect of electron beam radiation on polylactic acid (PLA) where an increase in the electron beam dose resulted in an increase in both moduli [254].

Tan Delta should be considered the most important value as this is where the bulk of the glass transition takes place at this value (Table 3-6). Overall, DMA analysis would indicate that cross-linking occurred, and as a result, both modulus storage and loss increased.

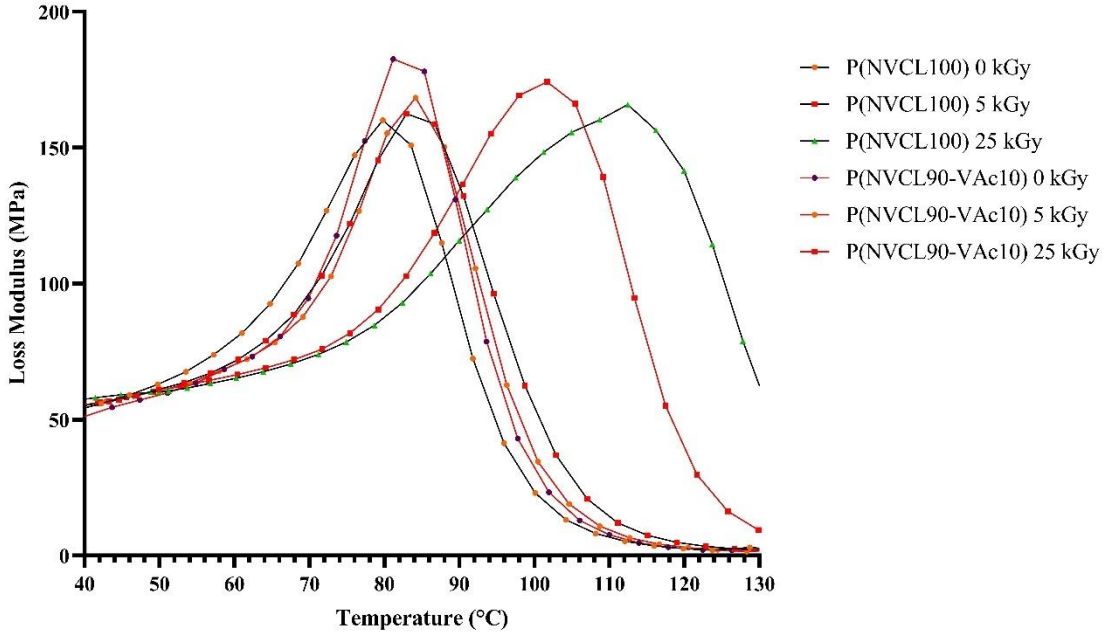

Figure 3-23: Loss Modulus (MPa) reported using DMA measurement. Mean DMA data is presented (n = 2).

Table 3-6: Summary of the results obtained from DMA (n=2) analysis; the dynamic glass transition for the onset of storage modulus and the peak of loss and tan delta modulus

Polymer Code	Storage Modulus range (°C)	Loss Modulus range (°C)	Tan Delta range (°C)
PNVCL 0 kGy	75.0-78.0	78.9-81.5	101.6-103
PNVCL 5 kGy	69.6-71.2	83.2-85.2	107.5-109.7
PNVCL 25 kGy	75.2-77.2	111.0-113.8	153.6-156.6
P(NVCL90-VAc10) 0 kGy	63.5-66.1	78.1-79.5	100.0-101.6
P(NVCL90-VAc10) 5 kGy	68.0-71.2	83.2-85.0	102.6-106.1
P(NVCL90-VAc10) 25 kGy	75.3-81.1	99.2-104.2	123.2-127.8

3.2.5. Swelling studies

Swelling studies below the phase transition temperature (<20 °C) examined the effect of electron beam dose, as physical cross-linked PNVCL swelling behaviour is dependent on temperature. PNVCL is an amorphous polymer, and during the electron beam irradiation process, it has been reported that the amorphous regions of the polymer can experience cross-linking [255]. Figure 3-24 and Figure 3-25 illustrates the swelling behaviour of PNVCL based samples exposed to irradiation doses of between 0 and 50 kGy. Based on the results, the 25 and 50 kGy samples displayed the most significant swelling, which indicates that cross-linking occurred.

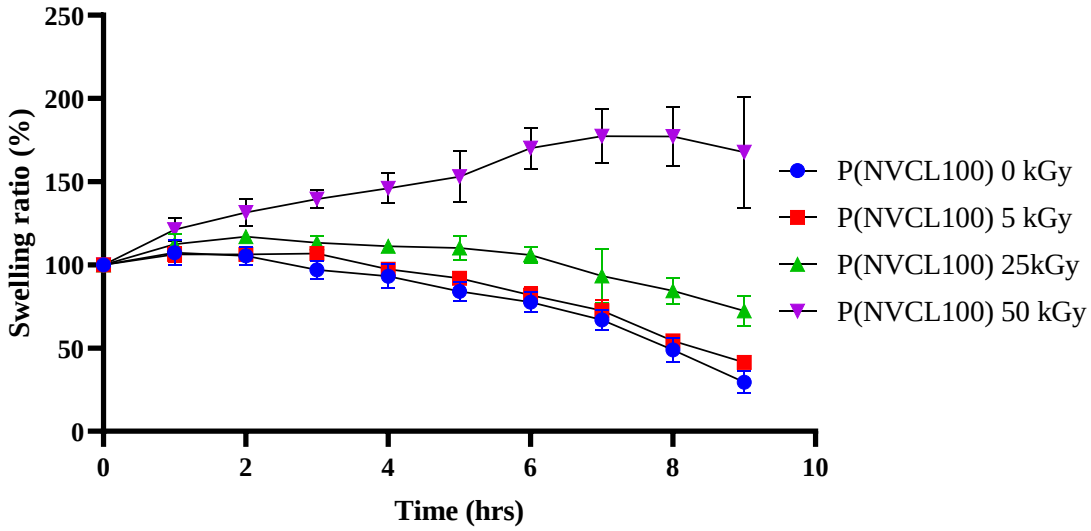

Figure 3-24: Swelling behaviour of PNVCL based samples at different irradiation doses tested at ambient temperature (< 20 °C). Swelling ratio (%) data are presented as mean±SD (n = 3).

In all cases, it was revealed that the swelling percentage was influenced by increasing irradiation dose. The increase in swelling percentage is likely due to the creation of chain branches or cross-link networks that are created through electron beam irradiation and attributed to the production of radiation free radicals. The creation of these cross-links was formed through hydrogen bonds during the electron beam process. The cross-links affected the entanglements of PNVCL chains, leading to an increased swelling ratio with an increase in irradiation dose. The results indicate that, initially, the swelling process for PNVCL based samples occurred primarily due to the water penetrating through capillarity and diffusion processes [256]. As outlined in Section 3.2.5, it was found that increasing the VAc content decreased the swelling ratio. However, in this body of work, increasing the electron beam dose lead to an increased swelling ratio and extended the breakdown rate.

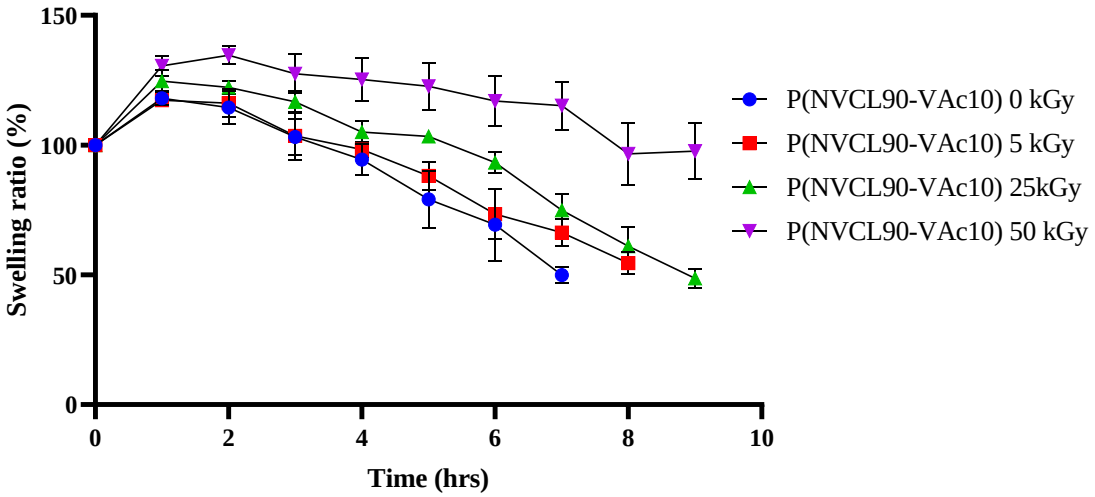

Figure 3-25: Swelling behaviour of PNVCL/VAc based samples at different irradiation doses tested at ambient temperature (< 20 °C). Swelling ratio (%) data are presented as mean±SD (n = 3).

Sharma *et al.* (2014) reported similar findings when studying the effects of gamma irradiation on Poly (acrylamide-aniline)-grafted gum ghatti hydrogels. The study indicated that increasing the irradiation dose increased the percent of swelling [257].

Cairns *et al.* (2011) stated that electron beam treatment could be used to control degradation profiles of poly (lactic acid). In the aforementioned study, the samples broke down more rapidly in aqueous media following electron beam exposure. It is therefore essential to carry out detailed testing on samples following electron beam or other sterilisation processes, as such processes can result in chain scission which can result in quicker breakdown rates of samples, or cross-linking which often results in extended breakdown rates [258].

3.2.6. Tensile testing

Tensile testing was used to analyse further the effect of electron beam irradiation on the mechanical properties of novel PNVCL samples. The Young's modulus, tensile strength, and percentage elongation of all PNVCL samples was to investigate further what effect electron beam exposure had on the materials. Based on the stress-strain measurements of the polymer, Young's modulus was used to confirm that the stiffness value for PNVCL based polymers increased as the irradiated dose increased (Figure 3-26).

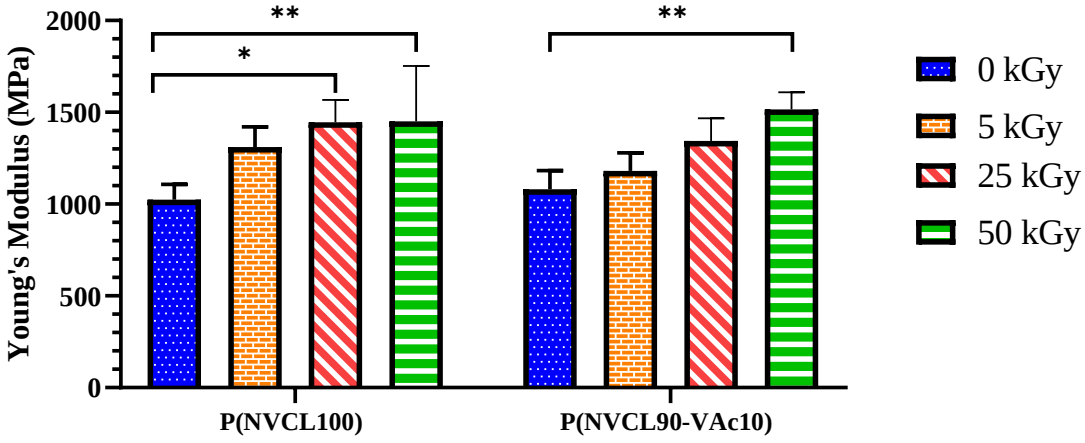

Figure 3-26: Statistical analysis of the interaction of electron beam irradiation on the irradiated samples measured by tensile testing. Young's Modulus (MPa) data are presented as mean±SD (n = 5). One-way ANOVA followed by Tukey multiple comparison test. Significantly different * $p < 0.05$; ** $p < 0.01$ and *** $p < 0.001$ vs. non-irradiated samples.

The tensile strength of all samples increased until they reached 25 kGy; at this point, a sharp decrease was demonstrated (Figure 3-28). Due to cross-linking, the

formation of 3-D networks can lead to an increase in tensile strength properties [235,259], though highly cross-linked structures can become more brittle, which was the case for 50 kGy samples. This would explain why 50 kGy samples were too brittle for use in the DMA analysis (Section 3.2.4.).

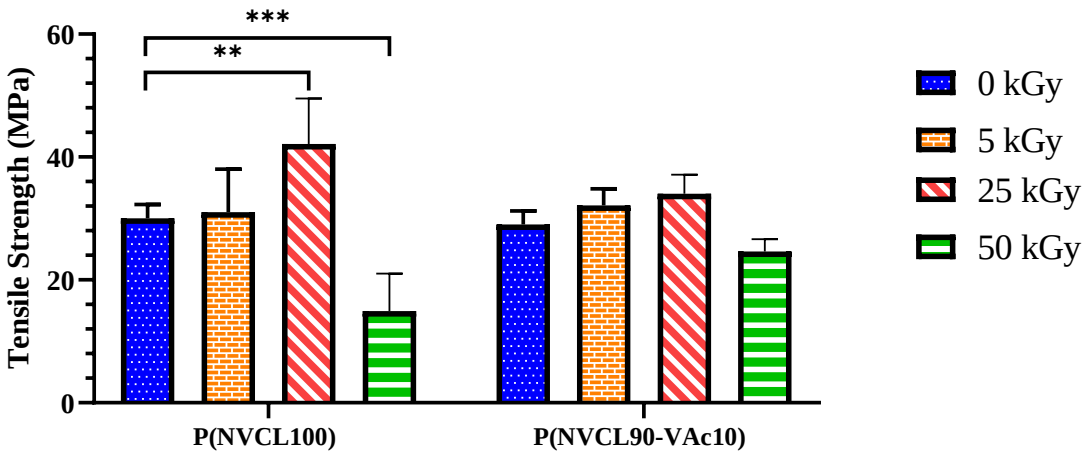

Figure 3-27: Statistical analysis of the interaction of electron beam irradiation on the irradiated samples measured by tensile testing. Tensile strength (MPa) data are presented as mean±SD (n = 5). One-way ANOVA followed by Tukey multiple comparison test. Significantly different ** $p < 0.01$ and *** $p < 0.001$ vs. non-irradiated samples.

Figure 3-28 illustrates the percentage elongation at break as a function of irradiated dose for PNVCL samples. The results show a decrease amongst all irradiated samples, in contrast to the control samples (0 kGy) for elongation at break. In the case of the 50 kGy samples, another sharp decrease was displayed. This was perhaps related to chain stretching of the PNVCL material because of an increase in the cross-link density. Chain stretching has been reported in other polymeric materials such as LDPE, following exposure to electron beam irradiation [260]. Table 3-7 provides a summary, tensile strength generally increased, with increasing dose of electron beam irradiation.

Figure 3-29 is a typical example of PNVCL samples after a tensile test. All samples broke within the gauge length. It is noted that at the highest dose of electron beam irradiation, samples PNVCL 50 kGy and PNVCL & VAc 50 kGy displayed a decrease in tensile strength and elongation at break.

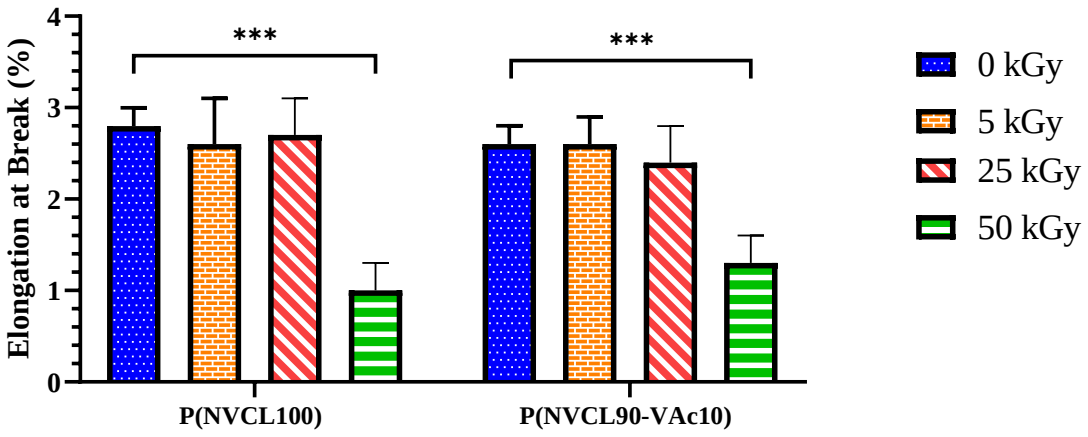

Figure 3-28: Statistical analysis of the interaction of electron beam irradiation on the irradiated samples measured by tensile testing. Elongation at break (%) data are presented as mean±SD (n = 5). One-way ANOVA followed by Tukey multiple comparison test. Significantly different *** $p < 0.001$ vs. non-irradiated samples.

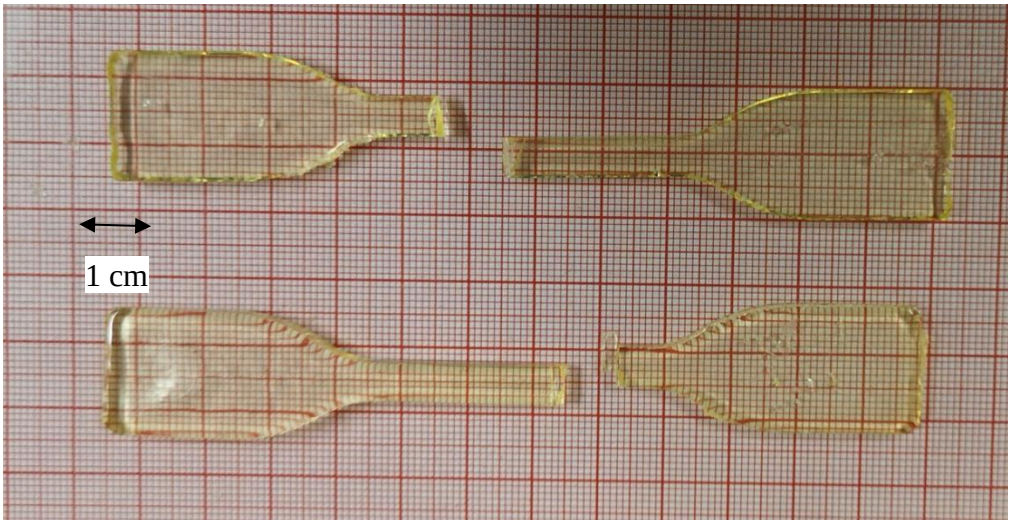

Figure 3-29: Typical example of tensile test samples after the break (PNVCL 0 kGy).

Tensile testing data revealed that the mechanical properties of PNVCL based samples were likely enhanced due to radiation cross-linking/branching, up until a critical point where mechanical properties exhibited a sharp decline. Once again, it is noteworthy that even at lower irradiation doses, obvious changes were observed in mechanical performance properties.

Table 3-7: Data collected for the mechanical testing of PNVCL based samples, data is presented as mean± relative standard deviation (RSD) (n = 5).

Polymer Code	Young's Modulus (MPa)	Relative standard deviation (%)	Tensile Strength (MPa)	Relative standard deviation (%)	Elongation at Break (%)	Relative standard deviation (%)
P(NVCL100) 0 kGy	1024.3	8.2	30	7.7	2.8	6.5
P(NVCL100) 5 kGy	1310.9	10.8	31	23.3	2.6	18.9
P(NVCL100) 25 kGy	1445.1	11.9	42.1	24.7	2.7	14.8
P(NVCL100) 50 kGy	1451.5	29.3	14.9	20.3	1	20.0
P(NVCL90-VAc10) 0 kGy	1081.5	9.8	29	7.3	2.6	7.7
P(NVCL90-VAc10) 5 kGy	1181.6	9.5	32.1	9.0	2.6	11.5
P(NVCL90-VAc10) 25 kGy	1344.1	12.1	34	10.3	2.4	16.7
P(NVCL90-VAc10) 50 kGy	1516.4	9.0	24.6	6.7	1.3	23.1

3.2.7. Differential scanning calorimetry

DSC measurements were conducted on the samples over a temperature range of 20-200 ºC for all samples. One broad transition was observed between 100-200 ºC for all non-irradiated and irradiated PNVCL samples. This transition was identified as the glass transition temperature (T_g). The irradiated samples showed an increase in T_g values, compared to non-irradiated samples. This is likely due to cross-linking occurring during electron beam exposure. The proposed cross-linking/side branching that occurred in PNVCL increased the molecular weight of the polymer, which would result in a more rigid structure, as discussed in Section 3.2.6. Figure 3-30 illustrates the glass transition temperatures for PNVCL based polymer samples at different irradiation doses. The proposed cross-linking/side branching in the polymers brings about a restriction in movement of the polymer chains. Similar trends were reported in Section 3.2.4 with regards to DMA analysis. Both the static (DSC) and dynamic glass transition temperature (DMA) exhibited an increase. This is further evidence that is branching or cross-linking is likely to have had occurred within the PNVCL samples.

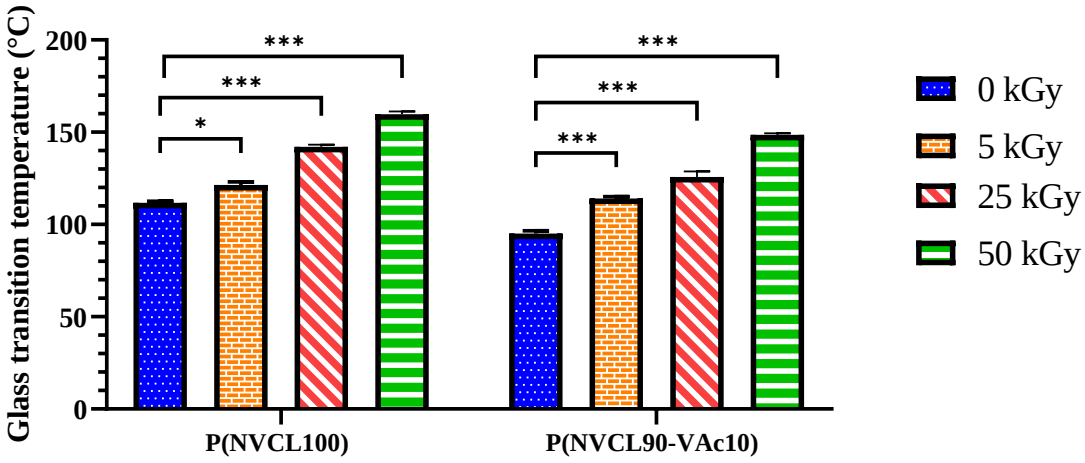

Figure 3-30: Statistical analysis of the interaction of electron beam irradiation on the irradiated samples measured by differential scanning calorimetry. Glass transition temperature (ºC) data are presented as mean±SD (n = 3). One-way ANOVA followed by Tukey multiple comparison test. Significantly different ** $p < 0.01$ and *** $p < 0.001$ vs. non-irradiated samples.

Shifting of the T_g to higher temperatures is another clear indication that cross-linking\side branching was induced by the irradiation of the PNVCL samples [211,212,261]. Any differences in T_g compared to literature can be associated with various factors, with M_w often cited as one of the significant contributors [213]. Other literature states that such radiation-induced reactions that cause an increase in the T_g may be a result of increased M_w and increased cross-link density among different regions of samples [262,263]. Similar trends were exhibited for both the homopolymer and novel copolymers in this study.

3.2.8. Melt Rheology

Melt rheology was conducted on non-irradiated and irradiated PNVCL based samples to determine the rheological properties. Melt rheology can be used to investigate the entanglements of the polymer. Therefore melt rheology was used to examine the effects of the electron beam. As previously discussed, side branching \ cross-linking occurs during the electron beam processing, which could result in an increased storage modulus. Also, rheological tests are sensitive to molecular chain entanglements or chain structure, such as small differences in chain length, branching or network, and these factors can cause large variations in flow behaviour [264]. To investigate the nature of the side branching \ cross-linking the relationship between G' (Storage modulus) and G'' (Loss modulus) was studied. The storage and loss modulus for parallel-plate rheology is determined as follows:

$$G' = \frac{2hM_0\cos\delta}{\pi r^4\phi_0} \qquad \text{Equation 3-5}$$

$$G'' = \frac{2hM_0\sin\delta}{\pi r^4\phi_0} \qquad \text{Equation 3-6}$$

Where ϕ_0 is the angular amplitude of oscillation, and M_0 is torque amplitude, and δ is the phase angle that represents the time-dependent behaviour of the viscoelastic material. Dynamic frequency sweeps were carried out in the viscoelastic region in order to study the microstructural changes and network formation of the PNVCL based samples while using the non-irradiated samples as the baseline. The frequency sweep was conducted at a percentage strain of 2%, which was within the linear viscoelastic region. All PNVCL samples were tested within a frequency range from 0.1 to 100 rad/s. The

dynamic frequency sweep scan measurements at 200 °C provided the data to plot graphs of G′, G″ and η* versus angular frequency (ω). Figure 3-31 and Figure 3-32 displays the relationship between G′ and ω, showing an increase in G′ as the radiation dose increased. There was a slight difference between the 0 and 5 kGy irradiated samples. However, between 5-50 kGy, a significant increase for G′ was noted. When a polymer is deformed at high angular frequencies, the entangled polymer chains do not have time to relax, so the modulus rises [265]. Overall the increase in *G′* indicates an intensification in side branching/cross-linking of PNVCL.

Complex viscosity (η∗) vs ω of the irradiated and non-irradiated PNVCL samples was measured from the G′ and G″ moduli and the angular frequency ω; the complex viscosity was calculated as:

$$|\eta^*| = \sqrt{\frac{(G'/\omega)^2}{(G''/\omega)^2}} \qquad \text{Equation 3-7}$$

Increasing the irradiation dose resulted in a decrease in η∗ , which correlates with findings in the literature for other polymers exposed to electron beam radiation [235,238,266]. With increasing ω, shear-thinning behaviour was displayed by the PNVCL samples (Figure 3-33 and Figure 3-34).

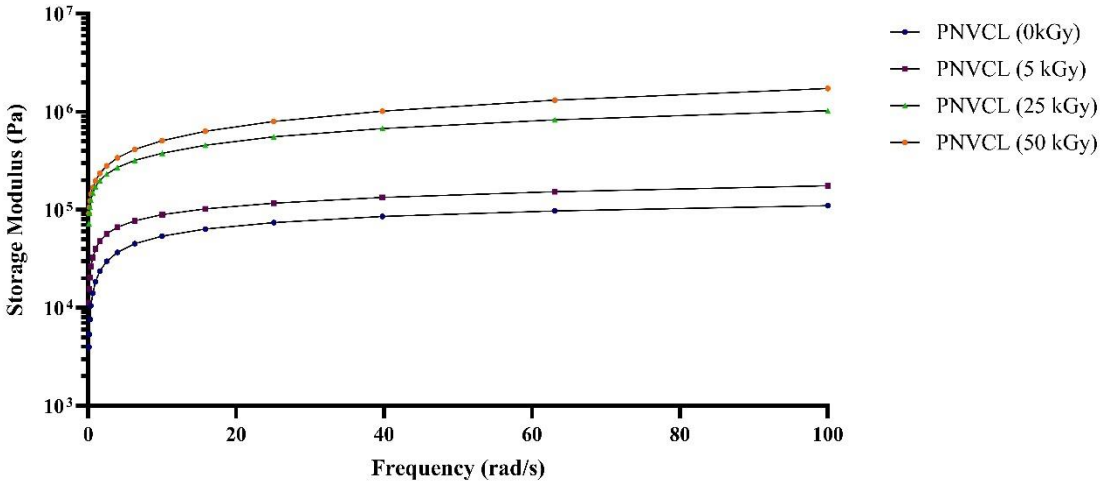

Figure 3-31: Storage modulus for PNVCL based samples Melt rheology storage modulus (Pa). Mean rheological data is presented (n = 2).

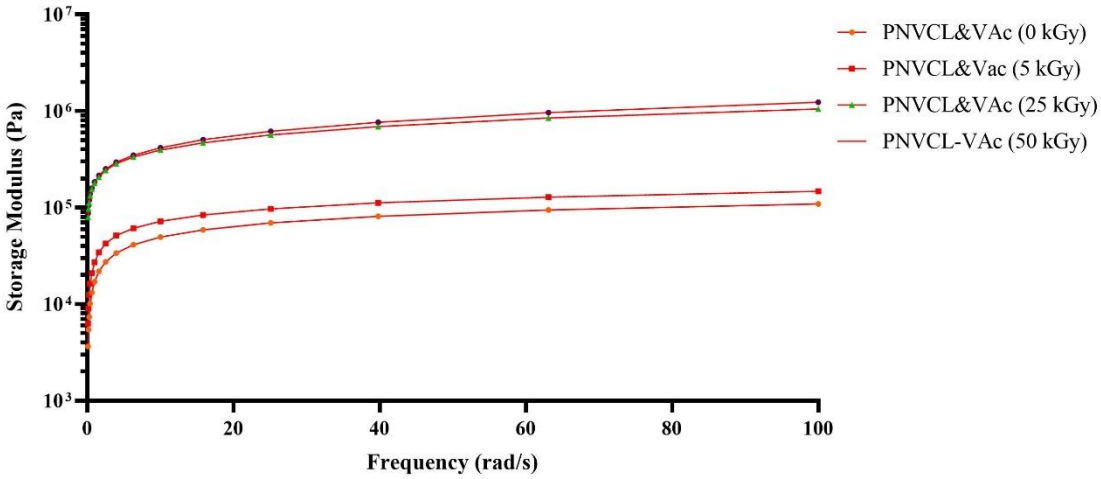

Figure 3-32: Storage modulus for PNVCL and VAc based samples. Melt rheology storage modulus (Pa). Mean rheological data is presented (n = 2).

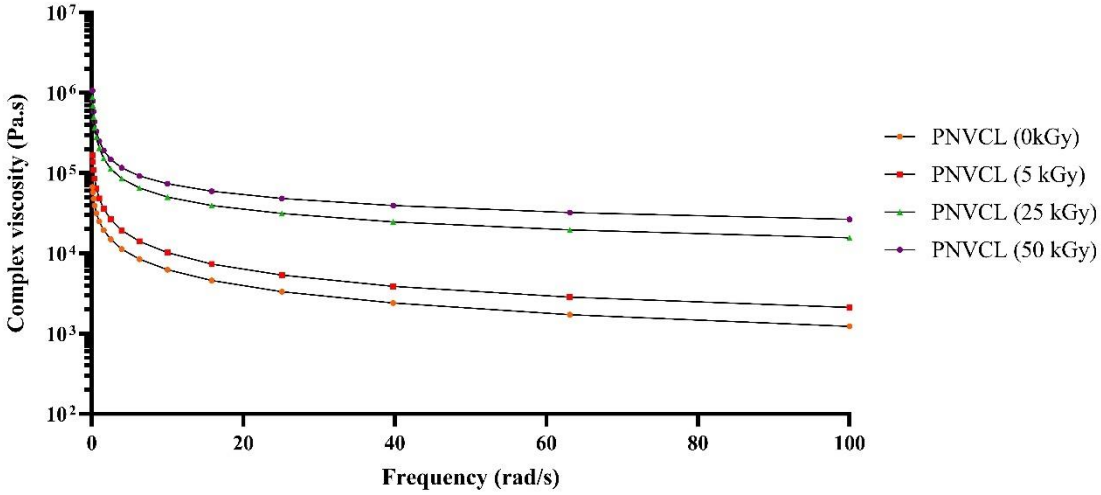

Figure 3-33: Complex viscosity versus angular frequency for non-irradiated and irradiated PNVCL based samples. Melt rheology complex viscosity (Pa.s). Mean rheological data is presented (n = 2).

Furthermore, in the low ω region of these pseudo-plastics, all the irradiated and non-irradiated samples can be classified as non-Newtonian, as they were dependent on

the shear rate to increase the viscosity [238]. In summary, it would appear that cross-linking/branching was existent for samples following electron beam exposure, which led to broadening of the molecular weight distribution, thus resulting in a decrease in the complex viscosity at high angular frequencies.

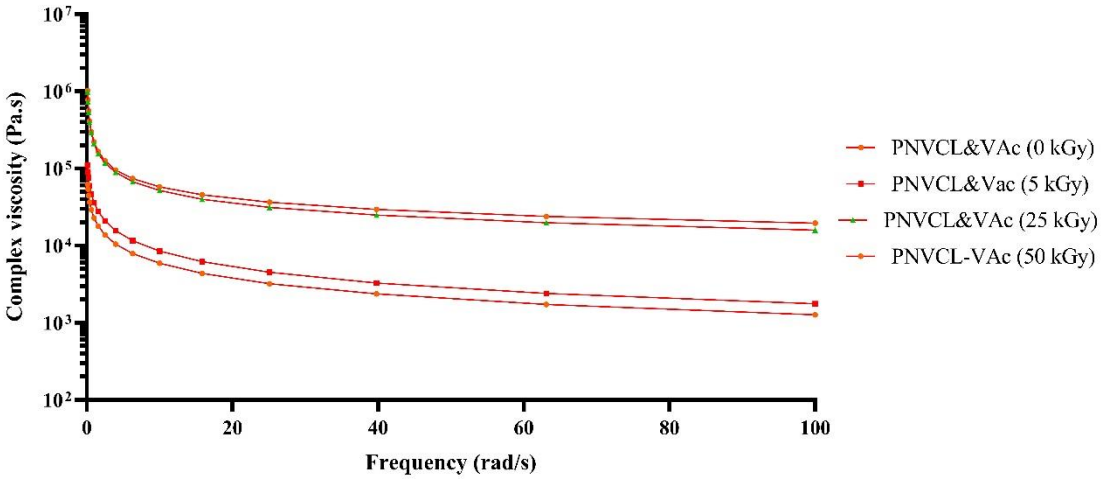

Figure 3-34: Complex viscosity versus angular frequency for non-irradiated and irradiated PNVCL and VAc based samples. Melt rheology complex viscosity (Pa.s). Mean rheological data is presented (n = 2).

3.2.9. Gel Permeation Chromatography

Gel Permeation Chromatography (GPC) analysis was conducted on all PNVCL based samples. Values from the unknown PNVCL samples are compared with the calibration graph to generate molecular weights and molecular weight averages with an (R^2) value of 0.9836. Table 3-8 summarises the results obtained using GPC measurement. Altering the irradiation dose led to an increase in the M_w. It is highly important to control the M_w and PDI, as the LCST of PNVCL is reported to be M_w dependent [218]. However, it has been reported the addition of a hydrophobic monomer such as vinyl acetate (VAc) can reduce the LCST from 32 °C to 26.5 °C as the content of VAc increases [267]. A typical GPC graph can be seen below in Figure 3-35. The GPC results revealed an increase in the average molecular weight when the irradiation dose increased. However, PNVCL 25 kGy and PNVCL 50 kGy samples (Table 3-8) are not displayed, as irradiated PNVCL's M_w is close to the detection limit of the GPC/column, preventing accurate determination for such samples. A similar finding was reported in the case of irradiation

of PNVCL homopolymer, whereby high irradiation doses led to difficulties in determining the M_w of PNVCL using GPC [268].

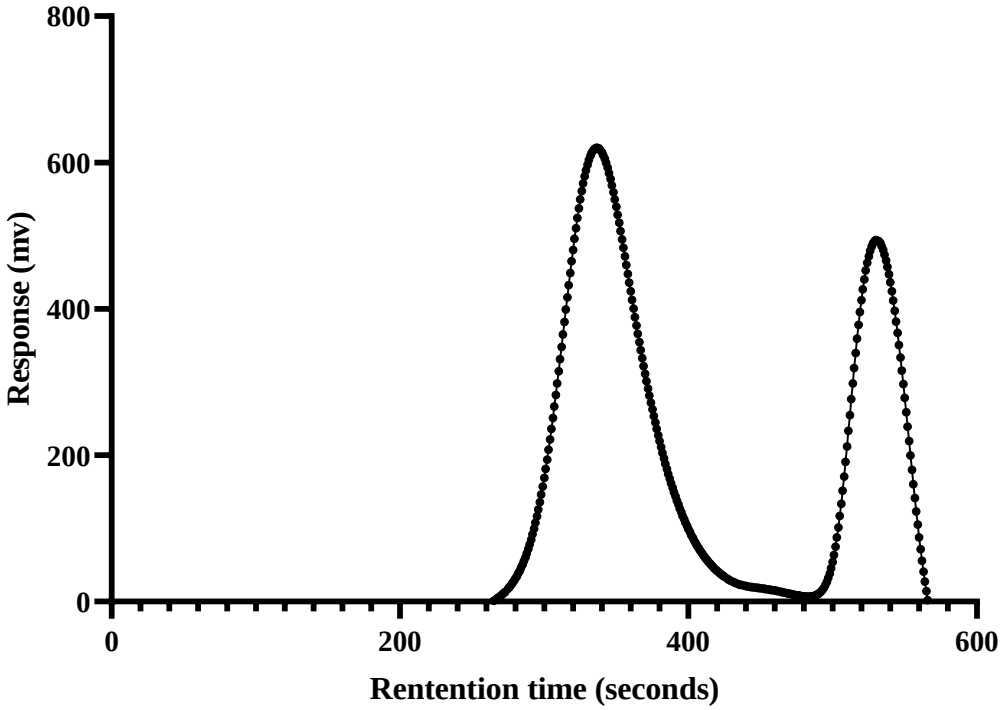

Figure 3-35: A typical GPC graph for PNVCL based samples.

Lim *et al*. (2007) grafted poly (*N*-vinylcaprolactam-co-*N*-isopropylacrylamide) (PNVCL-co-PNIPAm) onto tissue culture polystyrene (TCPS) by electron beam irradiation. Their results illustrated that with a change in temperature, the polymers could alter hydrophilic and hydrophobic surface properties. Above the LCST (37 °C), the surface was hydrophobic and cell-adhesive; below the LCST (32 °C), the surface changed to hydrophilic and was not cell adhesive, with no damage to the detached cells [269].

In summary, altering PNVCL molecular weight by electron beam exposure thus offers enormous potential benefits for biomedical applications such as drug delivery, cell detachment, and entrapment of enzymes, as even low electron beam irradiation doses can have significant effects on materials properties, and this should be given due consideration in the early stages of drug delivery system and medical device development. This study highlights the potential of modulating the M_w of novel polymers based on PNVCL, using electron beam irradiation. It is also very interesting to note the significant increases in M_w even at low irradiation doses, which are typically used in the sterilisation of medical devices. Given the critical relationship between the M_w and the LCST of

PNVCL, such analysis would thus be essential in medical device development and would be critically important particularly for thermogelling applications, as changes in M_w could significantly affect the gelling temperature.

Table 3-8: Molecular number (M_n), molecular weight (M_w) and polydispersity (PDI) results for irradiated PNVCL based samples.

Polymer Code	M_n	M_w	PDI
PNVCL 0 kGy	12291	167974	13.6
PNVCL 5kGy	12566	172805	13.7
PNVCL 25 kGy	NA	NA	NA
PNVCL 50 kGy	NA	NA	NA
P(NVCL90-VAc10) 0 kGy	20658	239484	11.5
P(NVCL90-VAc10) 5 kGy	19509	271888	15.2
P(NVCL90-VAc10) 25 kGy	11716	298177	23.2
P(NVCL90-VAc10) 50 kGy	13016	424907	32.6

3.2.10. Colourimetry

Colourimetry measurements were conducted on the PNVCL based samples before and after the irradiation process (Figure 3-36). The exposure rate of the electron beam irradiated samples ranged from between 0 and 50 kGy. The Hunter *b* value demonstrated an increase from -0.60 to 37.01 as the electron beam irradiation dose increased. Consequently, the irradiated samples became more yellowish. For the PNVCL-VAc copolymer sample (0 kGy), the Hunter *b* value was -0.03. However, with an increase in irradiation dose, notable differences between samples was observed, with increases in ΔE values for all irradiated specimens. An explanation for such changes after exposure to irradiation could be related to the entrapment of free-radicals [270]. Murray *et al*. (2016) found that with an increase in the electron beam dose (50 kGy) an overall colour change (ΔE) occurred, for polyether-block-amide (PEBA) samples [29]. Figure 3-36 provides an overview of the Hunter *b* value obtained from the colourimetry measurement. Overall in Table 3-9 it is displayed that colourimetry measurements indicate that PNVCL homopolymer and its copolymers with VAc are sensitive to electron beam processing, which led to discolouration in the samples. It was noted that samples containing VAc displayed less colour change at high irradiation doses when compared to the homopolymer. Such colour changes can be indicative of polymer degradation, however as shown in the previous sections in many cases, mechanical properties were enhanced.

That said, colour changes such as those displayed at the higher irradiation doses would be highly undesirable, especially for medical device products and drug delivery systems; thus, such analysis is of great importance.

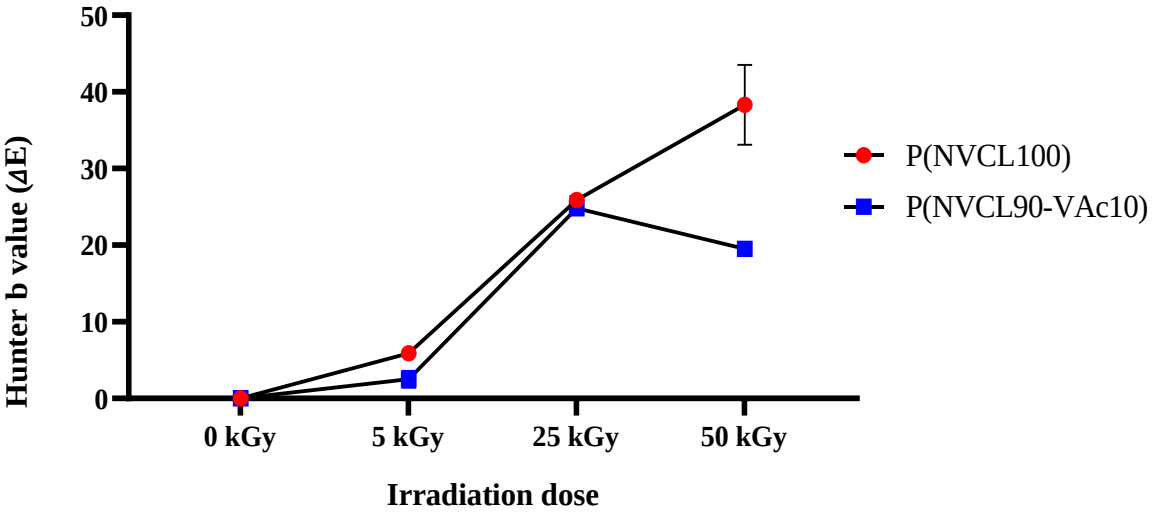

Figure 3-36: *ΔE* values versus E-beam irradiation dose for PNVCL based samples. Colourimetry measurements Hunter b value (ΔE) data are presented as mean±SD (n = 10).

Table 3-9: Colorimetry measurement of PNVCL based samples are presented as mean±SD (n = 10).

Polymer Code	L*	a*	b*	ΔE
P(NVCL100) 0 kGy	82.1±0.0	-0.01±0.0	-0.6±0.0	0±0.0
P(NVCL100) 5 kGy	84.2±3.1	-0.4±0.1	3.9±2.2	5.89±0.9
P(NVCL100) 25 kGy	66.1±0.3	0.6±0.1	19.7±0.4	25.9±0.5
P(NVCL100) 50 kGy	75.5±0.7	3.2±1.2	37.0±5.2	38.3±5.2
P(NVCL90-VAc10) 0 kGy	82.6±0.0	-0.1±0.0	-0.03±0.0	0.0±0.0
P(NVCL90-VAc10) 5 kGy	84.3±0.2	-0.3±0.1	1.1±2.0	2.5±1.1
P(NVCL90-VAc10) 25 kGy	65.9±0.1	-0.5±0.1	18.4±0.4	24.8±0.3
P(NVCL90-VAc10) 50 kGy	77.5±1.7	-1.0±0.0	18.7±0.4	19.5±0.6

3.2.11. Shore D Hardness

Figure 3-37 illustrates the results obtained from the Shore D hardness test for the non-irradiated and irradiated PNVCL based samples. All samples were tested for a period of 30 seconds at room temperature.

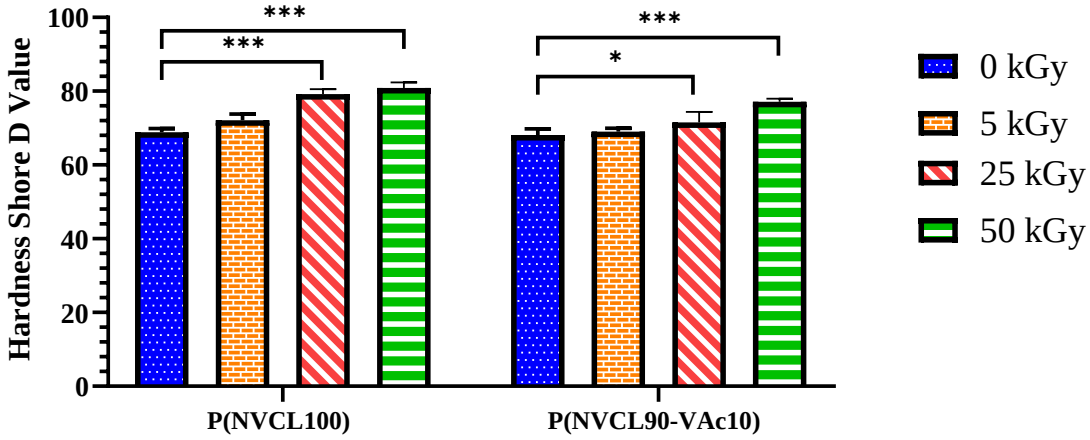

Figure 3-37: Statistical analysis of the interaction of electron beam irradiation on the irradiated samples measured by Shore D Hardness. Shore D data are presented as mean±SD (n = 10). One-way ANOVA followed by Tukey multiple comparison test. Significantly different ** $p < 0.01$ and *** $p < 0.001$ vs. non-irradiated samples.

The penetration depth-averaged between 68.9 and 97.2 D scale. Overall, there were statistically significant differences between samples at 25-50 kGy dose for PNVCL. However, in regards to samples that were dosed at 5 kGy, there were no significant differences between sample means ($P>0.05$) in the copolymer compared with non-irradiated PNVCL based samples. Based on these results, the increase in the hardness of the material is likely related to the formation of side branching or cross-linking.

3.2.12. Phase transition determination

3.2.12.1. UV-spectrometry

UV-spectroscopic measurement was carried out to observe the effects of the electron beam irradiation on PNVCL based samples phase transition temperature. The LCST of PNVCL can be altered by adjusting its molecular weight [170,208]. For

example, increases in M_w have been reported to result in a decreased phase transition, [191]. The current study indicates that exposing PNVCL based samples to electron beam irradiation increased the polymer chain length, as outlined in the previous sections. This, in turn, resulted in a decrease in phase transition upon polymer molecular weight increase, similar results were also seen in sol-gel transition measurements. It was also noted that the phase transition of PNVCL based samples was dependent on the irradiation dose as presented below in Figure 3-38, additionally, similar trends were found for rheological measurement (Section 3.2.12.2.). For non-irradiated PNVCL, the phase transition was within the range previously reported [42,217,218].

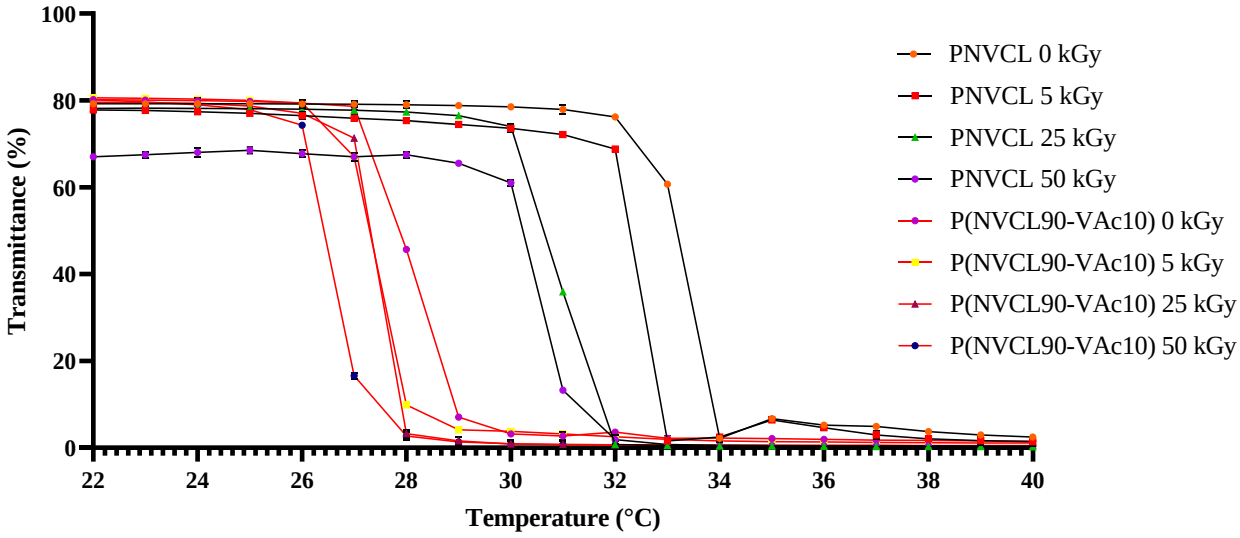

Figure 3-38: UV-spectroscopic measurement illustrating the phase transition of PNVCL based samples (5 wt%) at different radiation doses. UV-spectroscopy data are presented as mean±SD (n = 3).

These results imply that PNVCL matches Type 1 Flory-Huggins demixing behaviour, which states that increased molecular weight results in a decrease in phase transition temperature [23]. These results are in agreement with the results obtained in the previous sections. To date, this is the first study to report the adjustment of PNVCL phase transition using industrial-scale electron beam irradiation, under typical conditions for sterilising medical devices and also at higher irradiation doses. These findings are of great importance given the crucial role of the phase transition in many potential PNVCL based medical devices, and drug delivery systems, particularly as the LCST was significantly

reduced even at low irradiation doses typically in the range used for medical device sterilisation.

3.2.12.2. Sol-gel transition

The sol-gel transition for PNVCL based samples was measured using the tube inversion method (Figure 3-39) and rheological analysis (Figure 3-40) to examine the effects of electron beam irradiation on the polymers phase transitions, the results of which are summarised in Table 3-10. The transition temperatures were determined using a flow (sol)-no flow (gel) principle with a temperature increment of 1 °C per step for both methods.

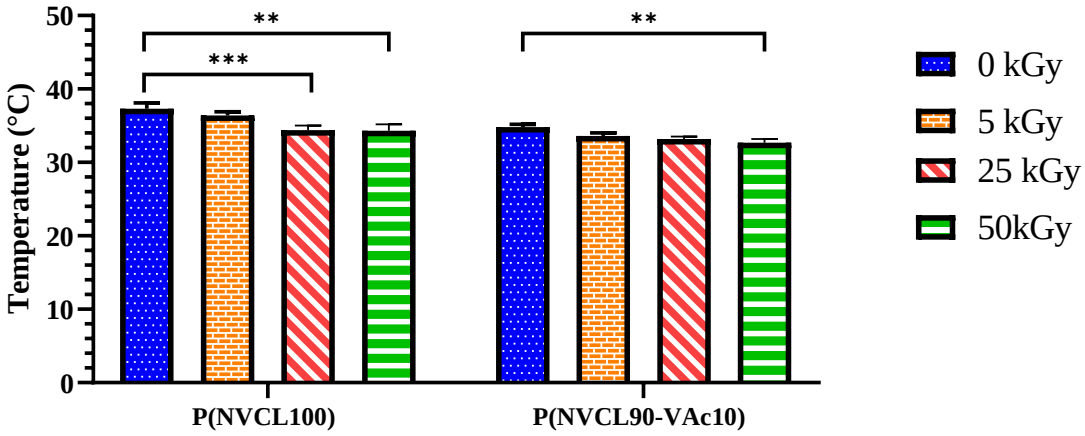

Figure 3-39: Statistical analysis of the interaction of electron beam irradiation on the irradiated samples measured by sol-gel transition measurement. Thermogelling data are presented as mean±SD (n = 5). One-way ANOVA followed by Tukey multiple comparison test. Significantly different ** $p < 0.01$ and *** $p < 0.001$ vs. non-irradiated samples.

The thermogelling capabilities of PNVCL were found to be affected by the electron beam process. This is a result that is advantageous for biomedical applications [226], as having the ability to control the molecular weight of the PNVCL post polymerisation is desirable. Similar trends were established using the sol-gel method in comparison to the results obtained for LCST (Table 3-10).

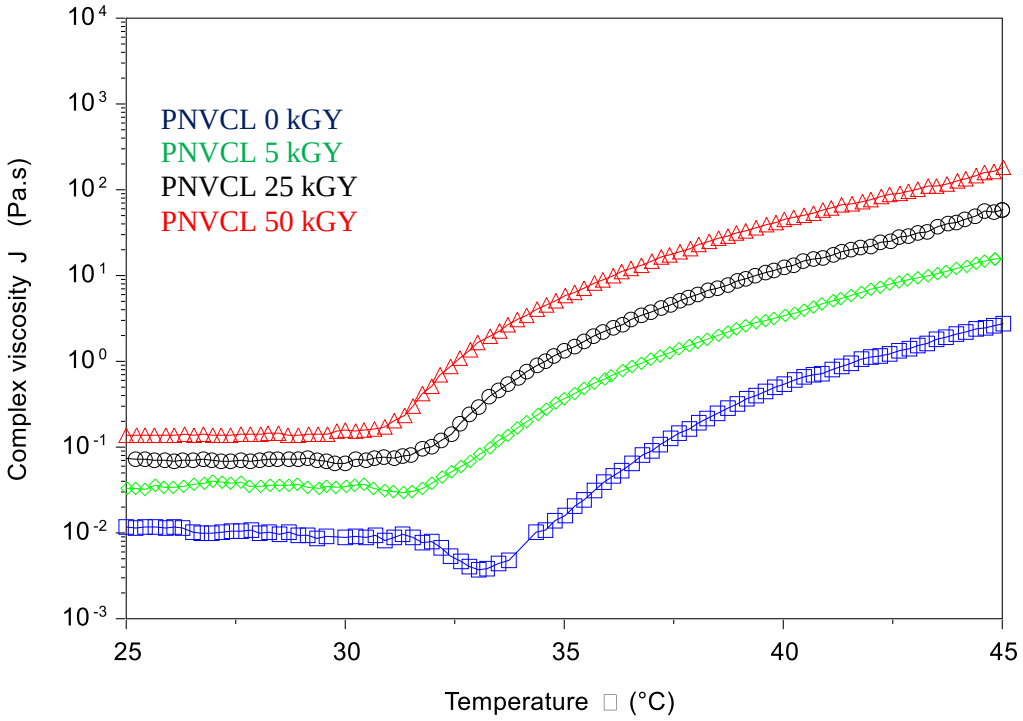

Figure 3-40: Complex viscosity vs temperature for PNVCL based samples at different electron beam doses.

The rheological analysis was used to examine the effects of the polymer in aqueous solutions. All of the samples exhibited a transition that was identified as the LCST and/or Sol-gel transition between 25 and 45 °C. Samples containing VAc displayed a slightly lower sol-gel transition temperature compared to PNVCL homopolymer samples, which is due to the incorporated VAc hydrophobic segment. Figure 3-40 displays a representative diagram for PNVCL (0 kGy) and PNVCL (5, 25 and 50 kGy), whereby it can be seen that, with an increase in the electron beam dose, the complex viscosity of the PNVCL solutions also increased. Additionally, a shift in LCST to lower temperatures was observed. This correlates very well with GPC findings discussed previously. For all samples, the complex viscosity started to increase between 32-34 °C and increased rapidly as the temperature increased. It can also be seen that the onset of the complex viscosity increase was lower as the electron beam dose was increased [271].

Table 3-10: Phase transition (LCST) and sol-gel transition results for PNVCL based samples (5wt%) which was established using UV-spectrometry and tube inversion methods.

Polymer Code	**LCST range as determined by UV-spectrometry *(°C)***	**LCST range as determined by Rheological analysis *(°C)***	***Sol-gel* range as determined by Tube inversion method *(°C)***	***Sol-gel* range as determined by Rheological analysis *Sol-gel (°C)***
P(NVCL100) 0 kGy	31.7-33.3	41.2-44.	37.3-38.1	44.5-47.1
P(NVCL100) 5kGy	30.7-32.5	34.7-36.5	35.9-36.9	42.1-45.1
P(NVCL100) 25 kGy	29.3-31.1	33.835.2	33.8-35	38.8-40.4
P(NVCL100) 50 kGy	29.4-31.4	34.4-37.2	33.4-35.2	35.9-39.3
P(NVCL90-VAc10) 0 kGy	27.2-29.0	27.7-30.1	34.8-35.2	43.1-45.3
P(NVCL90-VAc10) 5 kGy	26.8-28.0	28.9-30.5	33.2-34.0	36.6-37.8
P(NVCL90-VAc10) 25 kGy	26.9-27.5	27.2-30.6	32.9-33.5	35.8-39.2
P(NVCL90-VAc10) 50 kGy	25.7-27.3	27.0-29.6	32.2-33.2	33.4-37.2

It can be concluded from Sol-gel and UV-spectroscopy analysis that PNVCL retained its phase transition capabilities after electron beam processing. Additionally, it was proven that industrial-scale electron beam radiation, even at relatively low doses, had the ability to alter the phase transition and thermogelling properties of the temperature-responsive polymers, which is a crucial feature which should be given due consideration when designing medical devices or controlled drug delivery systems with such smart polymers.

3.2.13. Summary

There is limited literature available that examines the effects of modifying PNVCL based polymers by electron beam irradiation and as a means of potentially enhancing properties such as the LCST and mechanical behaviour. Irradiation doses

typical of those used in medical device sterilisation were used, and also higher doses were trialled on selected samples. The initial work focused on exploring the novel use of an industrial scale electron beam irradiator and optimising the operational conditions to sterilise temperature-responsive polymers. Electron beam irradiation provides a fast and reliable method of sterilisation to the medical device industry. Chemical indicators indicate that the smart materials were sterilised at all doses trialled. To achieve a more in-depth knowledge of the polymer modifications triggered by irradiation exposure, three key areas were examined, which included chemical, thermal and structural analysis. It was found that the electron beam dose could be used as a means of controlling key properties of PNVCL. The obtained smart polymers resulted in considerable modifications to the properties of the materials as analysed using ATR-FTIR, GPC, DSC, UV-spectroscopy, DMA, tensile testing and swelling studies. At a radiation absorbed dose of 50 kGy, decreases in PNVCL mechanical properties were observed for tensile testing. Increased swelling capacity was an indication that side branching/cross-linking had taken place. Also, it was noted that the higher the irradiation dose which samples were subjected to, the greater the subsequent percentage swelling. UV-spectroscopy was used to examine the phase transition behaviour, where a decrease in the LCST was found upon irradiation of all samples. This decrease is considered a result of increased molecular weight experienced during the electron beam process. It was also identified that the phase transition of the PNVCL solutions decreased with increasing irradiation dose. Electron beam irradiation results demonstrate that this method allowed functional modification to sterilised temperature-responsive polymers compared to standard methods.

In summary, PNVCL thermosensitivity and mechanical properties could be altered by utilising electron beam irradiation. Such enhancements allow the opportunity to tailor further such smart materials for a medical device or targeted drug delivery applications using this methodology. Although the electron beam approach showed great potential for formulation modification and sterilisation in one step, attaining ongoing/frequent access to the commercial-scale equipment was not possible. Thus in the next section, formulation *via* melt processing was used as an alternative novel approach for enhancing the properties of the smart PNVCL materials for potential implantable apllications.

3.3. Hot-melt extrusion trials of temperature-responsive polymer Poly (*N*-vinylcaprolactam): proof of concept

3.3.1. Preface

In this section, the potential of utilising PNVCL as part of a melt processed blend was investigated. To date, a large body of literature has been devoted to developing temperature-responsive polymers that can be formulated into new smart materials. However, the utilisation of these polymers has not been explored in conjunction with melt processing techniques such as hot-melt extrusion (HME).

Researchers today are focusing on general principles regarding the formulation and process development [272]. Successful melt processing of PNVCL would render the smart polymers more widely useable for many biomedical applications and as carriers for multi-drug delivery systems. Such polymers can be tailored for targeted delivery and trigger the release of the drug [189]. If successful, melt processing of PNVCL based formulations would greatly expand the polymers potential applications.

Polymers such as Poly (vinyl pyrrolidone) (PVP) and Soluplus which is a hydrophilic polyvinyl caprolactam graft copolymer (PEG6000/vinyl caprolactam/vinyl acetate copolymer) are polymers commonly melt processed and used to develop amorphous solid dispersions (ASD), they have overcome poor drug solubility, and have gained considerable interest in the pharmaceutical industry over the past decade. The difference between Soluplus and PNVCL is that Soluplus is a graft copolymer, where as PNVCL is developed in this study as a random copolymer.

Although PNVCL is an attractive temperature-responsive polymer, it has never been utilised in a melt processed formulation. Temperature-responsive polymers are commonly synthesised at a small scale; however, currently, there is no literature on the melt processing of PNVCL or other such smart temperature-sensitive polymers. This study will, therefore, attempt to exploit the use of such materials in a multiphase formulation consisting of temperature-responsive polymers and traditional sustained-release materials. Figure 3-41 displays the different methods that were used in an attempt to melt process the novel PNVCL based formulations.

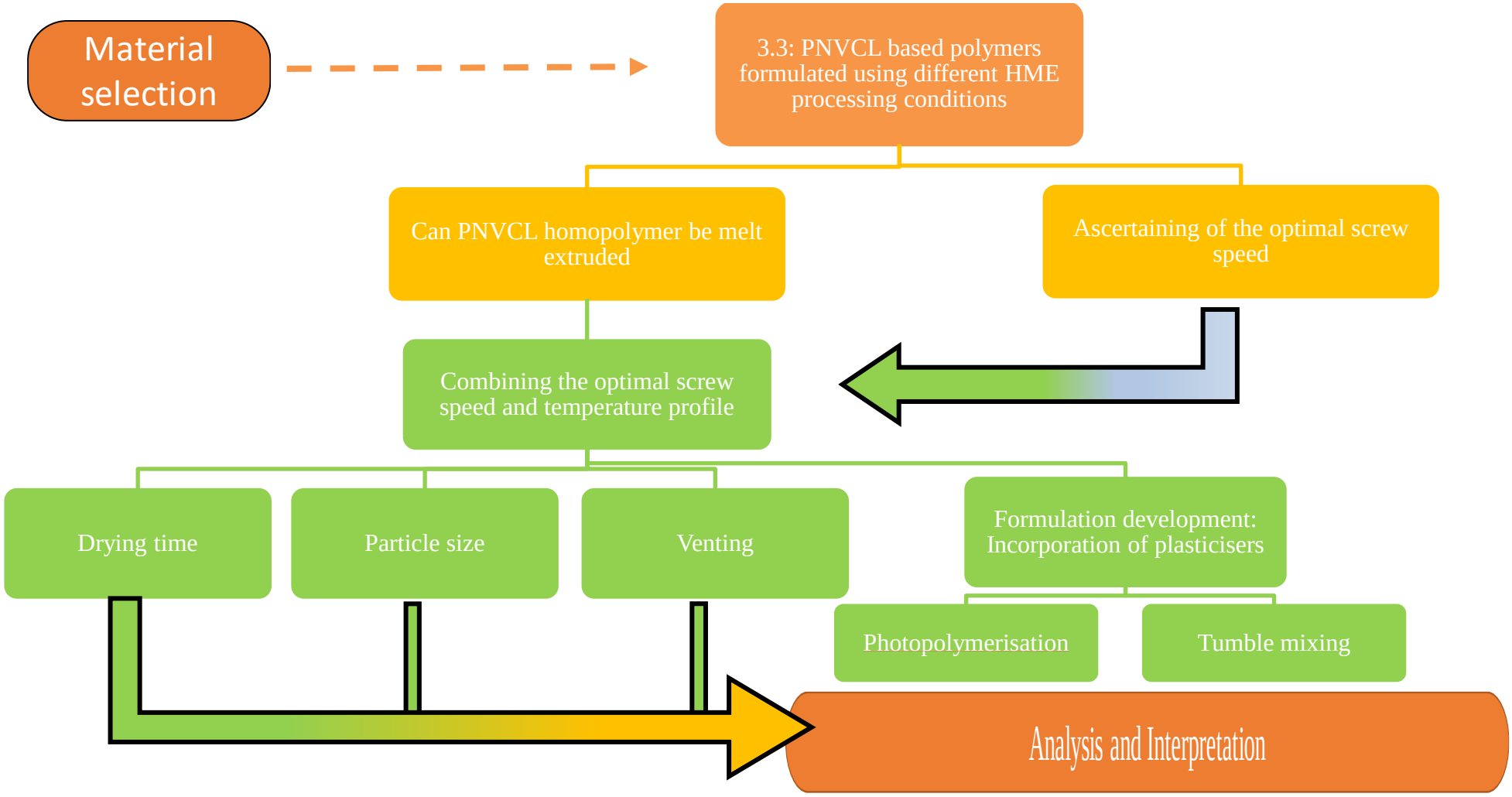

Figure 3-41: Workflow for initial hot-melt extrusion trails carried out on smart PNVCL based materials in this study.

3.3.2. Effect of varying processing parameters

It is essential to optimise the smart polymer formulations in order to achieve the desired end-use requirements. HME processing parameters for the extruder should be investigated to a similar degree as the novel formulations themselves since these will have a significant impact on the final product's characteristics [273]. Optimising HME processing parameters allows for better final product quality. In this section of work, in order to investigate the melt processability of PNVCL, two main processing parameters were initially optimised: temperature and screw speed using an APV Baker extruder.

3.3.2.1. Temperature

Temperature is the most important factor to account for in the HME process. Temperature has a significant impact on the processing properties of a polymer, as it dictates the rheological behaviour of the polymer, making it a priority parameter to be analysed [274]. In order to melt process any amorphous polymer, the processing temperature must be higher than its glass transition temperature (T_g). When melt processing a semi-crystalline polymer, for example, polyethene, the processing temperature must be higher than its melt temperature (T_m) but below its degradation temperature (T_{deg}). Temperature greatly affects the melt viscosity of a polymer, with increasing temperature providing a catalyst for easier polymer flow. For example, at low temperatures, where the polymer melt demonstrates high viscosity, this results in high torque in the extruder and at raised temperatures, it results in reduced torque due to the lower melt viscosity. However, excessive temperature will result in polymer degradation [273]. HME was initially carried out at three different temperature profiles, an overview of the melt processing parameters used can be seen in Table 3-12. The temperature profiles primarily chosen were based on previous DSC results for PNVCL, where the T_g was determined to be approximately 110.74 °C. However, the T_g of PNVCL can be as high as 145-147 °C, depending on M_w [211,212]; this should be taken into consideration when melt processing such polymers.

Processing conditions are governed by both the extrusion temperature and the shear rate/screw speed. In order to melt-process an amorphous polymer, the processing temperature should be 30 °C greater than the glass transition temperature of the polymer.

Due to the frictional force of the screws, the shear rate/screw speed generates up to 80 % of the heat within the barrel.

The initial extrusion temperature was thus chosen following DSC analysis. For example, when the glass transition temperature of the polymer is in the range of 140 °C the processing temperature should be around 170 °C. However, rheological measurements give us a more accurate picture of the extrusion temperature as it provides the melt viscosity of the polymer at a specific temperature over a range of shear rates. From the rheology results, the melt viscosity curve measurement was used as another means of ascertaining the appropriate melt processing range. The decomposition temperature of PNVCL is reported to be in the range of 350 °C and 380 °C [275]. After extrusion, there was an increase in the yellowing/blackening of the sample, particularly so using the highest temperature profile, which could be observed visually. This yellowing/blackening behaviour suggested possible thermal and oxidative degradation of PNVCL [276].

These findings indicate that temperature Profile 3 as described in Section 2.3.1.1 used an extrusion temperature of 160 °C and a screw speed of 20 RPM, is the most attractive temperature profile to melt process PNVCL. Melt processing within this temperature range corresponds to that for melt processing PVP [277]. However, temperature Profile 3 still resulted in high percentage torque values (Figure 3-42). In order to further improve upon this, screw speed was investigated. Temperature Profile 3 was the most attractive profile, as lower temperatures have the advantage of limiting the possibility of thermal degradation [278].

3.3.2.2. Screw speed

The second operating parameter investigated was screw speed, which affects several factors in the HME process such as shear rate, particle size, mixing and residence time [273]. Understanding these processing parameters leads to improved quality in final product characteristics. For example, processing at low screw speeds increases the likelihood of thermal degradation due to the longer residence time. On the other hand, the polymer may reach its T_{deg} if the screw speed is excessively increased due to the heat produced by the frictional heat of the screws [279].

In order to evaluate the effects of screw speed, torque output and visual observations were made. As a polymer degrades, the processed sample will appear to

change colour. This change in colour, such as yellowing/blackening, indicates possible degradation of the polymer [276]. The maximum screw speed used herein was 60 RPM, as any further increase resulted in high torque values. In order to evaluate the effects of screw speed, torque output and visual observations were made. Torque is normally measured in Newtons per meter, but in relation to the extruder, torque is measured as a percentage (%) of maximum motor load. It is effectively a measure of how difficult it is to turn the extruder screw at a given temperature profile, which is an indirect measurement of polymer melt viscosity. The minimum screw speed was set to 20 RPM. Any possible degradation of the PNVCL sample at this screw speed is likely to be caused by the increased residence time. Residence time is the duration of time that the polymer is in the extruder barrel. Overall it was found that, with an increase in screw speed, the torque output increased, and PNVCL samples appeared to change to a yellow/black colour. However, with a decrease in screw speed, the appearance of extruded PNVCL improved somewhat indicating that the shear rate has a significant effect on the processability (i.e. lack of process-induced degradation) of the smart polymers.

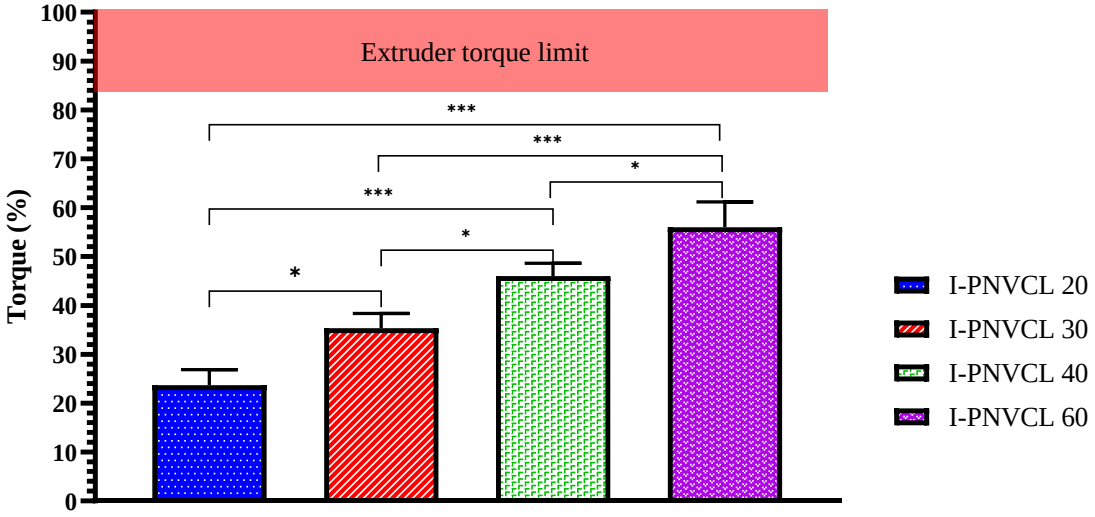

Figure 3-42: Statistical analysis of the effect of screw speed (RPM) on PNVCL based samples measured by the extruder torque. Extruder torque (%) data are presented as mean±SD (n = 3). One-way ANOVA followed by Tukey multiple comparison test. Significantly different * $p < 0.05$; ** $p < 0.01$ and *** $p < 0.001$ vs. each screw speed.

Figure 3-43: Typical appearance of extruded PNVCL samples after modifying the temperature (Profile 3) and screw speed (20 RPM).

Based on visual observations and extruder torque levels, the optimum screw speed was 20 RPM, resulting in the lowest torque values. However, extruded PNVCL samples experienced die swell, which may have been due to moisture content or other process-related factors. Overall it was found that PNVCL homopolymer at this M_w was very difficult to melt extrude, despite using the optimised screw speed and temperature profile. Figure 3-43 displays PNVCL samples melt-processed using the optimum screw speed and temperature profiles. The physical appearance of these samples suggested that further investigation would be beneficial to determine the effects of moisture content and particle size on melt processing.

3.3.2.3. Effects of moisture content and particle size

As discussed previously, the investigation of screw speed and temperature showed that even though PNVCL could be extruded by controlling the temperature and screw speeds, further material optimisation would be essential if the systems were to have potential as drug delivery carriers and for a commercially viable process to be developed. The next section focuses on investigating the moisture content and particle size of PNVCL samples.

3.3.2.3.1. Establishing moisture content of PNVCL

Due to the hydrophilic nature of PNVCL, it has a strong interaction with water. When a polymer is heated, its chains begin to move more freely. This weakens the force that bonds the water molecules to the PNVCL chain. During the initial HME process, it is believed that PNVCL had water molecules entrapped in the polymer matrix. This can result in cosmetic problems or hydrolysis, which is a chemical reaction that breaks covalent bonds between polymer chains. It can also reduce the molecular weight and mechanical properties. To overcome these issues, moisture content and venting during processing was investigated.

Materials like non-polar polyethylene will not interact with polar water. However, in most cases, polymers exhibit some level of polarity and therefore are capable of absorbing a certain amount of moisture from the atmosphere. The amount of moisture that any given polymer can absorb depends upon the chemistry of the polymer and the atmospheric conditions to which it is exposed. Nylon (Polyamide) is a highly polar polymer that can absorb 8-9% water depending on the material when taken to the point of saturation. However, even moisture levels of 0.07% can cause processing issues such as cosmetic problems on a part surface if the material is exposed to the temperatures of melt processing. Some polymers undergo more significant changes if they are processed in the presence of too much moisture. These materials enter into a chemical reaction with the moisture, which is called hydrolysis. This mechanism breaks the covalent bonds in the polymer chain, reducing the molecular weight of the polymer and potentially resulting in a significant reduction in mechanical properties [280].

A Mettler toledo moisture analyser was used to determine the optimum drying time for the PNVCL samples. The samples were placed into an oven at 90 ºC and were measured at 1-hour intervals until there was no moisture detected. Results are displayed in Figure 3-44; It is evident that undried PNVCL retained a high amount of moisture at 3.1 %, which in turn can lead to processing problems. Additionally, there was a significant decrease in the moisture content of the PNVCL matrix after each hour. After the 3rd hour, the moisture content of the PNVCL matrix could not be detected by the moisture analyser, thus indicating that there was no moisture left. Therefore, a drying time of 3 hours at a temperature of 90 ºC was used before all melt processing trials for the remainder of this study.

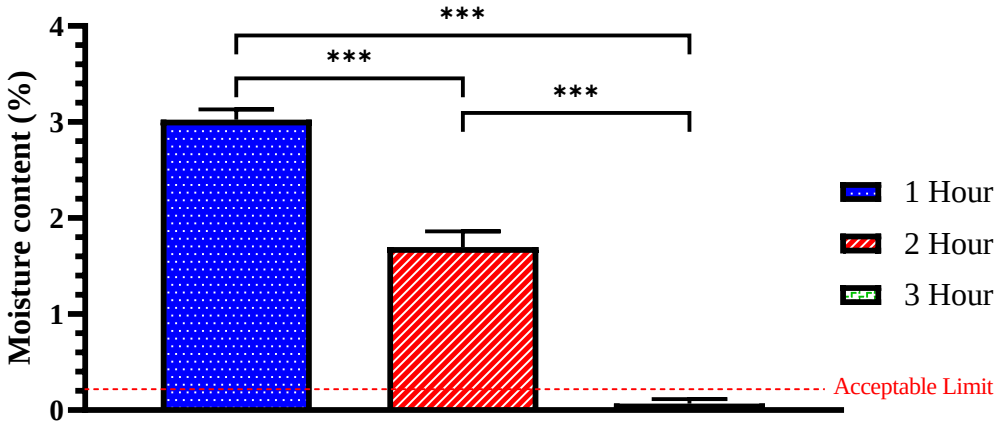

Figure 3-44: Statistical analysis of the Moisture content of PNVCL samples measured using a moisture analyser. Moisture content (%) data is presented as mean±SD (n = 3). One-way ANOVA followed by Tukey multiple comparison test. Significantly different * $p < 0.05$; ** $p < 0.01$ and *** $p < 0.001$.

To further improve the melt processing procedure, a vent was incorporated into the extruder, which is displayed in Figure 3-45. Venting is used in HME when volatiles must be removed in order to make a satisfactory product. With regards to venting, the barrel has a hole in it which is located downstream near the die.

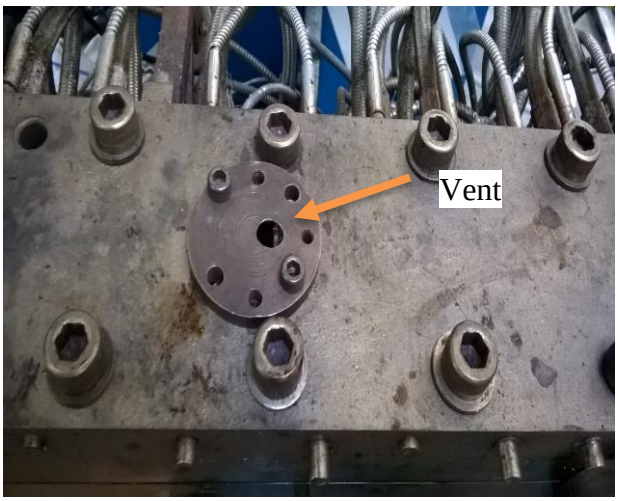

Figure 3-45: The incorporation of a vent during the initial hot-melt extrusion trials.

During the extrusion process, when the polymer reaches the vent, it is hot enough for the water molecules to be released out of the polymer chain. This physical alteration to the processing system had a significant impact on the processing of PNVCL, which can be seen in Figure 3-47.

3.3.2.3.2. Particle size

Improper flow of a powder blend through the extruder hopper can lead to a range of extrusion related defects. Therefore, improving or optimising the particle size can be an efficient method to enhance the mixing and flow properties. The resulting particle size as illustrated in Figure 3-46 for the two different methods, Colortronic granulator (Middle) and a planetary mono mill (Right) compared to the original PNVCL sample (left). The majority of the PNVCL powder (60 wt%) was found in size range between 220 and 420 µm as a result of milling the samples. Ayyub *et al*. (2019) found that optimising the melt mixing of Soluplus and APAP was beneficial as all samples exhibited a broad particle size. A small percentage (10%) was found between 420 and 850 µm, while the majority of the powders were found in the size range between 200 and 420 µm [281]. Similar results were found in this study.

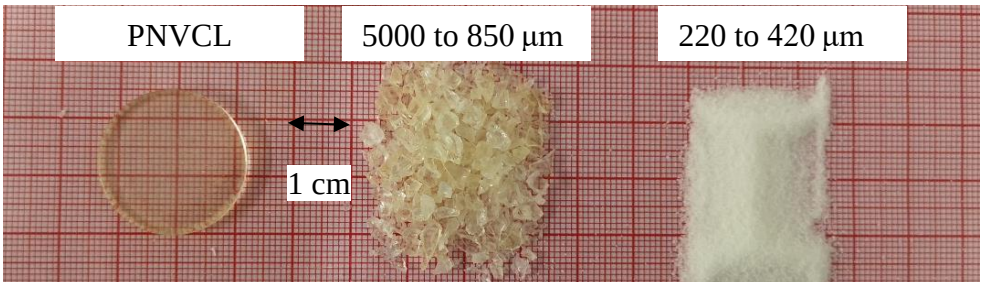

Figure 3-46: A summary of the particle size of PNVCL from photopolymerisation to granulates and powder.

While establishing the processability of PNVCL samples, it was found that a low processing temperature profile and a low screw speed was the best approach to extrude PNVCL. Additionally, improving other process parameters such as drying times and venting also aided the process of eliminating moisture in the PNVCL sample.

Overall a suitable temperature profile and screw speed were obtained while minimising the moisture content and particle size. Figure 3-47 below displays the resulting PNVCL sample after melt processing with reduced moisture content and particle size. Reducing the moisture content and particle size had a considerable impact on the melt processing of the PNVCL. Samples were much easier to melt process without a large die swell. Additionally, PNVCL samples became more uniform and consistent, which is an indication that it was able to flow better during melt processing. Though the reduction in particle size and moisture content resulted in significant improvements, the

incorporation of a plasticising agent was investigated to enhance the melt processability of PNVCL further.

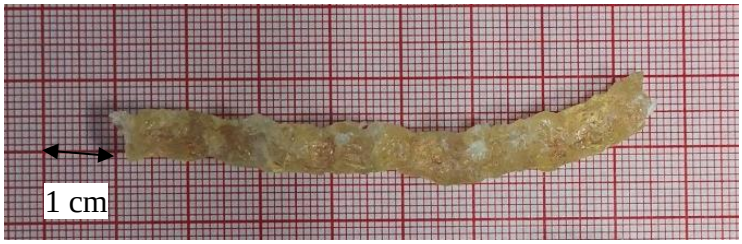

Figure 3-47: PNVCL sample processed using Temperature Profile 3 and a screw speed of 20 RPM, with the reduced moisture content and particle size.

3.3.2.4. Processing trials of temperature-responsive polymer PNVCL with the incorporation of plasticisers

This section deals with incorporating plasticisers into PNVCL polymer matrix to improve the melt processability. The plasticisers were incorporated into PNVCL by two methods, (i) during melt processing and (ii) during photopolymerisation, in an attempt to improve the melt flow properties of PNVCL based samples. The addition of a plasticiser is a common strategy to aid the melt processing of a polymer. The primary purpose of adding plasticisers is to increase the free volume between polymer chains, which usually results in lower melt viscosity. Plasticisers are commonly small molecules which can improve the processing conditions but also change the physicochemical properties of the final product and the release rate of API. There are many different types of plasticisers used in melt processing to reduce the polymer melt viscosity and to allow for better processing. Some of the conventional plasticisers are triethyl citrate (TEC), methylparaben (MP), polyethene glycol (PEG), citric acid monohydrate (CA MH), and acetyl tributyl citrate (ATBC) and Poloxamer 188. Below in Table 3-11 is a list of possible plasticisers that were considered for use in this study. The most promising plasticiser was PEG mainly due to its competitive price, and the fact that it comes in different molecular weights, which includes liquid and powder forms.

Table 3-11: Material selection matrix of suitable plasticisers [282].

Common plasticisers	Price	Non-toxic	A range of molecular weights	FDA approved	Total
Triethyl citrate (TEC)	3	1	0	1	5
Methylparaben (MP)	1	1	0	1	3
Polyoxyethylene (POE),	2	1	1	1	5
Polyethylene glycol (PEG)	3	1	1	1	6
Citric acid monohydrate (CA MH)	3	1	0	1	5
D-sorbitol	2	1	0	1	4
Poloxamer 188	1	1	0	1	3
Acetyltributyl citrate (ATBC)	2	1	0	1	4

Price: 1) Most expensive 2) Average 3) Less expensive

Non-toxic: 0) being toxic 1) Being Non-toxic

A range of molecular weights:0) not available in a range of molecular weights 1) Are available in a range of molecular weights

FDA approved; 0) not being FDA approved 1) being FDA approved

A study investigated plasticisers efficiency to improve the drug release properties for Eudragit® S100. TEC, MP, and PEG were found to be the most efficient plasticisers for Eudragit® S100 [282]. In this study, initially, three plasticisers were tested, PEO, PEG and D-sorbitol were all selected for use due to there excellent plasticising effects. PEG and PEO comes in a range of different molecular weights and has a low price; it is also safe to work with due to its biocompatible and non-toxic properties. D-sorbitol is non-toxic and could be used in some food contacting material. D-sorbitol has hydroxyl groups which make it an effective plasticiser for some -OH or –NH polymers [283].

Figure 3-48 displays the three different types of plasticisers PEO, PEG and D-sorbitol at 20 wt%. Samples containing D-sorbitol had lost all of their structure and melt strength and therefore did not maintain its shape during the extrusion process. In the case of samples containing PEO, the melt strength was greatly improved. However, a small amount of die swell occurred. Overall, the PNVCL samples containing PEG display the best result for surface appearance and consistency during the melt processing. Therefore PEG was selected to be further researched for melt processing at 10,000 and 35,000 M_w (powders). For photopolymerisation 600 and 1,000 M_w (liquids) were used as they can be introduced more easily during the photopolymerisation process.

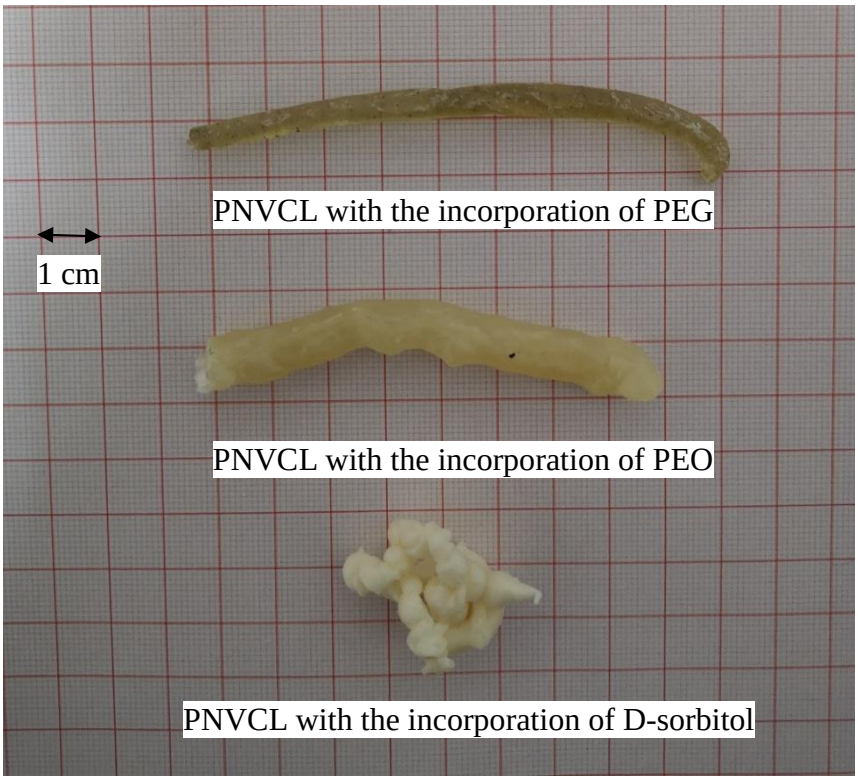

Figure 3-48: PNVCL samples after the incorporation of three different types of plasticisers PEO, PEG and D-sorbitol at 20 wt%.

During melt processing, the incorporation of the higher molecular weight PEG was introduced, resulting in P(NVCL90-PEG10-10000), P(NVCL80-PEG20-10000), P(NVCL90-PEG10-35000) and P(NVCL80-PEG20-35000) samples. A noticeable change in the processability of the samples was observed with the addition of PEG and all samples were substantially improved. Overall, introducing PEG during the melt processing aided PNVCL flow properties, which resulted in improved optical and textural properties of the samples (Figure 3-49). It is also noted that adding low M_w PEG 10,000 improved the surface properties and the consistency of melt-processed PNVCL.

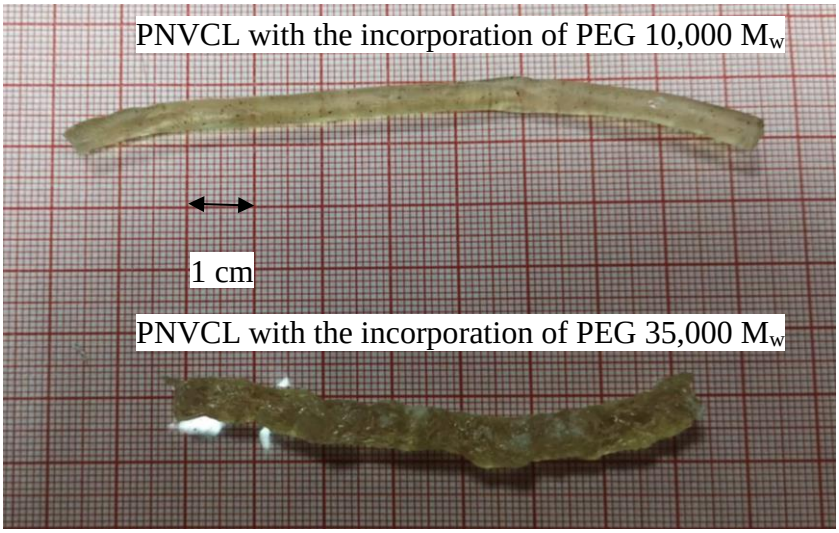

Figure 3-49: PNVCL samples after the incorporation of PEG during melt processing.

PEG was also added as a plasticiser at different molecular weights (600 and 1,000 M_w) during the free-radical polymerisation. Photopolymerisation is an attractive way of synthesising biomedical polymers, as reported in the previous sections [198]. In this study, physically cross-linked polymers based on PNVCL were synthesised *via* photopolymerisation, by incorporating PEG during the photopolymerisation step at different M_w of PEG 10 and 20 wt% (600 and 1,000 M_w) along with 0.1 wt% of a photoinitiator. After synthesising PNVCL-PEG copolymers *via* photopolymerisation, samples were then melt-processed.

A summary of the melt processing parameters used can be seen in Table 3-12 and the resultant extruded samples are displayed in Figure 3-50. This method of adding PEG prior to melt processing produced an improved homogeneous extrudate resulting in improved flowability, homogeneity and processability of the samples.

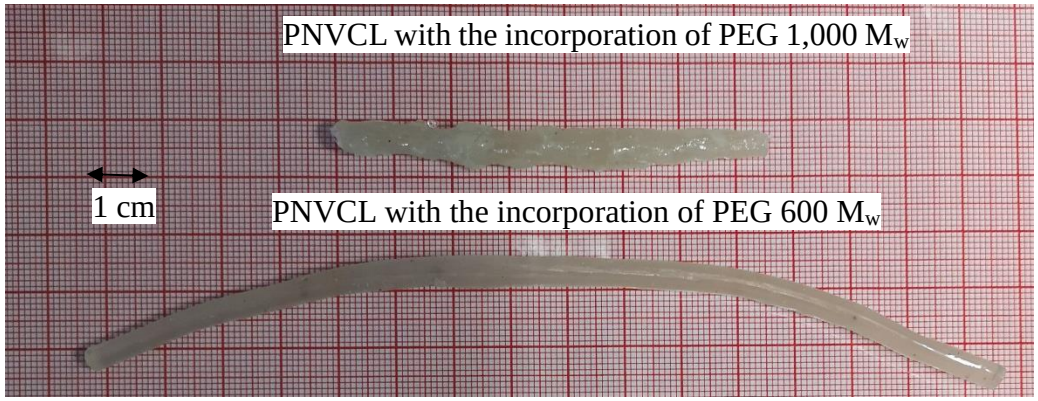

Figure 3-50: PNVCL-PEG samples prepared by photopolymerisation followed by melt processing trials.

3.3.3. Overview of melt processing trials

PNVCL was melt-processed this was achieved by optimising various processing factors such as temperature, screw speed, moisture content, particle size and the incorporation of a plasticiser, which is summarised in Table 3-12. PEG was incorporated into the PNVCL by two different methods, photopolymerisation and melt processing. PNVCL samples that were prepared by photopolymerisation were identified as the best samples using the optimised melt processing conditions and it had the lowest torque values (Figure 3-51). Subsequently, these samples were analysed and PNVCL was melt-processed using Profile 3 (160 °C) and 20 RPM to determine the effect melt processing had on the phase transition and the basic polymer properties. In summary, this section deals with the modification of a thermosensitive polymer when exposed to melt processing. This is important from a practical point of view as this polymer has to be fabricated in order to be used for potential biomedical applications. Throughout the literature, many authors and research groups have tried with some success to alter thermosensitive polymers through the synthesis process. However, this method has limitations that the present research aims to overcome by exploring innovative ways of altering PNVCL without relying on the polymer synthesis approach. This was done by taking advantage of HME technologies.

Table 3-12: Processing trials of PNVCL based samples using different melt processing parameters.

HME Formulation	Temperature (°C)	Screw speed (RPM)	Drying time (Hours)	Feed rate (Kg/h)	Residence time (min)	Particle size (µm)	Venting	Incorporation of plasticisers
I-P(NVCL100) (160 °C)	160 °C	40	NA	1-2	5-6	>500	No	NA
I-P(NVCL100) (170 °C)	170 °C	40	NA	1-2	5-6	>500	No	NA
I-P(NVCL100) (180 °C)	180 °C	40	NA	1-2	5-6	>500	No	NA
I-PNVCL 20	160 °C	20	NA	1-2	5-6	>500	No	NA
I-PNVCL 30	160 °C	30	NA	1-2	5-6	>500	No	NA
I-PNVCL 40	160 °C	40	NA	1-2	5-6	>500	No	NA
I-PNVCL 60	160 °C	20	NA	1-2	5-6	>500	No	NA
I-P(NVCL100) (170 °C)	160 °C	20	3	1-2	5-6	<500	Yes	NA
P(NVCL90-PEG10-1000)	160 °C	20	3	1-2	5-6	<500	Yes	Photo-polymerisation
P(NVCL90-PEG10-600)	160 °C	20	3	1-2	5-6	<500	Yes	Photo-polymerisation
P(NVCL80-PEG20-1000)	160 °C	20	3	1-2	5-6	<500	Yes	Photo-polymerisation
P(NVCL80-PEG20-600)	160 °C	20	3	1-2	5-6	<500	Yes	Photo-polymerisation
P(NVCL90-PEG10-10000)	160 °C	20	3	1-2	5-6	<500	Yes	Melt processing
P(NVCL90-PEG10-35000)	160 °C	20	3	1-2	5-6	<500	Yes	Melt processing
P(NVCL80-PEG20-10000)	160 °C	20	3	1-2	5-6	<500	Yes	Melt processing
P(NVCL80-PEG20-35000)	160 °C	20	3	1-2	5-6	<500	Yes	Melt processing
Legend: Extrudate quality		Poor		Medium		Good		

Extrudates quality can be defined as follows:
Poor samples showed characteristics of: Large die swell, Extruder torque in a high range 100-60 %, Samples had poor mechanical properties at die
Medium samples showed characteristics of: Medium die swell, Extruder torque in a high range 60-40 %, Samples had good mechanical properties at die
Good samples showed characteristics of: No die swell, Extruder torque in a high range 40-0 %, Samples had good mechanical properties at die

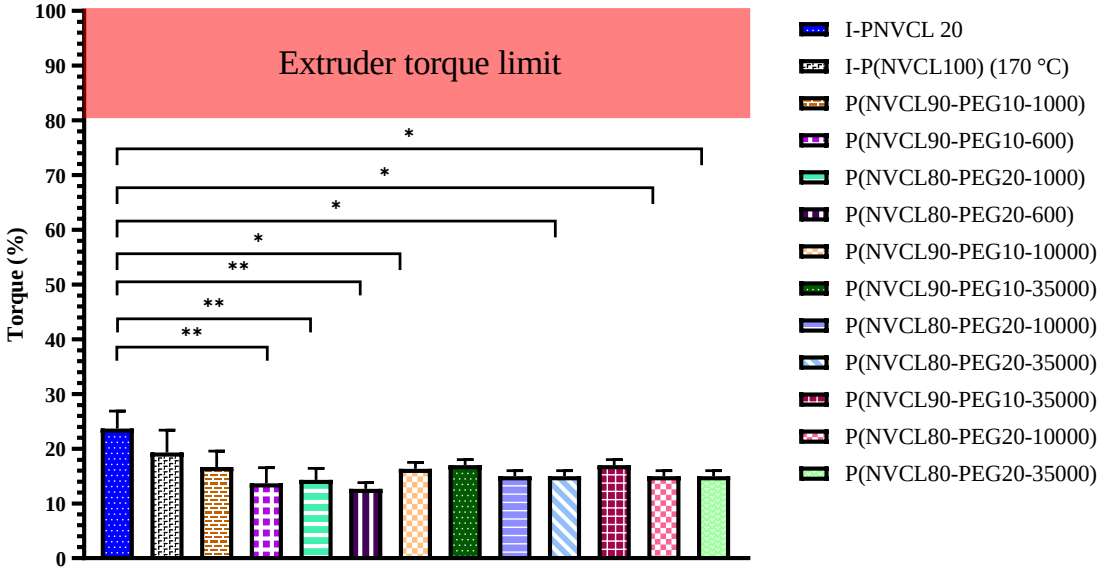

Figure 3-51: Statistical analysis of the torque (%) recorded during the melt processing trails. Torque (%) data are presented as mean±SD (n = 3). One-way ANOVA followed by Tukey multiple comparison test. * $p < 0.05$; ** $p < 0.01$ and *** $p < 0.001$ vs original processing conditions.

3.3.4. Characterisation Methods

3.3.4.1. ATR-FTIR

Extruded PNVCL samples exhibited a (C–H) band at ~2850 cm^{-1}, which is similar to that of the photopolymerised PNVCL. The retention of caprolactam functionality in the extruded PNVCL indicated that the HME process did not adversely affect the PNVCL polymer [42]. The most significant band of PNVCL is at 1620 cm^{-1}, which is associated with the C=O group. In the spectrum of the extruded PNVCL, the C=O were similar to the homopolymer sample, which is another indicator that HME did not significantly affect the extruded PNVCL. Based on Figure 3-52, unprocessed PNVCL demonstrated a broad band at ~3400 cm^{-1} related to O–H stretching, in contrast to the extruded PNVCL, which displayed a narrowing of the band. Similar results were found by Coates *et al.* (2003), who reported a decrease in the spectra intensity of polymers following extrusion. The O-H band comes from the hydrogen bonding and it can be seen that there is a lessening in the intensity the O-H band after extrusion [284].

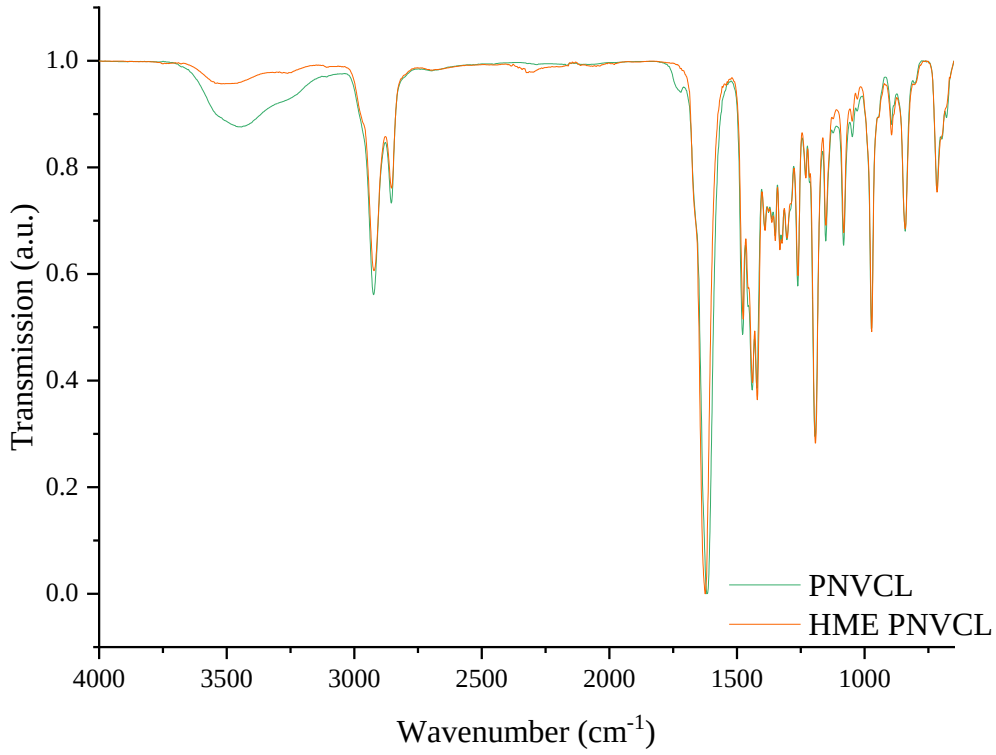

Figure 3-52: Normalised FTIR spectra of unprocessed PNVCL (green) and HME PNVCL samples following hot melt extrusion (Orange).

In the spectra of melt-processed PNVCL samples a narrowing of the O–H band would indicate HME changed the PNVCL hydrophobicity. This would have the potential to alter the swelling characteristics and more importantly, the phase transition behaviour of the polymer, as the phase transition is dependent on the hydrophilic to hydrophobic balance. Samples containing PEG exhibited a new peak in contrast to compounded PNVCL, which will be discussed further in Section 3.4. In summary, it was observed that the chemical composition of the PNVCL did not change, indicating PNVCL was not affected during the HME process.

3.3.5. Phase transition determination

Previous work in this study has shown 5 wt% to be an optimal concentration to detect the phase transition temperature. In this section, the phase transition was measured by employing three techniques to determine the effect of melt processing on PNVCL samples. Table 3-13 outlines a summary of the results obtained from each technique.

Similar trends were established; for example, the LCST of melt-processed PNVCL was found to increase. This increase is likely caused by decreases in M_w due to the HME process. The polymers developed have LCST in the range of 30-35 °C (Table 3-13).

Table 3-13: Phase transition temperature of melt-processed PNVCL based samples which were established using cloud point analysis and UV-spectrometry.

Gel code	LCST as determined by Cloud point (°C)	LCST as determined by UV-Spectrometry (°C)
PNVCL (5 wt%)	31.5-32.5	32.3-32.5
HME PNVCL (5 wt%)	32.9-33.5	33.0-33.4
P(NVCL90-PEG10-1000) (5 wt%)	34.0-34.2	32.5-32.9
P(NVCL90-PEG10-600) (5 wt%)	34.1-34.5	32.5-33.1
P(NVCL80-PEG20-1000) (5 wt%)	34.3-35.1	NA
P(NVCL80-PEG20-600) (5 wt%)	34.5-35.7	NA

3.3.5.1. Cloud point measurement

Cloud point measurement was carried out to ascertain the phase transition temperature range of the samples. Visual observations to detect the phase transition were used. Cloud point was defined as the temperature at which the first sign of turbidity occurred in the solution. PNVCL based samples showed a reversible phase transition in water [193]. It appears that the HME process caused an increase in the LCST, which is likely due to decreases in polymer M_w. Figure 3-53 exhibits the phase transition temperature range for PNVCL based samples. It also reveals that the incorporation of PEG polymer increases the phase transition behaviour for samples. This is likely due to PEG hydrophilic segment increasing the overall hydrophilicity of the polymer solution.

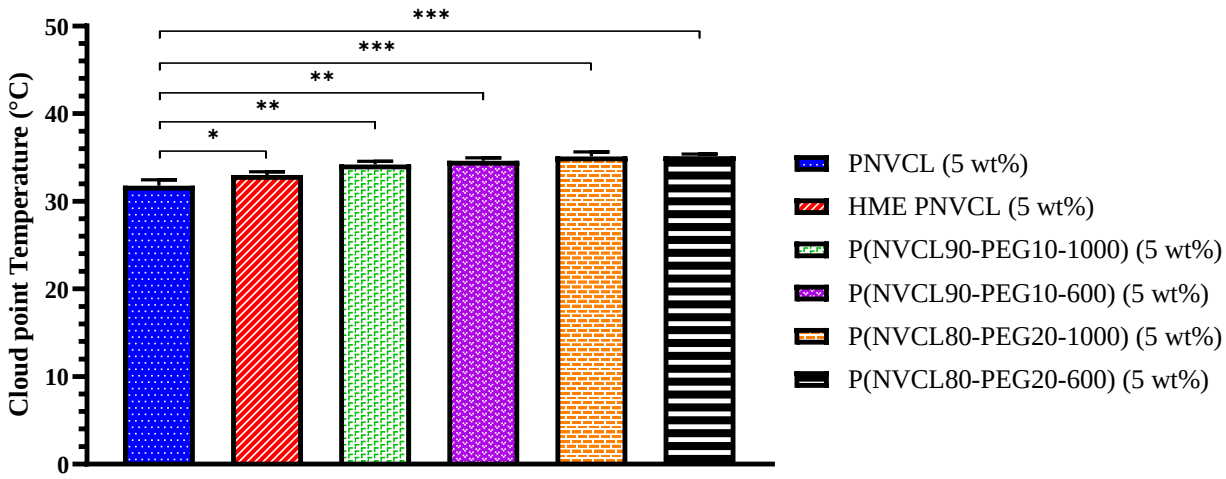

Figure 3-53**:** Statistical analysis of the interaction of melt processing on the PNVCL based samples (5 wt%) measured by the cloud point method. Phase transition data are presented as mean±SD (n = 5). One-way ANOVA followed by Tukey multiple comparison test. Significantly different * $p < 0.05$; ** $p < 0.01$ and *** $p < 0.001$ vs PNVCL (5 wt%) sample.

3.3.5.2. UV-spectroscopy

The LCST of aqueous solutions of unprocessed PNVCL and melt processed samples were also measured using UV-spectrometry. This technique measures the absorbance of a sample and is a commonly used test method for the determination of the phase transition [285]. All samples were analysed over a temperature range of 25-40 °C. UV-spectrometry results showed an increase in the phase transition temperature for all samples, which may be attributed to a decrease in PNVCL M_w compared to unprocessed PNVCL, this will be discussed further in Section 3.4. Figure 3-54 illustrates the LCST behaviour of unprocessed PNVCL (5 wt%) and melt processed P(NVCL100) (5 wt%). For the melt extruded samples, LCST was recorded. However, comparing unprocessed P(NVCL100) (5 wt%) to HME samples, the transmittance % was reduced. In the case where PEG was incorporated at a loading of 20wt%, the samples could not be accurately read, due to the low transmittance %. Overall, PNVCL and HME PNVCL exhibit the phase transition over a 1-2 °C range and have a similar profile. However, the incorporation of PEG into PNVCL changes the phase transition over a broader temperature range.

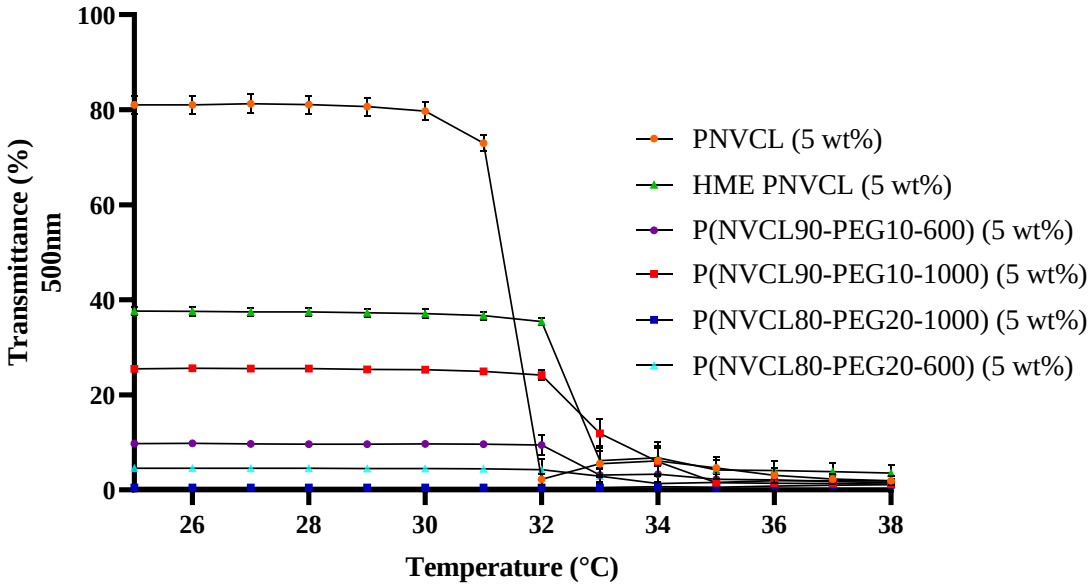

Figure 3-54: UV- spectroscopy illustrating the LCST of unprocessed P(NVCL100) (5 wt%) and melt processed PNVCL based samples (5 wt%). Phase transition transmittance (%) data are presented as mean±SD (n = 3).

3.3.6. Sol-gel transition

In this section, the sol-gel transition was measured using the tube inversion method to investigate the effects of the HME process and the compositions of PNVCL based samples. Similar trends were established for the sol-gel transition in comparison to the results obtained for LCST. The smart polymers that were analysed herein had a sol-gel transition within the range of 37-42 °C (Table 3-14).

Table 3-14: Sol-gel transition of PNVCL based samples following melt processing established using the tube inversion method.

Gel code	Sol-Gel as determined by Tube Inversion Method (°C)
PNVCL (5 wt%)	36.8-37.8
HME PNVCL100 (5 wt%)	37.5-38.2
P(NVCL90-PEG10-1000) (5 wt%)	38.3-39.4
P(NVCL90-PEG10-600) (5 wt%)	38.5-39.5
P(NVCL80-PEG20-1000) (5 wt%)	NA
P(NVCL80-PEG20-600) (5 wt%)	NA

The tube inversion method was used in determining the sol-gel transition of unprocessed P(NVCL100) and all melt processed samples (5 wt%), within the range of 20-45 °C. At temperatures below the sol-gel transition, PNVCL remains as a solution; however, with rising temperatures, PNVCL can turn into a gel. This is due to the internal energy where the hydrogen bonds between PNVCL and water molecules would break. This increase in entropy in PNVCL leads to the hydrophobic side chains of PNVCL accumulating until gelation occurs [286]. Concentration affects the sol-gel transition, where increasing the concentration results in a decrease in the sol-gel transition temperature. However, with the addition of 20 wt% PEG, the sol-gel transition was weakened and the PNVCL system did not form a gel.

3.3.7. Summary

Physically cross-linked PNVCL was prepared using bulk photopolymerisation. PNVCL samples were then melt processed in an attempt to fabricate PNVCL for the first time using a novel melt processing approach. The results indicate that temperature and screw speed plays a vital role in the fabrication of PNVCL using HME. Extruding PNVCL at 160 °C (Profile 3), with low screw speed (20 RPM), resulted in optimal processing conditions. To further enhance the melt processability of PNVCL, moisture content, particle size and the incorporation of a plasticiser, PEG, was investigated *via* two methods, the incorporation of PEG into PNVCL by tumble mixing before melt processing, and by photopolymerisation prior to melt processing.

The ability to fine-tune smart polymer properties such as the LCST by melt processing is the key finding of this body of work. While incorporating PEG by photopolymerisation proved successful, for the remainder of the study PEG was added by tumble mixing prior to melt processing, as this would allow tailoring of the properties during the melt process. Thus, in the next section, PNVCL was further investigated by incorporating PEG during the melt processing step, whereby a small-scale extruder was used to reduce batch size.

3.4. In-depth hot-melt extrusion trials and analysis of temperature-responsive Poly (*N*-vinylcaprolactam) based smart polymer systems

3.4.1. Preface

In the previous section, it was found that twin-screw extrusion could be used to melt process PNVCL successfully. This has the potential to open up avenues in controlled drug delivery such as new methodologies to control and mix additives into PNVCL, including the ability to modify phase transition properties, allowing for the creation of a highly tailorable smart polymer system. A small-scale extruder was used to keep the material cost and batch size down. The PRISM TSE 16 is a bench-top twin-screw extruder which is used in the pharmaceutical industry [287]. It is known to achieve reliable scale-up, reduced time to market, and controlled, continuous processing. These types of twin-screw extruders offer flexible compounding configurations for small batches for either pilot-scale production or low volume manufacturing. They are also well-suited for research and development in the polymer, and pharmaceutical sectors [288]. If HME is proven successful in melt processing of PNVCL, it will have great potential for controlling the properties of the smart polymer using an unexplored approach. This section explores several different factors, including the development of a washing process, the addition of PEG during the melt processing and in-depth characterisation of the PNVCL samples. Figure 3-55 below shows a work breakdown structure for the evaluation of the effect of melt processing on washed and unwashed PNVCL based samples. In summary, the ability to melt, formulate and incorporate different materials into PNVCL by a continuous process could offer a more attractive smart polymer.

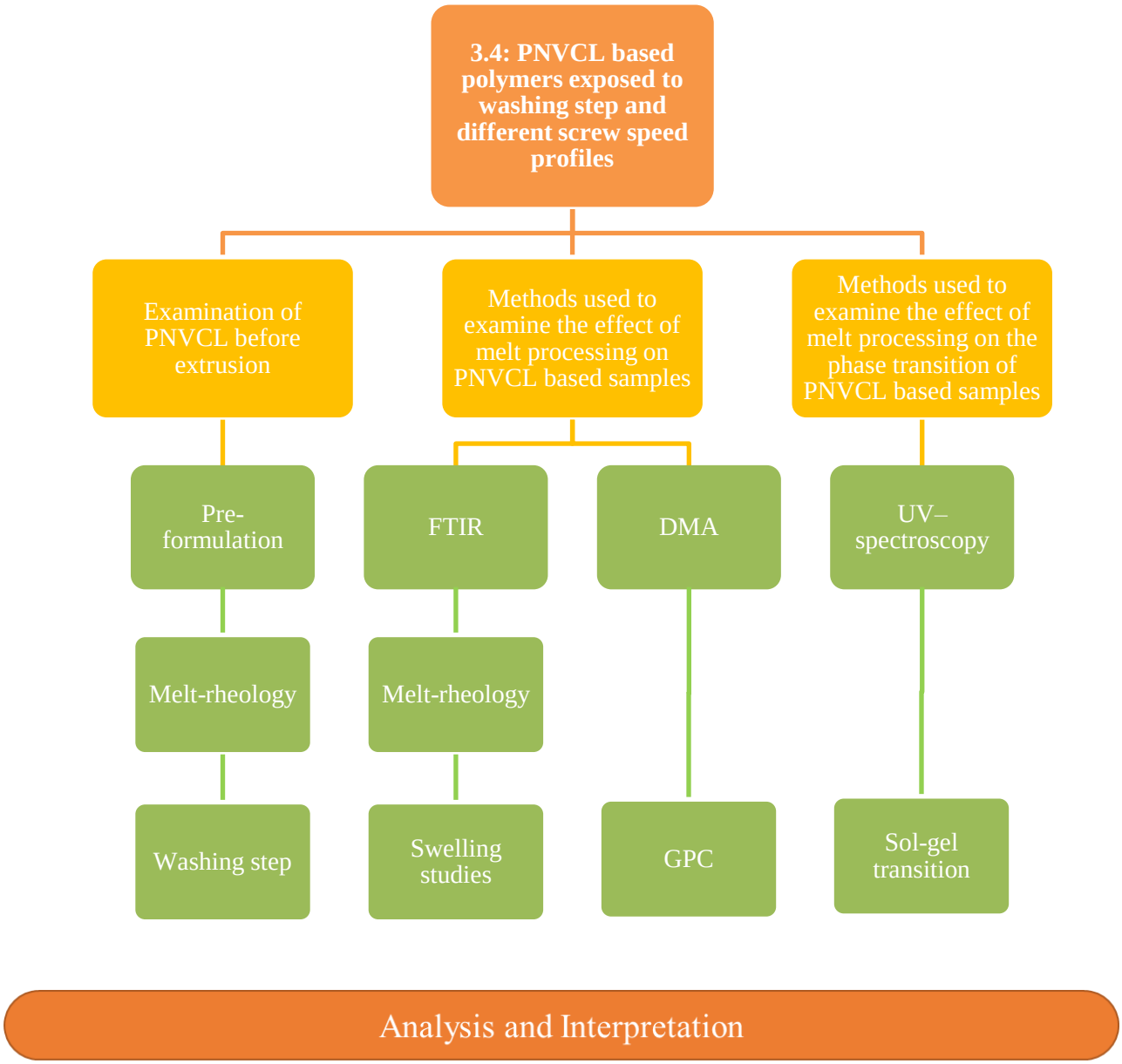

Figure 3-55: Work breakdown structure for the advanced evaluation of the effect of melt processing on PNVCL.

3.4.2. Pre-formulation characterisation

3.4.2.1. Melt Rheology

A rheological analysis was conducted on unprocessed PNVCL at three different temperatures, 180 °C, 190 °C and 200 °C, to investigate the melt viscosity of the polymer further. Melt viscosity is essential as it dictates if the polymer can be melt processed. Amplitude sweeps were used to determine the linear viscoelastic region of PNVCL

samples. It was found that all samples had a common viscoelastic region within around 2% strain. This strain was used for all frequency sweeps. Frequency sweeps used to determine the melt flow behaviour of PNVCL are displayed in Figure 3-56 and Figure 3-57.

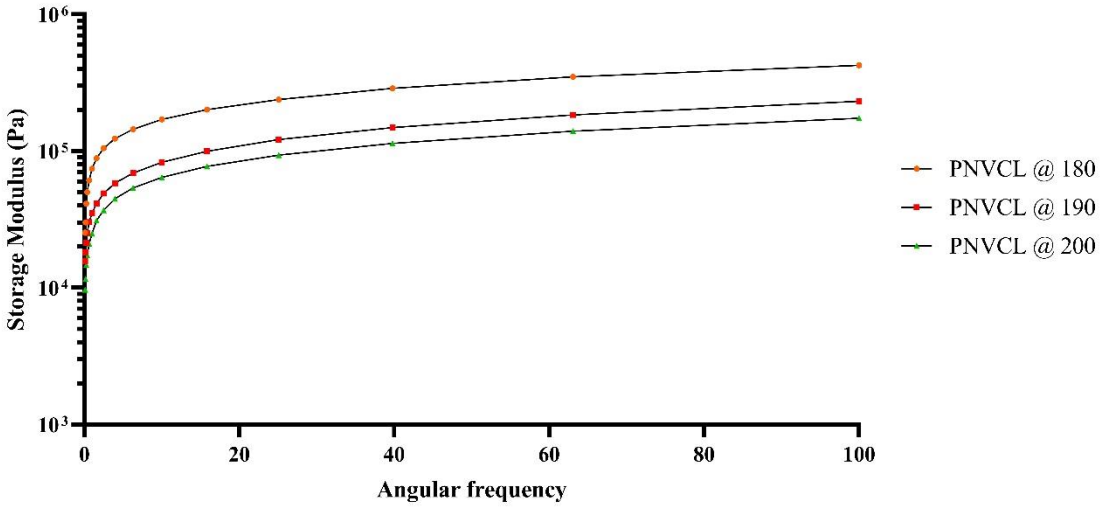

Figure 3-56: Storage modulus of unprocessed PNVCL at 180 °C, 190 °C and 200 °C. Melt rheology complex viscosity (Pa.s). Mean rheological data is presented (n = 2).

Figure 3-56 exhibits the typical entangled polymeric melt behaviour for PNVCL. It shows that when a low frequency is applied to PNVCL, there is an insufficient timescale to allow for the unravelling of polymeric entanglements [289]. Similar results were reported for PVP, where the authors generated rheological parameters at different temperatures and the findings were subsequently used to predict suitable HME processing conditions [290].

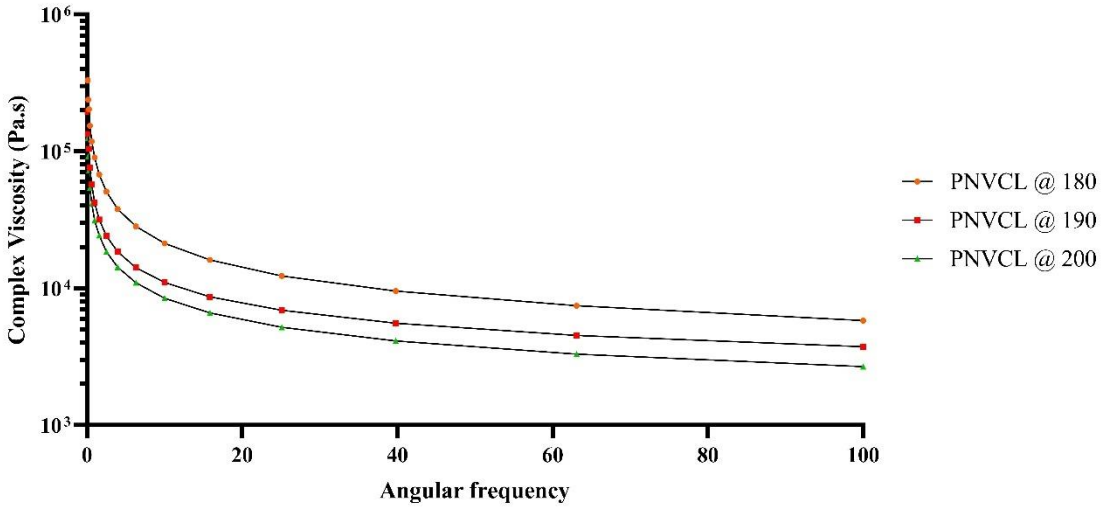

Figure 3-57: Complex viscosity of unprocessed PNVCL at 180, 190 and 200 °C. Melt rheology complex viscosity (Pa.s). Mean rheological data is presented (n = 2).

The complex viscosity was measured over a frequency range of 0.1 to 100 (rad/s) (Figure 3-57). It was found that higher temperatures led to a decrease in complex viscosity of PNVCL. The PNVCL samples displayed a shear-thinning non-Newtonian behaviour at all temperatures; when angular frequency increased, a decrease in complex viscosity was observed. Therefore, 200 °C appeared to be an attractive temperature for the melt processing of PNVCL. At 200 °C, the complex viscosity dropped below 4000 Pa.s thus was within the range for a polymer to be considered to be extruded, as it was free-flowing under the applied stress [291]. Gupta *et al.* (2015) found for Soluplus, that once the complex viscosity dropped below 10,000 Pa.s and remained above 1000 Pa.s, the polymer could be considered processable, as it was free-flowing under the applied stress. At the same time, it was not so soft that it would reaggregate after extrusion [292].

Although, literature states that viscoelastic analysis serves as an excellent technique to identify the processing temperature before melt extrusion [289,292,293]. Melt rheology suffers from some limitations, such as not being able to reach the shear rates that the polymer would typically be exposed to in a twin-screw extruder. However, this limitation can be overcome by employing a time-temperature superposition. This is where the frequency sweeps are performed at different temperatures to determine temperature-dependent properties of linear viscoelastic polymer from known properties at a reference temperature. Also, another limitation of melt rheology is due to not knowing

the shear profile of the screws, thus predicting the shear rates which the polymer will be exposed to would be difficult. However, overall results indicate that the optimal processing temperature for PNVCL is around 200 ºC.

3.4.3. Processing and characterisation

Melt processing trials were required in order to determine the processability of PNVCL on the small-scale extruder. In order to melt process PNVCL, screw speed parameters were optimised based on the findings from Section 3.3. Before processing and characterising PNVCL, all samples were dried in a vacuum oven for 3 hours at 90 °C.

3.4.3.1. Effect of screw speed on extrudability of PNVCL

Rheological studies demonstrated that PNVCL, at 200 °C, had the lowest complex viscosity. The effect of screw speed was then investigated; this parameter impacts upon several factors in the HME process such as shear rate, particle size, mixing, the load of the barrel and residence time [273,291]. To evaluate the effects of screw speed, visual observations were made during processing as well as the measurement of the screw torque. The screw torque measurements obtained during the processing of the PNVCL based samples indicated that the polymer is quite challenging to melt process. In Section 3.2.8 and Section 3.4.2.1, it was found using rheological analysis that PNVCL has a high melt viscosity.

The maximum screw speed used in this study was 150 RPM and the minimum screw speed was set to 50 RPM. Below 50 RPM resulted in high torque values. Based on visual observation and torque measurement, the most favourable screw speed was 100 RPM, as it resulted in the lowest torque values. The findings also identified that samples that were processed at high screw speeds experienced die swell. Die swell occurs when molten polymer flows through the die. The polymer chains tend to align in the direction of flow and expand in the opposite direction, resulting in die swell. This is due to the viscoelastic properties of the material. Many different factors affect the die swell such as shear rate, shear stress and temperature as well as the diameter and length/diameter ratio of the extruder.

3.4.3.2. Effects of incorporation of the plasticiser

In the previous section, a number of different plasticisers were used to determine which plasticisers would be the best to improve the overall melt viscosity of the PNVCL samples. It was found that PEG improved the flowability of PNVCL, PEG (2000 M_w) was incorporated before melt processing. PEG (2000 M_w) was chosen and incorporated by melt processing as results from Section 3.3 showed that lower M_w of PEG displayed the best results. PEG was introduced to PNVCL by tumble mixing and subsequently melt processed using different concentrations (10 and 20 wt%) at a constant temperature of 200 °C and a screw speed of 100 RPM. In biomedical applications, PEG can be used to enhance the hydrophilicity of polymers, to increase water uptake, to increase porosity and therefore, to influence the degradation properties of the prepared formulations [13,294].

Furthermore, incorporating PEG into the PNVCL matrix during the extrusion process aided the processability of the polymer. Processing observations for the PNVCL-PEG samples showed an improvement in flowability of the polymer and reduced torque.

3.4.4. Overview of Processing

A small-scale extruder was used to reduce material cost. Different screw speeds were trialled 50, 100 and 150 RPM. Torque measurement results indicated that an increase in the concentration of the plasticiser leads to a proportional decrease in the melt viscosity of the polymers. Also, using the small-scale extruder along with the new processing parameters, improved the visual appearance of the samples, as displayed in Figure 3-58. A summary of the processing parameters and samples extruded can be seen in Table 3-15 and Figure 3-60.

Table 3-15: Melt processing trials of PNVCL based samples using the small-scale prism extruder.

HME Formulation	Temperature (°C)	Screw speed (RPM)	Drying time (Hours)	Feed rate (Kg/h)	Residence time (min)	Particle size (µm)	Venting	Incorporation of plasticisers
W-PNVCL 50	200	50	3	1-2	2-3	<500	No	Melt processing
W-PNVCL 100	200	100	3	1-2	2-3	<500	No	Melt processing
W-PNVCL 150	200	150	3	1-2	2-3	<500	No	Melt processing
UW-PNVCL 50	200	50	3	1-2	2-3	<500	No	Melt processing
UW-PNVCL 100	200	100	3	1-2	2-3	<500	No	Melt processing
UW-PNVCL 150	200	150	3	1-2	2-3	<500	No	Melt processing
W-PNVCL90-PEG10	200	100	3	1-2	2-3	<500	No	Melt processing
W-PNVCL80-PEG20	200	100	3	1-2	2-3	<500	No	Melt processing
UW-PNVCL90-PEG10	200	100	3	1-2	2-3	<500	No	Melt processing
UW-PNVCL80-PEG20	200	100	3	1-2	2-3	<500	No	Melt processing
Extrudates quality		Poor		Medium		Good		

Extrudates quality can be defined as follows:
Poor samples showed characteristics of: Large die swell, Extruder torque in a high range 100-60 %, Samples had poor mechanical properties at die.
Medium samples showed characteristics of: Medium die swell, Extruder torque in a high range 60-40 %, Samples had good mechanical properties at die.
Good samples showed characteristics of: No die swell, Extruder torque in a high range 40-0 %, Samples had good mechanical properties at die.

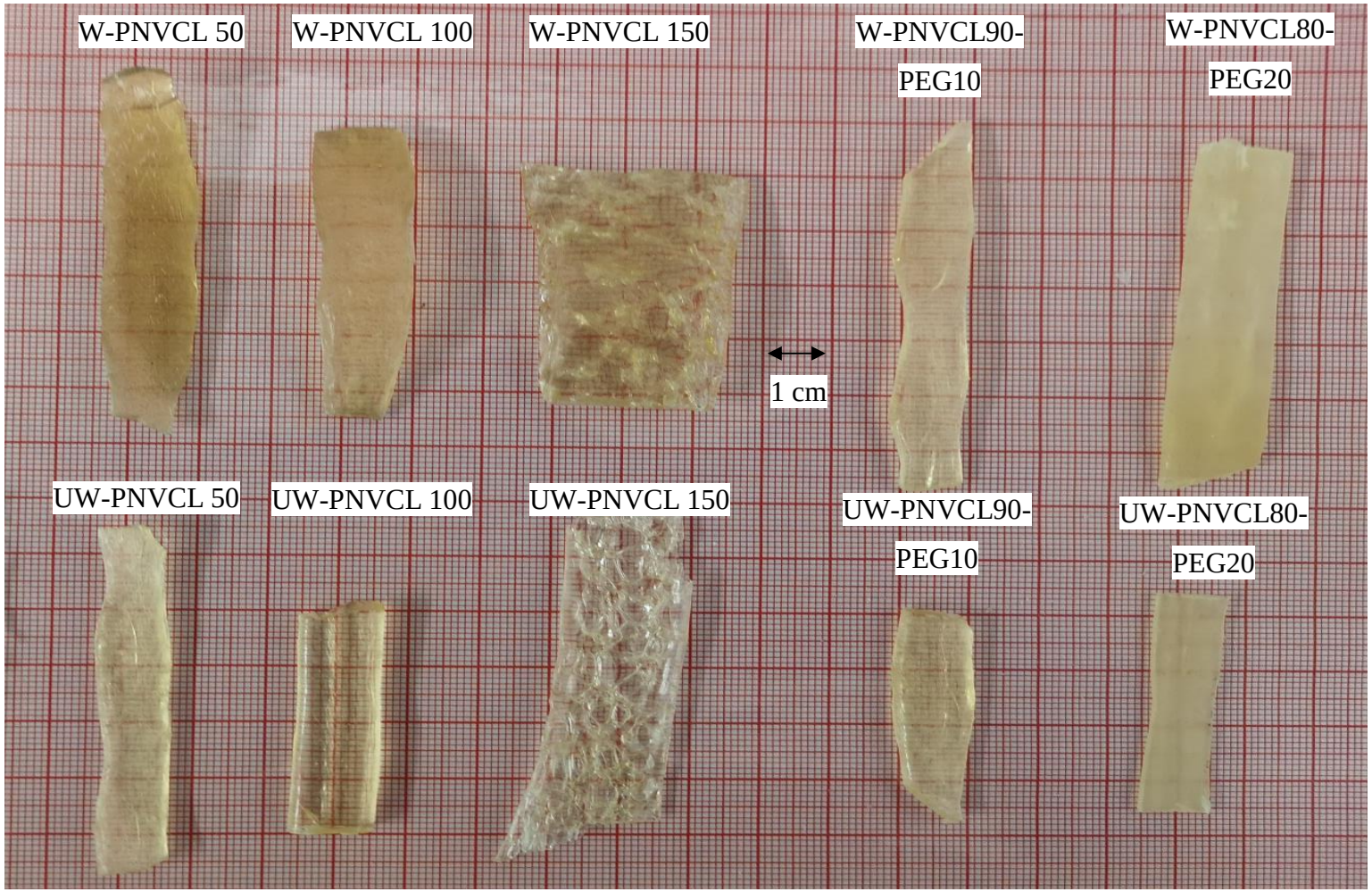

Figure 3-58: Washed and unwashed PNVCL based samples following melt processing at different screw speeds.

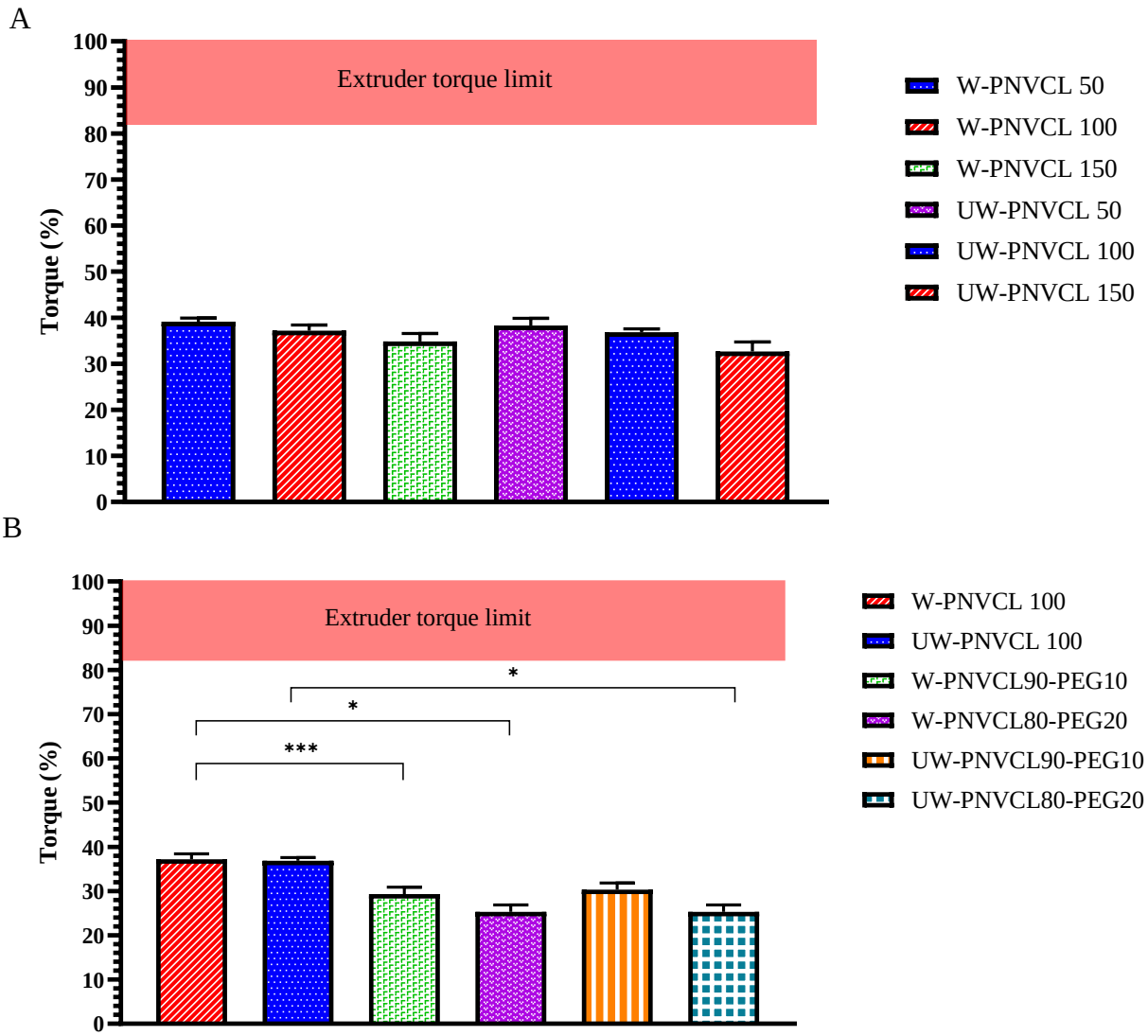

Figure 3-59: Statistical analysis of the interaction of A) melt processing trials of washed and unwashed samples measured by torque output data are presented as mean±SD (n = 5). One-way ANOVA followed by Tukey multiple comparison test, there was no significant difference found between the samples and the different screw speeds. B) Melt processing trial of the incorporation of PEG in PNVCL. Significantly different * $p < 0.05$ and *** $p < 0.001$.

3.4.5. Characterisation methods

3.4.5.1. Gel Permeation Chromatography

To determine the molecular weight distribution of a polymer sample, a calibration with standard polymers of known molecular weight must be performed. Values from the

unknown sample are then compared with the calibration graph to generate molecular weights and molecular weight averages with an (R^2) value of 0.9921. Chromatograms of PNVCL samples are presented in Figure 3-60, which were determined by GPC. The PNVCL samples with larger molecular weight, were eluted faster and had a smaller peak area, while the peak with smaller molecular weight were eluted slower and had a larger peak area.

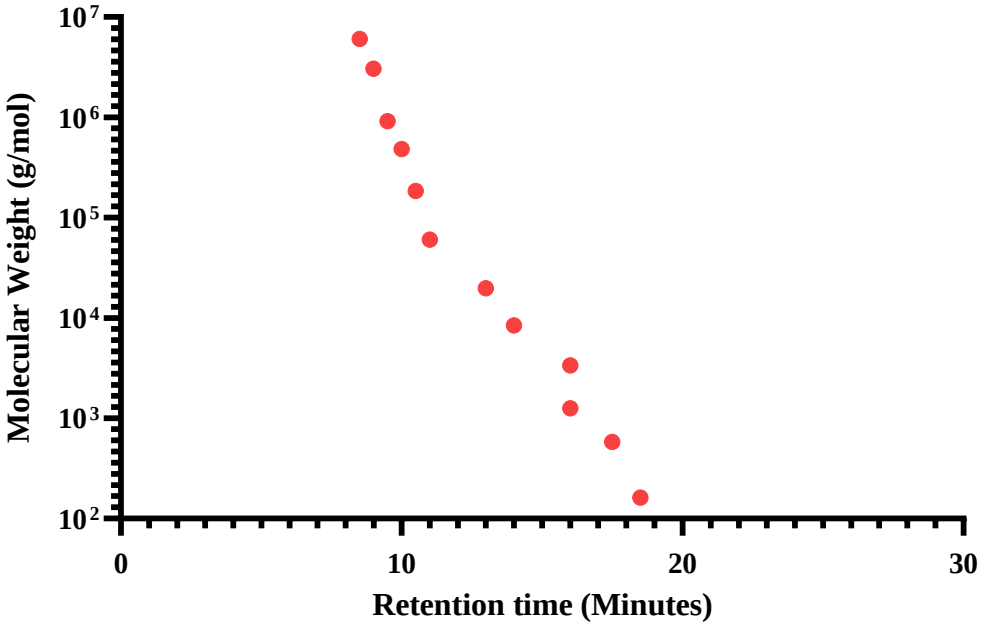

Figure 3-60: Calibration curve of standards by the GPC method

GPC analysis was conducted on extruded PNVCL based samples. It was found that PNVCL samples displayed increased molecular weight post-processing. This is an unusual occurrence because the molecular weight was expected to decrease due to the thermal energy PNVCL experienced during melt processing. The findings suggest that there was unreacted monomer molecules in the polymer, which may have caused an increase in molecular weight during the melt processing. Knowing this, it is possible that a reactive type extrusion occurred. To investigate this further, a washing step was developed, which involved washing PNVCL post polymerisation with *N*-pentane, followed by drying under vacuum at 60 °C to constant weight. Subsequently, PNVCL samples were processed using identical processing conditions as for the unwashed specimens.

In the case of washed PNVCL based samples, a reduction in the molecular weight was observed, with increasing screw speed. W-PNVCL 150 sample showed the most

significant reduction in molecular weight. The drop in molecular weight is most likely due to the high shear rates of the screws, which caused a decrease in molecular weight. However, in the case of the unwashed PNVCL samples, a much higher M_w was found. From GPC analysis (Table 3-16), it was found that HME could be used to modulate the molecular weight of PNVCL samples. Controlling PNVCL molecular weight will have a significant effect on its mechanical, swelling and phase transition behaviour [170,208]. It can thus be concluded, from the GPC study, that HME PNVCL samples have the potential to be further developed as smart drug carrier materials.

Table 3-16: Molecular number (M_n), molecular weight (M_w) and polydispersity (PDI) results for melt processed PNVCL based samples.

Polymer Code	M_n	M_w	PDI
W-PNVCL 50	6258	56337	9.0024
W-PNVCL 100	8403	40827	4.8586
W-PNVCL 150	2438	18465	7.5738
UW-PNVCL 50	48755	211034	4.3285
UW-PNVCL 100	63863	231156	3.6196
UW-PNVCL 150	89506	246866	2.7581
W-PNVCL90-PEG10	4812	50164	10.4248
W-PNVCL80-PEG20	24664	32103	1.3016
UW-PNVCL90-PEG10	106952	299916	2.8042
UW-PNVCL80-PEG20	114133	328865	2.8814

3.4.5.2. Washing step

Both N-pentane and xylene were initially used to remove any unreacted monomer. A small amount of residual monomer is often hard to identify by conventional polymer characterisation techniques. Recently a number of authors have used a solvent to reduce unreacted NVCL in samples. Lemus et al. (2017) removed unreacted monomers (NVCL and NVP) by dissolving the samples in dichloromethane, and precipitating them in diethyl ether. This step was repeated at least 3 times [295]. Eswaramma et al. (2017) removed NVCL from PNVCL by washing the PNVCL based polymer with a methanol-water mixture (4:2) for several cycles. The final solid obtained was first filtered and then dried at 40 °C until a constant weight was reached [154]. Additionally Ayon et al. (2014) used water at room temperature to remove unreacted NVCL. During the washing step, water was changed frequently for 5 days at room temperature to remove any unreacted monomers and other impurities [296].

Many washing methods for removing NVCL from PNVCL were developed in the literature. However, some methods would not work on the samples produced in this study. For examples using Ayon's *et al*. (2014) method, the fact that exposing PNVCL to the water at room temperature would breakdown the polymer unless the phase transition of the polymer is significantly lower than room temperature [296]. In this section, the rationale was that low weight percentages of photoinitiator would lead to a large amount of unreacted monomer. Therefore, to analyse the washing step, PNVCL samples were synthesised with 5 different concentrations of photoinitiator 0.01, 0.1, 0.5, 1 and 5 wt%. In order to examine if unreacted monomer remained within the PNVCL, samples were analysed before and after the washing step.

First, PNVCL samples were dried in a vacuum oven to determine the effect of using a drying step. The other steps involved soaking the PNVCL samples several times in *N*-pentane or xylene, both solvents were chosen due to their polarity, *N*- pentane and xylene are non-polar solvents. It is assumed that non-polar xylene and *N*-pentane would have dissolved the monomer and not the polymer as the polymer can be dissolved in water which is a polar solvent. In order to investigate the effects, the vacuum oven and washing of the polymer, sample were studied by IR spectrometry. Below in Figure 3-61 displayed PNVCL directly after the synthesising process. It can be seen, especially in the low concentration of Irgacure®184, that the amide group (C=O) at 1620 cm^{-1} appears to be in two separate peaks. The second peak arose around 1655 cm^{-1} which was identified as the vinyl segment of NVCL. With the increased concentration of Irgacure®184, the vinyl segment peak became weaker. This would suggest that increasing Irgacure®184 decreased the vinyl segment of the mixture. For example, low amounts of Irgacure®184 would lead to high levels of unreacted monomer, which will result in a high amount of the vinyl segment relating to NVCL being present. Additionally, another peak at 1390 cm^{-1} belongs to the aliphatic C–C bond in the backbone of the polymer. The presence of the 1390 cm^{-1} peak in conjunction with the absence of the related peaks, indicate that most unreacted monomer has been eliminated by the polymerisation reaction.

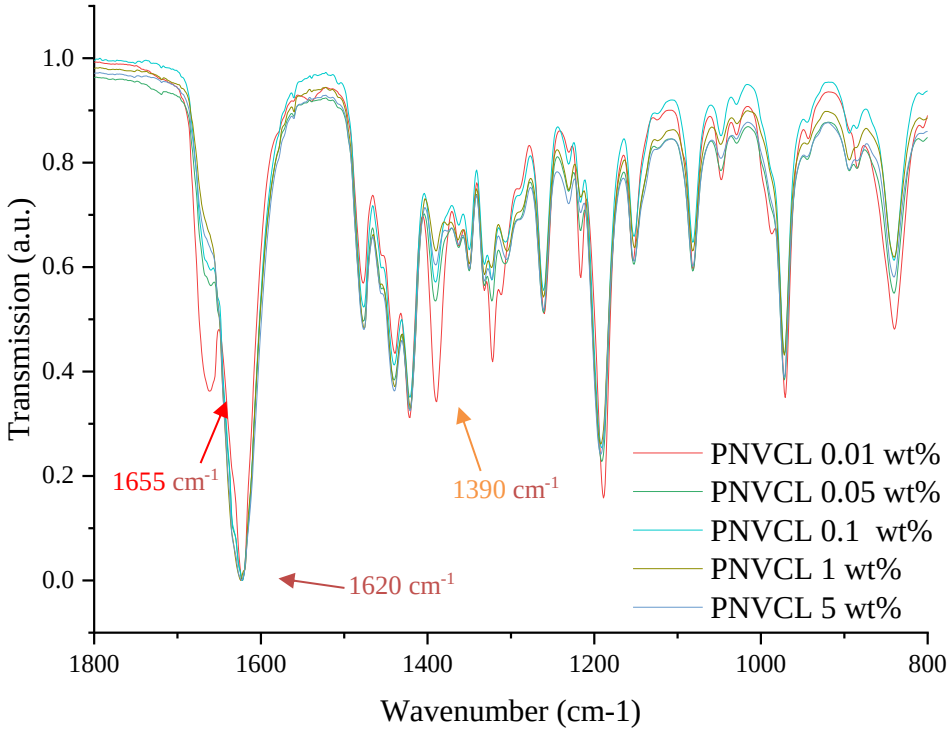

Figure 3-61: Normalised FTIR spectra of PNVCL samples with different concentrations of photoinitiator 0.01, 0.1, 0.5, 1 and 5 wt% of Irgacure®184 after the photopolymerisation process.

Regarding the removal of unreacted monomer used in this study and most other research papers, the normal procedure is to allow PNVCL to be dried to a constant weight in a vacuum oven. It is assumed that the unreacted monomer is removed during the vacuum oven process. Concerning the limitations of this method, it could be argued that there is a possibility of a small amount of unreacted monomer within the PNVCL as the scales would not be accurate enough to measure such a low amount of monomer.

Figure 3-62 displays PNVCL after vacuum drying at 40 ℃. It can be seen, especially with the lower concentration of Irgacure®184 (0.01 wt%) that there are two peaks still present in the spectrum at 1655 cm^{-1} (C=C) and 1620 cm^{-1} (C=O). However, for samples containing higher amounts of Irgacure®184, the intensity of the band at 1655 cm^{-1} (C=C) became weaker.

In summary, these results show that during this study, unreactive monomer may have been within the samples. However, the drying protocol used is a wildly acceptable

method to remove any unreactive monomer. Most research papers did not report these issues with PNVCL containing unreactive NVCL monomer. This may be due to the reason why most research groups do not normally use such a low amount of photoinitiator (0.01 wt%) during the polymerisation process, or a reason why the unreactive NVCL monomer was never tested.

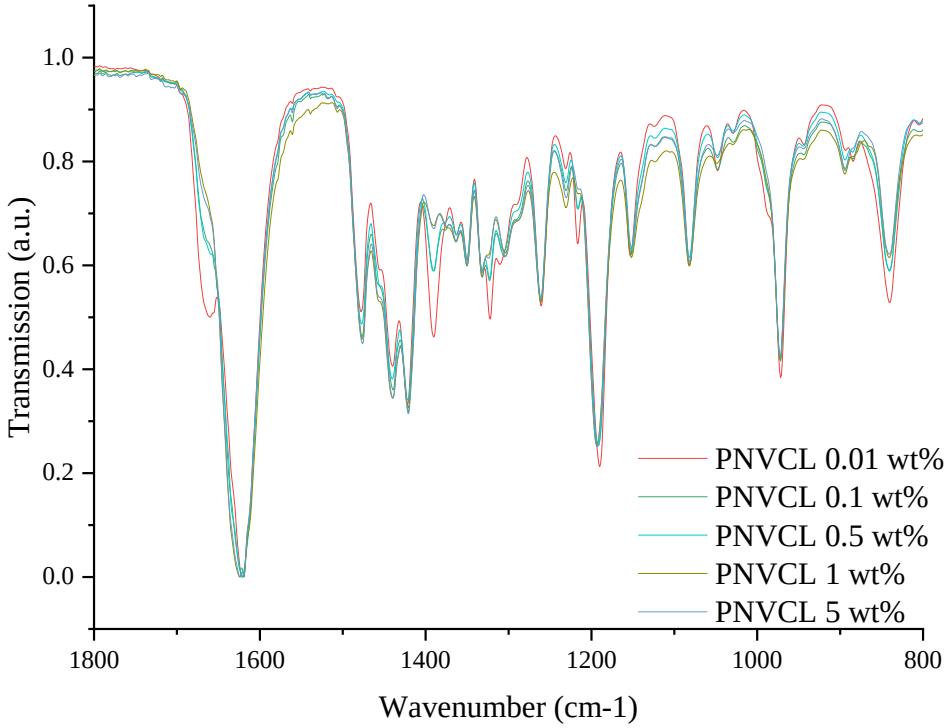

Figure 3-62: Normalised FTIR spectra of PNVCL samples with different concentrations of photoinitiator 0.01, 0.1, 0.5, 1 and 5 wt% of Irgacure®184 after vacuum drying at 40 °C.

N-pentane and xylene were used to determine the effect on the PNVCL samples. After vacuum drying the samples were then soaked in the solvents to determine if they would reduce any unreactive monomer within the samples. Figure 3-63 display the FTIR spectrum of PNVCL samples washed with *N*-pentane. It can be seen that an apparent reduction in both the bands at 1655 cm^{-1} (C=C) and 1390 cm^{-1} (C–C) compared to the samples dried in the vacuum oven.

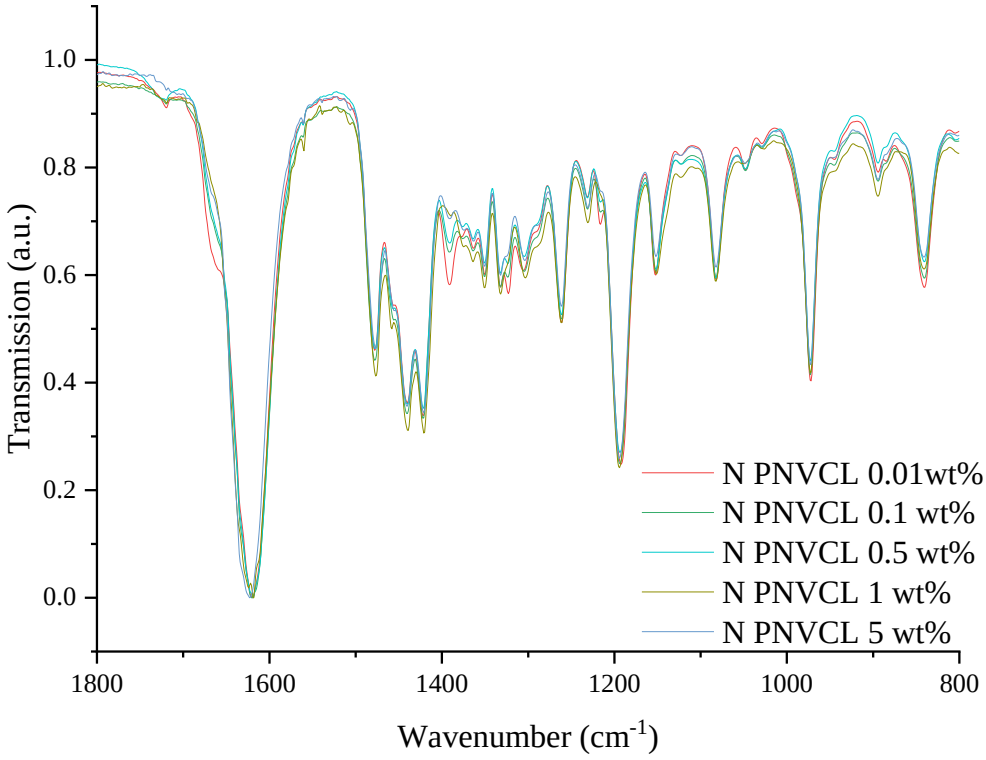

Figure 3-63: Normalised FTIR spectra of PNVCL samples with different centration of Irgacure®184 after washing the samples in *N*-pentane.

In Figure 3-64 displayed the PNVCL samples that were soaked in xylene. Again, there were noticeably decreased in the bands at 1655 cm^{-1} (C=C) and 1390 cm^{-1} (C–C), which were believed to be unreactive NVCL monomers. Overall, in summary, it was found that just using a vacuum oven to remove any unreacted monomers was not sufficient. It was only using a solvent and soaking the PNVCL samples several times that the unreacted monomer was removed. Samples washed with *N*-pentane were chosen to be used for the rest of the study as it was a more feasible option.

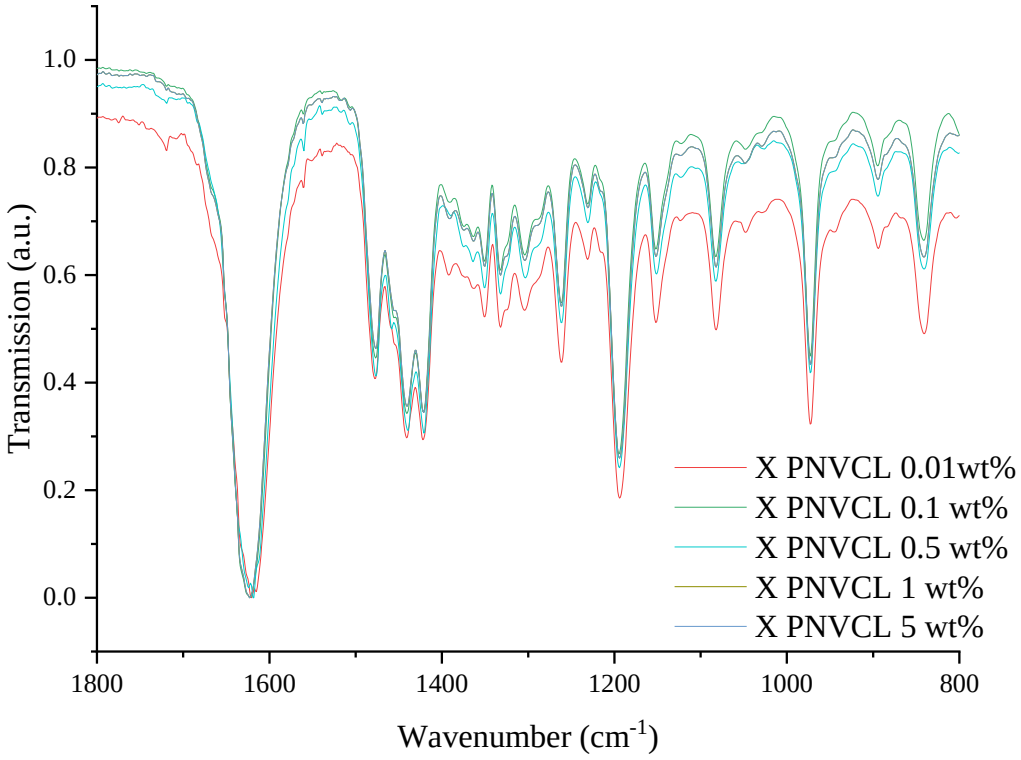

Figure 3-64: Normalised FTIR spectra of PNVCL samples with different centration of Irgacure®184 after washing the samples in *N*-pentane.

3.4.5.3. ATR-FTIR

In this section, ATR-FTIR was conducted on PNVCL based samples to determine the effects of HME processing (Figure 3-65). All extruded PNVCL samples exhibited a carbonyl band (C=O) which was observed at 1620 cm^{-1}, which is similar to that of the photopolymerised PNVCL. Overall, PNVCL samples that experienced the washing step and different screw speeds exhibited no significant shifts in band position, or new band formations occurred during the HME process. The results also indicated no degradation or formation of covalent links occurred between the materials.

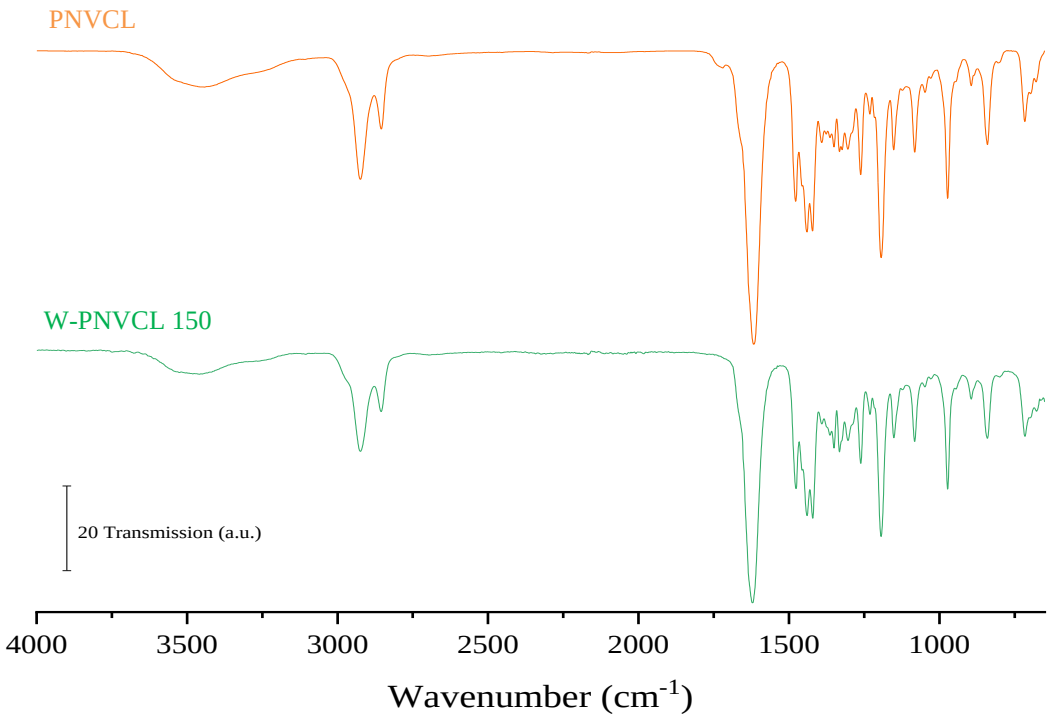

Figure 3-65: Typical FTIR spectra of washed PNVCL and Unwashed PNVCL 150 samples processed at 200 ºC.

Compounded PNVCL-PEG extruded samples can be seen in Figure 3-66. The wavelength at ~3400 cm^{-1} (O–H groups) displayed increases in intensity, corresponding to the hydrophilic nature of PEG.

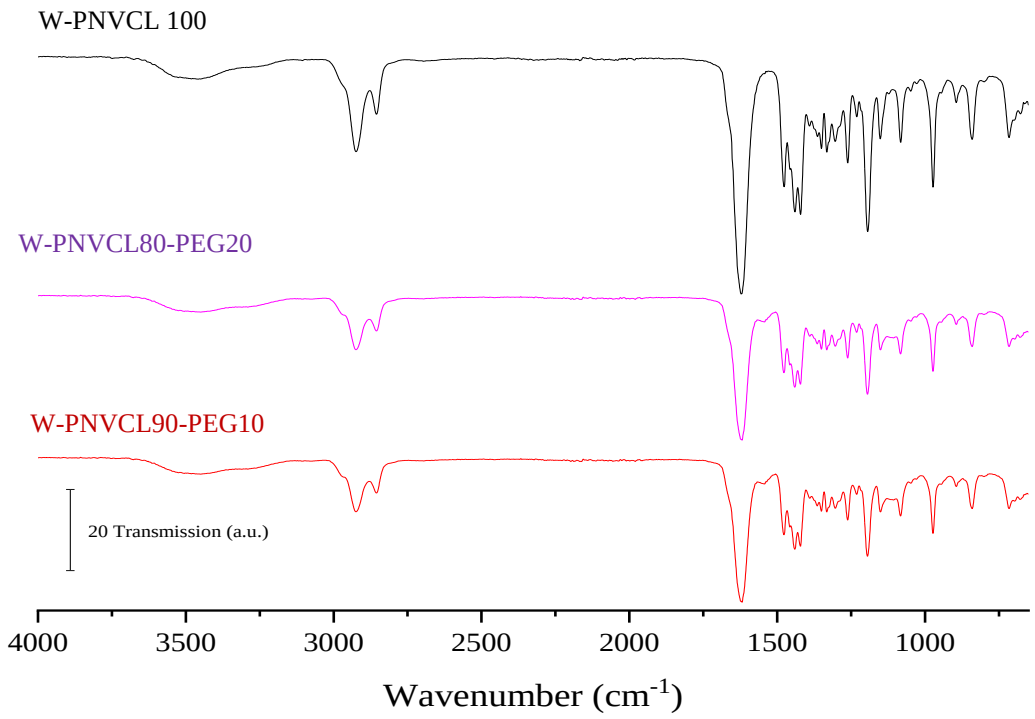

Figure 3-66: Typical FTIR spectra of washed PNVCL 100 W-P(NVCL80-PEG20) and W-P(NVCL80-PEG20). Highlighted in blue is PEG distinguishing band (C–O–C).

Given the changes in M_w, outlined in the previous section and proposed reaction of unreacted monomers during the melt processing of unwashed samples, one may have expected significant changes in the FTIR spectra of these samples, though this proved not to be the case. Advanced analytical testing such an NMR could be used to investigate this further but is beyond the scope of this study at this point.

Barmpalexis *et al.* (2013) studied the miscibility of PVP-PEG by FTIR spectroscopy which showed that PVP-PEG was miscible due to the hydrogen-bonding between the hydrogen atom of PEG terminal groups and the electronegative oxygen atom in the carbonyl groups of the monomer units of the PVP chains [297]. Figure S 6-1 in the appendix displays a summary of the peaks obtained for unwashed samples, which can be found in the supporting information. In the study herein, the addition of such bands with the PNVCL and PEG mixtures were observed when compared with unprocessed polymers.

3.4.5.4. Melt Rheology

Frequency sweeps on selected samples of PNVCL were carried out at 200 °C. Storage, loss modulus and complex viscosity were measured over angular frequency. During melt processing at higher screw speeds, PNVCL underwent die swell; from the rheological analysis, the results indicate that PNVCL has a high storage modulus (Figure 3-67 and Figure 3-68) which is related to the memory effect of the polymer. Storage modulus for unwashed PNVCL displayed an increase with increased screw speed. However, for washed PNVCL, the opposite effect occurred where a decrease was displayed with increasing screw speed.

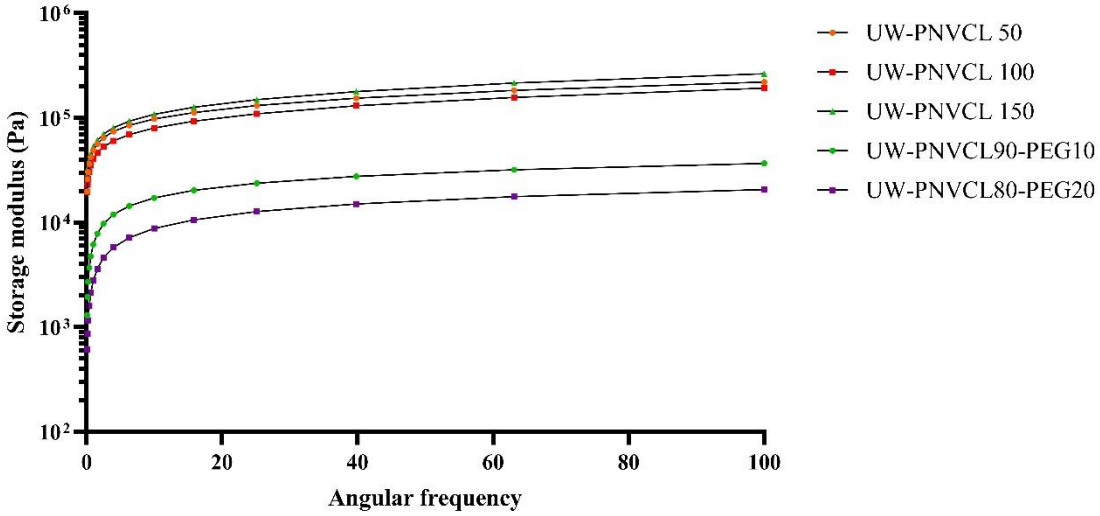

Figure 3-67: Storage modulus vs angular frequency for unwashed PNVCL based samples. Melt rheology storage modulus (Pa). Mean rheological data is presented (n = 2).

Figure 3-67 to Figure 3-70 inclusive display that all samples containing PEG exhibited a drop in both the storage modulus and the complex viscosity. With an increased concentration of PEG, a further reduction in the modulus was displayed for all samples. This was due to PEG's low molecular weight intermeshing between the PNVCL polymer chains and allowing them to move more freely. The molecular weight of a polymer is directly related to the polymer melt viscosity [249].

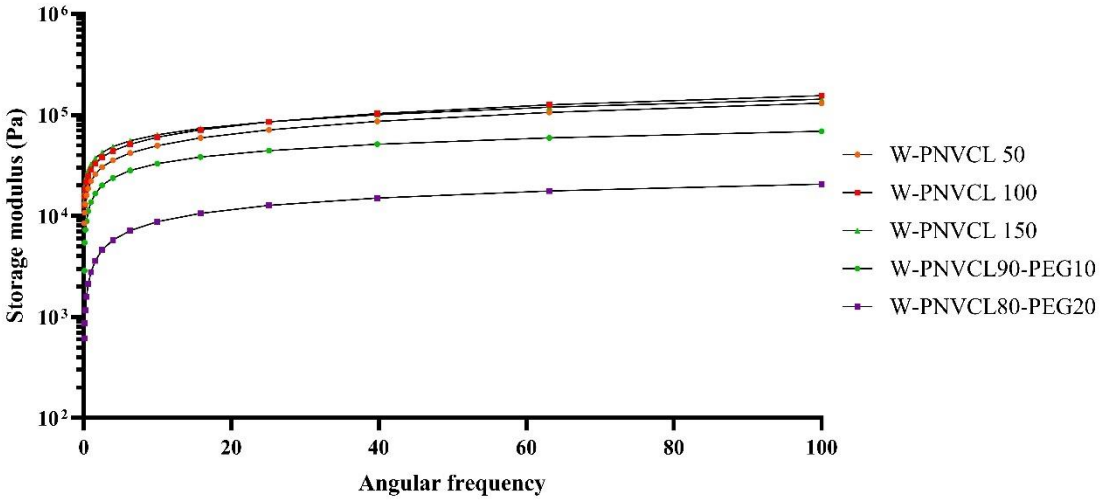

Figure 3-68: Storage modulus vs angular frequency for washed PNVCL based samples. Melt rheology storage modulus (Pa). Mean rheological data is presented (n = 2).

Figure 3-69 shows the complex viscosity for unwashed PNVCL samples; it shows that an increase in the complex viscosity occurred with an increase in screw speeds. This corresponds with results in Section 3.4.5.1. Polymers with high molecular weight will exhibit higher complex viscosity. This is further evidence that an increase in the M_w occurs during melt processing of unwashed samples.

Displayed in Figure 3-70 is the complex viscosity vs angular frequency for washed PNVCL based samples. It shows that higher screw speeds resulted in a lower complex viscosity. This is a direct result of the PNVCL M_w decreasing. The addition of PEG lowered the complex viscosity in all cases, washed and unwashed, and the low M_w PEG aided the melt processing of PNVCL.

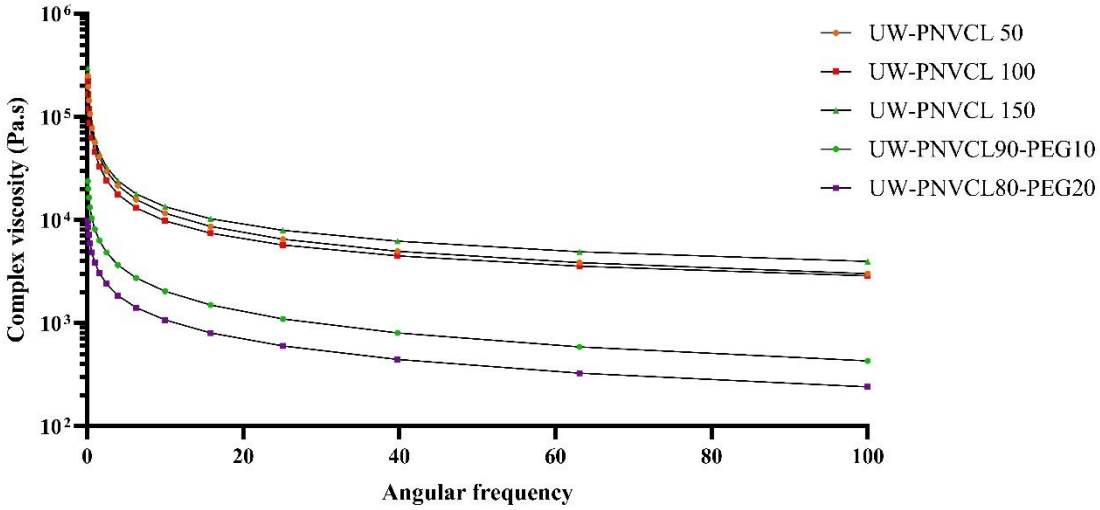

Figure 3-69: Complex viscosity vs angular frequency for unwashed samples. Melt rheology complex viscosity (Pa.s) data are presented as mean (n = 2). Mean rheological data is presented

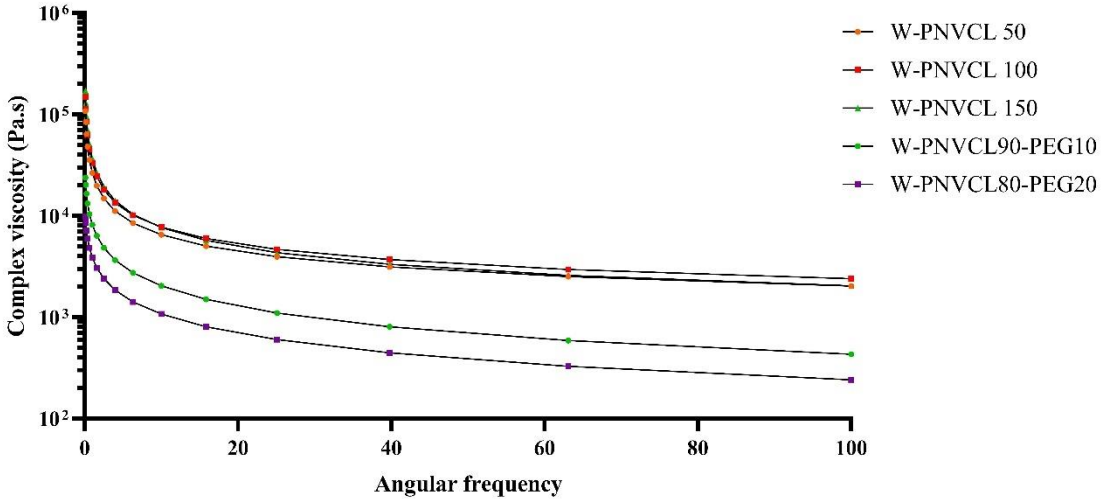

Figure 3-70: Complex viscosity vs angular frequency for washed PNVCL based samples. Melt rheology complex viscosity (Pa.s). Mean rheological data is presented data are presented as mean (n = 2). Dynamic Mechanical Analysis

Thermal analysis was also conducted using DMA measurements on all melt processing PNVCL based samples. DMA measurements were carried out over a temperature range of 20-200 ºC for all samples at a rate of 3 °C/min. DMA is extensively used in material science and research. The technique involves applying an oscillatory force to the PNVCL samples and monitoring the response over a temperature range. One

beneficial aspect of DMA is that it is more sensitive to the glass transition than DSC. As illustrated in Figure 3-71, a transition was observed between 60-180 ºC for all the PNVCL based samples. All samples exhibited a broad transition, which was identified as the linear viscosity-elastic region. Results showed that the T_g of melt processed PNVCL samples were found to be dependent on the screw speed used in the HME process (below in Table 3-17). Also, supplementary information is displayed in the appendix (Figure S 6-5-Figure S 6-13).

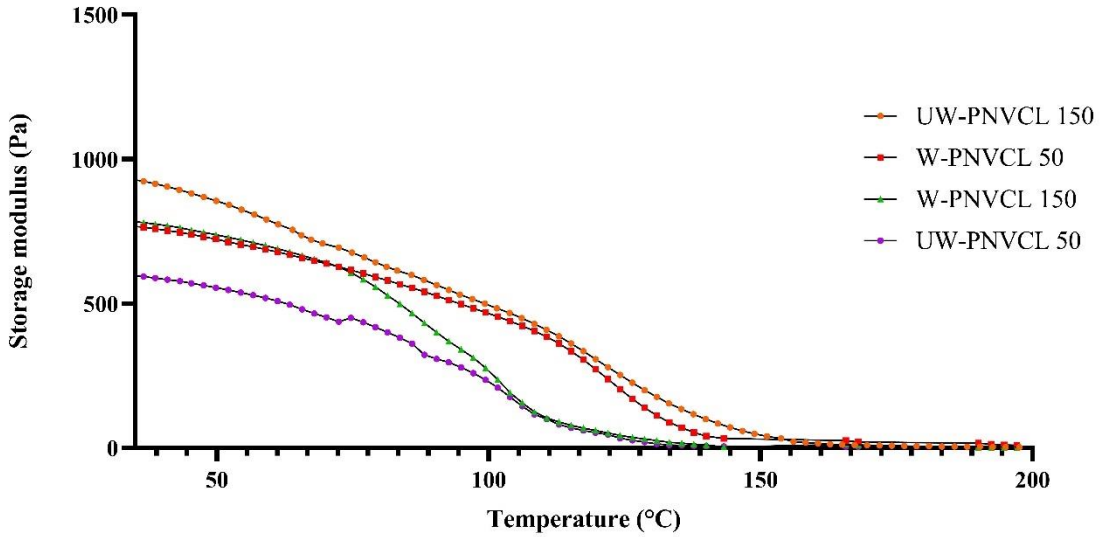

Figure 3-71: Storage modulus representing washed and unwashed PNVCL based samples at melt processing screw speeds of 50 and 150 RPM. Mean DMA data is presented (n = 2).

From the results, it can be observed that as the temperature increased the E′ decreased which is due to a reduction of stiffness, indicating that the material is undergoing a transition from a glassy to a rubbery state. Samples that were processed at higher screw speeds (150 RPM) led to the most significant changes. Washed and unwashed PNVCL 50 samples displayed a similar E′ at lower temperatures. A dramatic decrease in the unwashed PNVCL 50 sample identified the storage modulus at approximately 70 °C. This decrease in the slope is related to the molecular mobility that occurs as a result of increased temperature. The incorporation of PEG into the PNVCL matrix showed a decrease in T_g values of the samples (Figure 3-72). This indicates that

the incorporation of PEG has a plasticising effect on PNVCL samples, which was also noted in melt rheology Section 3.4.2.1.

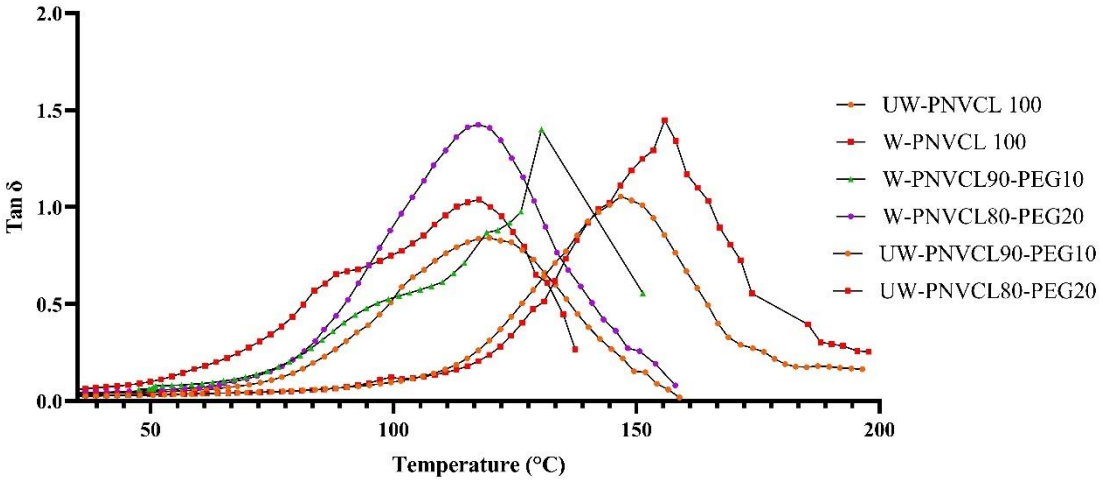

Figure 3-72: Tan δ vs temperature values with the incorporation of PEG into PNVCL. Mean DMA data is presented (n = 2).

In summary, DMA studies between washed and unwashed PNVCL samples displayed a difference in the T_g, suggesting that PNVCL was affected by this washing process. Lower M_w constituents of the polymers may have been removed during the washing procedure, and this may explain this behaviour. The screw speed was also again found to affect the T_g of PNVCL based samples.

Table 3-17: Summary of results obtained from DMA analysis after HME processing of PNVCL based.

Polymer Code	Storage Modulus (°C)	Loss Modulus (°C)	Tan Delta (°C)
W-PNVCL 50	100.1-101.7	78.8-83.6	114.0-115.2
W-PNVCL 100	113.7-114.1	98.7-102.1	132.1-134.5
W-PNVCL 150	117.3-124.3	105.1-107.3	143.4-146.4
UW-PNVCL 50	135.1-139.5.5	120.9-126.1	145.3-148.5
UW-PNVCL 100	136.9-7137.1	125.6-126.0	154.1-155.5
UW-PNVCL 150	145.5-148.4	120.2-121.4	149.9-153.7
W-PNVCL90-PEG10	101.9-109.7	88.4-94.0	121.7-126.5
W-PNVCL80-PEG20	93.4-99.0	82.888.0	115.8-120.4
UW-PNVCL90-PEG10	107.3-112.9	91.0-94.0	120.0-126.6
UW-PNVCL80-PEG20	74.8-77.8	84.4-89.0	116.4-118.0

3.4.5.5. Swelling studies

Extruded samples were placed in distilled water and their swelling ratio was investigated over an 8 hour period, at room temperature (Figure 3-73). The washed PNVCL 50 sample showed the highest degree of swelling, while increased screw speed led to a decrease in the swelling ratio. With the incorporation of PEG, a further reduction in the swelling ratio was exhibited. The influence of HME on the swelling of washed PNVCL resulted in a decrease in the swelling ratio, which is likely due to a reduction in the molecular weight.

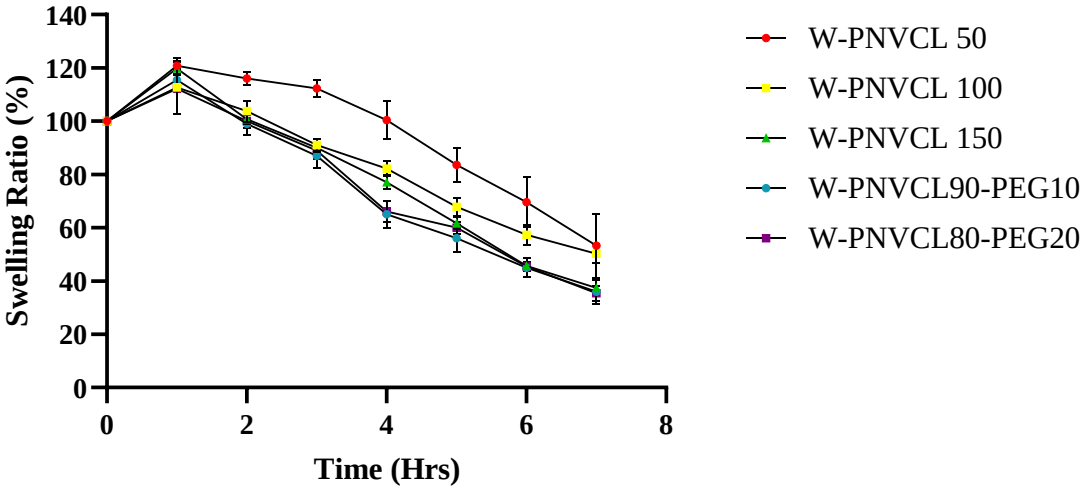

Figure 3-73: Swelling studies on washed PNVCL based samples at room temperature. Swelling ratio (%) data are presented as mean±SD (n = 3).

Figure 3-74 illustrates the swelling behaviours obtained for the unwashed PNVCL based samples. Once again, it can be seen that an increase in the screw speed led to a slight change in the swelling properties of PNVCL samples. However, in this case, it is noted that the unwashed PNVCL 50 samples had the lowest swelling degree; this is due to the molecular weight changes, which were reported previously, due to reaction of unreacted monomers in the unwashed samples during melt processing.

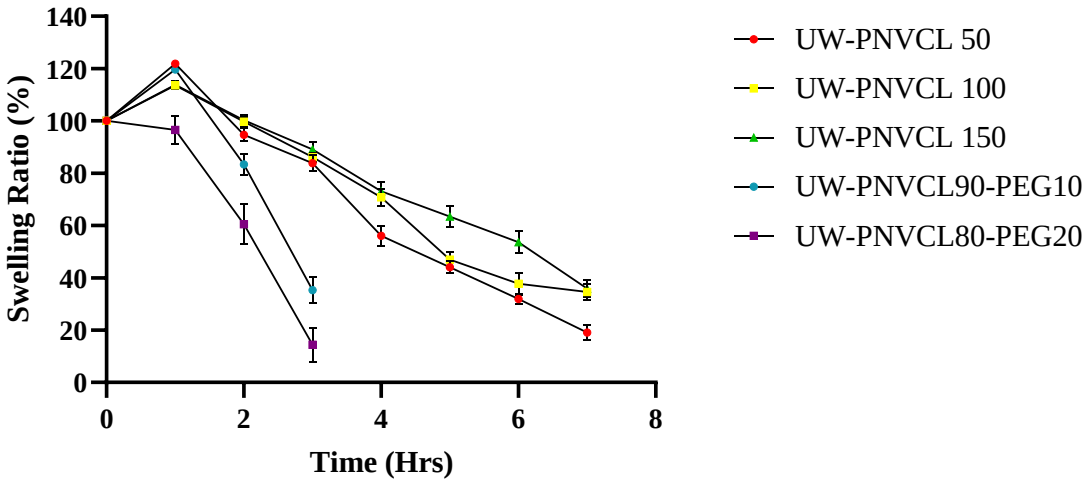

Figure 3-74: Swelling studies of Unwashed PNVCL based samples containing PEG at room temperature. Swelling ratio (%) data are presented as mean±SD (n = 3).

For samples containing PEG, the maximum swollen weight had been reached after 1 hour for all samples. When the maximum swollen weight was reached, the polymers began to break down. Samples containing the highest percentage of PEG led to a quicker breakdown rate; this is due to PEG being highly water-soluble and being a highly hydrophilic polymer. Similar findings have been reported by Perissutti *et al.* (2002), who incorporated hydrophilic PEG into a drug-polymer blend [298].

Thus, there is the possibility of adding a range of hydrophilic polymers to tailor the swelling characteristics, adding to the advantages of the HME process, as there is much research on the breakdown behaviour of PNVCL for drug release. Overall, the incorporation of PEG into the PNVCL polymeric matrix had a more significant impact on the swelling and breakdown rate of PNVCL based samples compared to screw speed.

3.4.6. Phase transition determination

3.4.6.1. UV-spectroscopy

In the design of temperature-responsive polymers, the phase transition is a highly significant element. It is well-known that PNVCL phase transition is affected by its molecular weight. With an increase in molecular weight, the phase transition is expected to decrease, which is based on the changes in the polymer-solvent interaction [191].

Figure 3-75 below shows the difference in the phase transition of unwashed PNVCL samples. There was minimal difference between unwashed samples processed at 50 and 100 RPM. However, with regards to samples processed at 150 RPM, a shift in the phase transition occurred towards lower temperatures. This is primarily due to the higher molecular weight of the unwashed samples at this processing speed. The result corresponds to the results found in the GPC analysis (Section 3.4.5.1).

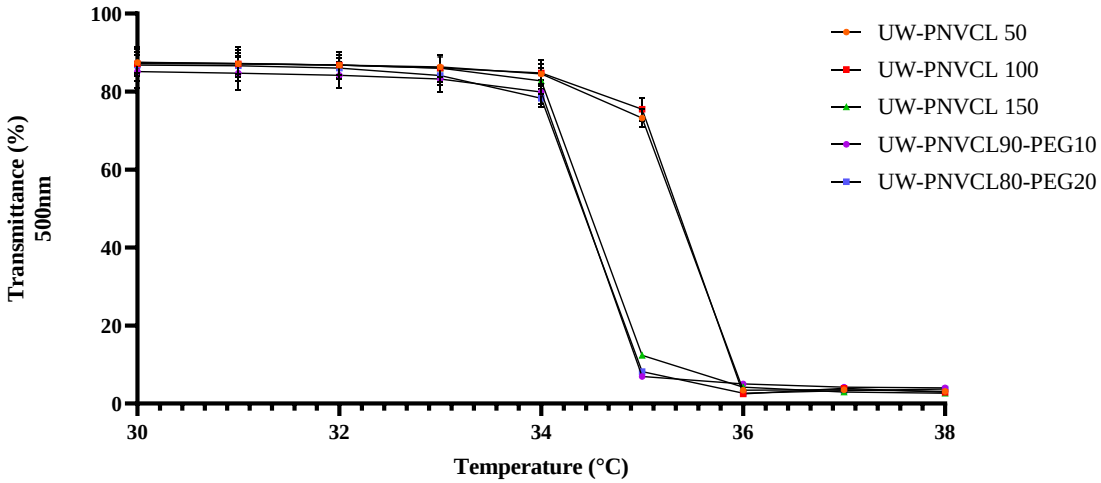

Figure 3-75: UV- spectroscopy illustrating the phase transition of unwashed PNVCL based samples. Phase transition transmittance (%) data are presented as mean±SD (n = 3).

It has been reported in the literature that when PNVCL solutions are introduced to an increased temperature, the polymer solutions undergo a coil-to-globule transition. This is where microscopic phase separation occurs when the PNVCL solution becomes cloudy above the phase transition, additionally increasing the temperature precipitation, which is due to the instability of the micro-separated phases. The carbonyl group of PNVCL interacting with water provides a smaller amount of water-structuring properties resulting in larger precipitation particles.

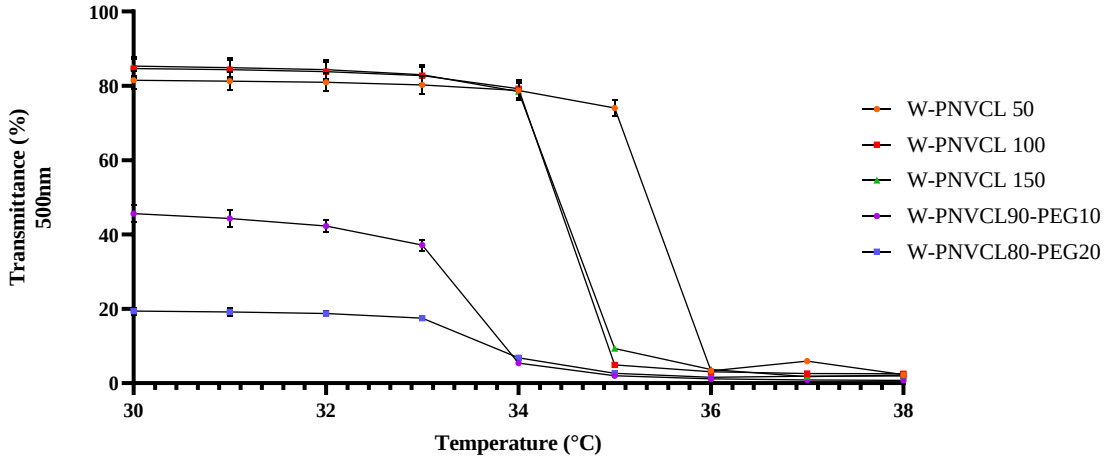

Figure 3-76: UV- spectroscopy illustrating the phase transition of washed PNVCL based samples. Phase transition transmittance (%) data are presented as mean±SD (n = 3).

Illustrated in Figure 3-76 above are PNVCL based samples that underwent the washing process; the samples displayed an increase in the phase transition temperature. The phase transition of PNVCL is a result of its chemical structure where the carbonyl group of the lactam ring can provide hydrogen bonding of PNVCL with water. Reviewing the washed samples, it was found that with increased screw speed, the phase transition temperature was lowered. It remains unclear as to why washed samples have a lower transmittance % with PEG. These results again correspond with the GPC results whereby all washed PNVCL samples showed a decrease in the molecular weight. This is a very significant finding as it proves that the LCST of this polymer can be modulated using a melt processing approach.

3.4.6.2. Sol-gel transition

Sol-gel measurement was only conducted on unwashed samples. Tube inversion method was used to determine if PNVCL thermo-gelling capabilities remained after melt processing. It was found that increased screw speed for unwashed samples led to a decrease in the thermo-gelling temperature (Figure 3-77). This correlates to results in Sections 3.4.6.2 and 3.4.5.1, where a decrease in the phase transition temperature was displayed, which is due to the molecular weight changes. However, for unwashed samples containing PEG, an increase in the thermo-gelling temperature was illustrated.

It is suggested from the literature that at temperatures below the sol-gel transition, PNVCL remains as a solution, and in the course of increasing the temperature, PNVCL turns into a gel. This is due to the internal energy where the hydrogen bonds between PNVCL and water molecules would break. This increase in entropy in PNVCL leads to the hydrophobic side chains of PNVCL accumulating until gelation occurred [286]. It is assumed that the incorporation of PEG to PNVCL led to increasing the space between PNVCL side chains, which resulted in a higher sol-gel transition temperature. One limitation in this, found that the loading level of PEG is limited. This is due to increasing the PEG concentration as it can weaken the phase transition properties of PNVCL. Importantly, this study has demonstrated that temperature-responsive polymers can be melt processed and still retain their phase transition capabilities.

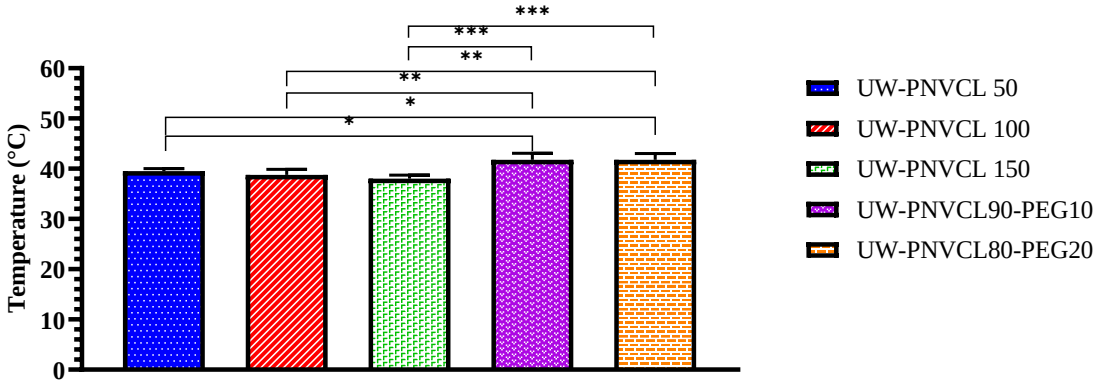

Figure 3-77: Statistical analysis of the interaction of melt processing on the unwashed samples measured using the tube inversion method. Sol-gel transition data are presented as mean±SD (n = 5). One-way ANOVA followed by Tukey multiple comparison test. Significantly different * $p < 0.05$; ** $p < 0.01$ and *** $p < 0.001$.

3.4.7. Summary

This is the first study to determine the melt processing capabilities of PNVCL, which indicates that it is a viable and novel option for the manufacture of smart polymer delivery systems with potential for implantable drug delivery applications (Figure 3-78). The properties of PNVCL can be tailored to be suitable for a one-step melt process. This is very important as melt processing techniques present many advantages over conventional fabrication methods. The incorporation of PEG served to decrease the melt viscosity of the polymer system. It was also observed in samples that M_w could be altered depending on the screw speed and washing process. It was found that increased screw

speed on washed samples led to a decreased M_w. This is a significant finding given that M_w is an essential factor in determining the phase transition of PNVCL. Overall, this study provides a novel approach for enhancing PNVCL properties by melt processing technique.

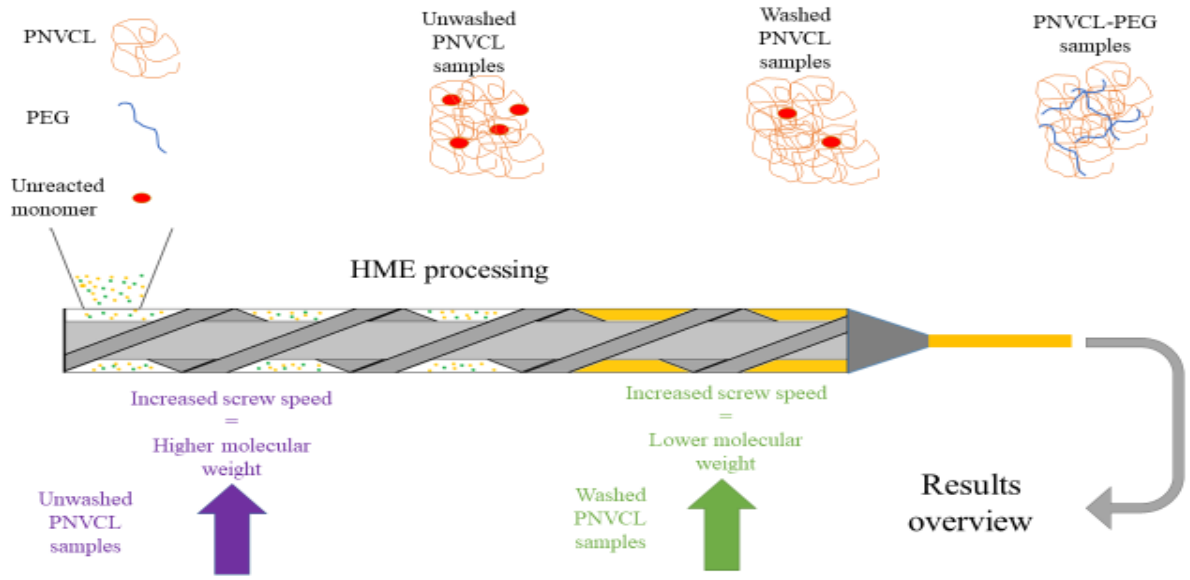

Figure 3-78: Research process visual overview of melt processing of PNVCL.

3.5. Potential platforms for drug delivery technology: Hot-melt extrusion of Poly (*N*-vinylcaprolactam)

3.5.1. Preface

In Sections 3.3 and 3.4, PNVCL was extensively studied and tailored for applications in HME. However, utilising melt processing to load a drug into a hydrogel matrix could offer great possibilities in smart delivery systems. Currently, smart polymers have gained a great deal of attention, mainly due to their unique characteristics that allow for site-specific drug release. These smart polymers hold many desirable characteristics for use as a drug carrier, which offers several advantages over traditional polymers. However, the drug loading capabilities of such smart polymers are very limited when compared to other systems that are prepared by HME processes. Traditionally smart polymers are loaded with drugs using two different methods, which is the current state of the art technology for these types of systems.

It was found from previous sections that physical cross-linked PNVCL can be used in melt processing. Therefore, the idea of this section is that a drug can be incorporated into a physically cross-linked hydrogel by melt processing. One advantage of this approach is that HME is a continuous process and both hydrophilic and hydrophobic drugs can be incorporated by this method. However, one major disadvantage is that the drug would have to be exposed to high temperatures and shear rates.

Overall, reviewing the literature and as discussed previously in Section 1.9, one limitation of hydrogels is how to get the drug into the polymer matrix efficiency. This section attempts to solve this issue by introducing the drug during melt processing.

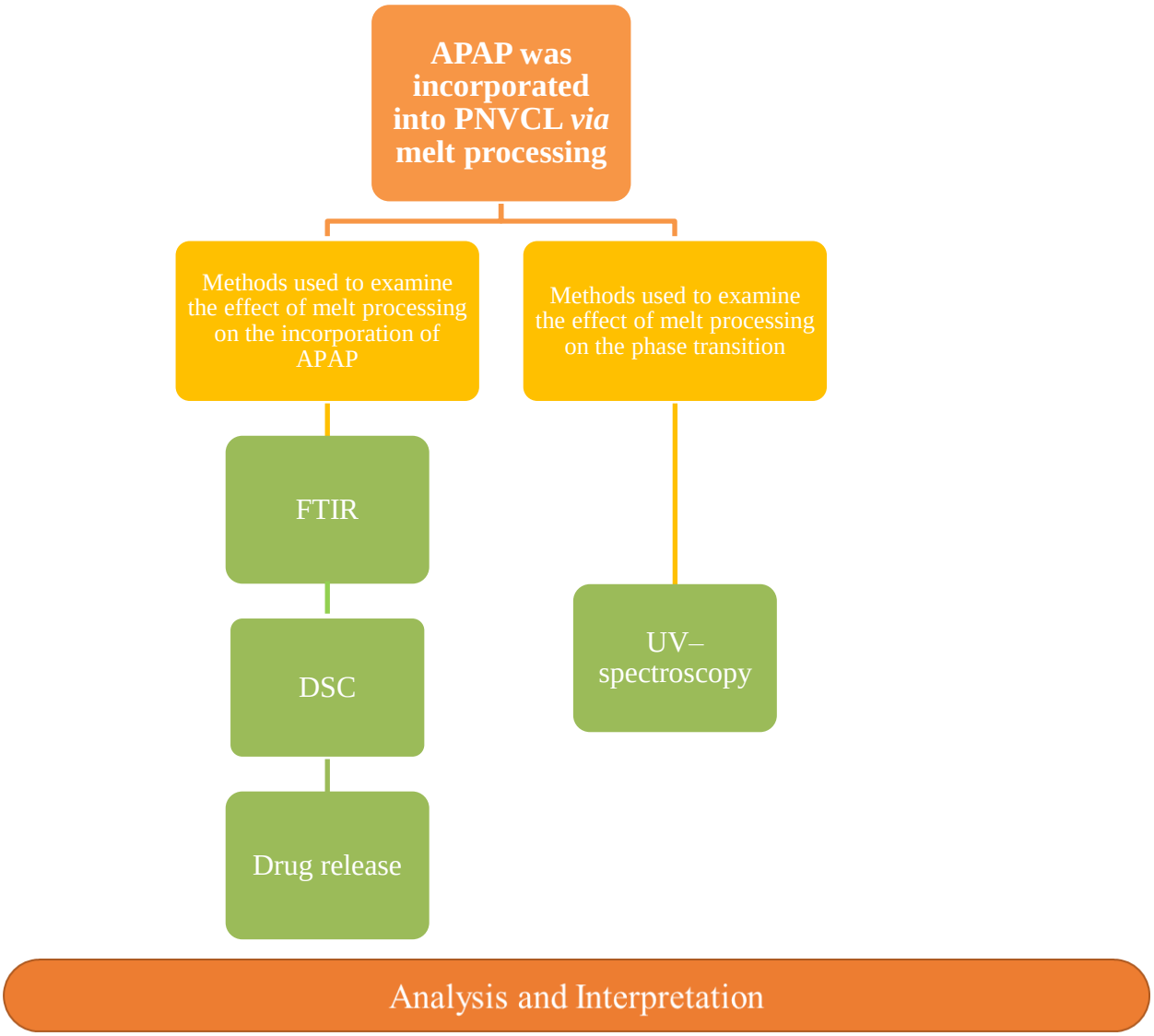

Figure 3-79: Workflow for Section 3.5 incorporating acetaminophen into PNVCL based samples.

In recent years, PNVCL has been proven to be biocompatible, with an increasing number of reports showing its applicability in drug delivery as a carrier system [23]. During the development of PNVCL, it was found that PNVCL could be either used as an implant or injectable system. Regarding the current methods of loading a drug into a hydrogel, melt processing of PNVCL has the potential to offer a number of benefits to an already popular smart hydrogel system. It will potentially allow for the creation of smart dosage forms that can respond to temperature and allow the drug to be released at a specific temperature, thus leading to more accurate and programmable drug delivery systems. This section aimed to investigate the possibility of loading a drug into PNVCL

by melt processing. To achieve this, a model drug was selected (APAP), which was added at 10, 20 and 30 wt%. In Figure 3-79 is the workflow for Section 3.5.

3.5.2. Processing observations

For smart hydrogels to be attractive in biomedical applications, some essential criteria must be met, these include efficient drug loading and controlled drug release [18]. Regarding drug loading, bioavailability and controlled drug release, HME is widely used in applications to enhance these properties [299]. To date, melt processing has not been used to load drug into smart negative temperature-sensitive polymers. Figure 3-80 is a schematic diagram of melt processing of PNVCL, PEG and APAP. Before processing and characterisation, all samples were dried in a vacuum oven at 90 °C for 3 hours. Based on the findings in the previous Section, the optimum processing conditions for PNVCL involved a temperature profile of 200 °C. The residence time of the samples in the extruder is approximately 2-3 minutes. Also, the most favourable screw speed was 100 RPM, as it resulted in the lowest torque values.

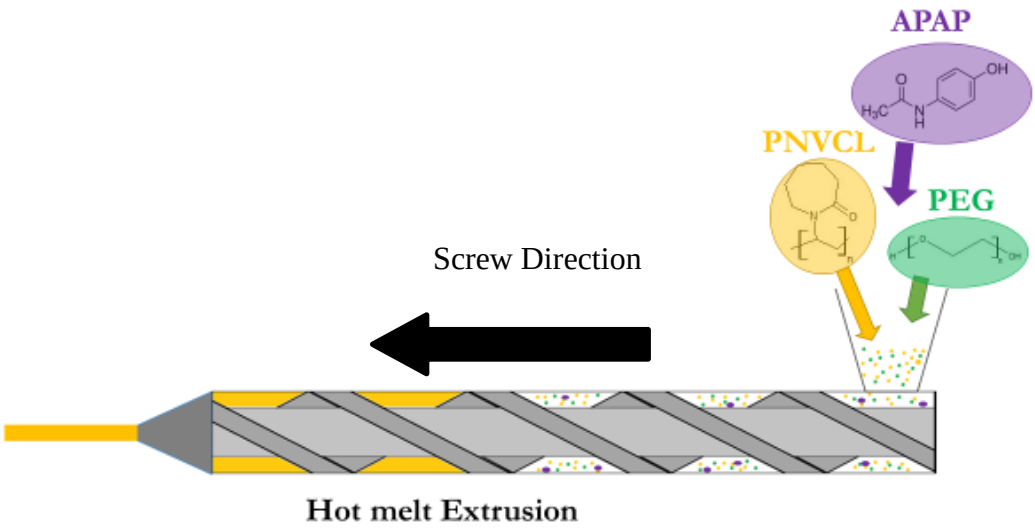

Figure 3-80: Schematic of melt processing PNVCL and APAP based samples.

Figure 3-81 below shows the torque values for the incorporation of APAP during melt processing. Increasing the concentration of APAP lowered the torque values, indicating that APAP acted as a plasticiser during melt processing. The thermal

decomposition of APAP in the literature shows only 5% weight loss upon heating above 300 °C [300]. Another study states that paracetamol degrades significantly above 200 °C. It was also found that when APAP is incorporated into the PVA, no appreciable mass loss is seen, suggesting the polymer is stabilising the drug [301].

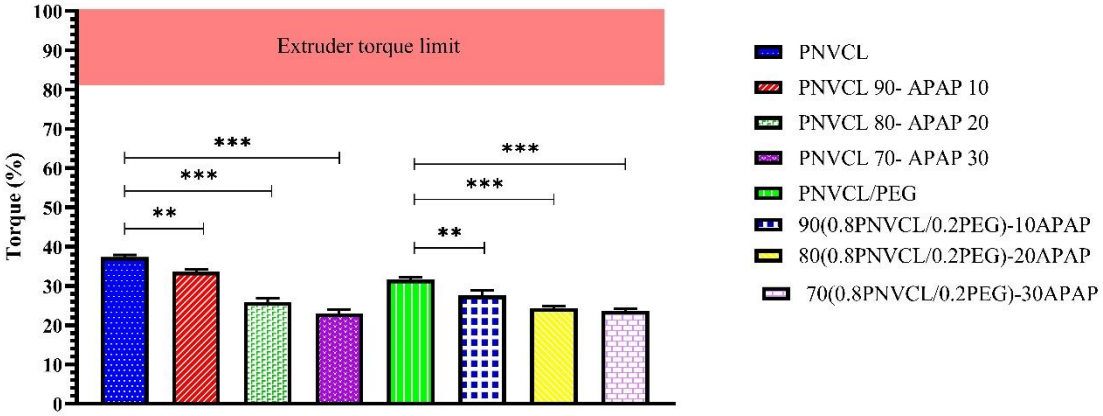

Figure 3-81: Statistical analysis of the of torque (%) recorded during the melt processing trails of PNVCL based samples containing APAP. Torque (%) data are presented as mean±SD (n = 3). One-way ANOVA followed by Tukey multiple comparison test. Significantly different * $p < 0.05$; ** $p < 0.01$ and *** $p < 0.001$ vs original processing conditions.

APAP is a well-known drug which is commonly used in melt processing to model the initial drug release profile. During melt processing, the APAP is dispersed and dissolved into a polymeric matrix to produce drug delivery systems such as tablets, capsules, films and implants via oral, transdermal and transmucosal routes [131,302]. In Table 3-18 is a summary of the processing conditions used for each sample, with a temperature of 200 ℃ and a screw speed of 100 RPM, samples display excellent mechanical properties at die and also the extruder torque was within the range of 40-20 %, the resulting samples are demonstrated in Figure 3-82. Samples containing 10-20 wt% of APAP appeared to improve the surface finish, however, with 30 wt% samples appeared to have some defects such as cracks forming when cooled down.

APAP is used in many studies as a model compound for the critical examination of the dissolution behaviour of pharmaceutical systems. Treenate et al. (2017) investigated the drug release profiles of pH-sensitive hydrogels composed of

hydroxyethylacryl chitosan (HC) and sodium alginate (SA). The hydrogels were cross-linked using different ionic cross-linkers. The drug release profiles were studied using APAP as a soluble model drug. The amount of APAP released in the simulated gastric fluid was relatively low (<20%). In simulated intestinal fluid, the burst release of APAP was controlled by increasing the HC cross-linkers content [303].

Sami et al. (2017) similarly used APAP as a model drug, and reported the formulation of hydrogel-based biopolymers chitosan and guar gum. The oral ingestion of APAP is associated with gastric tract and liver complications, which led the authors to examine the release rate of transdermal drug delivery systems as an alternative. After characterisation, the formulated hydrogel was employed for the preparation of drug encapsulated transdermal patch. The drug release was then studied using an avian skin model. It was shown that the formulated hydrogels could be safely used as a dermal patch for the sustained drug release of APAP [304].

As seen above, APAP has been used with many different methods to investigate the release profile of the delivery systems.

Table 3-18: Melt processing trials of PNVCL based samples with different contents of APAP and PEG.

HME Formulation	Temperature (°C)	Screw speed (RPM)	Drying time (Hours)	Feed rate (Kg/h)	Residence time (min)	Particle size (µm)	Venting	Incorporation of plasticisers
HME PNVCL	200	100	3	1-2	2-3	<500	No	Melt processing
PNVCL 90- APAP10	200	100	3	1-2	2-3	<500	No	Melt processing
PNVCL 80- APAP 20	200	100	3	1-2	2-3	<500	No	Melt processing
PNVCL 70- APAP 30	200	100	3	1-2	2-3	<500	No	Melt processing
HME PNVCL/PEG	200	100	3	1-2	2-3	<500	No	Melt processing
90(0.8PNVCL/0.2PEG)-10APAP	200	100	3	1-2	2-3	<500	No	Melt processing
80(0.8PNVCL/0.2PEG)-20APAP	200	100	3	1-2	2-3	<500	No	Melt processing
70(0.8PNVCL/0.2PEG)-30APAP	200	100	3	1-2	2-3	<500	No	Melt processing
Extrudate quality		Poor		Medium		Good		

Extrudates quality can be defined as follows:
Poor samples showed characteristics of: Large die swell, Extruder torque in a high range 100-60 %, Samples had poor mechanical properties at die
Medium samples showed characteristics of: Medium die swell, Extruder torque in a high range 60-40 %, Samples had good mechanical properties at die
Good samples showed characteristics of: No die swell, Extruder torque in a high range 40-0 %, Samples had good mechanical properties at die

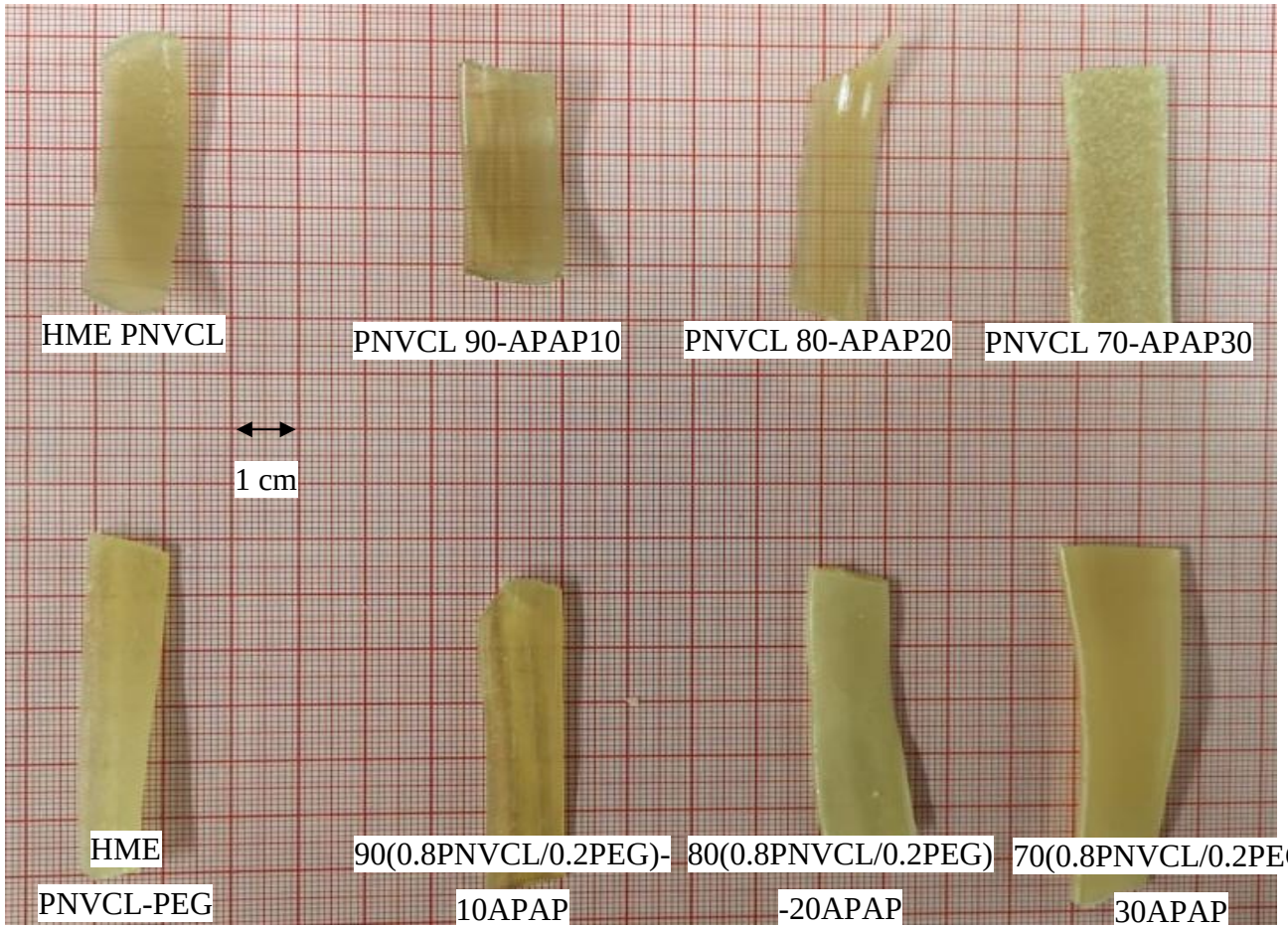

Figure 3-82: Picture of extrudates after melt processing PNVCL based samples with incorporated APAP.

3.5.3. ATR-FTIR

ATR-FTIR was carried out on all PNVCL based samples containing APAP to determine the potential intermolecular interactions of a drug into PNVCL by melt mixing. The main characteristic bands for APAP are 3324 cm^{-1} (N-H amide stretching), 3160 cm^{-1} (O-H stretching), 1656 cm^{-1} (C=O amide I stretching), 1565 cm^{-1} (C-N amide II stretching), where 1507 cm^{-1} and 1610 cm^{-1} corresponds to aromatic C-C stretching. These bands can be seen below in Figure 3-83 and Figure 3-84 [188,305]. The PNVCL characteristic band of the carbonyl (C=O) group was displayed in the region of 1619 cm^{-1} (Figure 3-83). However, with the incorporation of APAP, it was observed that the carbonyl (C=O) shifted to a lower frequency of 1589 cm^{-1}, indicating interaction with the carbonyl group of PNVCL.

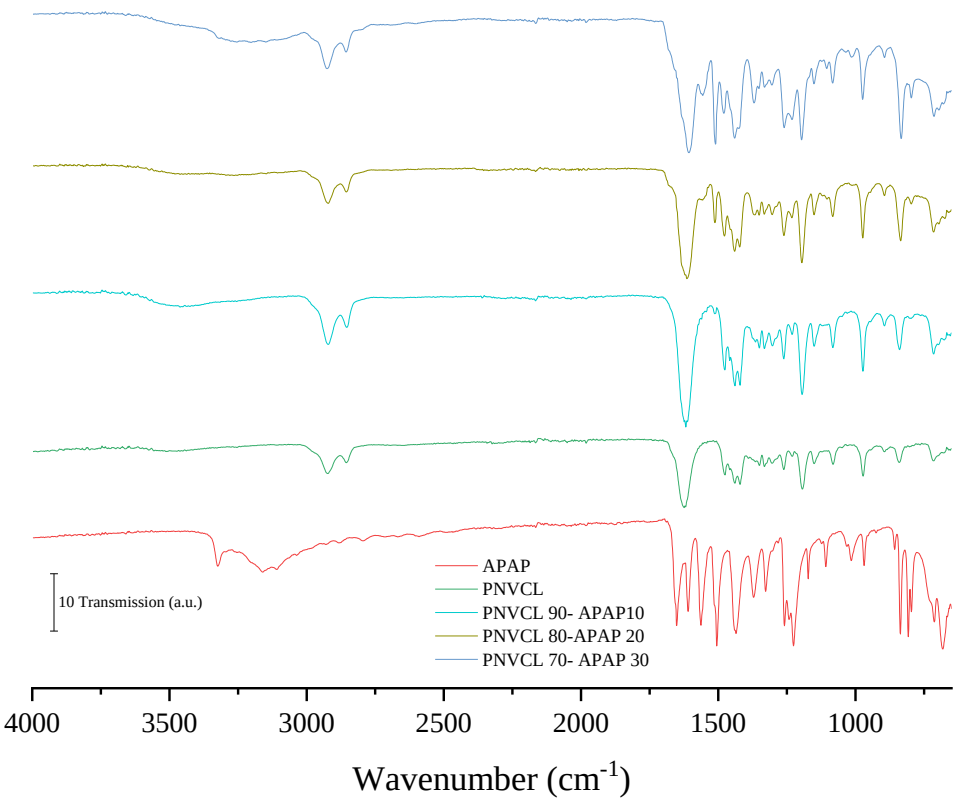

Figure 3-83: FTIR spectra of PNVCL and PNVCL-APAP extrudates.

Displayed in Figure 3-84, is PNVCL-PEG samples extruded with the addition of APAP. This new band was again due to the presence of APAP, as discussed above. Chan *et al.* (2015)

reported evidence of intermolecular interaction between drug (APAP) and PVP carriers [306]. This is consistent with the findings of this study.

Overall it is implied that hydrogen bond interactions are formed, which are associated with the C=O group of the PVP and the N-H or O-H groups of APAP [306–308]. Both Figure 3-83 and Figure 3-84, illustrates the possible hydrogen bond interaction between PNVCL and APAP. Furthermore, PNVCL and PNVCL-PEG samples containing APAP exhibit a new band. This band was within the region of 1700-1500 cm^{-1}; the new band was identified as one of APAP's characteristic band.

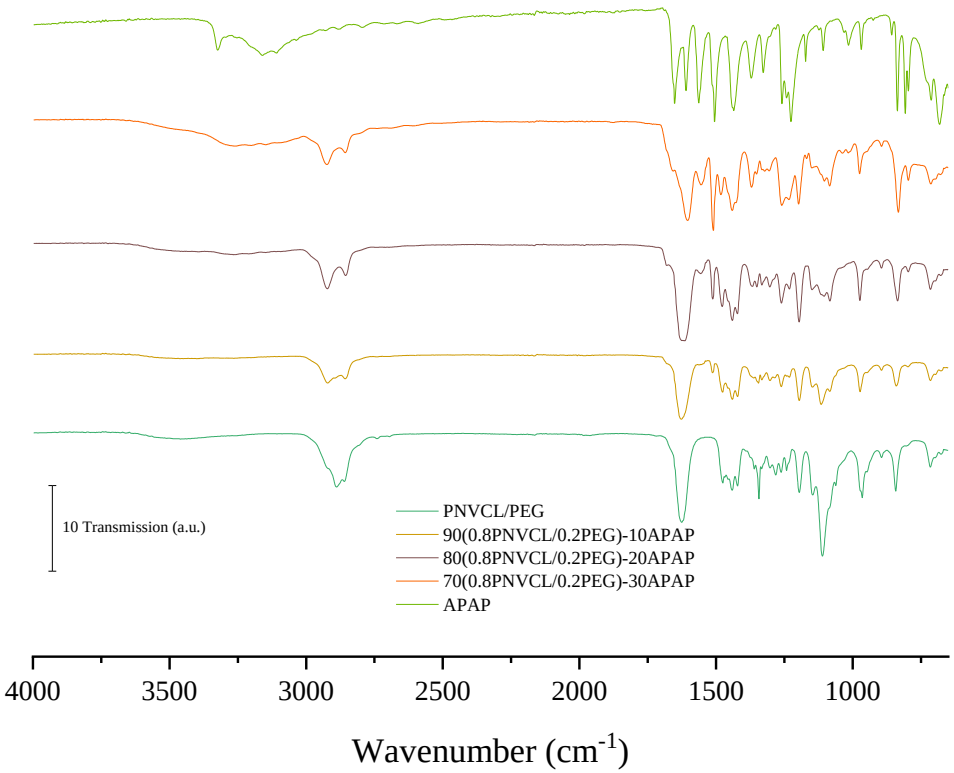

Figure 3-84: FTIR spectra of PNVCL-PEG extrudates containing APAP.

It is presumed from the ATR-FTIR analysis that polymer-drug interactions occurred. Evidence of these interactions was observed in the region of 1700-1500 cm^{-1} where a shift of the band attributed to the vibration of the C=O group of the PNVCL was recorded. It is assumed that the interactions are formed between the C=O group of the PNVCL and the N-H or O-H groups of APAP. Also, with increasing content of APAP, the band of the carbonyl (C=O) group 1619 cm^{-1} displayed shifts to lower wavenumbers which might indicate hydrogen bonding

between the polymer-drug. Possible hydrogen bond interactions of PNVCL and APAP indicated below in Figure 3-85.

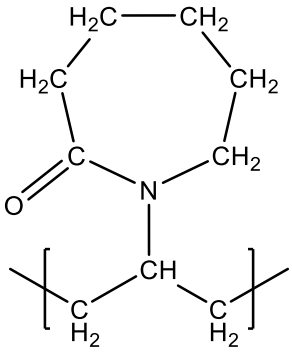

PNVCL

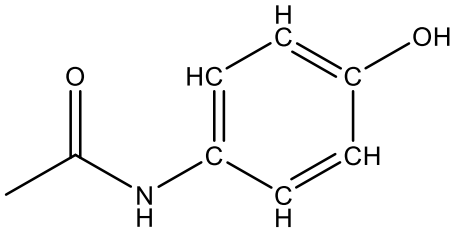

APAP

Possible hydrogen bonding

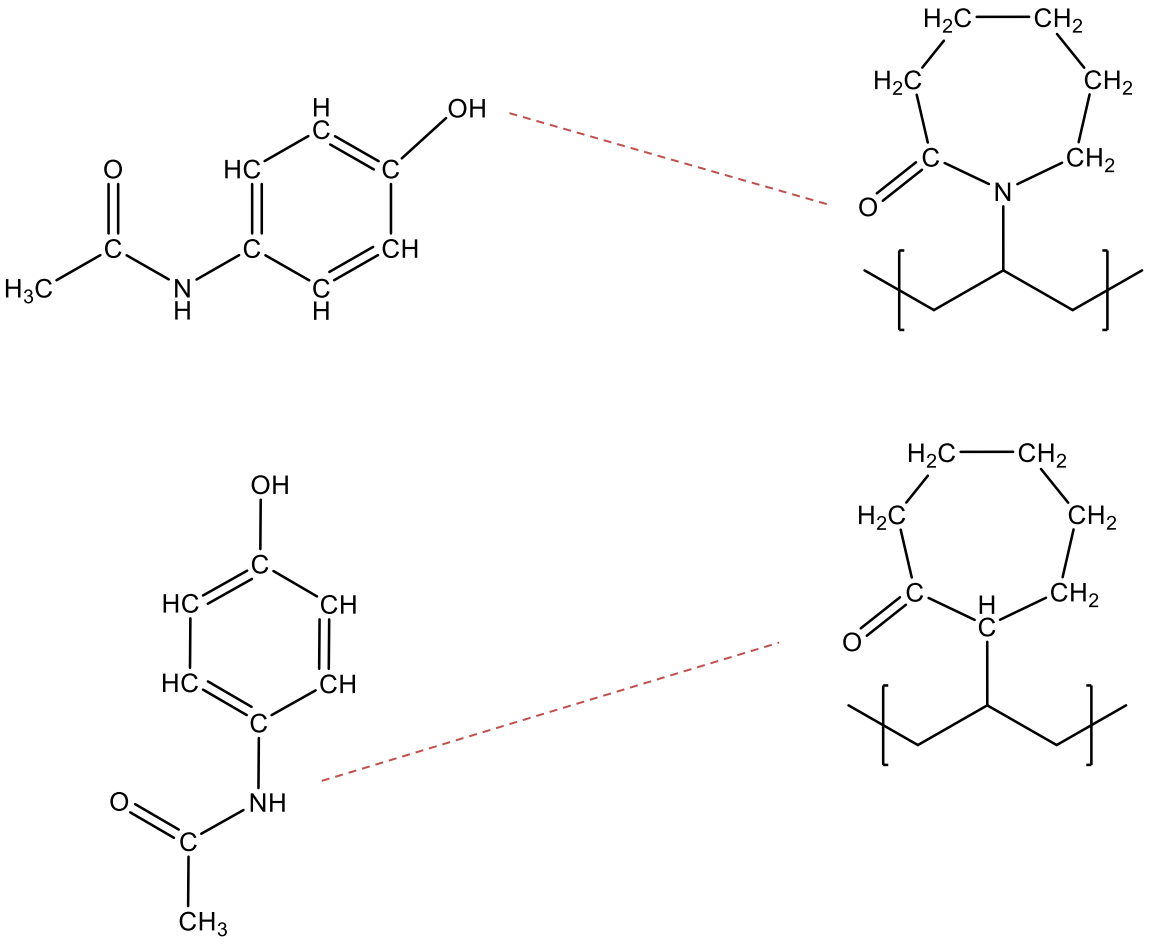

Figure 3-85: Possible hydrogen bond interactions of PNVCL and APAP indicated by red lines.

3.5.4. Differential scanning calorimetry

Drug-polymer extruded mixtures were also analysed using DSC to determine the solid state of APAP after its melt compounding with the polymeric matrix. The resulting thermographs are displayed in Figure 3-86 and Figure 3-87. As illustrated in Figure 3-86 A and Figure 3-87 A corresponding to the first heat cycle, the pure acetaminophen showed a melting peak in the region 169.5 ºC. Furthermore, this melting point suggests that APAP exists in its most stable form, Form I (monoclinic) [309,310]. However, observing the second heat cycle (B) as the melting point has shifted to a lower temperature of 159 °C, indicating that APAP may have changed forms. When the two heat cycles are compared, there is no cold crystallisation peak noted in the first heat cycle, thus indicating that the APAP is present in its crystalline form. However, upon observing the second heat cycle, it is apparent that the drug is in an amorphous form (Form II) with a glass transition temperature in the region of 24 °C, this finding is consistent with that of other studies [309,310]. Furthermore, the broad exothermal peak between 75 and 100 °C, with peak maxima around 80 °C, is typical of cold crystallisation process [310]. In addition, Rengarajan and Beiner reported similar results to support this. Rengarajan and Beiner also indicate that following cold crystallisation, the crystalline phase formed from form II, resulting in a melting point observed at 157 °C, which according to the literature, the melting temperature ranges from 154 to 160 °C [294,310].

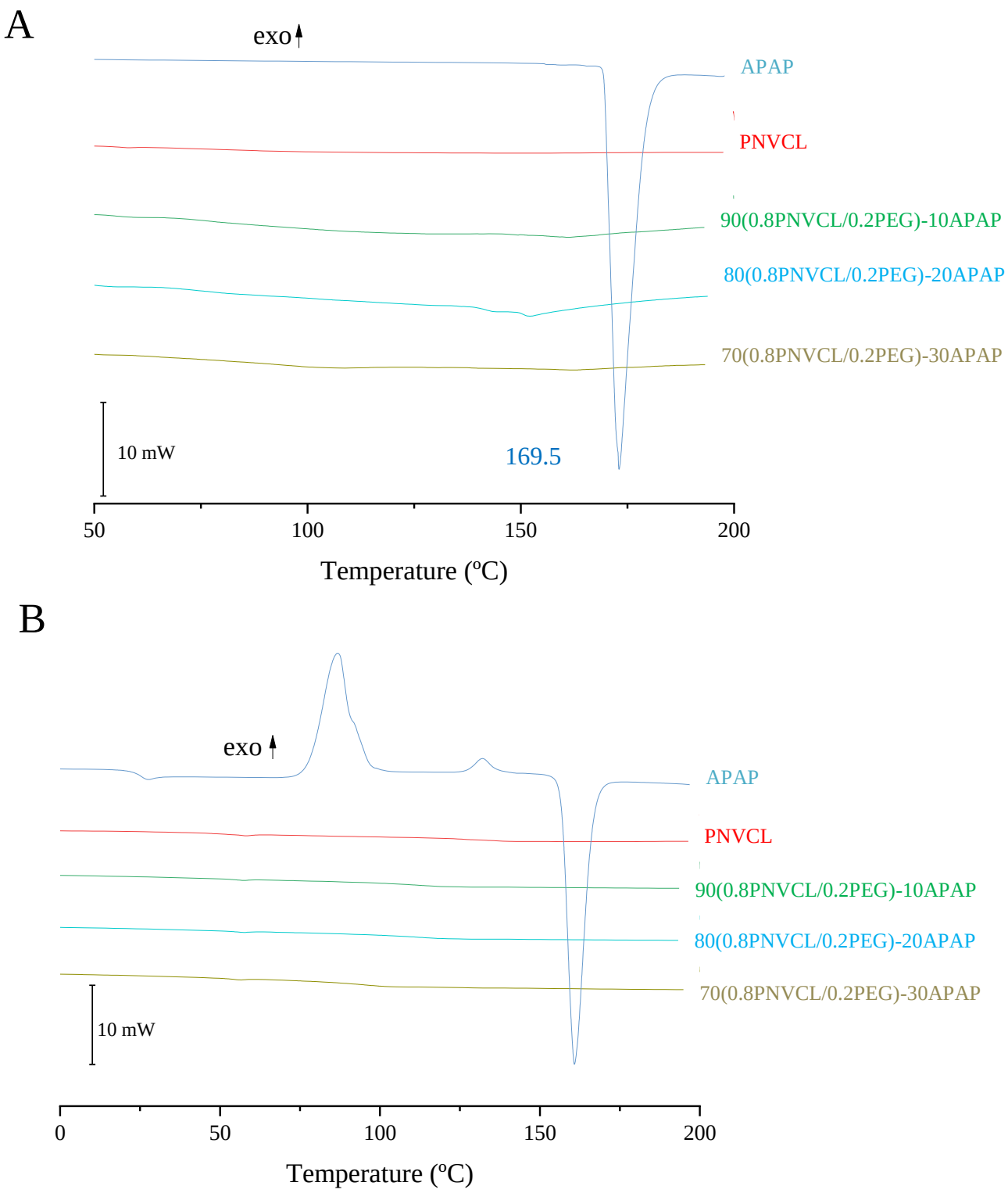

Figure 3-86: Thermographs illustrating the thermal transitions of PNVCL and APAP based extrudates (A) first heat cycle (B) second heat cycle.

Figure 3-86 exhibits the thermogram of APAP and PNVCL samples. PNVCL samples that had APAP incorporated displayed a reduction in the glass transition temperature from

126.6℃ to 98.8℃. In addition, APAP melting endotherm peaks had disappeared, which indicates the existence of APAP in an amorphous form Potentially due to the polymer-drug interaction during the HME process. Therefore, it is suggested that the presence of drug-polymer intermolecular interactions verified by FTIR may contribute to the stability of the drug in the amorphous state.

Figure 3-87 demonstrates the incorporation of APAP into PNVCL-PEG where similar results are displayed. A melting peak is observed on the second heating cycle at approximately 50 ℃, this was identified as PEG and is consistent with similar findings in the literature [311]. With the addition of APAP, the glass transition of the polymer was lowered from 107.5℃ to 84.3℃. Maniruzzaman *et al.* (2014) studied the polymer transformations of APAP in melt extruded Soluplus and vinylpyrrolidone-vinyl acetate copolymer (Kollidon). The experimental findings from the study showed that APAP transformed into a more stable form at temperatures varying from 112-120 ºC [312].

The results herein suggest that the incorporated APAP acted as a plasticiser for PNVCL based samples, as increasing the content of APAP led to a decrease in the glass transition temperature.

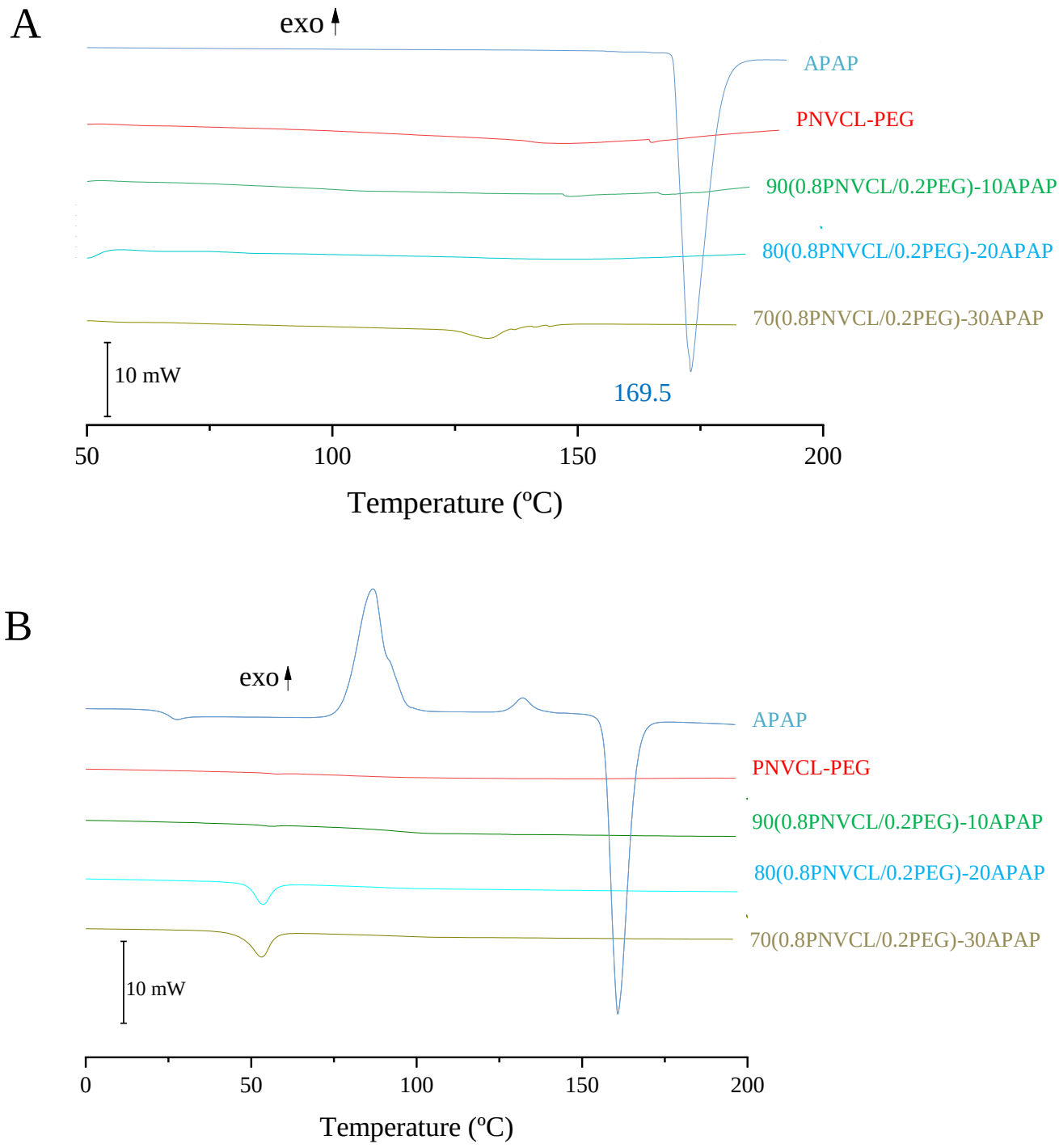

Figure 3-87: Thermographs illustrating the thermal transitions of PNVCL-PEG and APAP extrudates (A) first heat cycle (B) second heat cycle.

3.5.5. UV-spectroscopy

PNVCL based samples were tested for their phase transition temperature to determine the effect of APAP incorporation during melt processing on the cloud point behaviour. Samples containing APAP had a drastic effect on the phase transition temperature, increasing the content of APAP lowers and potentially weakens the phase transition (Figure 3-88). Incorporating 10 wt% of APAP into PNVCL, the phase transition was lowered to approximately 25 °C. However, the incorporation of 10 wt% APAP into PNVCL-PEG lowered the phase transition out of the UV-spectroscopy range. For all samples containing 20 wt% and 30 wt% APAP, the phase transition was also outside the range of the UV-spectroscopy. This was a very interesting finding as the drug incorporated had a significant effect on the phase transition temperature, which implies incorporating APAP into PNVCL could be a potential strategy to modulate the hydrophilic/hydrophobic balance of the system, which was previously discussed.

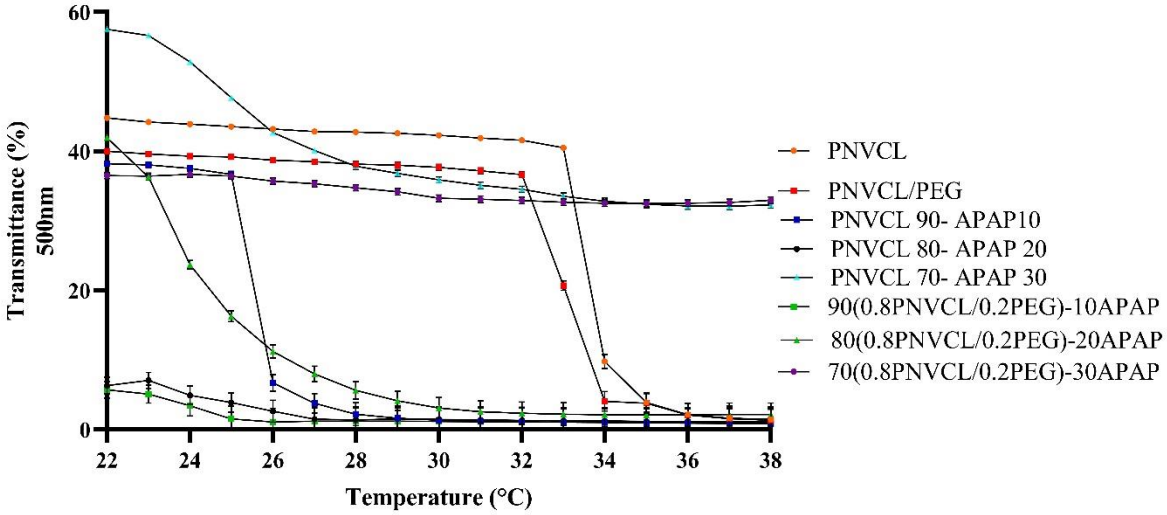

Figure 3-88: UV- spectroscopy analysis, which illustrates the phase transition of PNVCL based samples at different loading levels of APAP. UV-spectroscopy data are presented as mean±SD (n = 3).

3.5.6. Drug Release

A representative calibration curve of APAP in the HPLC method is shown below in Figure 3-89. A retention time of 1.6 minutes was noted for all runs. The linear regression data for

the calibration curve demonstrated an excellent linear relationship over the concentration range of 2.5 to 100 mg/100ml. Linearity was established by a correlation coefficient (R^2) value of 0.9902. A correlation coefficient is a statistical tool used to measure the degree or strength of this type of relationship. It was found that a high correlation coefficient value indicates a high level of a linear relationship between the concentration of APAP and peak area [313].

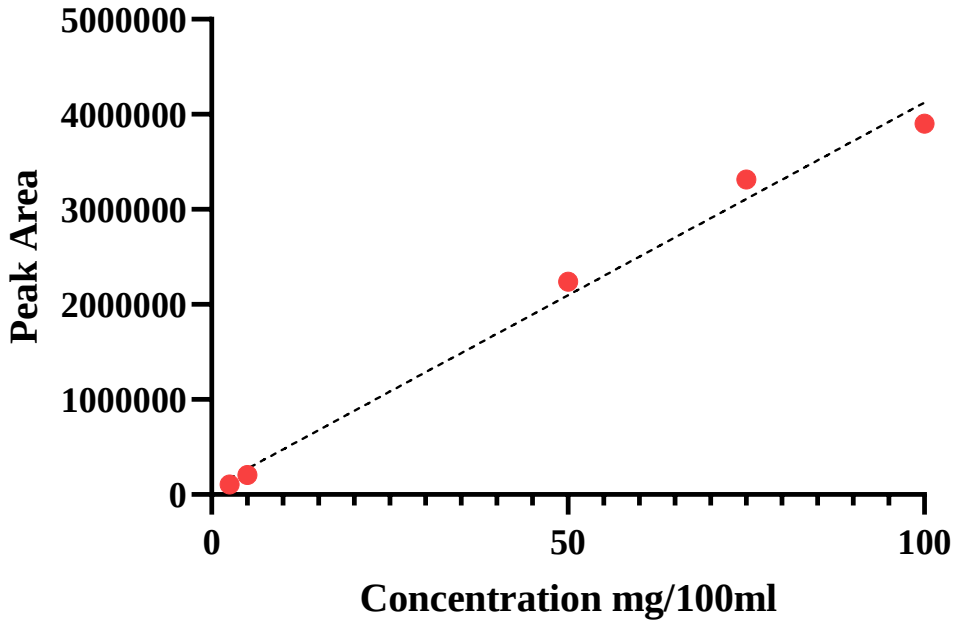

Figure 3-89: Calibration curve of APAP by the HPLC method

Sink conditions were applied. This refers to the ability of the dissolution media to dissolve at least 3 times the amount of drug present in the dosage form. The solubility of APAP in water is reported to be 12.78 g/kg (20 °C) [314]. To study the release of acetaminophen from the PNVCL matrix, drug release testing was performed by exposing manually-cut extrudates to phosphate buffer, pH 7.4; subsequent release profiles are displayed in Figure 3-90 and Figure 3-91. The extrudate weight was maintained consistently at 1.00g, with the sample dimensions approximately 3.5cm length, by 2mm wide and a thickness of 4mm. However, variations in sample surface area did occur due to the nature of the extrusion process and the requirement to ensure a consistent sample weight. A significant proportion of the samples exhibited 80% release after less than 120 hours.

The drug release profile of PNVCL and APAP (Figure 3-90) shows an extended-release profile, this is a result of PNVCL's phase transition (PNVCL 33-36 °C) , which turns the PNVCL segments into a hydrophobic state. The drug release behaviour was also influenced by the introduction of PEG in the PNVCL matrix, as samples which contained PEG exhibited

faster drug release. It is believed that the hydrophilic segment of PEG may have dissolved more rapidly compared to PNVCL, leading to pores in th PNVCL structure, changing the surface area and facilitating additional liquid ingress thus allowing APAP to release quicker. Papadimitriou et al. (2012) reported similar findings [315].Similarly, PNVCL release behaviour has been reported by Rejinold, who formulated biodegradable temperature-responsive chitosan-g-poly (*N*-vinylcaprolactam) nanoparticles for cancer drug delivery. The *in-vitro* drug release was higher at temperatures above the phase transition, compared to below the phase transition temperature. After the 72 hours, 40% of curcumin had been released at the above phase transition temperature of the system [120].

Liu *et al.* (2016) developed temperature-responsive nanofibers from poly (*N*-vinylcaprolactam-co-methacrylic acid) (PNVCL-*co*-MAA). Results showed that, by increasing the content of the hydrophobic monomer, NVCL, the drug release decreased. The hydrophilic captopril was released at a higher rate than the hydrophobic ketoprofen. Furthermore, they found that drug release characteristics were dependent on the portion of hydrophilic groups and hydrophobic groups in the copolymer [316].

Prabaharan *et al*. (2008) developed a novel pH and temperature-responsive polymer by using chitosan-g-PNVCL beads for the controlled release of the hydrophobic drug ketoprofen. The release behaviour of the chitosan-g-PNVCL beads was influenced by both the pH and temperature of the medium. The chitosan-g-PNVCL beads showed a compact structure, with reduced pore size and strong hydrophobic interactions with the drug molecules, resulting in a slow and steady release of the drug [317].

Comparing the results of the proposed method with those of the traditional methods shows that it is possible to load a drug into a physical crossed linked PNVCL hydrogel and achieve consistent release profiles

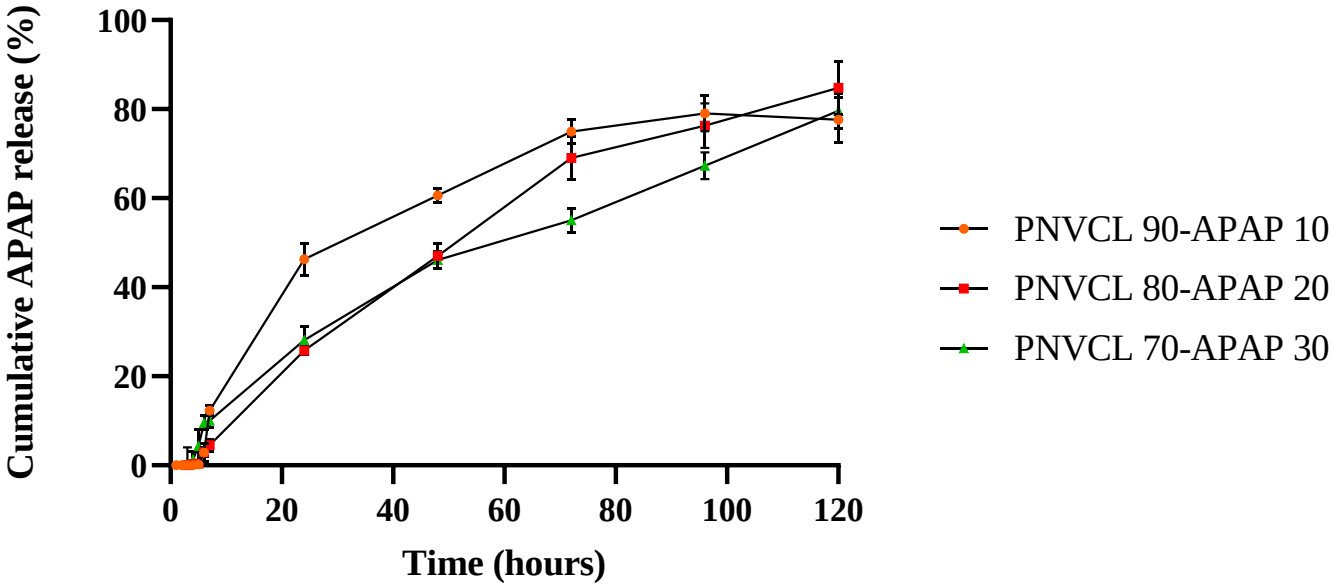

Figure 3-90: Drug release profile of different concentrations of APAP in PNVCL samples at 37 °C in phosphate buffer, pH 7.4.

This study allowed for the incorporation of a drug into the PNVCL by a HME method, also the drug release rate could be tailored by the variation of the concentration of APAP. An additional benefit of this study is that, unlike the usual procedures for preparing drug-hydrogels blends, which involve the use of organic solvents, this HME approach does not require the use of solvents. The tested samples showed great potential to be further developed into controlled, targeted drug delivery materials in order to enhance the therapeutic effects of the drug. The HME platform may be further developed to allow for delivery orally or by implantation, with subsequent targeting achieved by development of the tuning potential of the LCST of the hydrogel component to target release only in the case of inflammation etc.

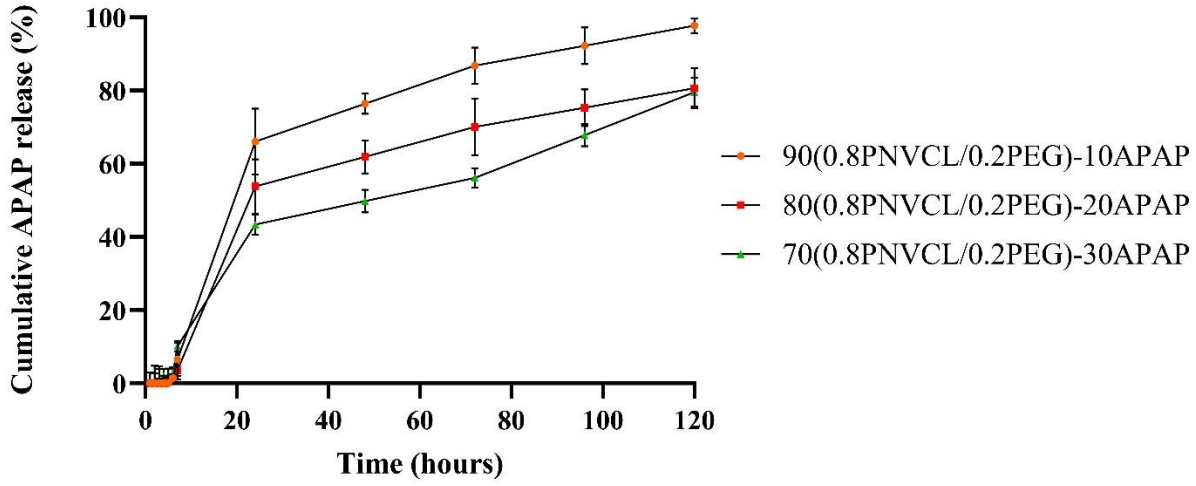

Figure 3-91: Drug release profile of different concentrations of APAP in PNVCL-PEG-based samples at 37 ℃ in phosphate buffer, pH 7.4.

3.5.7. Summary

Overall, this study demonstrates the successful loading of an active pharmaceutical ingredient into smart temperature-sensitive polymer materials *via* HME, and shows fundamental potential for oral or implantable systems. However, more research is still necessary to determine the drug release of a range of drugs as this study only focuses on APAP as a model drug. This is the first study to highlight the incorporation of a drug into PNVCL polymer by utilising HME to melt mix PNVCL and a drug efficiently and offers attractive possibilities for use in smart polymer drug delivery systems.

Chapter 4:

Conclusion

4. Conclusion

Although significant progress has been made in the controlled drug delivery area, more advances are yet to be made for treating many clinical disorders. While smart polymers show promise and have been researched widely in recent years, several drawbacks present themselves, which prevents them from achieving their true potential. This research addresses some of the key drawbacks while investigating the melt processing of smart temperature-sensitive polymers, developing a novel approach of incorporating active pharmaceutical ingredient into smart temperature-sensitive polymer materials and examining the effect of an industrial scale sterilisation method on the novel smart temperature-sensitive polymers.

In summary, successful polymerisation of NVCL-VAc monomers was achieved. Data confirmed this *via* FTIR and NMR. The LCST was determined by employing four different approaches: optical cloud point, UV-spectroscopy, DSC and Rheometry. This study demonstrates a better understanding of the LCST and sol-gel transition for PNVCL based samples, which were influenced by concentration and composition. The LCST of PNVCL was determined to be within the range of 32-35 °C, depending upon the polymer concentration in aqueous media. The LCST of the copolymers exhibited a decrease in a phase transition within the range of 26-33 °C. The sol-gel transition was determined to be within the range of 33.6-47.1 °C, depending on concentration and composition. PNVCL-VAc LCST and sol-gel transition can be controlled by concentration and composition and can be used as thermo-gelling systems, where the LCST of which should be below 37 °C so that when it is injected into the body, a sol-gel transition can occur. Finally, swelling studies were performed below and above LCST to determine the swelling and dissolution behaviour, which was found to be dependent on temperature.

The effects of electron irradiation on two different temperature-responsive polymers, poly (N-vinylcaprolactam) and its copolymer. To achieve in-depth knowledge of the polymers modifications triggered by irradiation exposure, three key areas were observed, which included chemical, thermal and structural analysis. The obtained polymers resulted in considerable modifications to the properties of the material as analysed by ATR-FTIR, GPC, DSC, UV–spectroscopy, DMA, tensile testing and swelling ratio studies. At a radiation concentration of 50 kGy, decreases in PNVCL mechanical properties were observed for tensile testing. UV-spectroscopy examined the phase transition behaviour, where a decrease in the phase transition temperature was found. This decrease is considered a result of a possible increased molecular

weight experienced during electron beam (cross-linking). It was identified that the phase transition of the PNVCL solutions decreased with the increasing irradiation dose. Altogether, electron irradiation results demonstrate that this method allowed functional modification to sterilised temperature-responsive polymers compared to standard methods and it also shows potential toward PNVCL based polymers to be used for emerging biomedical applications such as implantable drug delivery systems. These systems must be sterilised as it a key requirement, and until now the effect of electron irradiation on PNVCL was unknown.

Hot-melt extrusion was employed as a processing technique in a novel method to formulate a smart polymer-based upon PNVCL. It was found that PNVCL could be extruded above its glass transition temperature due to its amorphous nature. Processing parameters were established for PNVCL by varying the temperature, screw speed, and developing a drying procedure. However, with the ideal processing parameters established, a plasticiser was needed to improve the processing capability. PEG was incorporated into PNVCL by melt processing and photopolymerisation, with the photopolymerisation of the extruded PNVCL-PEG demonstrating, better processability characteristics, compared with melt–processing samples. However, it was found that the incorporation of PEG during the polymerisation process leads to a weakened phase transition temperature. The effects of HME on washed and unwashed PNVCL samples showed that the phase transition temperature could be altered due to a change in its molecular weight. In this section, it was determined that the melt processing of PNVCL is a viable option for the manufacture of smart polymers blends. The properties of PNVCL can be tailored by HME techniques, which presents advantages over conventional fabrication methods. This would benefit implantable drug delivery systems, as a major concern is the complexity of implantable systems and the cost-benefit ratio is an important parameter influencing patient acceptance and commercial success.

The successful loading of Acetaminophen into the Poly (*N*-vinylcaprolactam) matrix *via* HME demonstrated. ATR-FTIR spectra indicated that interactions occurred between PNVCL and of APAP. The results obtained from the DSC analysis suggested that the melting transitions got broader with APAP content. Therefore, this is mainly due to the higher fraction of the crystalline drug in the polymer. Drug release showed a lower drug loading of APAP and exhibited faster release compared to higher loaded formulations. This section is the first of its kind to report the use of a temperature-responsive polymer for targeted delivery systems *via* HME for PNVCL based polymers. This novel approach to incorporate drug into a smart polymer offers the possibility to formulate new implantable drug delivery systems.

There is a trend to make implantable drug delivery systems more cost-effective and patient-friendly. This trend indicates that future devices will probably be smaller, less invasive, and more site-specific. All these features will need to be accomplished while maintaining the dose at precise therapeutic levels for the desired duration. PNVCL based samples developed in this study show promise, where they could potentially be used in combination with current systems to add a targeting effect, creating a new class of implantable drug delivery system.

Chapter 5:

References

5. References

[1] G. Tiwari, R. Tiwari, S. Bannerjee, L. Bhati, S. Pandey, P. Pandey, B. Sriwastawa, Drug delivery systems: An updated review, Int. J. Pharm. Investig. 2 (2012) 2. https://doi.org/10.4103/2230-973x.96920.

[2] L.N. Sansom, Oral extended-release products, Aust. Prescr. 22 (1999) 88–90. https://doi.org/10.18773/austprescr.1999.072.

[3] J. Li, D.J. Mooney, Designing hydrogels for controlled drug delivery, Nat. Rev. Mater. 1 (2016) 16071. https://doi.org/10.1038/natrevmats.2016.71.

[4] J. Goole, K. Amighi, 3D printing in pharmaceutics: A new tool for designing customized drug delivery systems, Int. J. Pharm. 499 (2016) 376–394. https://doi.org/10.1016/j.ijpharm.2015.12.071.

[5] A.B.C. Shargel, L., Wu-Pong, S., & Yu, Applied Biopharmaceutics & Pharmacokinetics, Sixth Edit, Appleton & Lange Reviews/McGraw-Hill, Medical Pub. Division, New York, NY, 2005.

[6] J. Nielsen, S.O.W. Jensen, R.B. Friis, J.B. Valentin, C.U. Correll, Comparative Effectiveness of Risperidone Long-Acting Injectable vs First-Generation Antipsychotic Long-Acting Injectables in Schizophrenia: Results From a Nationwide, Retrospective Inception Cohort Study, Schizophr. Bull. 41 (2015) 627–636. https://doi.org/10.1093/schbul/sbu128.

[7] B.J. Boyd, C.A.S. Bergström, Z. Vinarov, M. Kuentz, J. Brouwers, P. Augustijns, M. Brandl, A. Bernkop-Schnürch, N. Shrestha, V. Préat, A. Müllertz, A. Bauer-Brandl, V. Jannin, Successful oral delivery of poorly water-soluble drugs both depends on the intraluminal behavior of drugs and of appropriate advanced drug delivery systems, Eur. J. Pharm. Sci. 137 (2019) 104967. https://doi.org/https://doi.org/10.1016/j.ejps.2019.104967.

[8] B. Chertok, M. Webber, M. Succi, R. Langer, Drug Delivery Interfaces in the 21st Century: From Science Fiction Ideas to Viable Technologies, Mol. Pharm. 10 (2013). https://doi.org/10.1021/mp4003283.

[9] H.J.T.C. Bennink, The pharmacokinetics and pharmacodynamics of Implanon®, a single-rod etonogestrel contraceptive implant, Eur. J. Contracept. Reprod. Heal. Care. 5 (2000) 12–20.

https://doi.org/10.1080/13625187.2000.12067162.

[10] D. Taylor, The Pharmaceutical Industry and the Future of Drug Development, in: Pharm. Environ., The Royal Society of Chemistry, 2016: pp. 1–33. https://doi.org/10.1039/9781782622345-00001.

[11] A. Dalmoro, G. Lamberti, G. Titomanlio, A.A. Barba, M. d'Amore, Enteric Micro-Particles for Targeted Oral Drug Delivery, AAPS PharmSciTech. 11 (2010) 1500–1507. https://doi.org/10.1208/s12249-010-9528-3.

[12] C.G. Pitt, Z.-W. Gu, R.W. Hendren, J. Thompson, M.C. Wani, Triggered drug delivery systems, J. Control. Release. 2 (1985) 363–374. https://doi.org/https://doi.org/10.1016/0168-3659(85)90058-6.

[13] N. Kamaly, B. Yameen, J. Wu, O.C. Farokhzad, Degradable controlled-release polymers and polymeric nanoparticles: Mechanisms of controlling drug release, Chem. Rev. 116 (2016) 2602–2663. https://doi.org/10.1021/acs.chemrev.5b00346.

[14] S. Jones, A. Taylor, P. Beales, Towards feedback-controlled nanomedicines for smart, adaptive delivery, Exp. Biol. Med. 244 (2018). https://doi.org/10.1177/1535370218800456.

[15] K. Park, Controlled drug delivery systems: past forward and future back, J. Control. Release. 190 (2014) 3–8. https://doi.org/10.1016/j.jconrel.2014.03.054.

[16] Y.H. Yun, B.K. Lee, K. Park, Controlled Drug Delivery: Historical perspective for the next generation, J. Control. Release. 219 (2015) 2–7. https://doi.org/10.1016/j.jconrel.2015.10.005.

[17] H. He, Q. Liang, M.C. Shin, K. Lee, J. Gong, J. Ye, Q. Liu, J. Wang, V. Yang, Significance and strategies in developing delivery systems for bio-macromolecular drugs, Front. Chem. Sci. Eng. 7 (2013) 496–507. https://doi.org/10.1007/s11705-013-1362-1.

[18] N.K. Singh, D.S. Lee, In situ gelling pH- and temperature-sensitive biodegradable block copolymer hydrogels for drug delivery, J. Control. Release. 193 (2014) 214–227. https://doi.org/10.1016/j.jconrel.2014.04.056.

[19] M.R. Matanović, J. Kristl, P.A. Grabnar, Thermoresponsive polymers: Insights into decisive hydrogel characteristics, mechanisms of gelation, and promising biomedical applications, Int. J. Pharm. 472 (2014) 262–275.

https://doi.org/10.1016/j.ijpharm.2014.06.029.

[20] H.K. Makadia, S.J. Siegel, Poly Lactic-co-Glycolic Acid (PLGA) as Biodegradable Controlled Drug Delivery Carrier, Polymers (Basel). 3 (2011) 1377–1397. https://doi.org/10.3390/polym3031377.

[21] H. Priya James, R. John, A. Alex, K.R. Anoop, Smart polymers for the controlled delivery of drugs - a concise overview, Acta Pharm. Sin. B. 4 (2014) 120–127. https://doi.org/10.1016/j.apsb.2014.02.005.

[22] S. Gao, G. Tang, D. Hua, R. Xiong, J. Han, S. Jiang, Q. Zhang, C. Huang, Stimuli-responsive bio-based polymeric systems and their applications, J. Mater. Chem. B. 7 (2019) 709–729. https://doi.org/10.1039/C8TB02491J.

[23] N.A. Cortez-Lemus, A. Licea-Claverie, Poly(N-vinylcaprolactam), a comprehensive review on a thermoresponsive polymer becoming popular, Prog. Polym. Sci. 53 (2016) 1–51. https://doi.org/10.1016/j.progpolymsci.2015.08.001.

[24] A. Moghanjoughi, A. Khoshnevis, A. Dorna Zarrabi, A concise review on smart polymers for controlled drug release, Drug Deliv. Transl. Res. 6 (2016) 333–340. https://doi.org/10.1007/s13346-015-0274-7.

[25] E. Andrzejewska, Free Radical Photopolymerization of Multifunctional Monomers, in: T.B.T.-T.-D.M.U.T.P. Baldacchini (Ed.), Three-Dimensional Microfabr. Using Two-Phot. Polym. Fundam. Technol. Appl., William Andrew Publishing, Oxford, 2016: pp. 62–81. https://doi.org/10.1016/B978-0-323-35321-2.00004-2.

[26] D.J. Overstreet, H.A. Von Recum, B.L. Vernon, Drug delivery applications of injectable biomaterials, Inject. Biomater. (2011) 95–141. https://doi.org/10.1533/9780857091376.2.95.

[27] K.M.S. Cheng, Chain Scission and Oxidation, Radiat. Process. Polym. Mater. Its Ind. Appl. (2012) 201–247. https://doi.org/doi:10.1002/9781118162798.ch7.

[28] W.J. Rogers, 7 - Sterilisation techniques for polymers, in: S. Lerouge, A.B.T.-S. of B. and M.D. Simmons (Eds.), Woodhead Publ. Ser. Biomater., Woodhead Publishing, 2012: pp. 151–211. https://doi.org/https://doi.org/10.1533/9780857096265.151.

[29] K.A. Murray, J.E. Kennedy, V. Barron, B. McEvoy, O. Vrain, D. Ryan, R. Cowman, C.L. Higginbotham, Effects of electron beam irradiation on the property behaviour of poly(ether-block-amide) blended with various stabilisers, Radiat. Phys. Chem. 110

(2015) 24–37. https://doi.org/10.1016/j.radphyschem.2015.01.009.

[30] S.E. Moulton, G.G. Wallace, 3-dimensional (3D) fabricated polymer based drug delivery systems, J. Control. Release. 193 (2014) 27–34. https://doi.org/10.1016/j.jconrel.2014.07.005.

[31] S.A. Khaled, J.C. Burley, M.R. Alexander, C.J. Roberts, Desktop 3D printing of controlled release pharmaceutical bilayer tablets, Int. J. Pharm. 461 (2014) 105–111. https://doi.org/10.1016/j.ijpharm.2013.11.021.

[32] A. Gupta, M.A. Khan, Consistency of Pharmaceutical Products: An FDA Perspective on Hot-Melt Extrusion Process, in: A.M. Repka, N. Langley, J. DiNunzio (Eds.), Melt Extrus. SE - 17, Springer New York, New York, NY, 2013: pp. 435–445. https://doi.org/10.1007/978-1-4614-8432-5_17.

[33] H. Yuan, Q. Ma, L. Ye, G. Piao, The Traditional Medicine and Modern Medicine from Natural Products, Molecules. 21 (2016) 559. https://doi.org/10.3390/molecules21050559.

[34] P. Gayatri, C. Dalwadi, Recent Patents on Stimuli Responsive Hydrogel Drug Delivery System, Recent Pat. Drug Deliv. Formul. 7 (2013). https://doi.org/10.2174/1872211307666131118141600.

[35] R. Quinn, Rethinking antibiotic research and development: World War II and the penicillin collaborative, Am. J. Public Health. 103 (2013) 426–434. https://doi.org/10.2105/AJPH.2012.300693.

[36] R.A. Bader, Fundamentals of Drug Delivery, in: Eng. Polym. Syst. Improv. Drug Deliv., John Wiley & Sons Ltd., Hoboken, New Jersey., 2013: pp. 1–28. https://doi.org/10.1002/9781118747896.ch1.

[37] B. Mishra, B.B. Patel, S. Tiwari, Colloidal nanocarriers: a review on formulation technology, types and applications toward targeted drug delivery, Nanomedicine Nanotechnology, Biol. Med. 6 (2010) 9–24. https://doi.org/10.1016/j.nano.2009.04.008.

[38] Y. Zhang, H.F. Chan, K.W. Leong, Advanced materials and processing for drug delivery: the past and the future, Adv. Drug Deliv. Rev. 65 (2013) 104–120. https://doi.org/10.1016/j.addr.2012.10.003.

[39] G.G. de Lima, D. Kanwar, D. Macken, L. Geever, D.M. Devine, M.J.D. Nugent, Smart Hydrogels: Therapeutic Advancements in Hydrogel Technology for Smart Drug

Delivery Applications, in: V.K. Thakur, M.K. Thakur (Eds.), Handb. Polym. Pharm. Technol., 1st ed., John Wiley & Sons, Inc., 2015: pp. 1–16. https://doi.org/10.1002/9781119041559.ch1.

[40] A.S. Hoffman, Hydrogels for biomedical applications, Adv. Drug Deliv. Rev. 64 (2012) 18–23. https://doi.org/10.1016/j.addr.2012.09.010.

[41] Y. Jiang, J. Chen, C. Deng, E.J. Suuronen, Z. Zhong, Click hydrogels, microgels and nanogels: Emerging platforms for drug delivery and tissue engineering, Biomaterials. 35 (2014) 4969–4985. https://doi.org/10.1016/j.biomaterials.2014.03.001.

[42] B. Lee, A. Jiao, S. Yu, J.B. You, D.H. Kim, S.G. Im, Initiated chemical vapor deposition of thermoresponsive poly (N-vinylcaprolactam) thin films for cell sheet engineering, Acta Biomater. 9 (2013) 7691–7698. https://doi.org/10.1016/j.actbio.2013.04.049.

[43] D. Darwis, P. Stasica, M.T. Razzak, J.M. Rosiak, Characterization of poly(vinyl alcohol) hydrogel for prosthetic intervertebral disc nucleus, Radiat. Phys. Chem. 63 (2002) 539–542. https://doi.org/10.1016/S0969-806X(01)00636-3.

[44] A.S. HOFFMAN, Hydrogels for Biomedical Applications, Ann. N. Y. Acad. Sci. 944 (2006) 62–73. https://doi.org/10.1111/j.1749-6632.2001.tb03823.x.

[45] S. Chaterji, I.K. Kwon, K. Park, Smart polymeric gels: Redefining the limits of biomedical devices, Prog. Polym. Sci. 32 (2007) 1083–1122. https://doi.org/10.1016/j.progpolymsci.2007.05.018.

[46] Y. Samchenko, Z. Ulberg, O. Korotych, Multipurpose smart hydrogel systems, Adv. Colloid Interface Sci. 168 (2011) 247–262. https://doi.org/10.1016/j.cis.2011.06.005.

[47] A. Mandal, J.R. Clegg, A.C. Anselmo, S. Mitragotri, Hydrogels in the clinic, Bioeng. Transl. Med. 5 (2020) e10158–e10158. https://doi.org/10.1002/btm2.10158.

[48] L.M. Geever, C.L. Higginbotham, J.G. Lyons, J.E. Kennedy, History and continued development of drug delivery systems based on smart negative temperature sensitive hydrogels, in: D.B. Stein (Ed.), Handb. Hydrogels Prop. Prep. Appl., Nova Science Publishers, 2011: pp. 103–140.

[49] S.T. Nedorost, Generalized dermatitis in clinical practice, Athlone Institute of Technology, 2012. https://doi.org/10.1007/978-1-4471-2897-7.

[50] S.K. H. Gulrez, S. Al-Assaf, G. O, Hydrogels: Methods of Preparation, Characterisation and Applications, Prog. Mol. Environ. Bioeng. - From Anal. Model. to Technol. Appl.

(2011). https://doi.org/10.5772/24553.

[51] W.E. Hennink, C.F. van Nostrum, Novel crosslinking methods to design hydrogels, Adv. Drug Deliv. Rev. 64 (2012) 223–236. https://doi.org/10.1016/j.addr.2012.09.009.

[52] T.R. Hoare, D.S. Kohane, Hydrogels in drug delivery: Progress and challenges, Polymer (Guildf). 49 (2008) 1993–2007. https://doi.org/10.1016/j.polymer.2008.01.027.

[53] J. Xu, X. Liu, X. Ren, G. Gao, The role of chemical and physical crosslinking in different deformation stages of hybrid hydrogels, Eur. Polym. J. 100 (2018) 86–95. https://doi.org/10.1016/j.eurpolymj.2018.01.020.

[54] M. Hamidi, A. Azadi, P. Rafiei, Hydrogel nanoparticles in drug delivery, Adv. Drug Deliv. Rev. 60 (2008) 1638–1649. https://doi.org/10.1016/j.addr.2008.08.002.

[55] S. Argin, P. Kofinas, Y.M. Lo, The cell release kinetics and the swelling behavior of physically crosslinked xanthan-chitosan hydrogels in simulated gastrointestinal conditions, Food Hydrocoll. 40 (2014) 138–144. https://doi.org/10.1016/j.foodhyd.2014.02.018.

[56] S.C. Lee, I.K. Kwon, K. Park, Hydrogels for delivery of bioactive agents: A historical perspective, Adv. Drug Deliv. Rev. 65 (2013) 17–20. https://doi.org/10.1016/j.addr.2012.07.015.

[57] P. Matricardi, C. Di Meo, T. Coviello, W.E. Hennink, F. Alhaique, Interpenetrating polymer networks polysaccharide hydrogels for drug delivery and tissue engineering, Adv. Drug Deliv. Rev. 65 (2013) 1172–1187. https://doi.org/10.1016/j.addr.2013.04.002.

[58] S. Ganguly, P.P. Maity, S. Mondal, P. Das, P. Bhawal, S. Dhara, N.C. Das, Polysaccharide and poly(methacrylic acid) based biodegradable elastomeric biocompatible semi-IPN hydrogel for controlled drug delivery, Mater. Sci. Eng. C. 92 (2018) 34–51. https://doi.org/10.1016/j.msec.2018.06.034.

[59] A. Lohani, G. Singh, S.S. Bhattacharya, A. Verma, Interpenetrating Polymer Networks as Innovative Drug Delivery Systems, J. Drug Deliv. 2014 (2014) 1–11. https://doi.org/10.1155/2014/583612.

[60] K. Madhusudana Rao, B. Mallikarjuna, K.S.V. Krishna Rao, S. Siraj, K. Chowdoji Rao, M.C.S. Subha, Novel thermo/pH sensitive nanogels composed from poly(N-vinylcaprolactam) for controlled release of an anticancer drug, Colloids Surfaces B

Biointerfaces. 102 (2013) 891–897. https://doi.org/10.1016/j.colsurfb.2012.09.009.

[61] S.J. Buwalda, K.W.M. Boere, P.J. Dijkstra, J. Feijen, T. Vermonden, W.E. Hennink, Hydrogels in a historical perspective: from simple networks to smart materials., J. Control. Release. 190 (2014) 254–73. https://doi.org/10.1016/j.jconrel.2014.03.052.

[62] P. Matricardi, C. Di Meo, T. Coviello, W.E. Hennink, F. Alhaique, Interpenetrating Polymer Networks polysaccharide hydrogels for drug delivery and tissue engineering., Adv. Drug Deliv. Rev. 65 (2013) 1172–87. https://doi.org/10.1016/j.addr.2013.04.002.

[63] A.S. Hoffman, Stimuli-responsive polymers: Biomedical applications and challenges for clinical translation, Adv. Drug Deliv. Rev. 65 (2013) 10–16. https://doi.org/10.1016/j.addr.2012.11.004.

[64] N.A. Peppas, D.S. Van Blarcom, Hydrogel-based biosensors and sensing devices for drug delivery, J. Control. Release. 240 (2016) 142–150. https://doi.org/10.1016/j.jconrel.2015.11.022.

[65] Q. Chai, Y. Jiao, X. Yu, Hydrogels for Biomedical Applications: Their Characteristics and the Mechanisms behind Them, Gels. 3 (2017) 6. https://doi.org/10.3390/gels3010006.

[66] S. Parveen, R. Misra, K.S. Sanjeeb, Nanoparticles: a boon to drug delivery, therapeutics, diagnostics and imaging., Nanomedicine. 8 (2012) 147–66. https://doi.org/10.1016/j.nano.2011.05.016.

[67] Frost & Sullivan, Targeted Drug Delivery--Technologies and Applications (Technical Insights), (2012) 1–60.

[68] D. Klinger, K. Landfester, Stimuli-responsive microgels for the loading and release of functional compounds: Fundamental concepts and applications, Polymer (Guildf). 53 (2012) 5209–5231. https://doi.org/10.1016/j.polymer.2012.08.053.

[69] R.A. Siegel, Stimuli sensitive polymers and self regulated drug delivery systems: A very partial review, 190 (2014) 337–351.

[70] E. Cabane, X. Zhang, K. Langowska, C.G. Palivan, W. Meier, Stimuli-responsive polymers and their applications in nanomedicine., Biointerphases. 7 (2012) 9. https://doi.org/10.1007/s13758-011-0009-3.

[71] E. Cabane, X. Zhang, K. Langowska, C.G. Palivan, W. Meier, Stimuli-responsive polymers and their applications in nanomedicine, Biointerphases. 7 (2012) 1–27.

https://doi.org/10.1007/s13758-011-0009-3.

[72] B. Singh, R.K. Khurana, B. Garg, S. Saini, R. Kaur, Stimuli-responsive systems with diverse drug delivery and biomedical applications: Recent updates and mechanistic pathways, Crit. Rev. Ther. Drug Carrier Syst. 34 (2017) 209–255. https://doi.org/10.1615/CritRevTherDrugCarrierSyst.2017017284.

[73] S. Kozanoğlu, T. Özdemir, A. Usanmaz, Polymerization of N-vinylcaprolactam and characterization of poly(N-vinylcaprolactam), J. Macromol. Sci. Part A Pure Appl. Chem. 48 (2011) 467–477. https://doi.org/10.1080/10601325.2011.573350.

[74] D. Chitkara, A. Shikanov, N. Kumar, A.J. Domb, Biodegradable injectable in situ depot-forming drug delivery systems, Macromol. Biosci. 6 (2006) 977–990. https://doi.org/10.1002/mabi.200600129.

[75] D. Schmaljohann, Thermo- and pH-responsive polymers in drug delivery., Adv. Drug Deliv. Rev. 58 (2006) 1655–70. https://doi.org/10.1016/j.addr.2006.09.020.

[76] J. Niskanen, H. Tenhu, How to manipulate the upper critical solution temperature (UCST)?, Polym. Chem. 8 (2017) 220–232. https://doi.org/10.1039/c6py01612j.

[77] E. Fleige, M. a Quadir, R. Haag, Stimuli-responsive polymeric nanocarriers for the controlled transport of active compounds: concepts and applications., Adv. Drug Deliv. Rev. 64 (2012) 866–84. https://doi.org/10.1016/j.addr.2012.01.020.

[78] A. Imaz, J.I. Miranda, J. Ramos, J. Forcada, Evidences of a hydrolysis process in the synthesis of N-vinylcaprolactam-based microgels, Eur. Polym. J. 44 (2008) 4002–4011. https://doi.org/10.1016/j.eurpolymj.2008.09.027.

[79] K. Madhusudana Rao, B. Mallikarjuna, K.S. V Krishna Rao, S. Siraj, K. Chowdoji Rao, M.C.S. Subha, Novel thermo/pH sensitive nanogels composed from poly(N-vinylcaprolactam) for controlled release of an anticancer drug., Colloids Surf. B. Biointerfaces. 102 (2013) 891–7. https://doi.org/10.1016/j.colsurfb.2012.09.009.

[80] X.M. Liu, L.S. Wang, L. Wang, J. Huang, C. He, The effect of salt and pH on the phase-transition behaviors of temperature-sensitive copolymers based on N-isopropylacrylamide, Biomaterials. 25 (2004) 5659–5666. https://doi.org/10.1016/j.biomaterials.2004.01.019.

[81] A. Benrebouh, D. Avoce, X.X. Zhu, Thermo- and pH-sensitive polymers containing cholic acid derivatives, Polymer (Guildf). 42 (2001) 4031–4038.

https://doi.org/https://doi.org/10.1016/S0032-3861(00)00837-5.

[82] F. Eeckman, A.J. Moës, K. Amighi, Evaluation of a new controlled-drug delivery concept based on the use of thermoresponsive polymers, Int. J. Pharm. 241 (2002) 113–125. https://doi.org/https://doi.org/10.1016/S0378-5173(02)00198-9.

[83] S. Mendrek, A. Mendrek, H.-J. Adler, A. Dworak, D. Kuckling, Temperature-sensitive behaviour of poly(glycidol)-b-poly(N-isopropylacrylamide) block copolymers, Colloid Polym. Sci. 288 (2010) 777–786. https://doi.org/10.1007/s00396-010-2203-0.

[84] N. V Gupta, Archive of SID Preparation and characterization of superporous hydrogels as gastroretentive drug delivery system for rosiglitazone maleate Archive of SID, 18 (2010) 200–210.

[85] G.H. Gao, Y. Li, D.S. Lee, Environmental pH-sensitive polymeric micelles for cancer diagnosis and targeted therapy., J. Control. Release. 169 (2013) 180–4. https://doi.org/10.1016/j.jconrel.2012.11.012.

[86] F.-J. Xu, E.-T. Kang, K.-G. Neoh, pH- and temperature-responsive hydrogels from crosslinked triblock copolymers prepared via consecutive atom transfer radical polymerizations., Biomaterials. 27 (2006) 2787–97. https://doi.org/10.1016/j.biomaterials.2006.01.003.

[87] T. Ishida, Y. Okada, T. Kobayashi, H. Kiwada, Development of pH-sensitive liposomes that efficiently retain encapsulated doxorubicin (DXR) in blood, Int. J. Pharm. 309 (2006) 94–100. https://doi.org/10.1016/j.ijpharm.2005.11.010.

[88] N.K. Singh, Q.V. Nguyen, B.S. Kim, D.S. Lee, Nanostructure controlled sustained delivery of human growth hormone using injectable, biodegradable, pH/temperature responsive nanobiohybrid hydrogel, Nanoscale. 7 (2015) 3043–3054. https://doi.org/10.1039/c4nr05897f.

[89] J.G. Lyons, C.L. Higginbotham, P. Blackie, Development of novel monolithic matrices for drug delivery using conventional and non-conventional polymer processing technologies., Athlone Institute of Technology, 2007.

[90] C. McConville, P. Tawari, W. Wang, Hot melt extruded and injection moulded disulfiram-loaded PLGA millirods for the treatment of glioblastoma multiforme via stereotactic injection, Int. J. Pharm. 494 (2015) 73–82. https://doi.org/10.1016/j.ijpharm.2015.07.072.

[91] I. Zembko, I. Ahmed, A. Farooq, J. Dail, P. Tawari, W. Wang, C. Mcconville, Development of disulfiram-loaded poly(lactic-co-glycolic acid) wafers for the localised treatment of glioblastoma multiforme: A comparison of manufacturing techniques, J. Pharm. Sci. 104 (2015) 1076–1086. https://doi.org/10.1002/jps.24304.

[92] D.Y. Arifin, L.Y. Lee, C.H. Wang, Mathematical modeling and simulation of drug release from microspheres: Implications to drug delivery systems, Adv. Drug Deliv. Rev. 58 (2006) 1274–1325. https://doi.org/10.1016/j.addr.2006.09.007.

[93] K.L. Poetz, H.S. Mohammed, B.L. Snyder, G. Liddil, D.S.K. Samways, D.A. Shipp, Photopolymerized cross-linked thiol–ene polyanhydrides: erosion, release, and toxicity studies, Biomacromolecules. 15 (2014) 2573–2582.

[94] S. You, Z. Yang, C.H. Wang, Toward Understanding Drug Release from Biodegradable Polymer Microspheres of Different Erosion Kinetics Modes, J. Pharm. Sci. 105 (2016) 1934–1946. https://doi.org/10.1016/j.xphs.2016.04.002.

[95] J. Heller, J. Barr, Poly (ortho esters) from concept to reality, Biomacromolecules. 5 (2004) 1625–1632. https://doi.org/10.1021/bm040049n.

[96] L.L. Lao, N.A. Peppas, F.Y.C. Boey, S.S. Venkatraman, Modeling of drug release from bulk-degrading polymers, Int. J. Pharm. 418 (2011) 28–41. https://doi.org/10.1016/j.ijpharm.2010.12.020.

[97] C. Li, J. Wang, Y. Wang, H. Gao, G. Wei, Y. Huang, H. Yu, Y. Gan, Y. Wang, L. Mei, H. Chen, H. Hu, Z. Zhang, Y. Jin, Recent progress in drug delivery, Acta Pharm. Sin. B. 9 (2019) 1145–1162. https://doi.org/10.1016/j.apsb.2019.08.003.

[98] S.-Y. Lin, Thermoresponsive gating membranes embedded with liquid crystal(s) for pulsatile transdermal drug delivery: An overview and perspectives, J. Control. Release. 319 (2020) 450–474. https://doi.org/https://doi.org/10.1016/j.jconrel.2019.12.046.

[99] H.-Q. Wu, C.-C. Wang, Biodegradable Smart Nanogels: A New Platform for Targeting Drug Delivery and Biomedical Diagnostics, Langmuir. 32 (2016) 6211–6225. https://doi.org/10.1021/acs.langmuir.6b00842.

[100] H. Ichikawa, Y. Fukumori, A novel positively thermosensitive controlled-release microcapsule with membrane of nano-sized poly(N-isopropylacrylamide) gel dispersed in ethylcellulose matrix, J. Control. Release. 63 (2000) 107–119. https://doi.org/10.1016/S0168-3659(99)00181-9.

[101] D. Jones, Pharmaceutical Applications of Polymers for Drug Delivery, Rapra Technology Limited, 2004. https://books.google.ie/books?id=VQOZ0zrEB9IC.

[102] M.L.B.T.-S. to M. the D.R. from P.S. Bruschi, ed., 2 - Modification of drug release, in: Woodhead Publishing, 2015: pp. 15–28. https://doi.org/https://doi.org/10.1016/B978-0-08-100092-2.00002-3.

[103] P. Colombo, R. Bettini, N.A. Peppas, Observation of swelling process and diffusion front position during swelling in hydroxypropyl methyl cellulose (HPMC) matrices containing a soluble drug., J. Control. Release. 61 (1999) 83–91. https://doi.org/10.1016/s0168-3659(99)00104-2.

[104] J. Killion, Development of novel hydrogel based composites for bone regeneration application, Athlone Insitute of Technoology, 2015.

[105] J.M. Rosiak, P. Ulański, L.A. Pajewski, F. Yoshii, K. Makuuchi, Radiation formation of hydrogels for biomedical purposes. Some remarks and comments, Radiat. Phys. Chem. 46 (1995) 161–168. https://doi.org/https://doi.org/10.1016/0969-806X(95)00007-K.

[106] C. Chang, B. Duan, J. Cai, L. Zhang, Superabsorbent hydrogels based on cellulose for smart swelling and controllable delivery, Eur. Polym. J. 46 (2010) 92–100. https://doi.org/https://doi.org/10.1016/j.eurpolymj.2009.04.033.

[107] A. Pourjavadi, P.E. Jahromi, F. Seidi, H. Salimi, Synthesis and swelling behavior of acrylatedstarch-g-poly (acrylic acid) and acrylatedstarch-g-poly (acrylamide) hydrogels, Carbohydr. Polym. 79 (2010) 933–940. https://doi.org/https://doi.org/10.1016/j.carbpol.2009.10.021.

[108] C. Demitri, F. Scalera, M. Madaghiele, A. Sannino, A. Maffezzoli, Potential of Cellulose-Based Superabsorbent Hydrogels as Water Reservoir in Agriculture, Int. J. Polym. Sci. 2013 (2013) 435073. https://doi.org/10.1155/2013/435073.

[109] I.B. Wong, S.C. Teoh, A.E. Yeoh, G. Lingam, Sustained-release ganciclovir implant as prophylaxis for cytomegalovirus retinitis in a child undergoing bone marrow transplantation, Eye. 27 (2013) 890–891. https://doi.org/10.1038/eye.2013.81.

[110] A. Kumar, J. Pillai, Chapter 13 - Implantable drug delivery systems: An overview, in: A.M.B.T.-N. for the E. of C. Grumezescu Tissues and Organs (Ed.), William Andrew Publishing, 2018: pp. 473–511. https://doi.org/https://doi.org/10.1016/B978-0-12-

813665-2.00013-2.

[111] Y. Onuki, U. Bhardwaj, F. Papadimitrakopoulos, D.J. Burgess, A review of the biocompatibility of implantable devices: current challenges to overcome foreign body response, J. Diabetes Sci. Technol. 2 (2008) 1003–1015. https://doi.org/10.1177/193229680800200610.

[112] L.G. De Oliveira, L.A. Figueiredo, G.M. Fernandes-Cunha, D.M. Marina Barcelos, L.A. Machado, G.R. Dasilva, D.M. Sandra Aparecida Lima, Methotrexate Locally Released from Poly(e-Caprolactone) Implants: Inhibition of the Inflammatory Angiogenesis Response in a Murine Sponge Model and the Absence of Systemic Toxicity, J. Pharm. Sci. 104 (2015) 3731–3742. https://doi.org/https://doi.org/10.1002/jps.24569.

[113] M. Rahimi, H. Mobedi, A. Behnamghader, In situ-forming PLGA implants loaded with leuprolide acetate/β-cyclodextrin complexes: mathematical modelling and degradation, J. Microencapsul. 33 (2016) 355–364. https://doi.org/10.1080/02652048.2016.1194905.

[114] E. Skorupska, A. Jeziorna, S. Kazmierski, M.J. Potrzebowski, Recent progress in solid-state NMR studies of drugs confined within drug delivery systems, Solid State Nucl. Magn. Reson. 57–58 (2014) 2–16. https://doi.org/10.1016/j.ssnmr.2013.12.001.

[115] S. Parveen, R. Misra, S.K. Sahoo, Nanoparticles: A boon to drug delivery, therapeutics, diagnostics and imaging, Nanomedicine Nanotechnology, Biol. Med. 8 (2012) 147–166. https://doi.org/10.1016/j.nano.2011.05.016.

[116] Frost & Sullivan, Targeted Drug Delivery--Technologies and Applications (Technical Insights), 2012.

[117] X.J. Loh, In-Situ Gelling Polymers, 2015. https://doi.org/10.1007/978-981-287-152-7.

[118] F. Quan, A. Zhang, F. Cheng, L. Cui, J. Liu, Y. Xia, Biodegradable polymeric architectures via reversible deactivation radical polymerizations, Polymers (Basel). 10 (2018) 758. https://doi.org/10.3390/polym10070758.

[119] T.N. Vo, A.K. Ekenseair, F.K. Kasper, A.G. Mikos, Synthesis, Physicochemical Characterization, and Cytocompatibility of Bioresorbable, Dual-Gelling Injectable Hydrogels, Biomacromolecules. 15 (2014) 132–142. https://doi.org/10.1021/bm401413c.

[120] N. Sanoj Rejinold, M. Muthunarayanan, V. V. Divyarani, P.R. Sreerekha, K.P. Chennazhi, S. V. Nair, H. Tamura, R. Jayakumar, Curcumin-loaded biocompatible

thermoresponsive polymeric nanoparticles for cancer drug delivery, J. Colloid Interface Sci. 360 (2011) 39–51. https://doi.org/10.1016/j.jcis.2011.04.006.

[121] J. Gan, X. Guan, J. Zheng, H. Guo, K. Wu, L. Liang, M. Lu, Biodegradable, thermoresponsive PNIPAM-based hydrogel scaffolds for the sustained release of levofloxacin, RSC Adv. 6 (2016) 32967–32978. https://doi.org/10.1039/C6RA03045A.

[122] M. Prabaharan, J.J. Grailer, D. a Steeber, S. Gong, Thermosensitive micelles based on folate-conjugated poly(N-vinylcaprolactam)-block-poly(ethylene glycol) for tumor-targeted drug delivery., Macromol. Biosci. 9 (2009) 744–53. https://doi.org/10.1002/mabi.200800366.

[123] N. a. Cortez-Lemus, A. Licea-Claverie, Poly(N-vinylcaprolactam), a comprehensive review on a thermoresponsive polymer becoming popular, 2015. https://doi.org/10.1016/j.progpolymsci.2015.08.001.

[124] G. Venkatareddy, M.. Subha, C. Rao, B. Yerriswamy, L.N. Reddy, V. Prasad, Controlled release studies of 5-Fluorouracil through poly (vinyl caprolactum-co-vinyl acetate) microspheres, Asian J. Pharm. 4 (2010) 200. https://doi.org/10.4103/0973-8398.72118.

[125] M. Prabaharan, J.J. Grailer, D. a Steeber, S. Gong, Stimuli-responsive chitosan-graft-poly(N-vinylcaprolactam) as a promising material for controlled hydrophobic drug delivery., Macromol. Biosci. 8 (2008) 843–51. https://doi.org/10.1002/mabi.200800010.

[126] I.S. Cho, C.G. Park, B.K. Huh, M.O. Cho, Z. Khatun, Z. Li, S.-W. Kang, Y. Bin Choy, K.M. Huh, Thermosensitive hexanoyl glycol chitosan-based ocular delivery system for glaucoma therapy., Acta Biomater. 39 (2016) 124–32. https://doi.org/10.1016/j.actbio.2016.05.011.

[127] B. Subia, J. Kundu, S. C., Biomaterial Scaffold Fabrication Techniques for Potential Tissue Engineering Applications, in: Tissue Eng., 2010: pp. 141–159. https://doi.org/10.5772/8581.

[128] C.Y. Xu, R. Inai, M. Kotaki, S. Ramakrishna, Aligned biodegradable nanofibrous structure: A potential scaffold for blood vessel engineering, Biomaterials. 25 (2004) 877–886. https://doi.org/10.1016/S0142-9612(03)00593-3.

[129] C. Arpagaus, N. Schafroth, Spray dried biodegradable polymers for controlled drug

delivery systems, 2011.

[130] M. Maniruzzaman, J.S. Boateng, M.J. Snowden, D. Douroumis, A Review of Hot-Melt Extrusion: Process Technology to Pharmaceutical Products, ISRN Pharm. 2012 (2012) 1–9. https://doi.org/10.5402/2012/436763.

[131] J. Baronsky-Probst, C. V. Möltgen, W. Kessler, R.W. Kessler, Process design and control of a twin screw hot melt extrusion for continuous pharmaceutical tamper-resistant tablet production, Eur. J. Pharm. Sci. 87 (2016) 14–21. https://doi.org/10.1016/j.ejps.2015.09.010.

[132] H. Patil, R. V. Tiwari, M.A. Repka, Hot-Melt Extrusion: from Theory to Application in Pharmaceutical Formulation, AAPS PharmSciTech. 17 (2016) 20–42. https://doi.org/10.1208/s12249-015-0360-7.

[133] D. Puppi, F. Chiellini, A.M. Piras, E. Chiellini, Polymeric materials for bone and cartilage repair, Prog. Polym. Sci. 35 (2010) 403–440. https://doi.org/10.1016/j.progpolymsci.2010.01.006.

[134] D. Leister, T. Geilen, K. Geissler, Twin screw extrusion techniques and practice, in: Hot-Melt Extrus. Pharm. Appl., 1st ed., John Wiley & Sons Ltd., The Atrium, Southern Gate, Chichester, West Sussex, Untied Kingdom, 2012: pp. 43–62.

[135] G. Verreck, The Influence of Plasticizers in Hot-Melt Extrusion, in: D. Douroumis (Ed.), Hot-Melt Extrus. Pharm. Appl., 1st ed., John Wiley & Sons Ltd., Chichester, UK., 2012: pp. 93–112. https://doi.org/10.1002/9780470711415.ch5.

[136] A. Gupta, M.A. Khan, Hot-Melt Extrusion: An FDA Perspective on Product and Process Understanding, in: Hot-Melt Extrus. Pharm. Appl., John Wiley & Sons Ltd., The Atrium, Southern Gate, Chichester, West Sussex, Untied Kingdom, 2012: pp. 323–331. https://doi.org/10.1002/9780470711415.ch15.

[137] A. Almeida, B. Claeys, J.P. Remon, C. Vervaet, Hot-Melt Extrusion Developments in the Pharmaceutical Industry, in: Hot-Melt Extrus. Pharm. Appl., 1st ed., John Wiley & Sons Ltd., The Atrium, Southern Gate, Chichester, West Sussex, Untied Kingdom, 2012: pp. 43–69. https://doi.org/10.1002/9780470711415.ch3.

[138] P. Gill, T.T. Moghadam, B. Ranjbar, Differential scanning calorimetry techniques: applications in biology and nanoscience, J. Biomol. Tech. 21 (2010) 167–193. https://pubmed.ncbi.nlm.nih.gov/21119929.

[139] I.M. Kalogeras, W. Brostow, Glass Transition Temperatures in Binary Polymer Blends, J. Polym. Sci. Part B Polym. Phys. 47 (2009) 80–95. https://doi.org/10.1002/polb.21616.

[140] K. Jin, J.M. Torkelson, Tg and Tg breadth of poly(2,6-dimethyl-1,4-phenylene oxide)/polystyrene miscible polymer blends characterized by differential scanning calorimetry, ellipsometry, and fluorescence spectroscopy, Polymer (Guildf). 65 (2015) 233–242. https://doi.org/https://doi.org/10.1016/j.polymer.2015.04.016.

[141] H. Bourara, S. Hadjout, Z. Benabdelghani, A. Etxeberria, Miscibility and hydrogen bonding in blends of poly(4-vinylphenol)/Poly(vinyl methyl ketone), Polymers (Basel). 6 (2014) 2752–2763. https://doi.org/10.3390/polym6112752.

[142] S. Sridhar, R.S. Veerapur, M.B. Patil, K.B. Gudasi, T.M. Aminabhavi, Matrimid polyimide membranes for the separation of carbon dioxide from methane, J. Appl. Polym. Sci. 106 (2007) 1585–1594. https://doi.org/10.1002/app.26306.

[143] B. Démuth, Z.K. Nagy, A. Balogh, T. Vigh, G. Marosi, G. Verreck, I. Van Assche, M.E. Brewster, Downstream processing of polymer-based amorphous solid dispersions to generate tablet formulations, Int. J. Pharm. 486 (2015) 268–286. https://doi.org/10.1016/j.ijpharm.2015.03.053.

[144] B.B. Patel, J.K. Patel, S. Chakraborty, D. Shukla, Revealing facts behind spray dried solid dispersion technology used for solubility enhancement, Saudi Pharm. J. 23 (2015) 352–365. https://doi.org/10.1016/j.jsps.2013.12.013.

[145] A.L. Sarode, H. Sandhu, N. Shah, W. Malick, H. Zia, Hot melt extrusion for amorphous solid dispersions: Temperature and moisture activated drug-polymer interactions for enhanced stability, Mol. Pharm. 10 (2013) 3665–3675. https://doi.org/10.1021/mp400165b.

[146] J.G. Lyons, H. Holehonnur, D.M. Devine, J.E. Kennedy, L.M. Geever, P. Blackie, C.L. Higginbotham, The incorporation of an organically modified layered silicate in monolithic polymeric matrices produced using hot melt extrusion, Mater. Chem. Phys. 103 (2007) 419–426. https://doi.org/10.1016/j.matchemphys.2007.02.080.

[147] E. Verhoeven, T.R.M. De Beer, E. Schacht, G. Van den Mooter, J.P. Remon, C. Vervaet, Influence of polyethylene glycol/polyethylene oxide on the release characteristics of sustained-release ethylcellulose mini-matrices produced by hot-melt extrusion: in vitro and in vivo evaluations, Eur. J. Pharm. Biopharm. 72 (2009) 463–470. https://doi.org/10.1016/j.ejpb.2009.01.006.

[148] D. Ma, A. Djemai, C.M. Gendron, H. Xi, M. Smith, J. Kogan, L. Li, Development of a HPMC-based controlled release formulation with hot melt extrusion (HME), Drug Dev. Ind. Pharm. 39 (2013) 1070–1083. https://doi.org/10.3109/03639045.2012.702350.

[149] C.R. Palem, S. Kumar Battu, S. Maddineni, R. Gannu, M.A. Repka, M.R. Yamsani, Oral transmucosal delivery of domperidone from immediate release films produced via hot-melt extrusion technology, Pharm. Dev. Technol. 18 (2013) 186–195. https://doi.org/10.3109/10837450.2012.693505.

[150] U.S. FDA, Technical Considerations for Additive Manufactured Medical Devices - Guidance for Industry and Food and Drug Administration Staff FDA 3D, 2017. https://www.fda.gov/downloads/MedicalDevices/DeviceRegulationandGuidance/GuidanceDocuments/UCM499809.pdf.

[151] N. Bhattarai, J. Gunn, M. Zhang, Chitosan-based hydrogels for controlled, localized drug delivery, Adv. Drug Deliv. Rev. 62 (2010) 83–99. https://doi.org/10.1016/j.addr.2009.07.019.

[152] I.I. Slowing, J.L. Vivero-Escoto, C.W. Wu, V.S.Y. Lin, Mesoporous silica nanoparticles as controlled release drug delivery and gene transfection carriers, Adv. Drug Deliv. Rev. 60 (2008) 1278–1288. https://doi.org/10.1016/j.addr.2008.03.012.

[153] K. Miladi, S. Sfar, H. Fessi, A. Elaissari, Drug carriers in osteoporosis: Preparation, drug encapsulation and applications, Int. J. Pharm. 445 (2013) 181–195. https://doi.org/10.1016/j.ijpharm.2013.01.031.

[154] S. Eswaramma, K.S.V.K. Rao, Synthesis of dual responsive carbohydrate polymer based IPN microbeads for controlled release of anti-HIV drug, Carbohydr. Polym. 156 (2017) 125–134. https://doi.org/10.1016/j.carbpol.2016.09.023.

[155] P. Ghasemiyeh, S. Mohammadi-Samani, Hydrogels as Drug Delivery Systems; Pros and Cons, Trends Pharm. Sci. 5 (2019) 7–24. https://doi.org/10.30476/TIPS.2019.81604.1002.

[156] E. Kahraman, S. Güngör, Y. Özsoy, Potential enhancement and targeting strategies of polymeric and lipid-based nanocarriers in dermal drug delivery, Ther. Deliv. 8 (2017) 967–985. https://doi.org/10.4155/tde-2017-0075.

[157] H. Liu, C. Wang, C. Li, Y. Qin, Z. Wang, F. Yang, Z. Li, J. Wang, A functional chitosan-based hydrogel as a wound dressing and drug delivery system in the treatment of wound

healing, RSC Adv. 8 (2018) 7533–7549. https://doi.org/10.1039/c7ra13510f.

[158] T. Zhao, Controlled / living Radical Polymerization of Multi-vinyl Monomer towards Hyperbranched Polymers for Biomedical Applications, Thesis. (2015) 254.

[159] C.G. Williams, A.N. Malik, T.K. Kim, P.N. Manson, J.H. Elisseeff, Variable cytocompatibility of six cell lines with photoinitiators used for polymerizing hydrogels and cell encapsulation, Biomaterials. 26 (2005) 1211–1218. https://doi.org/10.1016/j.biomaterials.2004.04.024.

[160] R. Rogers, Sterilisation of polymer healthcare products, 2005. http://books.google.com/books?hl=en&lr=&id=gPTDo2Esy1UC&oi=fnd&pg=PA1&dq=Sterilisation+of+Polymer+Healthcare+Products&ots=8aouuBmTvA&sig=CUPxzNP_8Ig228dGhaPYYr-O5cg.

[161] E. Kenny, L. Geever, C.L. Higginbotham, D. Devine, Processing, optimisation and characterisation of polymers for bone tissue engineering, Athlone Institute of Technology, 2013.

[162] Sterigenics, Sterilization Alternatives: Electron Beam Radiation, (2004). http://www.sterigenics.com/services/medical_sterilization/contract_sterilization/electron_beam_radiation/sterilization_alternatives__electron_beam_radiation.pdf.

[163] CDC, CDC Radiation Emergencies | Radiation Measurement, Centers Dis. Control Prev. (2014). https://emergency.cdc.gov/radiation/measurement.asp%0Ahttp://www.bt.cdc.gov/radiation/measurement.asp (accessed February 2, 2020).

[164] J.G. Drobny, Radiation technology for polymers, Boca Raton: CRC Press, 2010. https://doi.org/10.1201/b10304.

[165] S. Krainara, Electron beam irradiation and its applications EB irradiation Tasks Motivation, n.d. http://accelerator.slri.or.th/seminar/documents/ATD_SLRI_151015_02.pdf (accessed August 29, 2019).

[166] Radiation Processing Section - World at glance....., (n.d.). https://www.aeb.gov.lk/web/index.php?option=com_content&view=article&id=293&Itemid=243&lang=ta&limitstart=1 (accessed August 29, 2019).

[167] A. Ahmad, D.H. Mohd, I. Abdullah, Electron Beam Cross-linking of NR/LLDPE Blends

Azizan, Iran. Polym. J. 14 (2005) 505–510.

[168] A. Imaz, J. Forcada, Optimized buffered polymerizations to produce N-vinylcaprolactam-based microgels, Eur. Polym. J. 45 (2009) 3164–3175. https://doi.org/10.1016/j.eurpolymj.2009.08.003.

[169] L.M. Geever, Synthesis and characterisation of novel temperature sensitive hydrogels for controlled drug delivery Higher Education and Training Awards Council, Athlone Institute of Technology, 2008.

[170] S.F. Medeiros, A.M. Santos, H. Fessi, A. Elaissari, Stimuli-responsive magnetic particles for biomedical applications, Int. J. Pharm. 403 (2011) 139–161. https://doi.org/10.1016/j.ijpharm.2010.10.011.

[171] A. Imaz, J.I. Miranda, J. Ramos, J. Forcada, Evidences of a hydrolysis process in the synthesis of N-vinylcaprolactam-based microgels, Eur. Polym. J. 44 (2008) 4002–4011. https://doi.org/10.1016/j.eurpolymj.2008.09.027.

[172] V. Boyko, A. Pich, Y. Lu, S. Richter, K.F. Arndt, H.J.P. Adler, Thermo-sensitive poly(N-vinylcaprolactam-co-acetoacetoxyethyl methacrylate) microgels: 1 - Synthesis and characterization, Polymer (Guildf). 44 (2003) 7821–7827. https://doi.org/10.1016/j.polymer.2003.09.037.

[173] T. Inoue, G. Chen, K. Nakamae, A.S. Hoffman, Temperature sensitivity of a hydrogel network containing different LCST oligomers grafted to the hydrogel backbone, Polym. Gels Networks. 5 (1998) 561–575. https://doi.org/10.1016/S0966-7822(97)00029-4.

[174] M. Jannesari, J. Varshosaz, M. Morshed, M. Zamani, Composite poly(vinyl alcohol)/poly(vinyl acetate) electrospun nanofibrous mats as a novel wound dressing matrix for controlled release of drugs., Int. J. Nanomedicine. 6 (2011) 993–1003. https://doi.org/10.2147/ijn.s17595.

[175] N. Alhusein, P.A. de Bank, I.S. Blagbrough, A. Bolhuis, Killing bacteria within biofilms by sustained release of tetracycline from triple-layered electrospun micro/nanofibre matrices of polycaprolactone and poly(ethylene-co-vinyl acetate), Drug Deliv. Transl. Res. 3 (2013) 531–541. https://doi.org/10.1007/s13346-013-0164-9.

[176] A. Kermagoret, C.A. Fustin, M. Bourguignon, C. Detrembleur, C. Jérôme, A. Debuigne, One-pot controlled synthesis of double thermoresponsive N-vinylcaprolactam-based copolymers with tunable LCSTs, Polym. Chem. 4 (2013) 2575–2583.

https://doi.org/10.1039/c3py00134b.

[177] M.J. Roberts, M.D. Bentley, J.M. Harris, Chemistry for peptide and protein PEGylation, Adv. Drug Deliv. Rev. 64 (2012) 116–127. https://doi.org/10.1016/j.addr.2012.09.025.

[178] W. Brullot, N.K. Reddy, J. Wouters, V.K. Valev, B. Goderis, J. Vermant, T. Verbiest, Versatile ferrofluids based on polyethylene glycol coated iron oxide nanoparticles, J. Magn. Magn. Mater. 324 (2012) 1919–1925. https://doi.org/10.1016/j.jmmm.2012.01.032.

[179] K. Knop, R. Hoogenboom, D. Fischer, U.S. Schubert, Poly(ethylene glycol) in drug delivery: Pros and cons as well as potential alternatives, Angew. Chemie - Int. Ed. 49 (2010) 6288–6308. https://doi.org/10.1002/anie.200902672.

[180] A.A. Tager, A.P. Safronov, S. V. Sharina, I.Y. Galayev, Thermodynamics of aqueous solutions of polyvinylcaprolactam, Polym. Sci. U.S.S.R. 32 (1990) 469–474. https://doi.org/10.1016/0032-3950(90)90133-Q.

[181] S.M. Ponce-Vargas, N.A. Cortez-Lemus, A. Licea-Claveríe, Preparation of poly(N-Vinylcaprolactam) (NVCL) and statistical copolymers of NVCL with variable cloud point temperature by using a trithiocarbonate RAFT agent, Macromol. Symp. 325–326 (2013) 56–70. https://doi.org/10.1002/masy.201200045.

[182] H.A. Gaballa, L.M. Geever, J.A. Killion, C.L. Higginbotham, Synthesis and characterization of physically crosslinked N-vinylcaprolactam, acrylic acid, methacrylic acid, and N,N-dimethylacrylamide hydrogels, J. Polym. Sci. Part B Polym. Phys. 51 (2013) 1555–1564. https://doi.org/10.1002/polb.23369.

[183] S. Çavuş, E. Çakal, Synthesis and characterization of novel poly(N-vinylcaprolactam-co-itaconic acid) gels and analysis of ph and temperature sensitivity, Ind. Eng. Chem. Res. 51 (2012) 1218–1226. https://doi.org/10.1021/ie2008746.

[184] R.C. Mundargi, V. Rangaswamy, T.M. Aminabhavi, Poly(N-vinylcaprolactam-co-methacrylic acid) hydrogel microparticles for oral insulin delivery, J. Microencapsul. 28 (2011) 384–394. https://doi.org/10.3109/02652048.2011.576782.

[185] M.B. Dalton, S.C. Halligan, J.A. Killion, W. Wang, Y. Dong, M.J.D. Nugent, L.M. Geever, The Effect Acetic Acid has on Poly(N-Vinylcaprolactam) LCST for Biomedical Applications, Polym. - Plast. Technol. Eng. 57 (2018) 1165–1174. https://doi.org/10.1080/03602559.2017.1373400.

[186] A. Theis, T.P. Davis, M.H. Stenzel, C. Barner-Kowollik, Probing the reaction kinetics of vinyl acetate free radical polymerization via living free radical polymerization (MADIX), Polymer (Guildf). 47 (2006) 999–1010. https://doi.org/10.1016/j.polymer.2005.12.054.

[187] M. Maniruzzaman, M. Lam, C. Molina, A. Nokhodchi, Study of the Transformations of Micro/Nano-crystalline Acetaminophen Polymorphs in Drug-Polymer Binary Mixtures, AAPS PharmSciTech. 18 (2017) 1428–1437. https://doi.org/10.1208/s12249-016-0596-x.

[188] A. Ebrahimi, M. Saffari, F. Dehghani, T. Langrish, Incorporation of acetaminophen as an active pharmaceutical ingredient into porous lactose, Int. J. Pharm. 499 (2016) 217–227. https://doi.org/10.1016/j.ijpharm.2016.01.007.

[189] Y. Qiu, K. Park, Environment-sensitive hydrogels for drug delivery, Adv. Drug Deliv. Rev. 64 (2012) 49–60. https://doi.org/10.1016/j.addr.2012.09.024.

[190] E.S. Gil, S.M. Hudson, Stimuli-reponsive polymers and their bioconjugates, Prog. Polym. Sci. 29 (2004) 1173–1222. https://doi.org/10.1016/j.progpolymsci.2004.08.003.

[191] Q. Wu, L. Wang, X. Fu, X. Song, Q. Yang, G. Zhang, Synthesis and self-assembly of a new amphiphilic thermosensitive poly(N-vinylcaprolactam)/poly(ε-caprolactone) block copolymer, Polym. Bull. 71 (2014) 1–18. https://doi.org/10.1007/s00289-013-1041-x.

[192] X. Li, H. Zhong, X. Li, F. Jia, Z. Cheng, L. Zhang, J. Yin, L. An, L. Guo, Synthesis of attapulgite/N-isopropylacrylamide and its use in drug release, Mater. Sci. Eng. C. 45 (2014) 170–175. https://doi.org/10.1016/j.msec.2014.08.056.

[193] L.M. Geever, C.C. Cooney, J.G. Lyons, J.E. Kennedy, M.J.D. Nugent, S. Devery, C.L. Higginbotham, Characterisation and controlled drug release from novel drug-loaded hydrogels, Eur. J. Pharm. Biopharm. 69 (2008) 1147–1159. https://doi.org/10.1016/j.ejpb.2007.12.021.

[194] D. Wan, Q. Zhou, H. Pu, G. Yang, Controlled radical polymerization of N-vinylcaprolactam mediated by xanthate or dithiocarbamate, J. Polym. Sci. Part A Polym. Chem. 46 (2008) 3756–3765. https://doi.org/10.1002/pola.22722.

[195] T.M. Don, C.F. King, W.Y. Chiu, C.A. Peng, Preparation and characterization of chitosan-g-poly(vinyl alcohol)/poly(vinyl alcohol) blends used for the evaluation of blood-contacting compatibility, Carbohydr. Polym. 63 (2006) 331–339.

https://doi.org/10.1016/j.carbpol.2005.08.023.

[196] K. Kolter, A. Dashevsky, M. Irfan, R. Bodmeier, Polyvinyl acetate-based film coatings, Int. J. Pharm. 457 (2013) 470–479. https://doi.org/10.1016/j.ijpharm.2013.08.077.

[197] H. Priya James, R. John, A. Alex, K.R. Anoop, Smart polymers for the controlled delivery of drugs – a concise overview, Acta Pharm. Sin. B. 4 (2014) 120–127. https://doi.org/10.1016/j.apsb.2014.02.005.

[198] D.Y. Ko, U.P. Shinde, B. Yeon, B. Jeong, Recent progress of in situ formed gels for biomedical applications, Prog. Polym. Sci. 38 (2013) 672–701. https://doi.org/10.1016/j.progpolymsci.2012.08.002.

[199] J.A. Killion, L.M. Geever, D.M. Devine, J.E. Kennedy, C.L. Higginbotham, Mechanical properties and thermal behaviour of PEGDMA hydrogels for potential bone regeneration application, J. Mech. Behav. Biomed. Mater. 4 (2011) 1219–1227. https://doi.org/10.1016/j.jmbbm.2011.04.004.

[200] J.M.G. Cowie, V. Arrighi, Polymers : Chemistry and Physics of M O D E R N Materials, Third, CRC Press, Boca Raton, 2007.

[201] A. Guevara-Morales, U. Figueroa-López, Residual stresses in injection molded products, J. Mater. Sci. 49 (2014) 4399–4415. https://doi.org/10.1007/s10853-014-8170-y.

[202] Plastemart.com, Amorphous polymers can produce transparent clear products, Tech. Pap. Plast. . (n.d.). http://www.plastemart.com/plastic-technical-articles/Amorphous-polymers-can-produce-transparent-clear-products-/1354 (accessed September 8, 2020).

[203] S. Mukherjee, A. Gowen, A review of recent trends in polymer characterization using non-destructive vibrational spectroscopic modalities and chemical imaging, Anal. Chim. Acta. 895 (2015) 12–34. https://doi.org/10.1016/j.aca.2015.09.006.

[204] N.S. Allen, M. Edge, M. Rodriguez, C.M. Liauw, E. Fontan, Aspects of the thermal oxidation of ethylene vinyl acetate copolymer, Polym. Degrad. Stab. 68 (2000) 363–371. https://doi.org/10.1016/S0141-3910(00)00020-3.

[205] W. Qian, P. Xu, G. Lu, X. Huang, Synthesis of PAA-g-PNVCL Graft Copolymer and Studies on Its Loading of Ornidazole, Chinese J. Chem. 32 (2014) 1049–1056. https://doi.org/10.1002/cjoc.201400472.

[206] X. Liang, V. Kozlovskaya, C.P. Cox, Y. Wang, M. Saeed, E. Kharlampieva, Synthesis

and self-assembly of thermosensitive double-hydrophilic poly(N-vinylcaprolactam)-b-poly(N-vinyl-2-pyrrolidone) diblock copolymers, J. Polym. Sci. Part A Polym. Chem. 52 (2014) 2725–2737. https://doi.org/10.1002/pola.27291.

[207] M.L. Hans, A.M. Lowman, Biodegradable nanoparticles for drug delivery and targeting, Curr. Opin. Solid State Mater. Sci. 6 (2002) 319–327. https://doi.org/10.1016/S1359-0286(02)00117-1.

[208] S. Schwarz, S.M. Ponce-Vargas, A. Licea-Claverie, C. Steinbach, Chitosan and mixtures with aqueous biocompatible temperature sensitive polymer as flocculants, Colloids Surfaces A Physicochem. Eng. Asp. 413 (2012) 7–12. https://doi.org/10.1016/j.colsurfa.2012.03.048.

[209] G. Mittal, D.K. Sahana, V. Bhardwaj, M.N.V. Ravi Kumar, Estradiol loaded PLGA nanoparticles for oral administration: Effect of polymer molecular weight and copolymer composition on release behavior in vitro and in vivo, J. Control. Release. 119 (2007) 77–85. https://doi.org/10.1016/j.jconrel.2007.01.016.

[210] D. Li, H. Sun, J. Ding, Z. Tang, Y. Zhang, W. Xu, X. Zhuang, X. Chen, Polymeric topology and composition constrained polyether-polyester micelles for directional antitumor drug delivery, Acta Biomater. 9 (2013) 8875–8884. https://doi.org/10.1016/j.actbio.2013.06.041.

[211] V.T. Lebedev, G. Török, L. Cser, G. Káli, A.I. Sibilev, Molecular dynamics of poly (N-vinylcaprolactam) hydrate, Appl. Phys. A. 74 (2002) pp s478-s480.

[212] F. Meeussen, E. Nies, H. Berghmans, S. Verbrugghe, E. Goethals, F. Du Prez, Phase behaviour of poly(N-vinyl caprolactam) in water, Polymer (Guildf). 41 (2000) 8597–8602. https://doi.org/10.1016/S0032-3861(00)00255-X.

[213] J. Siepmann, N.A. Peppas, Modeling of drug release from delivery systems based on hydroxypropyl methylcellulose (HPMC), Adv. Drug Deliv. Rev. 64 (2012) 163–174. https://doi.org/10.1016/j.addr.2012.09.028.

[214] J.E. Chung, M. Yokoyama, M. Yamato, T. Aoyagi, Y. Sakurai, T. Okano, Thermo-responsive drug delivery from polymeric micelles constructed using block copolymers of poly(N-isopropylacrylamide) and poly(butylmethacrylate), J. Control. Release. 62 (1999) 115–127. https://doi.org/10.1016/S0168-3659(99)00029-2.

[215] L.M. Geever, D.M. Devine, M.J.D. Nugent, J.E. Kennedy, J.G. Lyons, A. Hanley, C.L.

Higginbotham, Lower critical solution temperature control and swelling behaviour of physically crosslinked thermosensitive copolymers based on N-isopropylacrylamide, Eur. Polym. J. 42 (2006) 2540–2548. https://doi.org/10.1016/j.eurpolymj.2006.06.002.

[216] S. Aerry, A. De, A. Kumar, A. Saxena, D.K. Majumdar, S. Mozumdar, Synthesis and characterization of thermoresponsive copolymers for drug delivery, J. Biomed. Mater. Res. - Part A. 101 A (2013) 2015–2026. https://doi.org/10.1002/jbm.a.34476.

[217] C.C. Ferraz, G.H.C. Varca, J.C. Ruiz, P.S. Lopes, M.B. Mathor, A.B. Lugão, E. Bucio, Radiation-grafting of thermo- and pH-responsive poly(N-vinylcaprolactam-co-acrylic acid) onto silicone rubber and polypropylene films for biomedical purposes, Radiat. Phys. Chem. 97 (2014) 298–303. https://doi.org/10.1016/j.radphyschem.2013.12.027.

[218] H.Y. Shi, L.M. Zhang, Phase-transition and aggregation characteristics of a thermoresponsive dextran derivative in aqueous solutions, Carbohydr. Res. 341 (2006) 2414–2419. https://doi.org/10.1016/j.carres.2006.06.015.

[219] L.M. Geever, C.M. Mínguez, D.M. Devine, M.J.D. Nugent, J.E. Kennedy, J.G. Lyons, A. Hanley, S. Devery, P.T. Tomkins, C.L. Higginbotham, The synthesis, swelling behaviour and rheological properties of chemically crosslinked thermosensitive copolymers based on N-isopropylacrylamide, J. Mater. Sci. 42 (2007) 4136–4148. https://doi.org/10.1007/s10853-006-0912-z.

[220] C. Scherzinger, A. Schwarz, A. Bardow, K. Leonhard, W. Richtering, Cononsolvency of poly-N-isopropyl acrylamide (PNIPAM): Microgels versus linear chains and macrogels, Curr. Opin. Colloid Interface Sci. 19 (2014) 84–94. https://doi.org/10.1016/j.cocis.2014.03.011.

[221] J.A. Killion, S. Kehoe, L.M. Geever, D.M. Devine, E. Sheehan, D. Boyd, C.L. Higginbotham, Hydrogel/bioactive glass composites for bone regeneration applications: Synthesis and characterisation, Mater. Sci. Eng. C. 33 (2013) 4203–4212. https://doi.org/10.1016/j.msec.2013.06.013.

[222] J.W. Jutai, S. Coulson, E. Russell-Minda, Technology and medicine, Technol. Psychol. Well-Being. 17 (2009) 206–226. https://doi.org/10.1017/CBO9780511635373.009.

[223] M.A. Ward, T.K. Georgiou, Thermoresponsive polymers for biomedical applications, Polymers (Basel). 3 (2011) 1215–1242. https://doi.org/10.3390/polym3031215.

[224] Z. Li, S. Cho, I.C. Kwon, M.M. Janát-Amsbury, K.M. Huh, Preparation and

characterization of glycol chitin as a new thermogelling polymer for biomedical applications, Carbohydr. Polym. 92 (2013) 2267–2275. https://doi.org/10.1016/j.carbpol.2012.11.068.

[225] D. Chitkara, A. Shikanov, N. Kumar, A.J. Domb, Biodegradable injectable in situ depot-forming drug delivery systems, Macromol. Biosci. 6 (2006) 977–990. https://doi.org/10.1002/mabi.200600129.

[226] S. Chen, H. Zhong, B. Gu, Y. Wang, X. Li, Z. Cheng, L. Zhang, C. Yao, Thermosensitive phase behavior and drug release of in situ N-isopropylacrylamide copolymer, Mater. Sci. Eng. C. 32 (2012) 2199–2204. https://doi.org/10.1016/j.msec.2012.05.052.

[227] S. Kempe, K. Mäder, In situ forming implants - An attractive formulation principle for parenteral depot formulations, J. Control. Release. 161 (2012) 668–679. https://doi.org/10.1016/j.jconrel.2012.04.016.

[228] J.K. Kim, H.W. Son, The rheological properties of polystyrene/poly(vinylmethylether) blend near the critical region and in the homogenous region, Polymer (Guildf). 40 (1999) 6789–6801. https://doi.org/10.1016/S0032-3861(99)00030-0.

[229] M. Kapnistos, A. Hinrichs, D. Vlassopoulos, S.H. Anastasiadis, A. Stammer, B.A. Wolf, Rheology of a lower critical solution temperature binary polymer blend in the homogeneous, phase-separated, and transitional regimes, Macromolecules. 29 (1996) 7155–7163. https://doi.org/10.1021/ma960835n.

[230] D. Gupta, C.H. Tator, M.S. Shoichet, Fast-gelling injectable blend of hyaluronan and methylcellulose for intrathecal, localized delivery to the injured spinal cord, Biomaterials. 27 (2006) 2370–2379. https://doi.org/10.1016/j.biomaterials.2005.11.015.

[231] R. Asasutjarit, S. Thanasanchokpibull, A. Fuongfuchat, S. Veeranondha, Optimization and evaluation of thermoresponsive diclofenac sodium ophthalmic in situ gels, Int. J. Pharm. 411 (2011) 128–135. https://doi.org/10.1016/j.ijpharm.2011.03.054.

[232] Radiological Protection Institute of Ireland, The Design of Diagnostic Medical Facilities where Ionising Radiation is used, ResearchGate. (2009) 113. https://www.researchgate.net/publication/235997041.

[233] MiniPhysics, The Electromagnetic Spectrum | Mini Physics - Learn Physics Online, (2017). https://www.miniphysics.com/electromagnetic-spectrum_25.html (accessed

October 23, 2019).

[234] S. Breiter, Membranes for oxygenators and plasma filters, in: M. Lysaght, T.J. Webster (Eds.), Biomater. Artif. Organs, Woodhead Publishing Limited, Germany, 2010: pp. 3–33. https://doi.org/10.1533/9780857090843.1.3.

[235] K.A. Murray, J.E. Kennedy, B. McEvoy, O. Vrain, D. Ryan, C.L. Higginbotham, The effects of high energy electron beam irradiation on the thermal and structural properties of low density polyethylene, Radiat. Phys. Chem. 81 (2012) 962–966. https://doi.org/10.1016/j.radphyschem.2011.09.011.

[236] Electron Beam (E-Beam) Sterilization | Sterigenics, (n.d.). https://sterigenics.com/technologies/electron-beam/ (accessed December 4, 2019).

[237] K.A. Murray, J.E. Kennedy, B. McEvoy, O. Vrain, D. Ryan, R. Cowman, C.L. Higginbotham, The influence of electron beam irradiation conducted in air on the thermal, chemical, structural and surface properties of medical grade polyurethane, Eur. Polym. J. 49 (2013) 1782–1795. https://doi.org/10.1016/j.eurpolymj.2013.03.034.

[238] K.A. Murray, J.E. Kennedy, B. McEvoy, O. Vrain, D. Ryan, R. Cowman, C.L. Higginbotham, The effects of high energy electron beam irradiation in air on accelerated aging and on the structure property relationships of low density polyethylene, Nucl. Instruments Methods Phys. Res. Sect. B Beam Interact. with Mater. Atoms. 297 (2013) 64–74. https://doi.org/10.1016/j.nimb.2012.12.001.

[239] S.C. Halligan, K.A. Murray, O. Vrain, J.G. Lyons, L.M. Geever, Controlling the thermosensitivity of poly(N-vinylcaprolactam) for smart glass applications via electron beam irradiation, Mater. Today Proc. 10 (2019) 430–435. https://doi.org/10.1016/j.matpr.2019.03.006.

[240] S. Dånmark, A. Finne-Wistrand, K. Schander, M. Hakkarainen, K. Arvidson, K. Mustafa, A.C. Albertsson, In vitro and in vivo degradation profile of aliphatic polyesters subjected to electron beam sterilization, Acta Biomater. 7 (2011) 2035–2046. https://doi.org/10.1016/j.actbio.2011.02.011.

[241] S.F. Medeiros, J.O.C. Filizzola, P.F.M. Oliveira, T.M. Silva, B.R. Lara, M. V. Lopes, B. Rossi-Bergmann, A. Elaissari, A.M. Santos, Fabrication of biocompatible and stimuli-responsive hybrid microgels with magnetic properties via aqueous precipitation polymerization, Mater. Lett. 175 (2016) 296–299. https://doi.org/10.1016/j.matlet.2016.04.004.

[242] E. Caló, V. V. Khutoryanskiy, Biomedical applications of hydrogels: A review of patents and commercial products, Eur. Polym. J. 65 (2015) 252–267. https://doi.org/10.1016/j.eurpolymj.2014.11.024.

[243] N.H.S. Estates., Health technical memorandum 2010. Part 3, Validation and verification : sterilization., 1998. https://www.gov.uk/government/uploads/system/uploads/attachment_data/file/170689/HTM_01-05_2013.pdf.

[244] International Atomic Energy Agency (IAEA), IAEA Annual Report 2015, 2015.

[245] S. Yasunaga, H. Murakami, Electron Beam Processing, in: T.B.T.-S. Sandle Sterilisation and Sterility Assurance for Pharmaceuticals (Ed.), Shinku, Woodhead Publishing, 1991: pp. 699–706. https://doi.org/10.3131/jvsj.34.699.

[246] Overview of a Gamma Irradiation Validation | TechTip | STERIS AST, (n.d.). https://www.steris-ast.com/tech-tip/overview-gamma-irradiation-validation/ (accessed January 31, 2020).

[247] J. a Sugranes, Basic Operating Principles and Validation of Electron Beam Irradiation Systems, J. Valid. Technol. (2005) 64–69. http://www.ivtnetwork.com/sites/default/files/Basic Operating Principles and Validation of Electron Beam Irradiation Systems.pdf.

[248] Fifth Report on Needs in Ionizing Radiation Council on Ionizing Radiation Measurements and Standards, 2011.

[249] K.A. Murray, J.E. Kennedy, B. McEvoy, O. Vrain, D. Ryan, R. Cowman, C.L. Higginbotham, Effects of temperature, packaging and electron beam irradiation processing conditions on the property behaviour of Poly (ether-block-amide) blends, Mater. Sci. Eng. C. 39 (2014) 380–394. https://doi.org/10.1016/j.msec.2014.03.021.

[250] A. Kumar, Deepak, S. Sharma, S. Afgan, R. Kumar, A.K. Keshari, R. Srivastava, Development of graft copolymer of carboxymethylcellulose and N-vinylcaprolactam towards strong antioxidant and antibacterial polymeric materials, Int. J. Biol. Macromol. 112 (2018) 780–787. https://doi.org/10.1016/j.ijbiomac.2018.02.030.

[251] S. Halligan, K. Murray, M. Hopkins, I. Rogers, J. Lyons, O. Vrain, L. Geever, Enhancing and controlling the critical attributes of poly (N-vinylcaprolactam) through electron beam irradiation for biomedical applications, J. Appl. Polym. Sci. 137 (2020)

48639. https://doi.org/10.1002/app.48639.

[252] S.C. Halligan, M.B. Dalton, K.A. Murray, Y. Dong, W. Wang, J.G. Lyons, L.M. Geever, Synthesis, characterisation and phase transition behaviour of temperature-responsive physically crosslinked poly (N-vinylcaprolactam) based polymers for biomedical applications, Mater. Sci. Eng. C. 79 (2017) 130–139. https://doi.org/10.1016/j.msec.2017.03.241.

[253] N. Saba, M. Jawaid, O.Y. Alothman, M.T. Paridah, A review on dynamic mechanical properties of natural fibre reinforced polymer composites, Constr. Build. Mater. 106 (2016) 149–159. https://doi.org/10.1016/j.conbuildmat.2015.12.075.

[254] M. Mansouri, A. Berrayah, C. Beyens, C. Rosenauer, C. Jama, U. Maschke, Effects of electron beam irradiation on thermal and mechanical properties of poly(lactic acid) films, Polym. Degrad. Stab. 133 (2016) 293–302. https://doi.org/10.1016/j.polymdegradstab.2016.09.005.

[255] M. Sabet, A. Hassan, M.U. Wahit, C.T. Ratnam, Mechanical, thermal and electrical properties of ethylene vinyl acetate irradiated by an electron-beam, Polym. - Plast. Technol. Eng. 49 (2010) 589–594. https://doi.org/10.1080/03602551003652755.

[256] E. Zavala-Lagunes, J.C. Ruiz, G.H.C. Varca, E. Bucio, Synthesis and characterization of stimuli-responsive polypropylene containing N-vinylcaprolactam and N-vinylimidazole obtained by ionizing radiation, Mater. Sci. Eng. C. 67 (2016) 353–361. https://doi.org/10.1016/j.msec.2016.05.044.

[257] K. Sharma, B.S. Kaith, V. Kumar, S. Kalia, V. Kumar, H.C. Swart, Synthesis and biodegradation studies of gamma irradiated electrically conductive hydrogels, Polym. Degrad. Stab. 107 (2014) 166–177. https://doi.org/10.1016/j.polymdegradstab.2014.05.014.

[258] M.L. Cairns, G.R. Dickson, J.F. Orr, D. Farrar, K. Hawkins, F.J. Buchanan, Electron-beam treatment of poly(lactic acid) to control degradation profiles, Polym. Degrad. Stab. 96 (2011) 76–83. https://doi.org/10.1016/j.polymdegradstab.2010.10.016.

[259] T. Oka, H. Kanbe, F. Yatagai, Y. Hama, Changes in the chemical structure and the mechanical properties of single-site polyethylene induced by ion-beam irradiation, Nucl. Instruments Methods Phys. Res. Sect. B Beam Interact. with Mater. Atoms. 208 (2003) 181–184. https://doi.org/10.1016/S0168-583X(03)00663-3.

[260] E. Oral, C. Godleski-Beckos, B.W. Ghali, A.J. Lozynsky, O.K. Muratoglu, Effect of cross-link density on the high pressure crystallization of UHMWPE, J. Biomed. Mater. Res. - Part B Appl. Biomater. 90 B (2009) 720–729. https://doi.org/10.1002/jbm.b.31340.

[261] S.H. Yoo, S. Park, Y. Park, D. Lee, H.I. Joh, I. Shin, S. Lee, Facile method to fabricate carbon fibers from textile-grade polyacrylonitrile fibers based on electron-beam irradiation and its effect on the subsequent thermal stabilization process, Carbon N. Y. 118 (2017) 106–113. https://doi.org/10.1016/j.carbon.2017.03.039.

[262] Y. Wang, D. Chen, Preparation and characterization of a novel stimuli-responsive nanocomposite hydrogel with improved mechanical properties, J. Colloid Interface Sci. 372 (2012) 245–251. https://doi.org/10.1016/j.jcis.2012.01.041.

[263] P.O. Guglielmi, E.G. Herbert, L. Tartivel, M. Behl, A. Lendlein, N. Huber, E.T. Lilleodden, Mechanical characterization of oligo(ethylene glycol)-based hydrogels by dynamic nanoindentation experiments, J. Mech. Behav. Biomed. Mater. 46 (2015) 1–10. https://doi.org/10.1016/j.jmbbm.2015.02.009.

[264] Y. Ma, F. He, H. Wang, H. Liu, Z. Wei, Effect of cross-linking on rheological properties and a model for flexibility-rigidity transition in SBS/PBMA LIPNs, J. Polym. Eng. 36 (2016) 149–156. https://doi.org/10.1515/polyeng-2015-0043.

[265] I.A. Hussein, Rheological investigation of the influence of molecular structure on natural and accelerated UV degradation of linear low density polyethylene, Polym. Degrad. Stab. 92 (2007) 2026–2032. https://doi.org/10.1016/j.polymdegradstab.2007.07.021.

[266] K.A. Murray, J.E. Kennedy, B. McEvoy, O. Vrain, D. Ryan, R. Cowman, C.L. Higginbotham, Effects of gamma ray and electron beam irradiation on the mechanical, thermal, structural and physicochemical properties of poly (ether-block-amide) thermoplastic elastomers, J. Mech. Behav. Biomed. Mater. 17 (2013) 252–268. https://doi.org/10.1016/j.jmbbm.2012.09.011.

[267] J. Liu, A. Debuigne, C. Detrembleur, C. Jérôme, Poly(N-vinylcaprolactam): A Thermoresponsive Macromolecule with Promising Future in Biomedical Field, Adv. Healthc. Mater. 3 (2014) 1941–1968. https://doi.org/10.1002/adhm.201400371.

[268] O. Sedláček, P. Černoch, J. Kučka, R. Konefal, P. Štěpánek, M. Vetrík, T.P. Lodge, M. Hrubý, Thermoresponsive Polymers for Nuclear

Medicine: Which Polymer Is the Best?, Langmuir. 32 (2016) 6115–6122. https://doi.org/10.1021/acs.langmuir.6b01527.

[269] Y.M. Lim, J.P. Jeun, J.H. Lee, Y.M. Lee, Y.C. Nho, Cell sheet detachment from poly(N-vinylcaprolactam-co-N- isopropylacrylamide) grafted onto tissue culture polystyrene dishes, J. Ind. Eng. Chem. 13 (2007) 21–26.

[270] R. Perera, C. Albano, J. González, P. Silva, M. Ichazo, The effect of gamma radiation on the properties of polypropylene blends with styrene-butadiene-styrene copolymers, Polym. Degrad. Stab. 85 (2004) 741–750. https://doi.org/10.1016/j.polymdegradstab.2003.09.020.

[271] S. Kametani, S. Sekine, T. Ohkubo, T. Hirano, K. Ute, H.N. Cheng, T. Asakura, NMR studies of water dynamics during sol-to-gel transition of poly (N-isopropylacrylamide) in concentrated aqueous solution, Polymer (Guildf). 109 (2017) 287–296. https://doi.org/10.1016/j.polymer.2016.12.063.

[272] B. Lang, J.W. McGinity, R.O. Williams, Hot-melt extrusion-basic principles and pharmaceutical applications, Drug Dev. Ind. Pharm. 40 (2014) 1133–1155. https://doi.org/10.3109/03639045.2013.838577.

[273] J. Thiry, F. Krier, B. Evrard, A review of pharmaceutical extrusion: Critical process parameters and scaling-up, Int. J. Pharm. 479 (2015) 227–240. https://doi.org/10.1016/j.ijpharm.2014.12.036.

[274] J. Vera-Sorroche, A. Kelly, E. Brown, P. Coates, N. Karnachi, E. Harkin-Jones, K. Li, J. Deng, Thermal optimisation of polymer extrusion using in-process monitoring techniques, Appl. Therm. Eng. 53 (2013) 405–413. https://doi.org/10.1016/j.applthermaleng.2012.04.013.

[275] V.H. Pino-Ramos, G.G. Flores-Rojas, C. Alvarez-Lorenzo, A. Concheiro, E. Bucio, Graft copolymerization by ionization radiation, characterization, and enzymatic activity of temperature-responsive SR-g-PNVCL loaded with lysozyme, React. Funct. Polym. 126 (2018) 74–82. https://doi.org/10.1016/j.reactfunctpolym.2018.03.002.

[276] A.L. Sarode, S. Obara, F.K. Tanno, H. Sandhu, R. Iyer, N. Shah, Stability assessment of hypromellose acetate succinate (HPMCAS) NF for application in hot melt extrusion (HME), Carbohydr. Polym. 101 (2014) 146–153. https://doi.org/10.1016/j.carbpol.2013.09.017.

[277] A.P. Simonelli, S.C. Mehta, W.I. Higuchi, Dissolution Rates of High Energy Polyvinylpyrrolidone (PVP)-Sulfathiazole Coprecipitates, J. Pharm. Sci. 58 (1969) 538–549. https://doi.org/10.1002/jps.2600580503.

[278] J.G. Moffat, S. Qi, D.Q.M. Craig, Spatial characterization of hot melt extruded dispersion systems using thermal atomic force microscopy methods: The effects of processing parameters on phase separation, Pharm. Res. 31 (2014) 1744–1752. https://doi.org/10.1007/s11095-013-1279-x.

[279] M.M. Crowley, F. Zhang, J.J. Koleng, J.W. McGinity, Stability of polyethylene oxide in matrix tablets prepared by hot-melt extrusion, Biomaterials. 23 (2002) 4241–4248. https://doi.org/10.1016/S0142-9612(02)00187-4.

[280] Why (and What) You Need to Dry : Plastics Technology, (n.d.) (1) Why (and What) You Need to Dry : Plastics Tech. https://www.ptonline.com/articles/why-and-what-you-need-to-dry%0Ahttp://www.ptonline.com/articles/why-and-what-you-need-to-dry (accessed December 16, 2019).

[281] K. Tousif Ayyub, K. Moravkar, M. Maniruzzaman, P. Amin, Effect of melt extrudability and melt binding efficiency of polyvinyl caprolactam polyvinyl acetate polyethylene glycol graft copolymer (Soluplus®) on release pattern of hydrophilic and high dose drugs, Mater. Sci. Eng. C. 99 (2019) 563–574. https://doi.org/10.1016/j.msec.2019.01.126.

[282] J.S. LaFountaine, J.W. McGinity, R.O. Williams, Challenges and Strategies in Thermal Processing of Amorphous Solid Dispersions: A Review, AAPS PharmSciTech. 17 (2016) 43–55. https://doi.org/10.1208/s12249-015-0393-y.

[283] H. Tian, D. Liu, Y. Yao, S. Ma, X. Zhang, A. Xiang, Effect of Sorbitol Plasticizer on the Structure and Properties of Melt Processed Polyvinyl Alcohol Films, J. Food Sci. 82 (2017) 2926–2932. https://doi.org/10.1111/1750-3841.13950.

[284] P.D. Coates, S.E. Barnes, M.G. Sibley, E.C. Brown, H.G.M. Edwards, I.J. Scowen, In-process vibrational spectroscopy and ultrasound measurements in polymer melt extrusion, Polymer (Guildf). 44 (2003) 5937–5949. https://doi.org/10.1016/S0032-3861(03)00544-5.

[285] E.M. Lee, S.Y. Gwon, Y.A. Son, S.H. Kim, Temperature-modulated quenching and photoregulated optical switching of poly(N-

isopropylacrylamide)/spironaphthoxazine/Rhodamine B hybrid in water, Spectrochim. Acta - Part A Mol. Biomol. Spectrosc. 94 (2012) 308–311. https://doi.org/10.1016/j.saa.2012.03.073.

[286] J. Wu, W. Wei, L.Y. Wang, Z.G. Su, G.H. Ma, A thermosensitive hydrogel based on quaternized chitosan and poly(ethylene glycol) for nasal drug delivery system, Biomaterials. 28 (2007) 2220–2232. https://doi.org/10.1016/j.biomaterials.2006.12.024.

[287] What is Pharmaceutical Grade Manufacturing?, (n.d.). https://www.nutrasciencelabs.com/blog/what-is-pharmaceutical-grade-manufacturing (accessed January 13, 2020).

[288] Extrusion & Compounding Equipment | Thermo Fisher Scientific - IE, (n.d.). https://www.thermofisher.com/ie/en/home/industrial/manufacturing-processing/extrusion-compounding-equipment.html (accessed January 13, 2020).

[289] F. Yang, Y. Su, L. Zhu, C.D. Brown, L.A. Rosen, K.J. Rosenberg, Rheological and solid-state NMR assessments of copovidone/clotrimazole model solid dispersions, Int. J. Pharm. 500 (2016) 20–31. https://doi.org/10.1016/j.ijpharm.2016.01.026.

[290] M.S. Dudhedia, A.M. Agrawal, Rheological study of copovidone and solid dispersion blend used for hot melt extrusion, J. Appl. Polym. Sci. 133 (2016) 1–9. https://doi.org/10.1002/app.43278.

[291] C. McConville, I. Major, B. Devlin, A. Brimer, Development of a multi-layered vaginal tablet containing dapivirine, levonorgestrel and acyclovir for use as a multipurpose prevention technology, Eur. J. Pharm. Biopharm. 104 (2016) 171–179. https://doi.org/10.1016/j.ejpb.2016.05.003.

[292] S.S. Gupta, T. Parikh, A.K. Meena, N. Mahajan, I. Vitez, A.T.M. Serajuddin, Effect of carbamazepine on viscoelastic properties and hot melt extrudability of Soluplus®, Int. J. Pharm. 478 (2015) 232–239. https://doi.org/10.1016/j.ijpharm.2014.11.025.

[293] J.S. LaFountaine, S. V. Jermain, L.K. Prasad, C. Brough, D.A. Miller, D. Lubda, J.W. McGinity, R.O. Williams, Enabling thermal processing of ritonavir-polyvinyl alcohol amorphous solid dispersions by KinetiSol® Dispersing, Eur. J. Pharm. Biopharm. 101 (2016) 72–81. https://doi.org/10.1016/j.ejpb.2016.01.018.

[294] G. Trichy Rengarajan, M. Beiner, Relaxation Behavior and Crystallization Kinetics of Amorphous Acetaminophen, Lett. Drug Des. Discov. 3 (2006) 723–730.

https://doi.org/10.2174/157018006778631938.

[295] N.A. Cortez-Lemus, A. Licea-Claverie, Preparation of a mini-library of thermo-responsive star (NVCL/NVP-VAc) polymers with tailored properties using a hexafunctional xanthate RAFT agent, Polymers (Basel). 10 (2017) 1–25. https://doi.org/10.3390/polym10010020.

[296] M.A. Gonzalez-Ayon, N.A. Cortez-Lemus, A. Zizumbo-Lopez, A. Licea-Claverie, Nanogels of poly(N-vinylcaprolactam) core and polyethyleneglycol shell by surfactant free emulsion polymerization, Soft Mater. 12 (2014) 315–325. https://doi.org/10.1080/1539445X.2014.914537.

[297] P. Barmpalexis, I. Koutsidis, E. Karavas, D. Louka, S.A. Papadimitriou, D.N. Bikiaris, Development of PVP/PEG mixtures as appropriate carriers for the preparation of drug solid dispersions by melt mixing technique and optimization of dissolution using artificial neural networks, Eur. J. Pharm. Biopharm. 85 (2013) 1219–1231. https://doi.org/10.1016/j.ejpb.2013.03.013.

[298] B. Perissutti, J.M. Newton, F. Podczeck, F. Rubessa, Preparation of extruded carbamazepine and PEG 4000 as a potential rapid release dosage form, Eur. J. Pharm. Biopharm. 53 (2002) 125–132. https://doi.org/10.1016/S0939-6411(01)00209-0.

[299] M. Stanković, H.W. Frijlink, W.L.J. Hinrichs, Polymeric formulations for drug release prepared by hot melt extrusion: application and characterization, Drug Discov. Today. 20 (2015) 812–823. https://doi.org/10.1016/j.drudis.2015.01.012.

[300] I. Tiffour, S. Bassaid, A. Dehbi, A. Belfedal, A.H.I. Mourad, A. Zeinert, Realization and characterization of a new organic thin film semiconductor, Surf. Rev. Lett. 26 (2019). https://doi.org/10.1142/S0218625X18501275.

[301] A. Goyanes, P. Robles Martinez, A. Buanz, A.W. Basit, S. Gaisford, Effect of geometry on drug release from 3D printed tablets, Int. J. Pharm. 494 (2015) 657–663. https://doi.org/10.1016/j.ijpharm.2015.04.069.

[302] W. Wang, Q. Kang, N. Liu, Q. Zhang, Y. Zhang, H. Li, B. Zhao, Y. Chen, Y. Lan, Q. Ma, Q. Wu, Enhanced dissolution rate and oral bioavailability of Ginkgo biloba extract by preparing solid dispersion via hot-melt extrusion, Fitoterapia. 102 (2015) 189–197. https://doi.org/10.1016/j.fitote.2014.10.004.

[303] P. Treenate, P. Monvisade, In vitro drug release profiles of pH-sensitive

hydroxyethylacryl chitosan/sodium alginate hydrogels using paracetamol as a soluble model drug, Int. J. Biol. Macromol. 99 (2017) 71–78. https://doi.org/10.1016/j.ijbiomac.2017.02.061.

[304] A.J. Sami, M. Khalid, T. Jamil, S. Aftab, S.A. Mangat, A.R. Shakoori, S. Iqbal, Formulation of novel chitosan guargum based hydrogels for sustained drug release of paracetamol, Int. J. Biol. Macromol. 108 (2018) 324–332. https://doi.org/10.1016/j.ijbiomac.2017.12.008.

[305] A. Jahangiri, M. Barzegar-Jalali, A. Garjani, Y. Javadzadeh, H. Hamishehkar, M. Rameshrad, K. Adibkia, Physicochemical characterization and pharmacological evaluation of ezetimibe-PVP K30 solid dispersions in hyperlipidemic rats, Colloids Surfaces B Biointerfaces. 134 (2015) 423–430. https://doi.org/10.1016/j.colsurfb.2015.07.025.

[306] S.Y. Chan, S. Qi, D.Q.M. Craig, An investigation into the influence of drug-polymer interactions on the miscibility, processability and structure of polyvinylpyrrolidone-based hot melt extrusion formulations, Int. J. Pharm. 496 (2015) 95–106. https://doi.org/10.1016/j.ijpharm.2015.09.063.

[307] U.E. Illangakoon, H. Gill, G.C. Shearman, M. Parhizkar, S. Mahalingam, N.P. Chatterton, G.R. Williams, Fast dissolving paracetamol/caffeine nanofibers prepared by electrospinning, Int. J. Pharm. 477 (2014) 369–379. https://doi.org/10.1016/j.ijpharm.2014.10.036.

[308] M. Rasekh, C. Karavasili, Y.L. Soong, N. Bouropoulos, M. Morris, D. Armitage, X. Li, D.G. Fatouros, Z. Ahmad, Electrospun PVP-indomethacin constituents for transdermal dressings and drug delivery devices, Int. J. Pharm. 473 (2014) 95–104. https://doi.org/10.1016/j.ijpharm.2014.06.059.

[309] G. Verstraete, W. De Jaeghere, J. Vercruysse, W. Grymonpré, V. Vanhoorne, F. Stauffer, T. De Beer, A. Bezuijen, J.P. Remon, C. Vervaet, The use of partially hydrolysed polyvinyl alcohol for the production of high drug-loaded sustained release pellets via extrusion-spheronisation and coating: In vitro and in vivo evaluation, Int. J. Pharm. 517 (2017) 88–95. https://doi.org/10.1016/j.ijpharm.2016.11.067.

[310] A. V. Healy, E. Fuenmayor, P. Doran, L.M. Geever, C.L. Higginbotham, J.G. Lyons, Additive manufacturing of personalized pharmaceutical dosage forms via stereolithography, Pharmaceutics. 11 (2019) 645.

https://doi.org/10.3390/pharmaceutics11120645.

[311] X. Wang, A. Michoel, G. Van den Mooter, Study of the phase behavior of polyethylene glycol 6000–itraconazole solid dispersions using DSC, Int. J. Pharm. 272 (2004) 181–187. https://doi.org/https://doi.org/10.1016/j.ijpharm.2003.11.026.

[312] M. Maniruzzaman, M.T. Islam, H.G. Moradiya, S.A. Halsey, I.J. Slipper, B.Z. Chowdhry, M.J. Snowden, D. Douroumis, Prediction of polymorphic transformations of paracetamol in solid dispersions, J. Pharm. Sci. 103 (2014) 1819–1828. https://doi.org/10.1002/jps.23992.

[313] K. Pramod, U.K. Ilyas, Y.T. Kamal, S. Ahmad, S.H. Ansari, J. Ali, Development and validation of RP-HPLC-PDA method for the quantification of eugenol in developed nanoemulsion gel and nanoparticles, J. Anal. Sci. Technol. 4 (2013) 16. https://doi.org/10.1186/2093-3371-4-16.

[314] R.A. Granberg, Å.C. Rasmuson, Solubility of Paracetamol in Pure Solvents, J. Chem. Eng. Data. 44 (1999) 1391–1395. https://doi.org/10.1021/je990124v.

[315] S.A. Papadimitriou, P. Barmpalexis, E. Karavas, D.N. Bikiaris, Optimizing the ability of PVP/PEG mixtures to be used as appropriate carriers for the preparation of drug solid dispersions by melt mixing technique using artificial neural networks: I, Eur. J. Pharm. Biopharm. 82 (2012) 175–186. https://doi.org/https://doi.org/10.1016/j.ejpb.2012.06.003.

[316] L. Liu, S. Bai, H. Yang, S. Li, J. Quan, L. Zhu, H. Nie, Controlled release from thermo-sensitive PNVCL-co-MAA electrospun nanofibers: The effects of hydrophilicity/hydrophobicity of a drug, Mater. Sci. Eng. C. 67 (2016) 581–589. https://doi.org/10.1016/j.msec.2016.05.083.

[317] M. Prabaharan, J.J. Grailer, D.A. Steeber, S. Gong, Stimuli-responsive chitosan-graft-Poly(N-vinylcaprolactam) as a promising material for controlled hydrophobic drug delivery, Macromol. Biosci. 8 (2008) 843–851. https://doi.org/10.1002/mabi.200800010.

Supporting Information

6. Supporting Information

6.1.1. ATR-FTIR

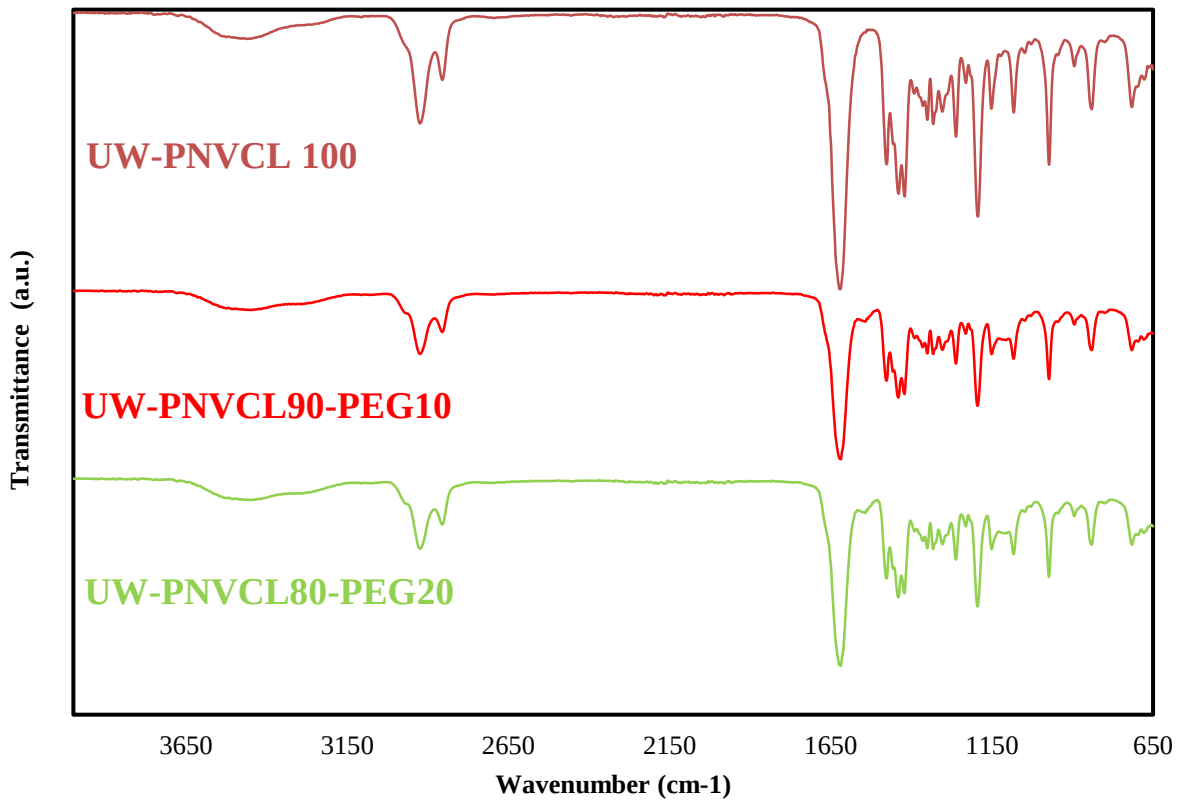

Figure S 6-1: FTIR spectrum for Unwashed PNVCL-PEG samples.

6.1.2. DMA

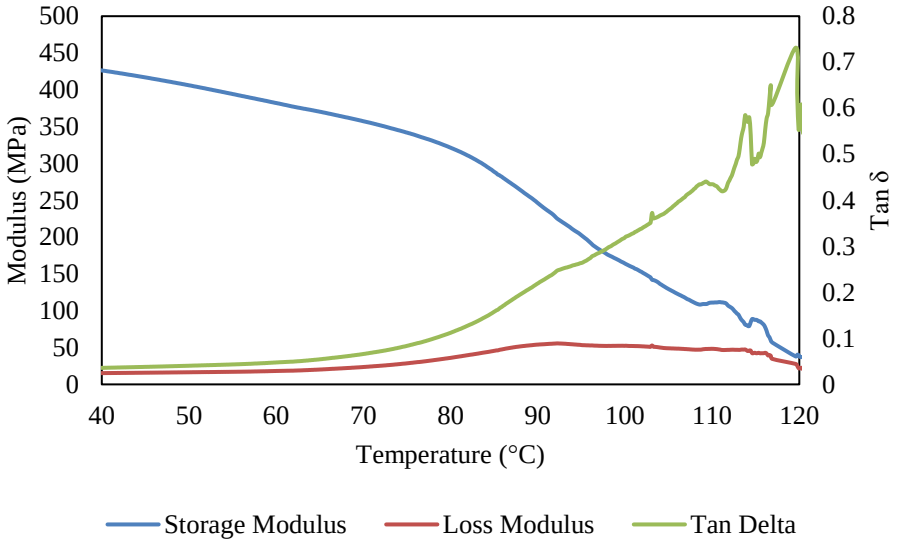

Figure S 6-2: W-PNVCL 50.

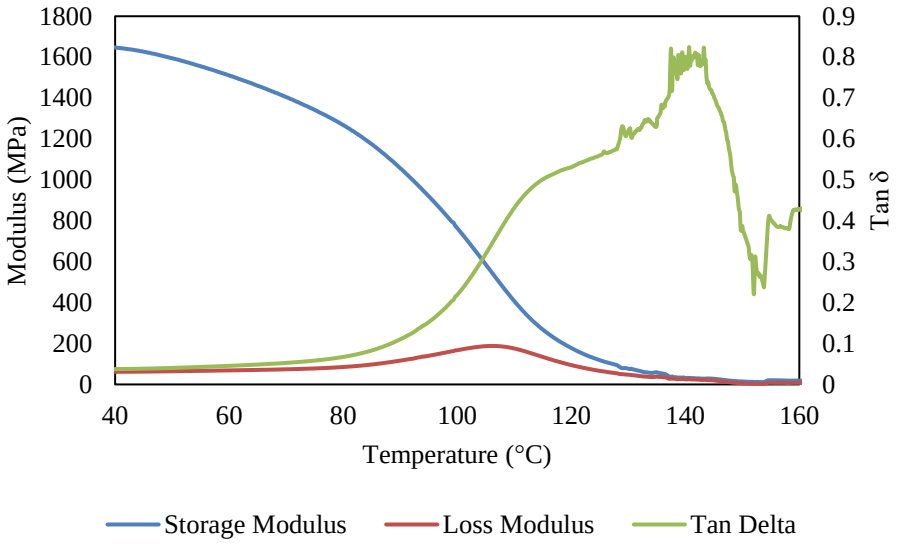

Figure S 6-3: W-PNVCL 100.

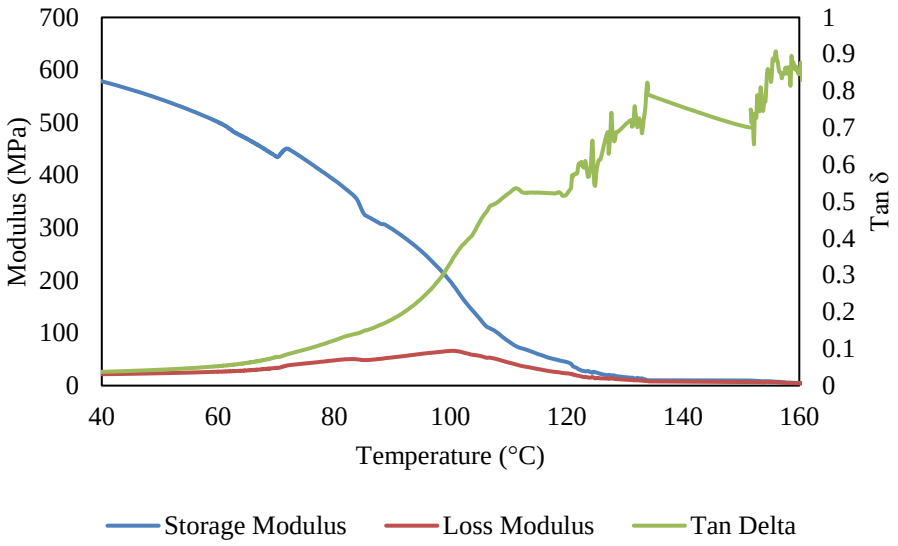

Figure S 6-4: W-PNVCL 150.

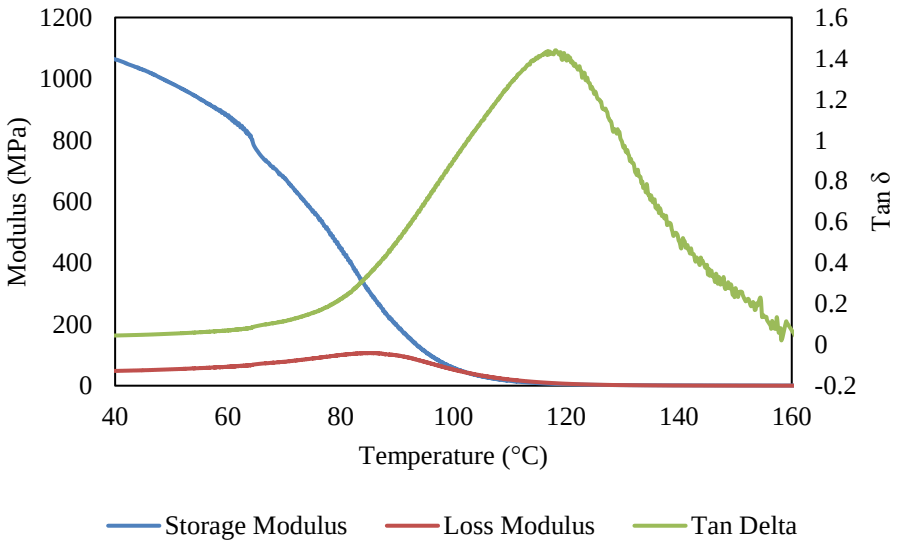

Figure S 6-5: W-PNVCL80-PEG20.

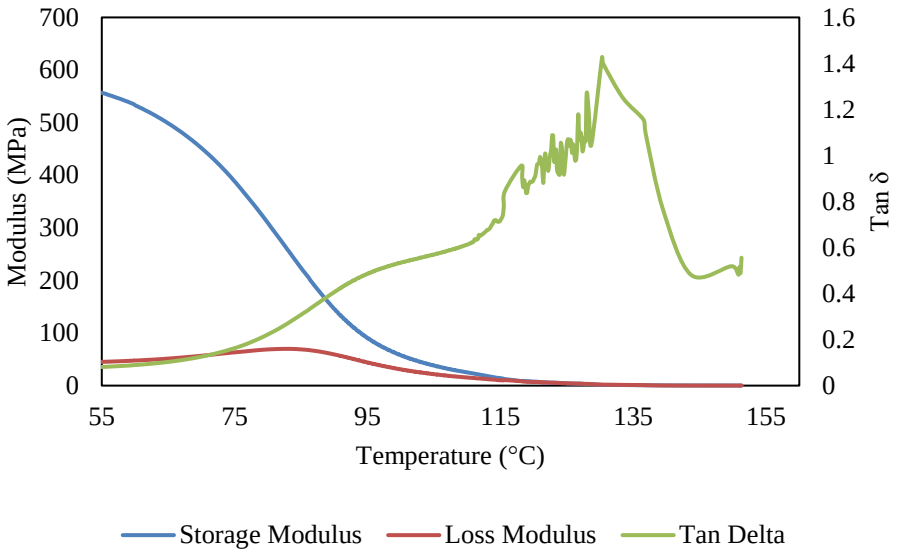

Figure S 6-6: W-PNVCL90-PEG10.

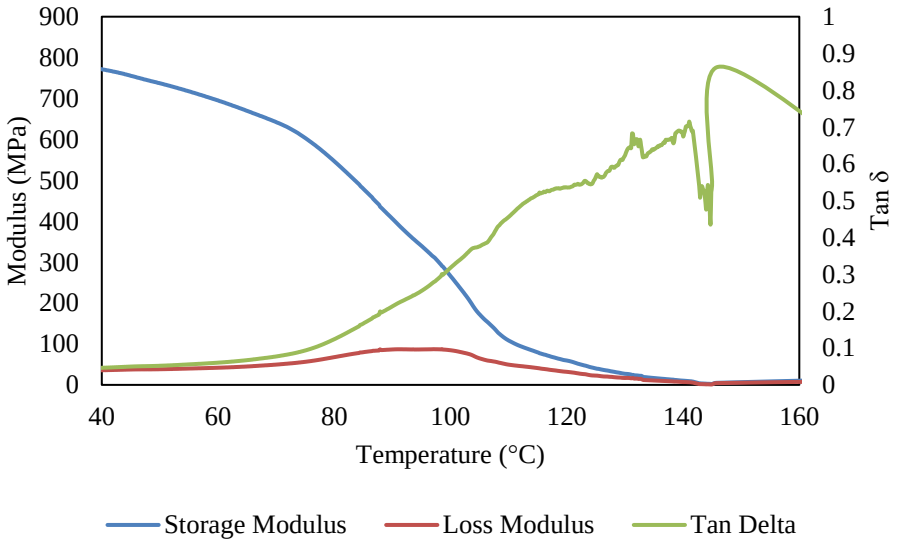

Figure S 6-7: UW-PNVCL 50.

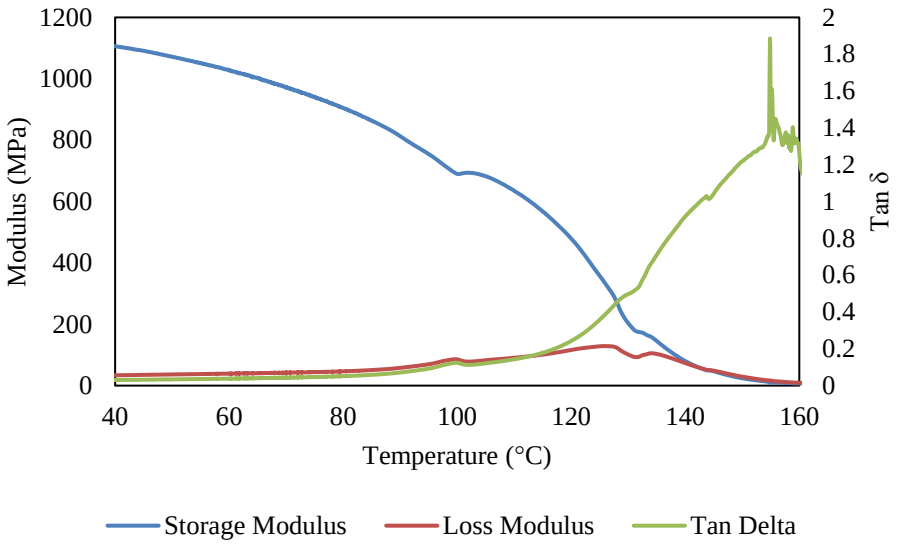

Figure S 6-8: UW-PNVCL 100.

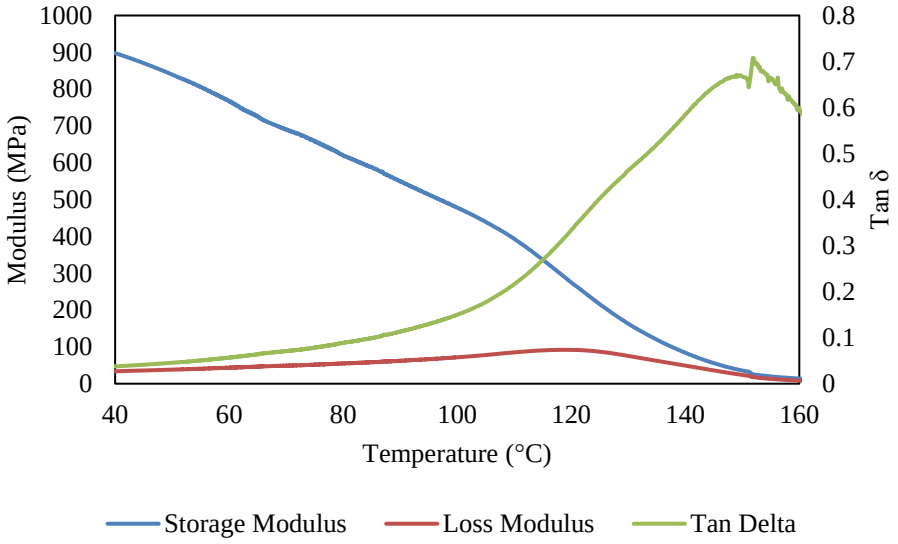

Figure S 6-9: UW-PNVCL 150.

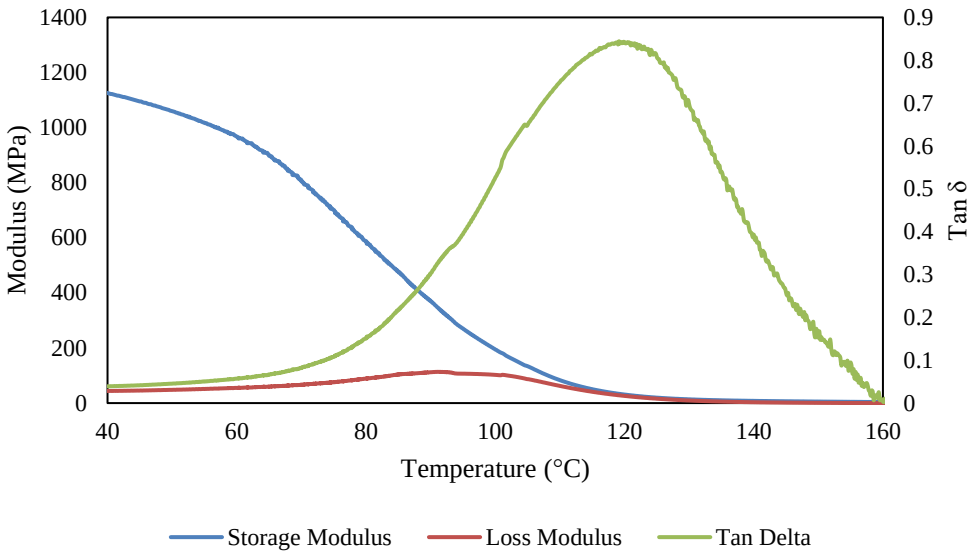

Figure S 6-10: W-PNVCL90-PEG10.

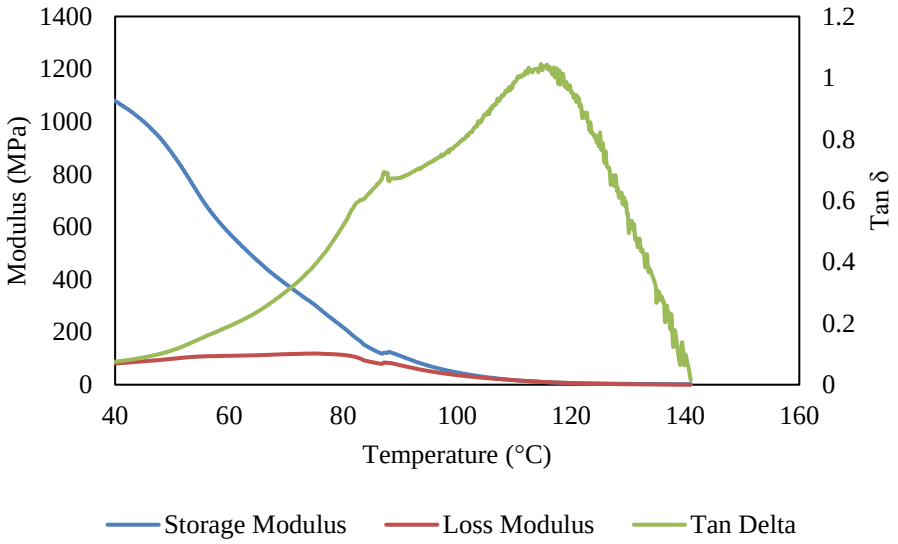

Figure S 6-11: W-PNVCL80-PEG20.

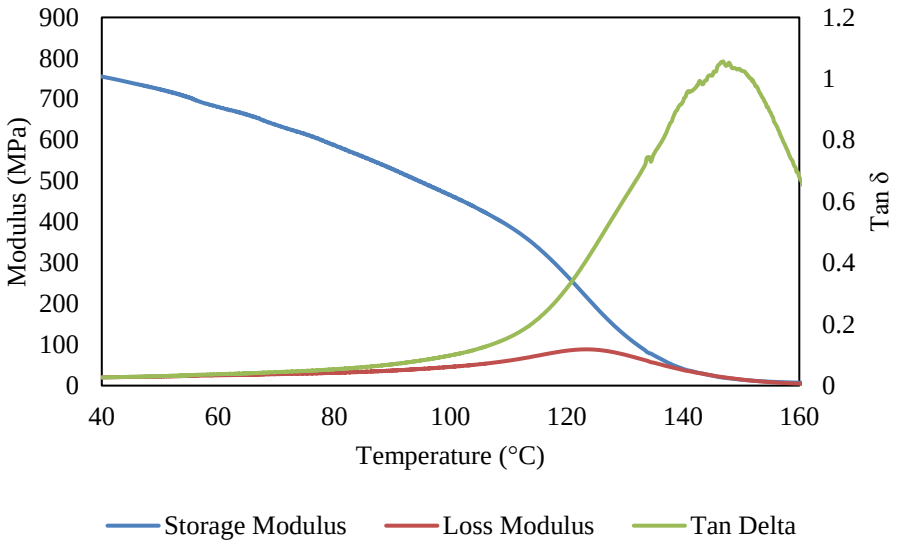

Figure S 6-12: W-PNVCL 50.

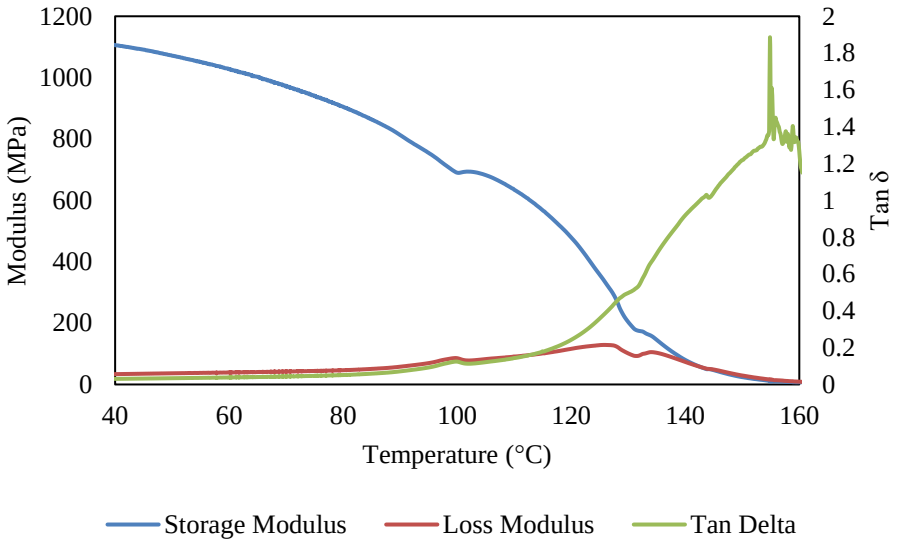

Figure S 6-13: UW-PNVCL 100.

Publication

7. Publication

Materials Science and Engineering C 79 (2017) 130–139

Contents lists available at ScienceDirect

Materials Science and Engineering C

journal homepage: www.elsevier.com/locate/msec

Synthesis, characterisation and phase transition behaviour of temperature-responsive physically crosslinked poly (*N*-vinylcaprolactam) based polymers for biomedical applications

Shane C. Halligan [a], Maurice B. Dalton [a], Kieran A. Murray [a], Yixiao Dong [b], Wenxin Wang [c], John G. Lyons [a], Luke M. Geever [a,*]

[a] Applied Polymer Technologies Gateway, Materials Research Institute, Athlone Institute of Technology, Dublin Road, Athlone, Co. Westmeath, Ireland
[b] Stanford University School of Medicine, Department of Surgery, 257 Campus Drive, GK-210, Stanford, CA 94305-5148, USA
[c] Charles Institute of Dermatology, School of Medicine and Medical Science, University College Dublin, Ireland

ARTICLE INFO

Article history:
Received 9 September 2016
Received in revised form 3 January 2017
Accepted 25 March 2017
Available online 29 March 2017

Keywords:
Poly (*N*-vinylcaprolactam)
Lower critical solution temperature transition
Temperature-responsive polymer
Sol-gel transition

ABSTRACT

Poly (*N*-vinylcaprolactam) (PNVCL) is a polymer which offers superior characteristics for various potential medical device applications. In particular it offers unique thermoresponsive capabilities, which fulfils the material technology constraints required in targeted drug delivery applications. PNVCL phase transitions can be tailored in order to suit the requirements of current and next generation devices, by modifying the contents with regard to the material composition and aqueous polymer concentration. In this study, physically crosslinked Poly (*N*-vinylcaprolactam)-Vinyl acetate (PNVCL-VAc) copolymers were prepared by photopolymerisation. The structure of the polymers was established by Fourier transform infrared spectroscopy, nuclear magnetic resonance and gel permeation chromatography. The polymers were further characterised using differential scanning calorimetry and swelling studies. Determination of the LCST of the polymers in aqueous solution was achieved by employing four techniques; cloud point, UV-spectrometry, differential scanning calorimetry and rheometry. Sol-gel transition was established using tube inversion method and rheological analysis. This study was conducted to determine the characteristics of PNVCL with the addition of VAc, and to establish the effects on the phase transition. The PNVCL based polymers exhibited a decrease in the LCST as the composition of VAc increased. Sol-gel transition could be controlled by altering the monomeric feed ratio and polymer concentration in aqueous milieu. Importantly all copolymers (10 wt% in solution) underwent gelation between 33.6 and 35.9 °C, and based on this and the other materials properties recorded in this study, these novel copolymers have potential for use as injectable *in situ* forming drug delivery systems for targeted drug delivery.

1. Introduction

Stimuli responsive polymers are known as polymers which experience moderately large and abrupt, physical or chemical changes in response to small external changes in environmental conditions [1]. Chemical stimuli, such as pH, ionic factors and chemical agents, will change the interactions between polymer chains or solvents at the molecular level. The physical stimuli, such as temperature, electric or magnetic fields and mechanical stress, will affect the level of various energy sources and alter molecular interactions at critical onset points [2,3]. Among all stimuli responsive polymers investigated, temperature responsive polymer systems have received significant interest, due to the fact that temperature is a vital physiological factor in the body which some disease manifest themselves by a change in temperature [3]. Temperature responsive polymers have allowed for novel developments in tissue engineering [4] and drug delivery carriers [5]. Drug delivery carriers which are based on temperature responsive polymers have superior characteristics such as controlling drug release rate and lowering toxicity which results in an enhanced controlled drug delivery system [6]. Common sources of toxicity include photoinitiators, and organic solvents [7]. However, improvements can be made by optimum selection of photoinitiators as well as photoinitiator concentration. Williams et al. found the toxicity of photoinitiators increased as the concentrations of the initiators increased and as UV exposure time increased [8]. Stimuli-responsive polymers are useful for controlling drug release profiles and interactions with cells. Stimuli-responsive drug carriers are constructed by introducing stimuli-responsive polymers into conventional drug carrier system. Stimuli-responsive drug carriers alter their physicochemical properties in response to ambient environment changes between normal and tumour tissues or applied

* Corresponding author.
E-mail address: lgeever@ait.ie (L.M. Geever).

http://dx.doi.org/10.1016/j.msec.2017.03.241
0928-4931/

physical stimuli to increase the cellular uptake and drug release rate [9, 10]. Temperature responsive injectable polymers are attractive for the use of controlled drug delivery systems, where the aqueous solution of these polymers can undergo a sol-gel transition in response to a change in temperature [11].

Polymers that exhibit a phase transition become less water-soluble as the temperature increases above the lower critical solution temperature (LCST). The LCST occurs, upon which the polymer changes its hydrophilic to hydrophobic balance and therefore, becomes less water-soluble which offers great opportunities for targeted drug delivery carriers [12]. Poly (*N*-vinylcaprolactam) (PNVCL) is acknowledged for its superior characteristics with regard to biocompatibility, solubility, thermosensitivity and having non-ionic and non-toxic features. Moreover, the LCST of PNVCL (32–34 °C) is near the range of physiological temperature [13]. The LCST behaviour of PNVCL is sensitive to alterations in the polymer concentration, the molecular weight of the polymer and also the composition of the solution [14]. Vinyl acetate (VAc) was selected due to its hydrophobic nature and its applications ranging from drug delivery and pharmaceuticals [15–17]. In a comprehensive review, PNVCL was found to have several biomedical applications, such as a matrix for microbial cell entrapment. Results show that enzymatic activities of the microorganisms decreased after cell entrapment in PNVCL gel. Another application for PNVCL was found as a cell culture scaffold. The large pore size and high surface area of PNVCL provides good support for cell growth and interconnected porosity provides better nutrient transfer for cell growth and proliferation [18].

Kermagoret et al. [19] successfully copolymerised NVCL for the first time in a controlled manner with *N*-vinyl pivalate (NVPi) and VAc, that allowed the authors to precisely tune the LCST. The copolymers were prepared by cobalt-mediated radical polymerisation (CMRP) using the bis-(acetylacetonato) cobalt (II) complex as a controlling agent.

Wan et al. [20] reported the synthesis of NVCL and vinyl acetate (VAc) block copolymers using the controlled radical polymerisation *via* macromolecular design by interchange of xanthate, *via* reversible addition-fragmentation chain transfer (RAFT).

Although the homopolymer has been synthesised by various methods of free-radical polymerisation [18], this is the first study to report the synthesis of PNVCL-VAc by free-radical photopolymerisation, using 1-hydroxycyclohexyl phenyl ketone to initiate the reaction. Altering the composition of VAc has the potential to affect the phase transition, swelling, dissolution and sol-gel transitions behaviour of the copolymers, which offers great possibilities for use in drug delivery systems.

2. Materials and methods

2.1. Materials

N-vinylcaprolactam (NVCL) was obtained from Sigma Aldrich Ireland with a molecular weight of 139.19 g mol^{-1} and storage temperature of 2–8 °C. 1-Hydroxycyclohexyl phenyl ketone (Irgacure® 184) was used to initiate the reaction of free-radical polymerisation. Vinyl acetate monomer (VAc) was obtained from Sigma Aldrich Ireland with a molecular weight of 86.09 g mol^{-1}.

2.2. Polymer synthesis

The polymers investigated in this study were prepared by free-radical polymerisation using ultraviolet (UV) light. These polymers were synthesised *via* physical crosslinking using a UV curing system (Dr. Gröbel UV-Electronik GmbH). This particular irradiation chamber is a controlled radiation source with 20 UV-tubes that provide a spectral range of between 315 and 400 nm at an average intensity of 10–13.5 mW/cm^2. The prepolymerised mixtures were prepared by combining desired amounts of the monomer NVCL with 5, 10 and 20 wt% of VAc and 0.1 wt% photoinitiator. The composition of the samples synthesised is listed in Table 1. The batches were placed in a 50 mL beaker and mixed using a magnetic stirrer for 20 min until a homogeneous mixture was obtained. The solutions were pipetted into silicone moulds that contained disc impressions (23 mm diameter, 2.2 mm thickness). Photopolymerisation was carried out for 30 min, at which time gelation occurred. All samples were cured in a silicone mould and prior to use, dried for 24 h in a vacuum oven at 40 °C.

2.2.1. Preparation of aqueous solutions

Homogeneous solutions of each sample were prepared by weighing appropriate amounts of the xerogel and distilled water, leaving these mixtures at room temperature until completely dissolved. These aqueous solutions were produced for subsequent use in LCST measurements.

2.3. Attenuated total reflectance Fourier transform infrared spectroscopy

Attenuated total reflectance Fourier transform infrared (ATR-FTIR) spectroscopy was carried out on a Perkin Elmer Spectrum One, fitted with a universal ATR sampling accessory. All data was recorded at room temperature (<20 °C), in the spectral range of 4000–650 cm^{-1}, utilising a 4 scan per sample cycle and a fixed universal compression force of 80 N. Subsequent analysis was performed using Spectrum software.

2.4. Nuclear magnetic resonance

^{1}H NMR was carried out on a 300 MHz Bruker NMR with MestReNova processing software. The chemical shifts were referenced to the lock chloroform ($CDCl_3$, 7.26 p.p.m.).

2.5. Gel permeation chromatography

Molecular weights and molecular weight distributions (M_w/M_n) of the polymer samples were determined using GPC (Agilent PL-GPC50) with RI detectors. The columns (30 cm PLgel Mixed-C, two in series) were eluted using chloroform and calibrated with poly(methyl methacrylate) (PMMA) standards. All calibrations and analysis were performed at 60 °C with a flow rate of 1 mL/min.

2.6. Differential scanning calorimetry

Differential scanning calorimetry studies were performed on all samples (TA Instrument DSC 2920 Modulated DSC). The DSC was calibrated with indium standards. The samples had a dry weight of between 8 and 12 mg. Aluminium pans were used to contain the samples for the DSC experiment. All samples were examined under a pure nitrogen atmosphere. During testing, each of the PNVCL-VAc samples was ramped from 20 °C to 200 °C at a rate of 10 °C/min.

2.7. Phase transition determination

2.7.1. Cloud point measurement

The LCST of polymer solutions can be determined by using a visual cloud point method. A sealed glass test tube with 75 mm path length was filled with selected polymer solutions and placed in a

Table 1
Compositions of physically crosslinked xerogels, containing 0.1 wt% of Irgacure® 184 and 5, 10 and 20 wt% of VAc.

Polymer code	PNVCL (wt%)	VAc (wt%)	Irgacure® 184 (wt%)
B1	100	0	0.1
B2	95	5	0.1
B3	90	10	0.1
B4	80	20	0.1

thermo-stable bath. The temperature was increased manually at a rate of <1 °C per 2 min, after the temperature reached a few degrees below the pre-estimated cloud point temperature. The LCST was recorded at the temperature at which the sample began to show the initial signs of becoming turbid.

2.7.2. Differential scanning calorimetry

Differential scanning calorimetry studies were performed on all aqueous polymer solutions (TA Instrument DSC 2920 Modulated DSC). The DSC was calibrated with indium standards. The samples had a weight between 8 and 12 mg. Aluminium pans were used to contain the samples for the DSC experiment. All samples were examined under a pure nitrogen atmosphere. All samples were ramped from 10 °C to 60 °C at a rate of 1 °C/min. The results were plotted as a function of heat flow (W/g) against temperature (°C).

2.7.3. UV-spectroscopy

The LCST behaviour of samples was also investigated using a UV-spectroscopy synergy HT BioTek plate reader. The transmittance of samples in aqueous polymer solutions was measured at 500 nm at intervals of 1 °C in the range of 25–44 °C. The solution was allowed to equilibrate at each temperature for 20 min before the transmittance was measured.

2.8. Swelling studies

After photopolymerisation the samples were placed in a vacuum oven for 24 h at 40 °C and the apparent dry weights (Wd) were measured. The samples were tested at room temperature (<20 °C) and 40 °C, below and above the LCST. Samples were placed in 50 mL of distilled water to determine their swelling ratio. The percentage of gel swelling was calculated using Eq. (1). All reported swelling studies were measured in distilled water. Tests were carried out in quintuplicate below and above LCST and the data was presented as mean ± SD.

$$\text{Swelling Ratio}\ (\%) = (\text{Wt}-\text{Wd}/\text{Wd})*100 \quad (1)$$

where Wt and Wd are the weights of the gels in the swelling state and the dried state, respectively.

2.9. Sol-gel transition

2.9.1. Tube inversion method

Aqueous polymer solutions (1 mL) of all samples were placed in 10 mm diameter glass tubes. Samples were kept at constant temperature for 10 min in a thermostated bath before inverting the tube at intervals of 1 °C. Before switching to the next temperature, the samples were cooled in an ice-water bath until the polymer solution became homogeneous. Gelation temperature was accounted as the temperature at which the polymer solution did not flow by inverting the tube.

2.9.2. Rheological testing

Dynamic rheological tests were conducted on aqueous polymer solutions with an Advanced rheometer AR 1000 (TA Instruments) fitted with a Peltier temperature control. The instrument was calibrated for inertia and mapped before use in all cases. The geometry used in this analysis was a 4 cm diameter cone steel plate. Aqueous polymer solutions of 1.5 mL were pipetted onto the Peltier plate. The sample gap was set at 0.5 mm for the studies carried out. To determine the phase transition temperature of the selected sample solutions, temperature ramp tests were performed. In this study the storage modulus (G′) and loss modulus (G″) were examined with change in temperature from 20 to 50 °C at the rate of 1 °C/min. Tests were conducted at 0.5% controlled strain which was within the linear viscoelastic region of the material and this was determined by stress sweep analysis.

3. Results and discussion

3.1. Preparation of samples

Accompanying the accelerated growth of biomedical technology, polymers that have the ability to be prepared under bio-friendly conditions are urgently needed. Ko et al. [21] reported that considering biomedical applications, the polymerisation involving high temperature or toxic metals should be avoided [21]. Therefore a more appealing method of polymer synthesis, namely photopolymerisation is considered in this study. Physically crosslinked polymers based on NVCL were synthesised *via* photopolymerisation by incorporating VAc at 5, 10 and 20 wt% along with 0.1 wt% Irgacure® 184 photoinitiator. Concentration levels of the photoinitiator were kept at 0.1 wt% as previous studies have shown that minimising photoinitiator concentration levels serve to enhance biocompatibility of the polymer [22]. All samples were optically transparent indicating that the polymers are amorphous and the chains sorted in a random fashion (Fig. 1) [23].

3.2. Attenuated total reflectance Fourier transform infrared spectroscopy

NVCL monomer and NVCL-VAc based copolymers were analysed using ATR-FTIR to determine if polymerisation had occurred. Prior to analysis, all samples were dried in a vacuum oven at 40 °C for 24 h. In the NVCL monomer spectrum (Fig. 2), a C═C band was recognised at 1655 cm^{-1}. Further characteristic signals of NVCL were detected for the amide group (C═O) at 1622 cm^{-1}, while the C—C for the aliphatic group in the caprolactam ring was observed at 1438 cm^{-1} in accordance with literature [4,24]. The stretching and bending vibrational bands of the C—H bond in the vinyl group (═CH and $=CH_2$) were observed at 3108 cm^{-1} and 989 cm^{-1}, respectively. For successful polymerisation of NVCL, the bands corresponding to the C═C and the C—H bond in the vinyl group of the NVCL monomer should disappear, as was the case in this study. PNVCL absorbs moisture which corresponds to the broad band at ~3400 cm^{-1} relates to the O—H stretching, this is associated with the polymers hydrophilic character. These

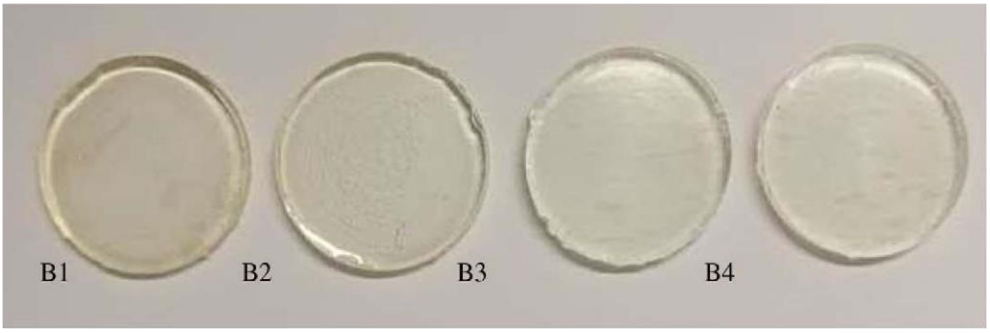

Fig. 1. PNVCL based samples were optically transparent where increasing the concentration of VAc slightly increased he transparency of the sample.

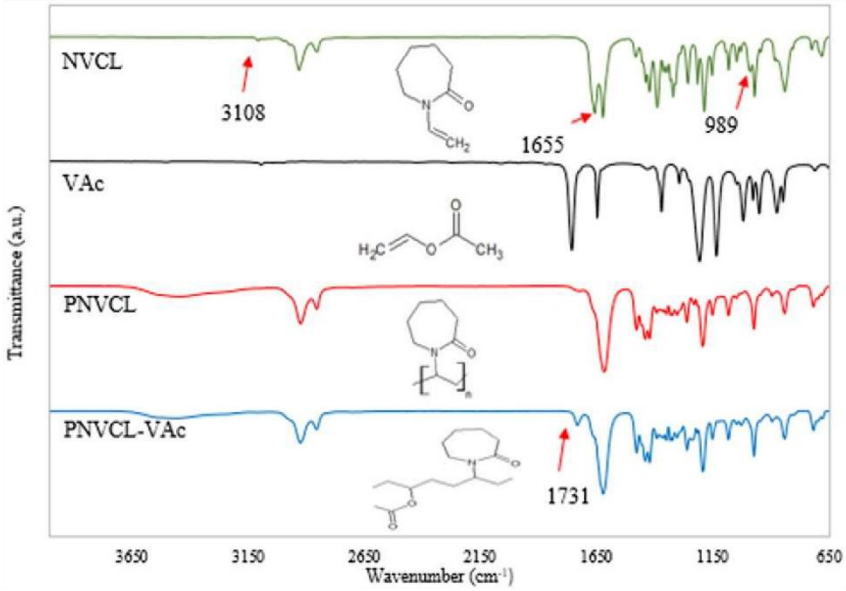

Fig. 2. FTIR spectra of NVCL, VAc, PNVCL and PNVCL-VAc copolymer (B4). Arrows mark the characteristics peaks of NVCL and additionally peak of VAc in samples B4.

findings correspond with other studies that involved successful polymerisation of PNVCL [4,14,24].

The PNVCL-VAc spectra exhibited new bands not typically associated with PNVCL, which indicates that the copolymer reaction successfully took place as represented in Fig. 2. One such band occurred at 1731 cm^{-1} which corresponds to the C═O stretching of the aliphatic ester group of VAc [25]. The C═O of the aliphatic ester group increased in intensity as the concentration of VAc increased in the samples. The wavelength at ~3400 cm^{-1} (O—H groups) exhibited a decrease in intensity at higher VAc loadings, corresponding to the more hydrophobic nature of VAc. Table 2 presents a summary of the bands obtained for NVCL and the novel copolymers synthesised.

The characteristic bands of PNVCL were also observed in the spectra of the copolymers, however there was no significant shift in the characteristic bands for samples B1-B4. For example, PNVCL C—N and —CH2 functional groups displayed no shift in position when it is compared with the addition of Vac. Similar finding was found when comparing NVCL and PNVCL where the changes in the conformation of the molecules and interaction of molecules upon polymerisation [26].

3.3. Nuclear magnetic resonance

Nuclear magnetic resonance was performed to further validate the findings of the FTIR analysis. As Fig. 3 showing, the polymer structures were characterised by ^{1}H NMR. The copolymer composition can be calculated from the integral data e, h and n assigned as indicated in Fig. 3.

Table 2
FTIR bands for NVCL and the novel copolymers synthesised.

Functional group	Shift (cm^{-1})				
	NVCL	B1	B2	B3	B4
Aliphatic C—H	2930,2853	2924,2854	2924,2855	2924,2856	2924,2857
Ketone C═O	1622	1617	1619	1920	1920
C—N	1481	1477	1477	1477	1477
—CH2	1438	1440	1440	1440	1440
C═C	1655	–	–	–	–
═CH and CH2	3108,989	–	–	–	–
O—H	–	3443	3432	3464	3457
Ester C═O	–	–	1731	1732	1732

The following equations (Eqs. (3-1)–(3-4)) demonstrate the calculating process:

$$m = e/3 \quad (3-1)$$

$$n = h/2 \quad (3-2)$$

$$VAc\% = m/(m+n) \times 100\% \quad (3-3)$$

$$PNVCL\% = n/(m+n) \times 100\% \quad (3-4)$$

The ^{1}H NMR spectrum of copolymer samples can be seen in Fig. 4. Fig. 4 shows, that the VAc% increased from B1 (100 NVCL) (0%) to B2 (95 NVCL-5VAc) as about 10%, and B3 (90 NVCL-10VAc) as about 16%. Qian et al. examined the chemical structure of PNVCL and copolymers by ^{1}H NMR, which found new resonance signals attributed to the protons of the addition of copolymers [27]. This is a further confirmation that polymerisation occurred [27–29].

3.4. Gel permeation chromatography

The release characteristics of polymer drug delivery systems is an important aspect and one such factor affecting the release rate of an entrapped drug is particle size. It is well known that it is possible to change the release rate of a drug by changing the copolymer composition as well as molecular weights of the polymer [30]. Table 3 summarises the results obtained for the molecular number (M_n), molecular weight (M_w) and polydispersity (PDI) of the samples. GPC analysis indicates that the M_w of PNVCL is 3932 g mol^{-1}. Altering the composition of NVCL and VAc during photopolymerisation resulted in an increase in the M_w and M_n, providing further evidence that a copolymerisation reaction has taken place. The LCST behaviour of PNVCL is known to be influenced by the M_w [31,32]. For example, increases in M_w have been reported to result in decreased LCST which has been attributed to an increase in the polymer hydrophilicity [3], and this is further investigated in Section 3.6.

The release rate of a drug can be affected by the M_w and composition of the polymer. Increase in the M_w of the polymer contributes to the decrease of the drug released. This is most likely as an increase in M_w increases the hydrophilicity of the polymer. Adjusting the M_w of a polymer it is possible to con rol the release rate of a drug. Mittal et al.

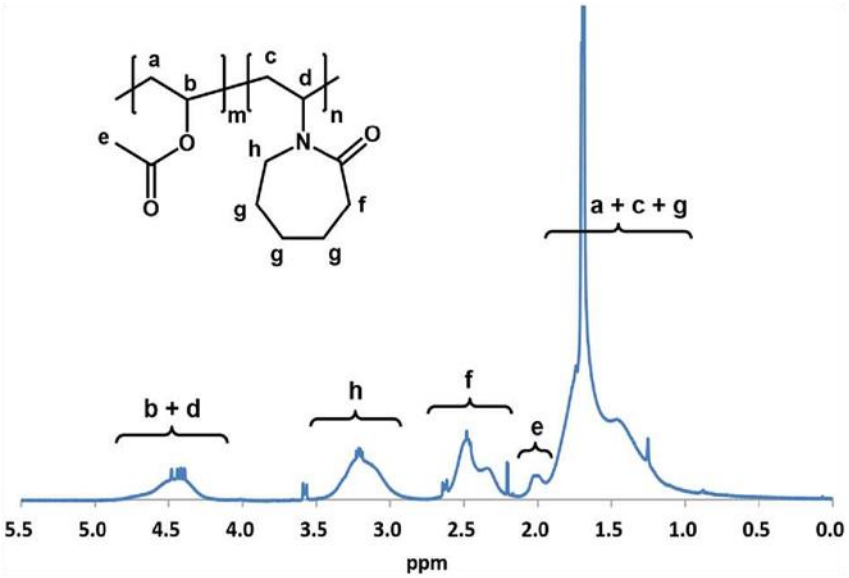

Fig. 3. ^{1}H NMR spectrum for the PNVCL-VAc copolymer in $CDCl_3$.

studied the effects of adjusting the M_w on the release behaviour of PLGA. Results showed drug release *in vitro* decreased with increase in M_w of poly (lactide-*co*-glycolide) (PLGA) [33]. Controlling the composition of polymer and copolymer is another possible way to control the release rate of a drug. Li et al. studied poly (ethylene glycol)–poly (lactide-*co*-glycolide) (PEG–PLGA) copolymers Doxorubicin (DOX), loaded into micelles through nanoprecipitation. The *in vitro* release behaviour could be adjusted by regulating the composition of the copolymer [34].

3.5. Differential scanning calorimetry

Studies of PNVCL have focused almost entirely on its behaviour in aqueous media with far fewer studies been done on the polymer in the solid state. Differential scanning calorimetry measurements were conducted over a temperature range of 20–200 °C for all samples. One broad transition was observed between 60 and 150 °C for all the NVCL based polymers and this transition was identified as the glass transition temperature (T_g). Table 4 summarises the glass transition results for each of the samples analysed. The T_g of a polymer is a distinguishing aspect in the design of a controlled drug delivery system. Lebedev et al. [35] reported a T_g for PNVCL at 147 °C while Meeussen et al. [36] reported a T_g of 145 °C [35,36]. For PNVCL homopolymer developed in this study, the T_g was determined to be approximately 110.7 °C (Fig. 5).

Difference in T_g compared to the literature can be associated with various factors though molecular weight is often cited as one of the major contributors [37]. The T_g of NVCL based copolymers was found to be dependent on the incorporation level of VAc, whereby increasing the composition lead to a decrease in glass transition value. This indicates that the incorporation of VAc has a plasticising effect on PNVCL. This is likely due to the VAc low molecular weight (86.09 g mol^{-1}) allowing greater flexibility in the polymers chains resulting in lowered T_g.

3.6. Phase transition determination

The LCST of temperature-responsive polymers plays a key role in designing a targeted drug delivery system, as the phase transition

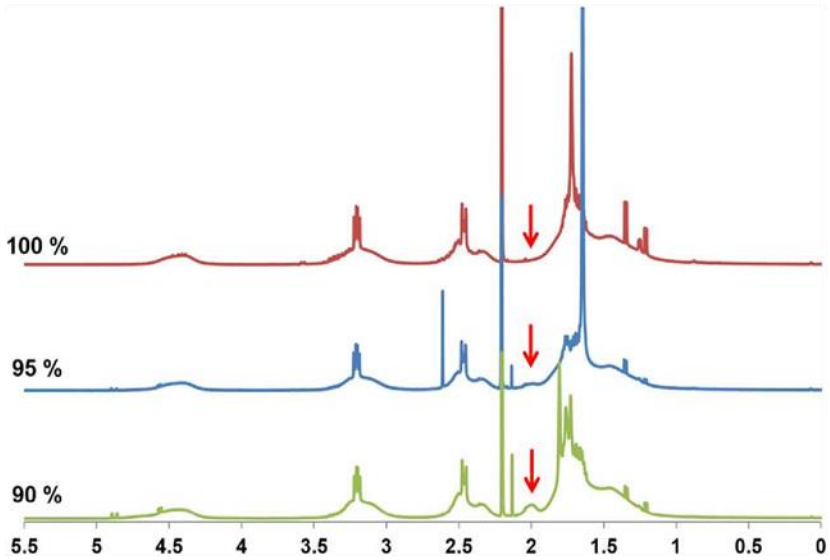

Fig. 4. ^{1}H NMR spectrum of different polymerisations of PNVCL-VAc copolymers. The arrows highlight the characteris ic peak attributed to the acetate.

Table 3
Molecular number (M_n), molecular weight (M_w) and polydispersity (PDI) results for NVCL based samples.

Sample	M_n	M_w	PDI
B1	388	3932	10.13
B2	2253	28,376	12.59
B3	2516	76,164	30.27

Table 4
Glass transition temperatures recorded for NVCL based samples.

Sample code	B1	B2	B3	B4
T_g values (°C)	110.74	103.33	91.21	75.61

temperature is the point at which the drug can be released [38]. The most important factors affecting the phase transition of PNVCL are M_w, copolymer composition and concentration in aqueous media. The LCST is expected to decrease with increasing polymer molecular weight based on the changes in the polymer solvent interaction. In this section, phase transition was measured by employing four techniques to determine the LCST (Table 5). By utilising each of these techniques, common trends were established, for example the LCST was found to be influenced by the monomeric feed ratio and the polymer concentration in solution at fixed molecular weight of PNVCL. The incorporation of a more hydrophobic monomer (VAc) to NVCL resulted in a decrease in the LCST, whereby the polymers developed in this study have LCST's in the range 26.2–34.5 °C (Table 5), which would be very favourable for potential biomedical thermogelling applications.

3.6.1. Cloud point measurements

Visual observation of LCST was initially employed to establish the phase transition behaviour. This testing was carried out to ascertain the range of LCST's for PNVCL based copolymers prior to more sophisticated phase transition testing. Cloud point was defined as the temperature at which the first sign of turbidity occurred in the solution [39]. Samples showed a reversible phase transition in water which was in agreement with literature [3]. The opaque solution slowly changed back to the transparent colourless solution as the temperature reduced.

Table 5
LCST of NVCL based samples which were established using cloud point, UV-spectrometry, DSC and rheological analysis.

Sample code	Cloud point (°C)	UV-spectrometry (°C)	DSC (°C)	Rheological analysis (°C)
B1 (3 wt%)	32 ± 0.5	32.4	32.5	31.6
B1 (5 wt%)	32 ± 0.5	32.5	32.7	32.3
B1 (10 wt%)	33 ± 0.5	33.4	34.5	33.5
B2 (10 wt%)	32 ± 0.5	31.4	32.4	32.9
B3 (10 wt%)	30 ± 0.5	29.4	30.8	29.2
B4 (10 wt%)	27 ± 0.5	26.4	26.2	26.2

It has been suggested that at a certain temperature, water becomes a poor solvent to the polymer, possibly due to the new and less polar polymer conformation, causing the prevalence of the polymer-polymer interaction and the growth of the polymer aggregates leading to phase separation [40]. As can be seen in Table 5, the cloud point analysis of copolymer samples resulted in a decrease in LCST with increased VAc incorporation during photopolymerisation.

3.6.2. Differential scanning calorimetry

Differential scanning calorimetry was also used to analyse the LCST behaviour. For PNVCL, Ferraz et al. [13] reported a LCST of 33–36 °C, while Shi & Zhang reported a LCST of around 32 °C. In this study, one transition was identified during the heating scan between 32 and 35 °C for all homopolymer samples and this transition was related to the LCST, which is in accordance with the values achieved by the previous authors [13,41]. In all cases the onset value of the endothermal peak was used to establish the LCST value. The relatively strong hydrogen bonds formed between water molecules and N—H or C═O groups in dilute solutions, become weaker and break as temperature is raised, resulting in the endothermic heat of phase separation [42]. Illustrated in Fig. 6 is a thermogram for PNVCL homopolymer (10 wt%) solution, where the onset value recorded was 34.5 °C. However, in some cases it was found there was a difference of over 2 °C between the calorimetric peak and onset values. It is understood that a small portion of the gel starts to undergo its phase transition at the onset temperature, while the majority experience the transition at the peak value [39,43]. The incorporation of VAc during polymerisation resulted in a decrease in the LCST (Table 5).

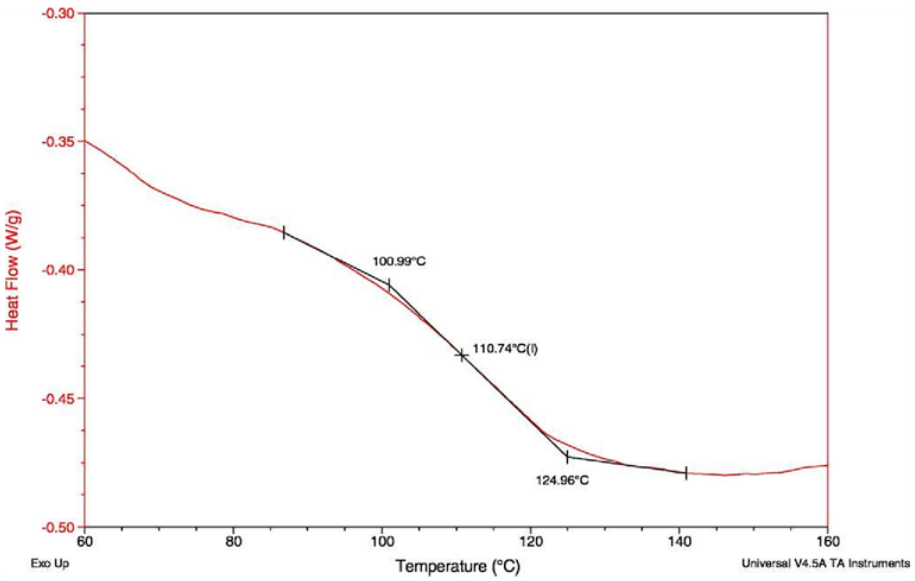

Fig. 5. A representative thermogram illustrating the glass transition of PNVCL homopolymer.

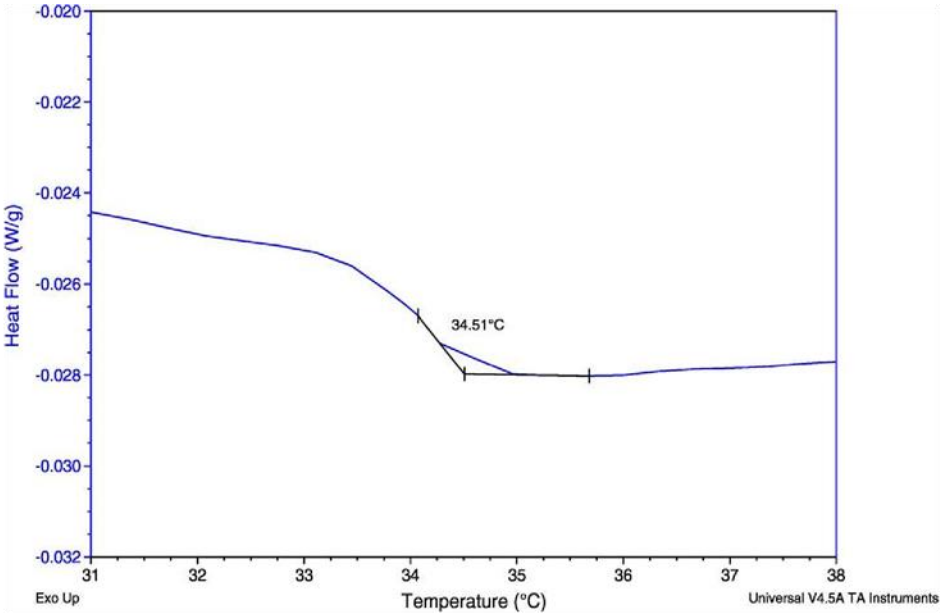

Fig. 6. A representative thermogram illustrating the LCST of PNVCL homopolymer (10 wt%) aqueous solution.

3.6.3. UV-spectrometry

Aqueous solutions of PNVCL homopolymer (3 wt%) and (10 wt%) were also investigated using UV-spectrometry. All samples were analysed over a temperature range of 25–44 °C. The image confined within Fig. 7 illustrates the phase transition behaviour of PNVCL, notable by the change in its optical transparency below (left) and above (right) the LCST. At temperatures below the LCST, PNVCL solution is transparent and colourless, while above the LCST the solution is opaque. The phase transition temperature obtained for PNVCL was within the range reported in previous observations [4,13,41]. Concentration affects the LCST due to the water content increasing the hydrogen bonding interactions among water and the polymer, which requires more thermal energy to break the water structure, resulting in an increase in the LCST. Furthermore, phase transitions of all NVCL-VAc copolymers were measured, with the LCST found to decrease almost linearly with increasing concentration of VAc.

3.7. Swelling studies

Negative temperature sensitive polymers have been proposed as smart solid dosage forms whereby active agent can be incorporated directly during polymerisation. Photopolymerisation is particularly suitable for development of such drug delivery systems as it is a quick and relatively mild form of polymerisation where no extremes of temperatures or toxic solvents are required. Swelling is one of the most important factors in controlling the release mechanisms for drug delivery systems [37]. Swelling studies were carried out on all samples above and below the LCST as was determined by previous phase transition experiments. At 1-hour time intervals, samples were removed from the swelling distilled water and blotted with filter paper to absorb excess water on surface, and then the samples were weighed. Fresh, distill water was preheated to the required temperature, before submerging the samples into distilled water. Graphical results are exhibited in Figs. 8 and 9 which display the polymer swelling behaviour below and above LCST. For samples below LCST, the maximum swollen weight had been reached after 1 h for all samples. Subsequent to maximum swollen weight being achieved, the polymer started to break down. After 6 h, the polymers had lost their structure and could not be weighed.

Contrasting swelling behaviour was observed for the PNVCL samples above LCST; within 6–24 h the peak swelling was achieved. Swelling studies were performed until the maximum swollen weight of the

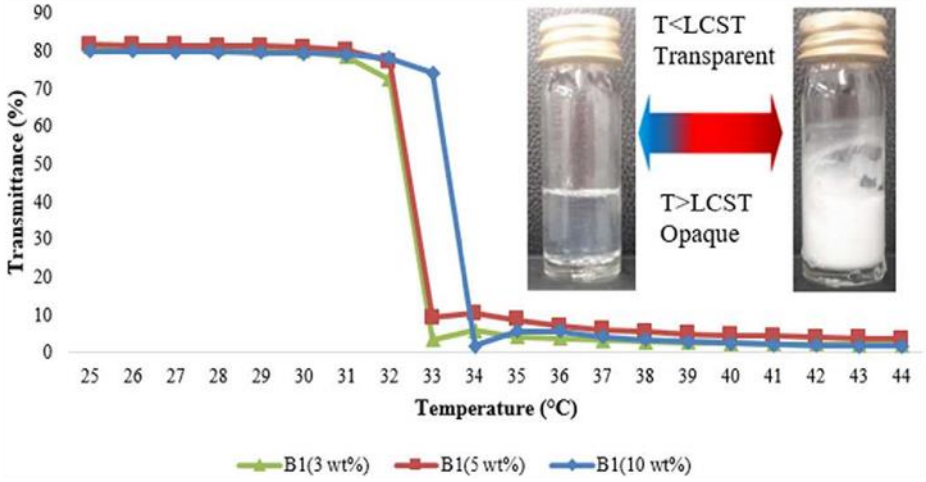

Fig. 7. UV-spectrometry analysis which illustrates the LCST of PNVCL homopolymer at different aqueous solution concentrations.

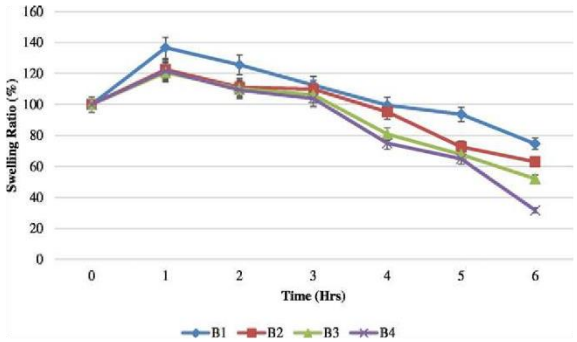

Fig. 8. Swelling behaviour of PNVCL based samples tested below LCST at 20 °C.

sample was achieved. When the temperature is below LCST, the hydrogen-bonding of the hydrophilic segments dominates the interaction between water and the polymer chains thus the polymer absorbs water which leads to the dissolution of polymer chains. When the temperature increases above the LCST, the polymer chains shrink and expel water molecules through hydrophobic segments, which results in the precipitation of polymer and a globular state appears [6]. Controlled swelling is required for tissue engineering and drug delivery which is influenced by the dissolution behaviour of the polymer [23,43].

3.8. Sol-gel transition

Thermogelling polymers that undergo sol-gel transition have proven to be appealing in biomedical fields particularly in potential drug delivery and injectable tissue engineering applications [37,39]. Injectable, *in situ* setting semi-solid drug depots are being established as alternative delivery systems [48]. Polymers with a sol-gel transition between room temperature and body temperature are predicted to be the most beneficial [49]. Thermogelling systems can comprise of drugs or cells and such systems aid in delivery to a desired site. During the sol-gel transition, all of the ingredients in the system form a matrix, whereby drugs can be released in a controlled manner [21]. In this section, sol-gel transition was measured using the tube inversion method and rheological analysis. Samples synthesised in this study had sol-gel transitions within the range 33.6–47.1 °C (Table 6). These novel copolymers could potentially be used as thermogelling systems, which should have a LCST below 37 °C so that the materials could undergo gelation when injected into the body [14,41].

Table 6
Sol-gel transition temperatures for PNVCL based samples which were established using tube inversion method and rheological analysis.

Sample code	Tube inversion method (°C)	Rheological analysis (°C)
B1 (3 wt%)	47.1 ± 0.5	45.8
B1 (5 wt%)	42.6 ± 0.5	42.7
B1 (10 wt%)	37.3 ± 0.5	37.6
B2 (10 wt%)	35.2 ± 0.5	35.9
B3 (10 wt%)	34.3 ± 0.5	34.2
B4 (10 wt%)	34.0 ± 0.5	33.6

3.8.1. Tube inversion method

The tube inversion technique was used in determining the sol-gel transition of all samples (3 wt% and 10 wt% aqueous solutions), within the range of 20–50 °C. At temperatures below the sol-gel transition, PNVCL remained as a colourless solution, while above the sol-gel transition the polymer transformed into a gel. Concentration affected the sol-gel transition, whereby increasing the concentration resulted in a decrease in the sol-gel transition temperature. Incorporating VAc during photopolymerisation also resulted in a decrease in the temperature of the thermogelling transition.

3.8.2. Rheological analysis

Dynamic temperature ramp tests were performed on all samples (3 wt% and 10 wt% aqueous solutions), where G′ and G″ were measured as a function of the temperature within the range 20–50 °C (Fig. 10). For the samples analysed in this work, the onset temperature for the LCST is marked with the arrow (↓) [51]. It is known that the elastic component (G′) dominates the LCST when it first responds and is more sensitive to temperature change than the loss modulus (G″) [52]. As the LCST is approached, the values for G′ (●) and G″ (○) increased until G′ and G″ were equal and this point is known as the sol-gel transition temperature [53,54]. The sol-gel transition temperature has a tendency to decrease when the concentration of polymer in solution is increased [54]. According to Fig. 10 marked with the arrow (↑), the sol-gel transition temperature for PNVCL homopolymer B1 (3 wt%) was 47 °C. The image confined within Fig. 10 illustrates the sol-gel transition behaviour for PNVCL; the LCST is the point at which the polymer changes colour but is still in solution (middle) and above the sol-gel transition (right) the sample has solidified. While reviewing the results for PNVCL homopolymer, increasing the concentration leads to a decrease in the gelling temperature, while incorporation of VAc also resulted in a decrease in LCST. The systems developed have the potential to gel at about 3–7 °C above the LCST depending on Vac incorporation level during photopolymerisation. The gelling point of the homopolymer (3–10 wt%

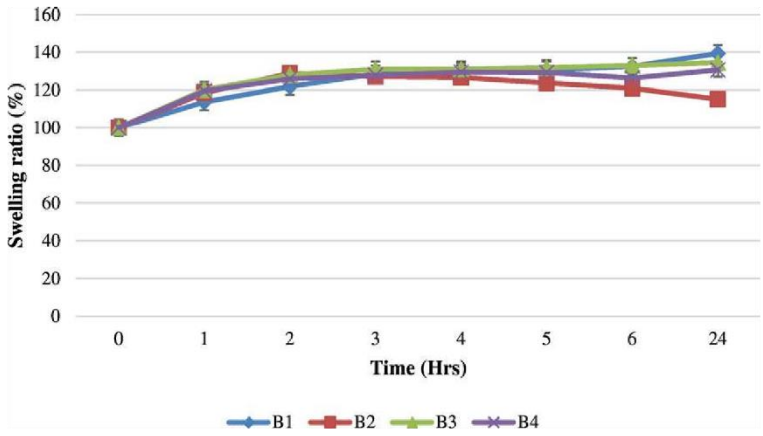

Fig. 9. Swelling behaviour of PNVCL based samples tested above LCST at 40 °C.

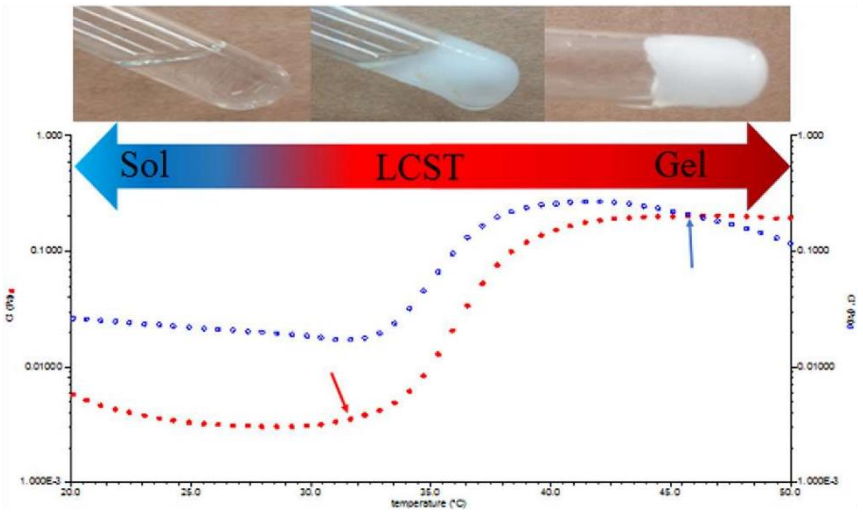

Fig. 10. A representative graph of G′ (●) and G″ (○) for PNVCL homopolymer (3 wt% aqueous solution). The onset temperature for the LCST is marked as the arrow (↓). The sol-gel transition temperature is marked as the arrow (↑) where G′ and G″ are equal.

in solution) was above 37 °C. Importantly all copolymers (10 wt% in solution) gelled between 33.6 and 35.9 °C. These novel copolymers could potentially be used as an injectable *in situ* forming drug delivery systems for local delivery of drug [48].

4. Conclusion

In summary, successful polymerisation of NVCL-VAc was achieved resulting in physical crosslinked polymers. This was confirmed with data *via* FTIR, NMR and GPC. The LCST was determined by employing four different approaches; optical cloud point, UV-spectroscopy, DSC and rheometry. This study allows much greater understanding of the LCST phase and sol-gel transition of novel PNVCL based copolymer systems, which were influenced by the concentration and monomeric feed ratio. The LCST of PNVCL was determined to be within the range of 31.–34.5 °C depending upon the polymer concentration in aqueous media. Also, copolymers exhibited a decrease in phase transition within the range of 26.2–32.9 °C. Sol-gel transition was determined to be within the range 33.6–47.1 °C, which was dependent on the concentration and composition. LCST and sol-gel transitions for PNVCL-VAc based samples were controlled by altering the monomeric feed ratio and concentration in aqueous solution, and based on the findings of this study have potential to be used as thermogelling systems in drug delivery applications.

References

[1] Y. Qiu, K. Park, Environment-sensitive hydrogels for drug delivery, Adv. Drug Deliv. Rev. 64 (2012) 49–60, http://dx.doi.org/10.1016/j.addr.2012.09.024.
[2] E.S. Gil, S.H. Hudson, Stimuli-reponsive polymers and their bioconjugates, Prog. Polym. Sci. 29 (2004) 1173–1222, http://dx.doi.org/10.1016/j.progpolymsci.2004.08.003.
[3] Q. Wu, L. Wang, X. Fu, X. Song, Q. Yang, G. Zhang, Synthesis and self-assembly of a new amphiphilic thermosensitive poly(N-vinylcaprolactam)/poly(e-caprolactone) block copolymer, J. Polym. Res. (2014) 1–18, http://dx.doi.org/10.1007/s00289-013-1041-x.
[4] B. Lee, A. Jiao, S. Yu, J.B. You, D.-H. Kim, S.G. Im, Initiated chemical vapor deposition of thermoresponsive poly(N-vinylcaprolactam) thin films for cell sheet engineering, Acta Biomater. 9 (2013) 7691–7698, http://dx.doi.org/10.1016/j.actbio.2013.04.049.
[5] A. Imaz, J. Forcada, Optimized buffered polymerizations to produce N-vinylcaprolactam-based microgels, Eur. Polym. J. 45 (2009) 3164–3175, http://dx.doi.org/10.1016/j.eurpolymj.2009.08.003.
[6] X. Li, H. Zhong, X. Li, F. Jia, Z. Cheng, L. Zhang, J. Yin, L. An, L. Guo, Synthesis of attapulgite/N-isopropylacrylamide and its use in drug release, Mater. Sci. Eng. C. Mater. Biol. Appl. 45 (2014) 170–175, http://dx.doi.org/10.1016/j.msec.2014.08.056.
[7] L.M. Geever, C.C. Cooney, J.G. Lyons, J.E. Kennedy, M.J.D. Nugent, S. Devery, C.L. Higginbotham, Characterisation and controlled drug release from novel drug-loaded hydrogels, Eur. J. Pharm. Biopharm. 69 (2008) 1147–1159, http://dx.doi.org/10.1016/j.ejpb.2007.12.021.
[8] C.G. Williams, A.N. Malik, T.K. Kim, P.N. Manson, J.H. Elisseeff, Variable cytocompatibility of six cell lines with photoinitiators used for polymerizing hydrogels and cell encapsulation, Biomaterials 26 (2005) 1211–1218, http://dx.doi.org/10.1016/j.biomaterials.2004.04.024.
[9] J. Akimoto, M. Nakayama, T. Okano, Temperature-responsive polymeric micelles for optimizing drug targeting to solid tumors, J. Control. Release 193 (2014) 2–8, http://dx.doi.org/10.1016/j.jconrel.2014.06.062.
[10] N. Rapoport, Physical stimuli-responsive polymeric micelles for anti-cancer drug delivery, Prog. Polym. Sci. 32 (2007) 962–990, http://dx.doi.org/10.1016/j.progpolymsci.2007.05.009.
[11] N.K. Singh, D.S. Lee, In situ gelling pH- and temperature-sensitive biodegradable block copolymer hydrogels for drug delivery, J. Control. Release 193 (2014) 214–227, http://dx.doi.org/10.1016/j.jconrel.2014.04.056.
[12] X.-M. Liu, L.-S. Wang, L. Wang, J. Huang, C. He, The effect of salt and pH on the phase-transition behaviors of temperature-sensitive copolymers based on N-isopropylacrylamide, Biomaterials 25 (2004) 5659–5666, http://dx.doi.org/10.1016/j.biomaterials.2004.01.019.
[13] C.C. Ferraz, G.H.C.C. Varca, J. Ruiz, P.S. Lopes, M.B. Mathor, A.B. Lugão, E. Bucio, Radiation-grafting of thermo- and pH-responsive poly(N-vinylcaprolactam-co-acrylic acid) onto silicone rubber and polypropylene films for biomedical purposes, Radiat. Phys. Chem. 97 (2014) 298–303, http://dx.doi.org/10.1016/j.radphyschem.2013.12.027.
[14] K. Madhusudana Rao, B. Mallikarjuna, K.S.V. Krishna Rao, S. Siraj, K. Chowdoji Rao, M.C.S. Subha, Novel thermo/pH sensitive nanogels composed from poly(N-vinylcaprolactam) for controlled release of an anticancer drug, Colloids Surf. B: Biointerfaces 102 (2013) 891–897, http://dx.doi.org/10.1016/j.colsurfb.2012.09.009.
[15] A. Theis, T.P. Davis, M.H. Stenzel, C. Barner-Kowollik, Probing the reaction kinetics of vinyl acetate free radical polymerization via living free radical polymerization (MADIX), Polymer (Guildf). 47 (2006) 999–1010, http://dx.doi.org/10.1016/j.polymer.2005.12.054.
[16] T. Don, C. King, W. Chiu, C. Peng, Preparation and characterization of chitosan-g-poly(vinyl alcohol)/poly(vinyl alcohol) blends used for the evaluation of blood-contacting compatibility, Carbohydr. Polym. 63 (2006) 331–339, http://dx.doi.org/10.1016/j.carbpol.2005.08.023.
[17] K. Kolter, A. Dashevsky, M. Irfan, R. Bodmeier, Polyvinyl acetate-based film coatings, Int. J. Pharm. 457 (2013) 470–479, http://dx.doi.org/10.1016/j.ijpharm.2013.08.077.
[18] N.A. Cortez-Lemus, A. Licea-Claverie, Poly(N-Vinylcaprolactam), a Comprehensive Review on a Thermoresponsive Polymer Becoming Popular, 2015http://dx.doi.org/10.1016/j.progpolymsci.2015.08.001.
[19] A. Kermagoret, C.-A. Fustin, M. Bourguignon, C. Detrembleur, C. Jérôme, A. Debuigne, One-pot controlled synthesis of double thermoresponsive N-vinylcaprolactam-based copolymers with tunable LCSTs, Polym. Chem. 4 (2013) 2575, http://dx.doi.org/10.1039/c3py00134b.
[20] D. Wan, Q. Zhou, H. Pu, G. Yang, Controlled Radical Polymerization of N -Vinylcaprolactam Mediated by Xanthate or Dithiocarbamate, 2008 3–7, http://dx.doi.org/10.1002/pola.
[21] D. Ko, U. Shinde, B. Yeon, B. Jeong, Recent progress of in-situ formed gels for biomedical applications, Prog. Polym. Sci. 38 (2013) 672, http://dx.doi.org/10.1016/j.progpolymsci.2012.08.002.
[22] J.A. Killion, L.M. Geever, D.M. Devine, J.E. Kennedy, C.L. Higginbotham, Mechanical properties and thermal behaviour of PEGDMA hydrogels for potential bone regeneration application, J. Mech. Behav. Biomed. Mater. 4 (2011) 1219–1227, http://dx.doi.org/10.1016/j.jmbbm.2011.04.004.

[23] J.M.G. Cowie, V. Arrighi, Polymers: Chemistry and Physics of m o d e r n Materials, Third CRC Press, Boca Raton, 2007.
[24] S. Kozanoğlu, Polymerization and Characterization of N-Vinylcaprolactam, Middle East Technical University, 2008.
[25] N.S. Allen, M. Edge, M. Rodriguez, C.M. Liauw, E. Fontan, Aspects of the thermal oxidation of ethylene vinyl acetate copolymer, Polym. Degrad. Stab. 68 (2000) 363–371, http://dx.doi.org/10.1016/S0141-3910(00)00020-3.
[26] S. Kozanoğlu, T. Özdemir, A. Usanmaz, Polymerization of N-Vinylcaprolactam and characterization of poly(N-Vinylcaprolactam), J. Macromol. Sci. A 48 (2011) 467–477, http://dx.doi.org/10.1080/10601325.2011.573350.
[27] W. Qian, P. Xu, G. Lu, X. Huang, Synthesis of PAA- *g* -PNVCL graft copolymer and studies on its loading of ornidazole, Chin. J. Chem. 32 (2014) 1049–1056, http://dx.doi.org/10.1002/cjoc.201400472.
[28] X. Liang, V. Kozlovskaya, C.P. Cox, Y. Wang, M. Saeed, E. Kharlampieva, Synthesis and self-assembly of thermosensitive double-hydrophilic poly(*N*-vinylcaprolactam)-*b*-poly(*N*-vinyl-2-pyrrolidone) diblock copolymers, J. Polym. Sci. A Polym. Chem. 52 (2014) 2725–2737, http://dx.doi.org/10.1002/pola.27291.
[29] Q. Wu, L. Wang, X. Fu, X. Song, Q. Yang, G. Zhang, Synthesis and self-assembly of a new amphiphilic thermosensitive poly(N-vinylcaprolactam)/poly(ε-caprolactone) block copolymer, Polym. Bull. 71 (2013) 1–18, http://dx.doi.org/10.1007/s00289-013-1041-x.
[30] M.L. Hans, A.M. Lowman, Biodegradable nanoparticles for drug delivery and targeting, Curr. Opin. Solid State Mater. Sci. 6 (2002) 319–327.
[31] S.F. Medeiros, A.M. Santos, H. Fessi, A. Elaissari, Stimuli-responsive magnetic particles for biomedical applications, Int. J. Pharm. 403 (2011) 139–161, http://dx.doi.org/10.1016/j.ijpharm.2010.10.011.
[32] S. Schwarz, S.M. Ponce-Vargas, A. Licea-Claverie, C. Steinbach, Chitosan and mixtures with aqueous biocompatible temperature sensitive polymer as flocculants, Colloids Surf. A Physicochem. Eng. Asp. 413 (2012) 7–12, http://dx.doi.org/10.1016/j.colsurfa.2012.03.048.
[33] G. Mittal, D.K. Sahana, V. Bhardwaj, M.N.V. Ravi Kumar, Estradiol loaded PLGA nanoparticles for oral administration: effect of polymer molecular weight and copolymer composition on release behavior in vitro and in vivo, J. Control. Release 119 (2007) 77–85, http://dx.doi.org/10.1016/j.jconrel.2007.01.016.
[34] D. Li, H. Sun, J. Ding, Z. Tang, Y. Zhang, W. Xu, X. Zhuang, X. Chen, Polymeric topology and composition constrained polyether-polyester micelles for directional antitumor drug delivery, Acta Biomater. 9 (2013) 8875–8884, http://dx.doi.org/10.1016/j.actbio.2013.06.041.
[35] V.T. Lebedev, G. Török, L. Cser, G. Káli, A.I. Sibilev, Molecular dynamics of poly (N-vinylcaprolactam) hydrate, Appl. Phys. A Mater. Sci. Process. 74 (2002) s478–s480.
[36] F. Meeussen, E. Nies, H. Berghmans, S. Verbrugghe, E. Goethals, F. Du Prez, Phase behaviour of poly (N-vinyl caprolactam) in water, 41 (2000) 8597–8602.
[37] J. Siepmann, N.A. Peppas, Modeling of drug release from delivery systems based on hydroxypropyl methylcellulose (HPMC), Adv. Drug Deliv. Rev. 64 (2012) 163–174, http://dx.doi.org/10.1016/j.addr.2012.09.028.
[38] J.E. Chung, M. Yokoyama, M. Yamato, T. Aoyagi, Y. Sakurai, T. Okano, Thermoresponsive drug delivery from polymeric micelles constructed using block copolymers of poly (N-isopropylacrylamide) and poly (butylmethacrylate), J. Control. Release 62 (1999) 115–127.
[39] L.M. Geever, D.M. Devine, M.J.D. Nugent, J.E. Kennedy, J.G. Lyons, A. Hanley, C.L. Higginbotham, Lower critical solution temperature control and swelling behaviour of physically crosslinked thermosensitive copolymers based on N-isopropylacrylamide, Eur. Polym. J. 42 (2006) 2540–2548, http://dx.doi.org/10.1016/j.eurpolymj.2006.06.002.
[40] S. Aerry, A. De, A. Kumar, A. Saxena, D.K. Majumdar, S. Mozumdar, Synthesis and characterization of thermoresponsive copolymers for drug delivery, J. Biomed. Mater. Res. A 101 (2013) 2015–2026, http://dx.doi.org/10.1002/jbm.a.34476.
[41] H.-Y. Shi, L.-M. Zhang, Phase-transition and aggregation characteristics of a thermoresponsive dextran derivative in aqueous solutions, Carbohydr. Res. 341 (2006) 2414–2419, http://dx.doi.org/10.1016/j.carres.2006.06.015.
[42] L.M. Geever, C.M. Mínguez, D.M. Devine, M.J.D. Nugent, J.E. Kennedy, J.G. Lyons, A. Hanley, S. Devery, P.T. Tomkins, C.L. Higginbotham, The synthesis, swelling behaviour and rheological properties of chemically crosslinked thermosensitive copolymers based on N-isopropylacrylamide, J. Mater. Sci. 42 (2007) 4136–4148, http://dx.doi.org/10.1007/s10853-006-0912-z.
[43] C. Scherzinger, A. Schwarz, A. Bardow, K. Leonhard, W. Richtering, Cononsolvency of poly-N-isopropyl acrylamide (PNIPAM): Microgels versus linear chains and macrogels, Curr. Opin. Colloid Interface Sci. 19 (2014) 84–94, http://dx.doi.org/10.1016/j.cocis.2014.03.011.
[48] D. Chitkara, A. Shikanov, N. Kumar, A.J. Domb, Biodegradable injectable in situ depot-forming drug delivery systems, Macromol. Biosci. 6 (2006) 977–990, http://dx.doi.org/10.1002/mabi.200600129.
[49] S. Chen, H. Zhong, B. Gu, Y. Wang, X. Li, Z. Cheng, L. Zhang, C. Yao, Thermosensitive phase behavior and drug release of in situ N-isopropylacrylamide copolymer, Mater. Sci. Eng. C 32 (2012) 2199–2204, http://dx.doi.org/10.1016/j.msec.2012.05.052.
[51] J.K. Kim, H.W. Son, The rheological properties of polystyrene/poly(vinylmethylether) blend near the critical region and in the homogenous region, Polymer (Guildf). 40 (1999) 6789–6801, http://dx.doi.org/10.1016/S0032-3861(99)00030-0.
[52] M. Kapnistos, A. Hinrichs, D. Vlassopoulos, S.H. Anastasiadis, A. Stammer, B.A. Wolf, Rheology of a lower critical solution temperature binary polymer blend in the homogeneous, phase-separated, and transitional regimes, 9297 (1996) 7155–7163.
[53] D. Gupta, C.H. Tator, M.S. Shoichet, Fast-gelling injectable blend of hyaluronan and methylcellulose for intrathecal, localized delivery to the injured spinal cord, Biomaterials 27 (2006) 2370–2379, http://dx.doi.org/10.1016/j.biomaterials.2005.11.015.
[54] R. Asasutjarit, S. Thanasanchokpibull, A. Fuongfuchat, S. Veeranondha, Optimization and evaluation of thermoresponsive diclofenac sodium ophthalmic in situ gels, Int. J. Pharm. 411 (2011) 128–135, http://dx.doi.org/10.1016/j.ijpharm.2011.03.054.

Journal of Applied Polymer Science

Enhancing and controlling the critical attributes of poly (*N*-vinylcaprolactam) through electron beam irradiation for biomedical applications

Shane Halligan,[1] **Kieran Murray**,[2] **Michael Hopkins**,[1] **Ian Rogers**,[1] **John Lyons**,[1] **Olivier Vrain**,[3] **Luke Geever**[1]

[1]Applied Polymer Technologies Gateway, Materials Research Institute, Athlone Institute of Technology, Ireland
[2]CelgenTek part of the Zimmer Biomet Group, Ireland
[3]STERIS Applied Sterilization Technologies, Ireland
Correspondence to: L. Geever (E-mail: lgeever@ait.ie)

ABSTRACT: The primary aim of this body of work is to investigate the effect of an industrial scale electron beam sterilization process on novel PNVCL-based smart polymers. There is limited literature available that examines the effects of modifying PNVCL by electron beam irradiation, and as a means of potentially enhancing properties such as the lower critical solution temperature and mechanical behavior. Physically crosslinked poly(*N*-vinylcaprolactam)–vinyl acetate (PNVCL–VAc) copolymers were prepared by photopolymerization and were subsequently exposed to ionizing radiation via electron beam technology. The mechanical characteristics and phase transitions of the physically crosslinked PNVCL samples were tailored by controlling the electron beam irradiation dose. Importantly, PNVCL and PNVCL–VAc samples (5 wt % in solution) underwent a phase transition between 33.5 and 26.5 °C, following electron beam irradiation. Furthermore, all samples displayed a Young's modulus between 1024.3 and 1516.4 MPa depending on the addition of copolymer and electron beam irradiation dose. The industrial scale electron beam sterilization process proved successful in enhancing/modifying many key smart polymer properties, and this ability to formulate and sterilize in one step could prove a very attractive approach for many biomedical applications. © 2019 Wiley Periodicals, Inc. J. Appl. Polym. Sci. **2019**, *137*, 48639.

Received 21 May 2019; accepted 5 October 2019
DOI: 10.1002/app.48639

INTRODUCTION

Sterilization of smart polymer materials is oftentimes overlooked until later in the technology development phase of medical devices or controlled drug delivery systems. However, given that sterilization has been reported to have a considerable effect on smart polymer properties, it is critically important to consider its effects sooner rather than later in the research and development phase. This body of work involved collaboration with STERIS Applied Sterilization Technologies, who carried out all sterilization trials free of cost on their commercial scale electron beam equipment.

Sterilization is essential for any medical device to be used in the body. It prevents against any microorganisms infringing on the body's defense mechanisms.[1] Commonly employed sterilization techniques include steam, ethanol immersion, dry heat, ethylene oxide, and radiation sterilization. There are many physical and chemical methods of sterilization. Chemical sterilization avoids increased temperatures but has the disadvantages of lengthy degassing times, potentially toxic residues, and geometric changes in the materials. An efficient and appealing alternative to these techniques is radiation sterilization. Radiation-induced chemical alterations, crosslinking and/or chain shortening are dependent on the dose and compositional ratios of the incorporated polymers.[2] Electron beam irradiation is currently being used in commercial applications which provides many companies with an effective and efficient means of sterilization, and also of enhancing the properties and performance of polymers and other materials.

Although there are many studies on the use of electron beam technology to enhance the properties and performance of conventional polymers,[3–5] far fewer studies focus on the use of sterilization methods on stimuli responsive polymers. One such polymer which has the potential to benefit from electron beam technology is poly(*N*-vinylcaprolactam) (PNVCL) as the polymer molecular weight (M_w) strongly influences the lower critical solution temperature (LCST) behavior. This is due to PNVCL having a Type I Flory–Huggins miscibility behavior, which by increasing the chain length of the polymer, the position of the LCST shifts

toward lower temperature. [6]Therefore, an understanding of the changes induced by irradiation sterilization is essential in the design of temperature-responsive polymers. Electron beam is by far the fastest and most cost-effective sterilization technology in commercial use today. The electron beam can affect the characteristics of polymers by undergoing simultaneous scission and crosslinking; however, in most cases, one process will dominate. Crosslinking can enhance the mechanical, thermal, and chemical properties, along with environmental and radiation stabilities. The ability to enhance polymer properties via irradiation processes has gained increased attention in the biomedical industry recently.[6,7]

Currently, there are a number of studies centered on altering the phase transition of PNVCL by the incorporation of hydrophilic and hydrophobic segments into PNVCL polymer matrix.[8,9] However, it is important to note that little information exists on the electron beam irradiation of PNVCL,[10,11] and current studies focus only on relatively low radiation doses. The current study focuses on PNVCL-based samples utilizing electron beam doses ranging from 0 to 50 kGy. By accurately controlling the electron beam dose rate, it is hoped that properties such as phase transition, mechanical properties, and swelling behavior could be manipulated and controlled.

EXPERIMENTAL SECTION

Materials

N-Vinylcaprolactam (NVCL) was obtained from Sigma-Aldrich Ireland Ltd. with a M_w of 139.19 g mol^{-1} and storage temperature of 2–8 °C. 1-hydroxycyclohexyl phenyl ketone (Irgacure 184) was used as a photoinitiator to initiate the reaction of free-radical polymerization. Vinyl acetate (VAc) monomer was obtained from Sigma-Aldrich Ireland Ltd. with a M_w of 86.09 g mol^{-1}.

Polymer Synthesis. The polymers investigated in this study were prepared by free-radical polymerization using ultraviolet (UV) light. These polymers were synthesized via physical crosslinking using a UV curing system (Dr Gröbel UV-Electronik GmbH) according to the previously reported procedure. [1–4] This particular irradiation chamber is a controlled radiation source with 20 UV-tubes that provide a spectral range of between 315 and 400 nm (UV-A radiation) at an average intensity of 10–13.5 mW/cm^2. The solutions were pipetted into silicone molds that contained disc and dumbbell specimen impressions. The composition of the samples synthesized is listed in Table I. All samples/xerogels were cured in a silicone mold and, before use, dried for 24 h in a vacuum oven at 40 °C. A xerogel is a solid formed from a gel by drying with unhindered shrinkage.

Table I. Compositions of Physically Crosslinked Xerogels, Containing 0.1 wt % of Irgacure 184 and 10 wt % of VAc

Polymer code	NVCL (wt %)	VAc (wt %)	Irgacure 184 (wt %)
PNVCL	100	0	0.1
PNVCL-VAc	90	10	0.1

Vacuum Packing. Vacuum packing was conducted on virgin PNVCL and PNVCL–VAc. In this section, only the tensile specimens and granules were vacuum packed. Vacuum packing was performed to ensure the samples were contained in a controlled environment. The sample size, weight, and orientation remained the same for all samples to facilitate consistency during the electron beam irradiation process.

Electron Beam Irradiation. A MEVEX high-energy electron beam irradiator was used to irradiate vacuum packed PNVCL and P(90 NVCL–10VAc) ASTM G49-85(2011) testing specimens, disc, and granules, at doses of 5, 25, and 50 kGy. The dose rate was approximately half of the total kGy per pass on each side to accomplish a uniform irradiation dose at room temperature. All samples were irradiated at room temperature at the STERIS facility (Tullamore, Ireland). All samples were exposed for about 5 s per pass. The period between the first and second pass was between 250 and 260 s. Each of the aforementioned times was calculated and evaluated by STERIS Applied Sterilization Technologies personnel. The nonirradiated samples served as a baseline for each of the results.[5,6]

Preparation of Aqueous Solutions. Homogeneous solutions of each sample were prepared by weighing appropriate amounts of the xerogels and distilled water (5 wt %), leaving these mixtures for a period of hours/days until completely dissolved. These aqueous solutions were produced for subsequent use in phase transition measurements.

Characterization Methods

Attenuated Total Reflectance Fourier Transform Infrared Spectroscopy. Attenuated total reflectance Fourier transform infrared (ATR–FTIR) spectroscopy was performed on a PerkinElmer Spectrum One, fitted with a universal ATR sampling accessory. All data were recorded at room temperature (< 20 °C), in the spectral range of 4000–650 cm^{-1}, utilizing four scans per sample cycle and a fixed universal compression force of 80 N. Subsequent analysis was performed using Spectrum software.

Swelling Studies. After photopolymerization, the samples were placed in a vacuum oven for 24 h at 40 °C, and the apparent dry weights (Wd) were measured. The samples were tested at room temperature (< 20 °C). Samples were placed in 50 mL of distilled water to determine their swelling ratio. The percentage of gel swelling was calculated using eq. (1). All reported swelling studies were measured in distilled water. Tests were carried out in quintuplicate below, and above phase transition and the data were presented as mean ± SD.

$$\text{Swelling ratio}\,(\%) = (\text{Wt} - \text{Wd})/\text{Wd}*100 \quad (1)$$

where Wt and Wd are the weights of the gels in the swelled state and the dried state, respectively.

Dynamic Mechanical Analysis. Dynamic mechanical analysis (DMA) measurements were performed on nonirradiated and irradiated samples with a TA Instruments DMA Q800. Samples with dimensions of 35 × 6 × 3 mm were clamped in the instrument using a dual cantilever. Each of the samples was heated from 20 to 160 °C at a rate of 3 °C/min while using the multifrequency strain mode. A constant frequency of 1 Hz was applied while a strain rate of 0.1% was used to calculate the viscoelastic behavior of the samples regarding the storage modulus (E'), loss modulus (E"), and tan delta (tan δ).

Gel Permeation Chromatography. Gel permeation chromatography (GPC) was carried out using a PL GPC-120 system. The GPC was set to a flow rate of 0.5 mL per minute with a mini-mixed D column with guard column fitted. The system was allowed to equilibrate at 40 °C for 24 h with chloroform circulating before the test took place. Agilent polystyrene standards were used as reference standards with a range from 3 000 000 to 162 g mol^{-1}.

Differential Scanning Calorimetry. Differential scanning calorimetry (DSC) studies were performed on all samples (TA Instrument DSC 2920 Modulated DSC). The DSC was calibrated with indium standards. The samples had a dry weight of between 8 and 12 mg. Aluminium pans were used to contain the samples. All samples were examined under a pure nitrogen atmosphere. During testing, each of the PNVCL–VAc samples was ramped from 20 to 200 °C at a rate of 10 °C/min.

Tensile Testing. Tensile testing of the nonirradiated and irradiated dumbbell specimens was performed to measure the tensile strength, Young's modulus, and percentage elongation at break. They were synthesized to dimensions of 33 × 6 × 3 mm (length of the narrow section × width of the narrow section × overall thickness) and had an overall length of 115 mm. The experiment was carried out per ASTM D638-03 except for implementing a crosshead speed of 50 mm/min. An Instron 3365 (Instron Ltd, UK) universal testing machine was employed to conduct each experiment where a 5 kN load cell was applied during the experiments with a gripper distance of 40 mm. Five tests were executed for each dose range, and the mean was calculated from each of the five results.

Colorimetry. Color measurements were performed according to ASTM D 1925 using a Lovibond RT600 sphere spectrophotometric colorimeter. Calibration was conducted on the instrument prior to testing using a calibration unit that was provided with the equipment (L = 94.91, a = −1.01, b = +0.09). All samples were stored in a dark area at room temperature for 1 week following irradiation before being tested. Five tests were performed on each sample from the different materials. Each test provided values for Hunter L [black (0) to white (100)], Hunter a [green (−) to red (+)], and Hunter b [blue (−) to yellow (+)]. The overall color difference (ΔE) was established by implementing statistical analysis of the ΔE values for L, a, and b. ΔE was calculated by using the following formula:

$$\Delta E = \sqrt{(\Delta L)^2 + (\Delta a)^2 + (\Delta b)^2} \quad (2)$$

where ΔE is expressed as the difference between the control sample and the irradiated sample color values.

Phase Transition Determination. ***UV–spectroscopy.*** The phase transition behavior of samples was also investigated using a UV–spectroscopy synergy HT BioTek plate reader. The transmittance of samples in aqueous polymer solutions was measured at 500 nm at intervals of 1 °C in the range of 25–44 °C. The solution was allowed to equilibrate at each temperature for 20 min before the transmittance was measured.

Tube inversion method. Aqueous polymer solutions (1 mL) of all samples were placed in 10 mm diameter glass tubes. Samples were kept at the constant temperature for 10 min in a thermostated bath, before inverting the tube at intervals of 1 °C. Before switching to the next temperature, the samples were cooled in an ice–water bath until the polymer solution became homogeneous. Gelation temperature was seen as the temperature at which the polymer solution did not flow by inverting the tube.

Results and Discussion

Preparation of Samples. Physically crosslinked polymers, based on NVCL, were synthesized via photopolymerization. The copolymers were synthesized by incorporating VAc 10 wt %, along with 0.1 wt % Irgacure 184 photoinitiators. Vacuum packing led to depleted oxygen content during the irradiation procedure, which minimized oxidative degradation, as there was no oxygen to react with the free radicals generated during the process.[7] Figure 1 demonstrates the color change of each sample, before and after irradiation (i.e., 0, 5, 25, and 50 kGy). As the irradiation dose increased from 5 to 50 kGy, a notable discoloration was observed; in particular, the 50 kGy samples turned a dark yellowish color.

Attenuated Total Reflectance Fourier Transform Infrared Spectroscopy. Electron beam irradiation can alter the physical and chemical properties of polymers. This can occur through

Figure 1. PNVCL-based samples were optically transparent, and increasing the irradiation dose of the electron beam from 0 to 50 kGy led to a color change in the samples. [Color figure can be viewed at wileyonlinelibrary.com]

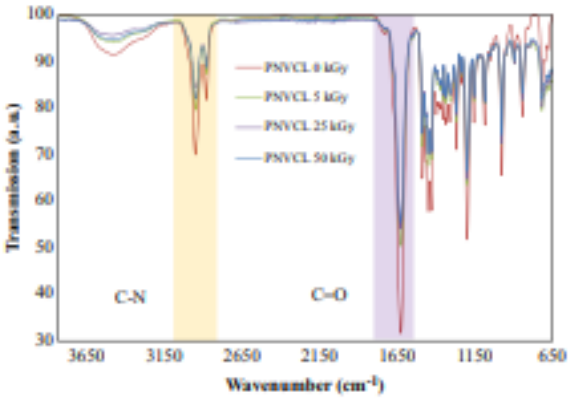

Figure 2. FTIR spectra of PNVCL before and after electron beam irradiation at 5, 25, and 50 kGy. [Color figure can be viewed at wileyonlinelibrary.com]

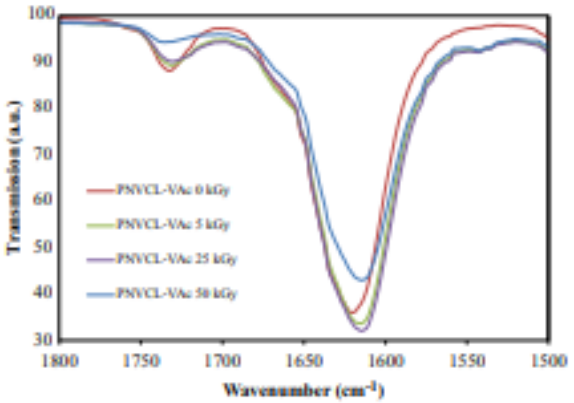

Figure 3. FTIR spectra of PNVCL90-VAc10 copolymer before and after electron beam irradiation at 5, 25, and 50 kGy. [Color figure can be viewed at wileyonlinelibrary.com]

main-chain scission (degradation) or crosslinking, which are reliant on the electron beam dose and copolymer ratios.[8] ATR–FTIR analysis was carried out on the irradiated and non-irradiated PNVCL-based samples, to ensure that electron beam irradiation did not lead to undesirable changes in the material (Figure 2). For example, it is essential to ensure that the caprolactam ring is present within the PNVCL structure. ATR–FTIR analysis confirmed that the caprolactam ring was detected in all PNVCL samples (Figure 2). All samples displayed the aliphatic (C—H) band, and the caprolactam ring was recognized at 2924 and 2850 cm^{-1}, while the C—C for the aliphatic group in the caprolactam ring was observed at 1438 cm^{-1}, in accordance with the literature.[9–11] The retention of caprolactam functionality in the PNVCL samples demonstrated that electron beam irradiation did not affect the structure of the material.[9,10,12] PNVCL absorbs moisture which corresponds to the broad band at ~3400 cm^{-1} which relates to the O—H stretching; this is associated with the polymers hydrophilic character. It was observed that increasing the irradiation dose lead to a decreased in this broad band. Additionally, another characteristic band of PNVCL is the carbonyl band (C═O) and the amide group peak (C—N) was also found at 1620 and 1453 cm^{-1}, respectively. The retention of these bands gives further evidence that the PNVCL structure was not affected during the electron beam process. The intensity of transmittance decreases regarding higher electron dosage may suggest crosslinking. For example, the reduction in the intensity of the O—H group at higher electron doses suggesting the crosslinking of PNVCL occurs due to the formation of hydrogen bonds by the free radicals released during electron beam irritation. This may indicate the crosslinking of the PNVCL through the covalent bond formation between carbon and hydrogen at higher dosages.[13]

The PNVCL—VAc spectra exhibited a band around ~1731 cm^{-1}, which corresponds to the C═O (Figure 3) stretching of the aliphatic ester group of VAc.[1,14] As illustrated in Figure 3, it was noted that there is a decrease in the intensity of the C═O. This reduction in intensity of the aliphatic ester group of VAc resulted from an increased irradiation dose. The reduction of intensity in the non-hydrogen-bonded C═O may be due to hydrolysis of the aliphatic ester group segment.

Swelling Studies. Swelling studies below the phase transition temperature (< 20 °C) examined the effect of electron beam dose, as physical crosslinked PNVCL swelling behavior is dependent on temperature. PNVCL is an amorphous polymer, and during the electron beam irradiation process, it has been reported that the amorphous regions of the polymer can experience crosslinking.[15] Figure 4 illustrates the swelling behavior of PNVCL-based samples exposed to irradiation doses of between 0 and 50 kGy. Based on the results, the 25 and 50 kGy samples displayed the most significant swelling, which indicates that crosslinking occurred. A similar trend was observed for the copolymers.

In all cases, it was revealed that the swelling percentage was influenced by increasing irradiation dose. The increase in swelling percentage is likely due to the creation of chain branches or crosslink networks that are created through electron beam irradiation and attributed to the production of radiation-free radicals. The creation of these crosslinks is likely a result of hydrogen bond formation during the electron beam process. The crosslinks affected the entanglements of PNVCL chains, leading to an increased swelling ratio with an increase of irradiation dose. The results indicate that, initially, the swelling process for PNVCL-based samples occurred primarily due to the water penetrating through capillarity and diffusion processes.[16]

Sharma *et al.* reported similar findings when studying the effects of gamma irradiation on poly(acrylamide-aniline)-grafted gum ghatti hydrogels. The study indicated that increasing the irradiation dose, increased the percent of swelling.[17] Cairns *et al.* stated that electron beam treatment could be used to control degradation profiles of poly(lactic acid). In the aforementioned study, the samples broke down more rapidly in aqueous media following electron beam exposure. It is therefore essential to carry out detailed testing on samples following electron beam or other sterilization processes, as such processes can result in chain scission which can result in quicker breakdown rates of samples, or crosslinking which often results in extended breakdown rates.[18]

Dynamic Mechanical Analysis. PNVCL testing in the literature mainly includes several chemical analyses and its behavior in

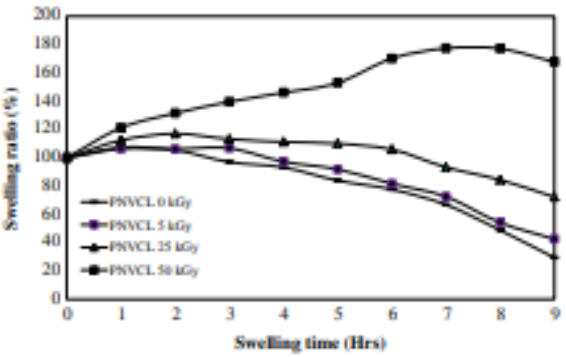

Figure 4. Swelling behavior of PNVCL-based samples at different irradiation doses tested at ambient temperature (< 20 °C). [Color figure can be viewed at wileyonlinelibrary.com]

aqueous solution. However, far fewer studies report the mechanical properties of PNVCL. The mechanical properties of the dry polymer should be taken into account to determine the effect of the electron beam irradiation. Also, this knowledge of PNVCL in a dry state could be useful for transportation and handing purposes for future biomedical applications. DMA measurements were conducted over a temperature range of 30–160 °C for selected samples (0–25 kGy), to examine the effect that electron beam irradiation had on the mechanical properties (Figure 5). All samples tested exhibited a broad transition, which was identified as the liner viscosity-elastic region. DMA measurements for PNVCL, which are presented in Figure 5 displays a graph representing the collected data for E′ and tan δ. The dynamic glass transition temperature (T_g) found using DMA can be interpreted in three ways. The first is at the temperature of the middle point of storage modulus vs temperature curve. The second measurement is the maximum temperature which loss modulus occurs, and finally, third is the maximum peak of Tan δ. Thus, T_g is the temperature range where a polymer changes from a "glassy," rigid, or hard state to a more compliant, pliable, or a "rubbery" state.[19]

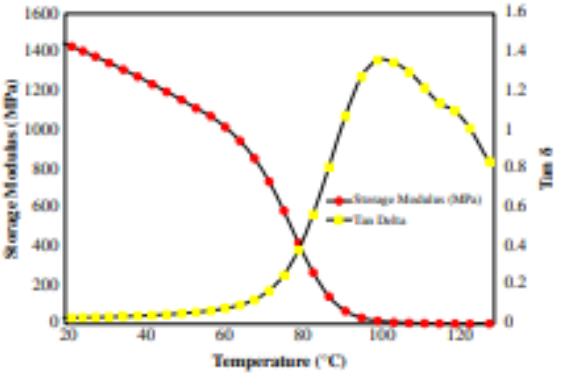

Figure 5. The collected data for storage modulus (E′) and tan δ for PNVCL homopolymer. [Color figure can be viewed at wileyonlinelibrary.com]

Figure 6 displays the storage (E′) and loss modulus (E″) vs temperature for selected samples analyzed. Table II is a summary of the results, it can be observed that, as the temperature increased, the E′ decreased. This is due to a reduction in stiffness, which is the material undergoing a transition from a glassy to a rubbery state. Samples that were irradiated at higher doses resulted in a greater E′, compared to those exposed to lower doses, this is similar to other reports in the literature.[20] In the case of PNVCL preirradiation (0 kGy), the storage modulus amounted to ~1450 MPa, which increased to ~1550 MPa for a dose of 25 kGy at 20 °C. E″ relates to energy dissipation within the PNVCL matrix. Therefore, increasing the temperature within the T_g range will result in an increase in the E″. As the temperature reaches the T_g, there is a reduction in the molecular friction, resulting in a peak in E″. The increases in E″ are likely a result of radiation-induced branching or crosslinking, which reduces this motion causing a slight shift of T_g to higher values.

Similar results were reported by Mansouri *et al.* who examined the effect of electron beam radiation on polylactic acid where an increase in the electron beam dose resulted in an increase in both storage and loss modulus.[20]

Gel Permeation Chromatography. GPC analysis was conducted on all PNVCL-based samples. Table III summarizes the molecular number (M_n), M_w, and polydispersity (PDI) data attained. Altering the irradiation dose led to an increase in the M_w. It is highly important to control the M_w and PDI, as the LCST of PNVCL is reported to be M_w dependent.[21] However, it has been reported that the addition of a hydrophobic monomer such as VAc can reduce the LCST from 32 to 26.5 °C as the content of VAc increases.[22] The GPC results revealed an increase in the average M_w when the irradiation dose increased. However, PNVCL 25 kGy and PNVCL 50 kGy samples (Table III) are not displayed, as irradiated PNVCL's M_w is close to the detection limit of the GPC/column, preventing accurate determination for such samples. A similar finding was reported in the case of irradiation of PNVCL homopolymer whereby high irradiation doses led to difficulties in determining the M_w of PNVCL using GPC.[23]

Lim *et al.* grafted PNVCL-*co*-*N*-isopropylacrylamide) (PNVCL-*co*-PNIPAm) onto tissue culture polystyrene by electron beam irradiation. Results illustrated that with a change in temperature, the polymers could alter hydrophilic and hydrophobic surface properties. Above the LCST (37 °C), the surface was hydrophobic and cell adhesive; below the LCST (32 °C), the surface changed to hydrophilic and was not cell adhesive, with no damage to the detached cells. [24] PNVCL is an attractive polymer for the biomedical field, and it also has emerging applications in other areas that are expected to grow, such as those related to nanotechnology rapidly.[25] This study highlights the potential of modulating the M_w of novel polymers based on PNVCL, using electron beam irradiation. It is also very interesting to note the significant increases in M_w even at low irradiation doses, which are used in the sterilization of medical devices. Given the critical relationship between the M_w and the LCST of PNVCL, such analysis would thus be essential in medical device development and would be critically important particularly for thermogelling applications, as changes in M_w could significantly affect the gelling temperature.

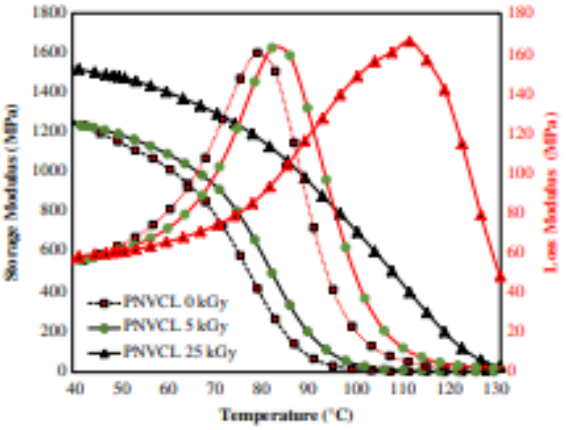

Figure 6. Storage modulus (MPa) and loss modulus (MPa) reported using DMA measurement. [Color figure can be viewed at wileyonlinelibrary.com]

Table II. Summary of the Results Obtained from DMA Analysis; the Dynamic Glass Transition for the Peak Value of Tan Delta Modulus

Polymer code	Tan delta (°C)
PNVCL 0 kGy	102.3
PNVCL 5 kGy	108.6
PNVCL 25 kGy	155.1
PNVCL-VAc 0 kGy	100.8
PNVCL-VAc 5 kGy	104.3
PNVCL-VAc 25 kGy	125.5

Table III. Molecular Number (M_n), Molecular Weight (M_w), and Polydispersity (PDI) Results for PNVCL-Based Samples

Polymer code	M_n (g mol^{-1})	Mw (g mol^{-1})	PDI
PNVCL 0 kGy	12 291	167 974	13.6664
PNVCL 5 kGy	12 566	172 805	13.7518
PNVCL 25 kGy	NA	NA	NA
PNVCL 50 kGy	NA	NA	NA
PNVCL-VAc 0 kGy	20 658	239 484	11.5928
PNVCL-VAc 5 kGy	19 509	298 177	15.2841
PNVCL-VAc 25 kGy	11 716	271 888	23.2066
PNVCL-VAc 50 kGy	13 016	424 907	32.645

In summary, altering PNVCL M_w by electron beam exposure thus offers enormous potential benefits for biomedical applications such as drug delivery, cell detachment, and entrapment of enzymes, and even low electron beam irradiation doses can have significant effects on materials properties, and this should be given due consideration in the early stages of medical device development.

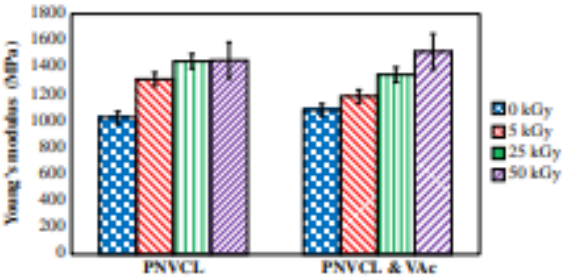

Figure 7. Young's modulus (MPa) for nonirradiated and irradiated samples. [Color figure can be viewed at wileyonlinelibrary.com]

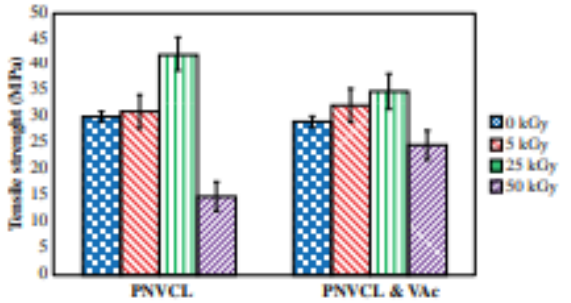

Figure 8. Tensile strength (MPa) for nonirradiated and irradiated samples. [Color figure can be viewed at wileyonlinelibrary.com]

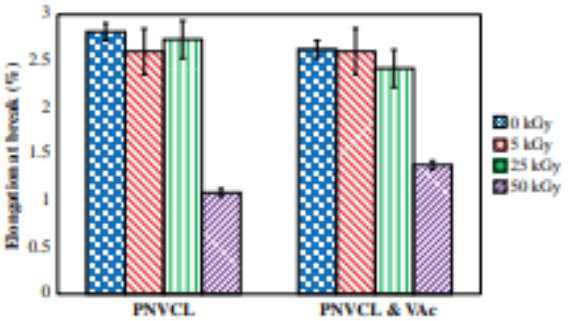

Figure 9. Elongation at break (%) for nonirradiated and irradiated samples. [Color figure can be viewed at wileyonlinelibrary.com]

Tensile Testing. Tensile testing was used to further analyze the effect of electron beam irradiation on the mechanical properties of novel PNVCL samples. The Young's modulus, tensile strength, and percentage elongation of all PNVCL samples were investigated to determine what effect electron beam exposure had on the material. Based on the stress–strain measurements of the polymer, Young's modulus was used to confirm that the stiffness value for PNVCL-based polymers increased as the irradiated dose increased (Figure 7).

The tensile strength of all samples increased gradually, until they reached 25 kGy, at this point, a sharp decrease was demonstrated

Table IV. Data Collected for the Mechanical Testing of PNVCL-Based Samples

Polymer code	Young's modulus (MPa)	Std. error	Tensile strength (MPa)	Std. error	Elongation at break (%)	Std. ERROR
PNVCL100 kGy	1024.3	83.5	30.0	2.3	2.8	0.2
PNVCL100 5 kGy	1310.9	110.3	31.0	7.0	2.6	0.5
PNVCL100 25 kGy	1445.1	122.1	42.1	7.4	2.7	0.4
PNVCL100 50 kGy	1451.5	300.2	14.9	6.1	1.0	0.3
PNVCL90-VAc10	1081.5	100.6	29.0	2.2	2.6	0.2
PNVCL90-VAc10 5 kGy	1181.6	97.6	32.1	2.7	2.6	0.5
PNVCL90-VAc10 25 kGy	1344.1	123.7	34.0	3.1	2.4	0.4
PNVCL90-VAc10 50 kGy	1516.4	92.1	24.6	2.0	1.3	0.3

(Figure 8). During the crosslinking process, the formation of three-dimensional networks can lead to an increase in tensile strength properties, though highly crosslinked structures can become more brittle.[5,26]

Figure 9 illustrates the percentage elongation at break as a function of irradiated dose for PNVCL samples. The results show a decrease among all irradiated samples, in contrast to the control samples (0 kGy) for elongation at break. In the case of the 50 kGy samples, another sharp decrease was displayed. This was perhaps related to chain stretching of the PNVCL material because of an increase in the crosslink density. Chain stretching has been reported in other polymeric materials such as LDPE, following exposure to electron beam irradiation.[27]

In summary (Table IV), tensile strength generally increased, with increasing dose of electron beam irradiation. However, at the highest dose of electron beam irradiation, samples PNVCL 50 kGy and PNVCL–VAc 50 kGy displayed a decrease in tensile strength and elongation at break. Tensile testing data revealed that the mechanical properties of PNVCL-based samples were likely enhanced due to radiation crosslinking/branching, up until a critical point where mechanical properties exhibited a sharp decline. Once again, it is noteworthy that even at lower irradiation doses obvious changes were observed in mechanical performance properties.

Differential Scanning Calorimetry. DSC measurements were conducted on xerogels over a temperature range of 20–200 °C for all samples. One broad transition was observed between 100 and 200 °C for the entire nonirradiated and irradiated PNVCL samples. This transition was identified as the T_g. The irradiated samples showed an increase in T_g values, compared to nonirradiated samples. This is likely due to crosslinking occurring during electron beam exposure. The crosslinking that occurred in PNVCL increased the M_w of the polymer, which would result in a more rigid structure, as discussed in DMA analysis. Figure 10 illustrates the T_g for PNVCL-based polymer samples at different irradiation doses. The proposed crosslinking in the polymers brings about a restriction in the polymer chains. The restricted movement of molecular chains and the shifting of the T_g to a higher temperature can also be observed in Section "Dynamic Mechanical Analysis" during DMA analysis (Figure 6). Both the static (DSC) and dynamic T_g (DMA) exhibited an increase. This is further evidence that branching or crosslinking is likely to have had occurred within the PNVCL samples.

Shifting of the T_g to higher temperatures is another clear indication that crosslinking was induced by the irradiation of the PNVCL samples.[28–30] Any differences in T_g compared to the

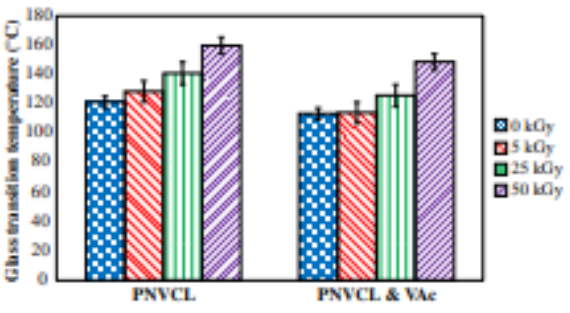

Figure 10. Glass transition temperature for nonirradiated and irradiated PNVCL-based samples. [Color figure can be viewed at wileyonlinelibrary.com]

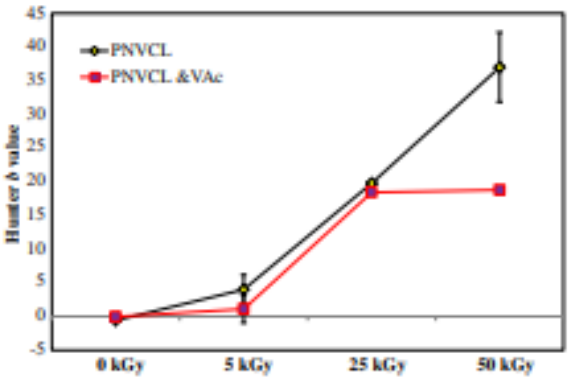

Figure 11. ΔE values vs E-beam irradiation dose for PNVCL-based samples. [Color figure can be viewed at wileyonlinelibrary.com]

Table V. Colorimetry Measurement of PNVCL-Based Samples

Polymer code	L*	Std. error	a*	Std. error	b*	Std. error	ΔE	Std. error
PNVCL100 0 kGy	82.1		0.01		−0.6		0	0
PNVCL100 5 kGy	84.2	3.1	−0.4	0.07	3.9	2.23	5.89	0.9
PNVCL100 25 kGy	66.1	0.3	0.6	0.07	19.7	0.371	25.9	0.4
PNVCL100 50 kGy	75.5	0.7	3.2	1.2	37.0	5.18	38.3	5.2
PNVCL90-VAc10	82.6		−0.1		−0.03		0.0	0.0
PNVCL90-VAc10 5 kGy	84.3	0.2	−0.3	0.1	1.1	2.03	2.5	1.1
PNVCL90-VAc10 25 kGy	65.9	0.07	−0.5	0.1	18.4	0.40	24.8	0.3
PNVCL90-VAc10 50 kGy	77.5	1.7	−1.0	0.0	18.7	0.36	19.5	0.6

*The significance of the asterisk is relation to the colourimetry measurement.

literature can be associated with various factors, with M_w often cited as one of the significant contributors.[31] Other literature states that such radiation-induced reactions that cause an increase in the T_g may be a result of increased M_w and increased crosslink density among different regions of samples.[32,33] Similar trends were exhibited for both the homopolymer and novel copolymers in this study.

Colorimetry. Colorimetry measurements were conducted on the PNVCL-based samples before and after the irradiation process (Figure 11). The exposure rate of the electron beam irradiated samples ranged from between 0 and 50 kGy. The Hunter *b* value demonstrated an increase from −0.60 to 37.01 as the electron beam irradiation dose increased. Consequently, the irradiated samples became more yellowish. For the PNVCL-VAc copolymer sample (0 kGy), the Hunter *b* value was −0.03. However, with an increase in irradiation dose, notable differences between samples were observed, with increases in ΔE values for all irradiated specimens. An explanation for such changes after exposure to irradiation could be related to the entrapment of free radicals.[34] Figure 11 provides an overview of the results obtained from the colorimetry measurement. Overall, colorimetry measurements indicate that PNVCL homopolymer and its copolymers with VAc are sensitive to electron beam processing which led to discoloration in the samples. It was noted that samples containing VAc displayed less color change at high irradiation doses when compared to the homopolymer (Table V). Such color changes can be indicative of polymer degradation; however, as shown in the previous sections, in many cases, mechanical properties were enhanced. That said, color changes such as those displayed at the higher irradiation doses would be highly undesirable especially for medical device products, thus such analysis is of great importance.

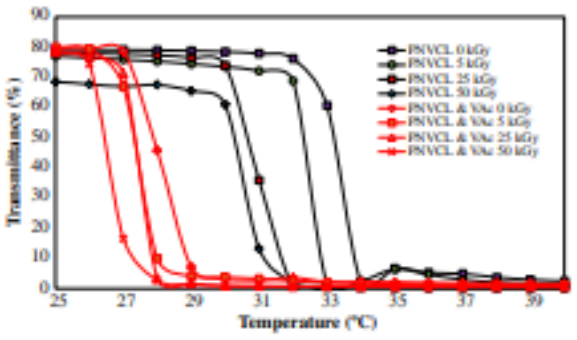

Figure 12. UV–spectroscopic measurement illustrating the phase transition of PNVCL-based samples (5 wt %) at different radiation doses. [Color figure can be viewed at wileyonlindibrary.com]

Phase Transition Determination. ***UV–spectroscopy.*** The UV–spectroscopic measurement was carried out to observe the effects of the electron beam irradiation on PNVCL-based samples phase transition temperature. The LCST of PNVCL can be altered by adjusting its M_w.[35,36] For example, increases in M_w has been reported to result in decreased phase transition, attributed to an increase in the polymer hydrophilicity.[37] This study showed that exposing PNVCL-based samples to electron beam irradiation increased the polymer chain length, as outlined in the previous

Table VI. Phase Transition (LCST) and Sol–Gel Transition Results for PNVCL-Based Samples (5 wt %) Which Were Established Using UV–Spectrometry and Tube Inversion Methods

Polymer code	UV–spectrometry LCST (°C)	Tube inversion method sol–gel (°C)
PNVCL100 0 kGy	33.5	37.3 ± 0.5
PNVCL100 5 kGy	31.6	36.4 ± 0.5
PNVCL100 25 kGy	30.2	34.4 ± 0.5
PNVCL100 50 kGy	30.4	34.3 ± 0.5
PNVCL90-VAc10 0 kGy	28.1	34.8 ± 0.5
PNVCL90-VAc10 5 kGy	27.4	33.6 ± 0.5
PNVCL90-VAc10 25 kGy	27.2	33.2 ± 0.5
PNVCL90-VAc10 50 kGy	26.5	32.7 ± 0.5

sections. This, in turn, resulted in a decrease in phase transition upon polymer M_w increase. It was also noted that the phase transition of PNVCL-based samples was dependent on the irradiation doses, as presented in Figure 12. For nonirradiated PNVCL, the phase transition was within the range previously reported.[10,21,38]

These results imply that PNVCL matches Type 1 Flory–Huggins demixing behavior, which states that increased M_w results in a decrease in phase transition temperature.[25] These results are in agreement with the results obtained in the previous sections. To date, this is the first study to report the adjustment of PNVCL phase transition using industrial-scale electron beam irradiation, under typical conditions for sterilizing medical devices and also at higher irradiation doses. These findings are of great importance, given the crucial role of the phase transition in many potential PNVCL-based medical devices, and drug delivery systems, particularly as the LCST was significantly reduced even at low irradiation doses typically in the range used for medical device sterilization.

Sol–gel transition. The sol–gel transition for PNVCL-based samples was measured using the tube inversion method and rheological analysis to examine the effects of electron beam irradiation on the polymers phase transitions, the results of which are summarized in Table VI. The transition temperatures were determined using a flow (sol)-no flow (gel) principle with a temperature increment of 1 °C per step for both methods. The thermogelling capabilities of PNVCL were found to be affected by the electron beam process. This is a result that is auspicious for biomedical applications, as having the ability to control the M_w of the PNVCL postpolymerization is desirable.[39] Similar trends were established using the sol–gel method in comparison to the results obtained for LCST (Table VI).

It can be concluded from sol–gel and UV–spectroscopy analysis that PNVCL retained its phase transition capabilities after electron beam processing. Additionally, it was proven that industrial-scale electron beam radiation, even at relatively low doses, had the ability to alter the phase transition and thermogelling properties of the temperature-responsive polymers, which is a crucial feature which should be given due consideration when designing medical devices or controlled drug delivery systems with such smart polymers.

CONCLUSION

The initial work focused on exploring the novel use of an industrial scale electron beam irradiator, and optimizing the operational conditions to sterilize temperature-responsive polymers. Electron beam irradiation provides a fast and reliable method of sterilization to the medical device industry. To achieve a more in-depth knowledge of the polymer modifications triggered by irradiation exposure, three key areas were examined which included chemical, thermal, and structural analysis. It was found that the electron beam dose could be used as a means of controlling key properties of PNVCL. The obtained smart polymers resulted in considerable modifications to the materials properties as analyzed by ATR–FTIR, GPC, DSC, UV–spectroscopy, DMA, tensile testing, and swelling studies. At a radiation concentration of 50 kGy, decreases in PNVCL mechanical properties were observed for tensile testing. Increased swelling behavior was an indication that crosslinking had taken place. Also, it was noted that the higher the irradiation dose which samples were subjected to, the greater the subsequent percentage swelling. UV–spectroscopy was used to examine the phase transition behavior, where a decrease in the LCST was found upon irridiation of all samples. This decrease is considered a result of increased M_w experienced during the electron beam process. It was also identified that the phase transition of the PNVCL solutions decreased with increasing irradiation dose. Electron beam irradiation results demonstrate that this method allowed functional modification to sterilized temperature-responsive polymers compared to standard methods.

In summary, PNVCL thermosensitivity and mechanical properties could be altered by utilizing electron beam. Such enhancements allows opportunity to further tailor such smart materials for medical device or targeted drug delivery applications using this methodology.

ACKNOWLEDGMENTS

This work was supported by the Athlone Institute of Technology Presidents Doctoral Scholarship fund. The authors also thank STERIS Applied Sterilization Technologies for their contribution to the work.

REFERENCES

1. Halligan, S. C.; Dalton, M. B.; Murray, K. A.; Dong, Y.; Wang, W.; Lyons, J. G.; Geever, L. M. *Mater. Sci. Eng. C.* **2017**, *79*, 130.
2. Dalton, M. B.; Halligan, S. C.; Killion, J. A.; Wang, W.; Dong, Y.; Nugent, M. J. D.; Geever, L. M. *Polym.- Plast. Technol. Eng.* **2017**, *57*, 1165.
3. Frost, M. J.; Lyons, S. G.; Geever, L. M. *Mater. Today Proc.* **2019**, *10*.
4. Gaballa, H. a.; Geever, L. M.; Killion, J. a.; Higginbotham, C. L. *J. Polym. Sci. Part B: Polym. Phys.* **2013**, *51*, 1555.
5. Murray, K. a.; Kennedy, J. E.; McEvoy, B.; Vrain, O.; Ryan, D.; Higginbotham, C. L. *Radiat. Phys. Chem.* **2012**, *81*, 962.
6. Murray, K. A.; Collins, M. N.; O, Sullivan, R. P.; Ren, G.; Devine, D. M.; Murphy, A.; Sadlo, J.; O, Sullivan, C.; McEvoy, B.; Vrain, O.; O, Neill, C.; Insley, G. *J. Mech. Behav. Biomed. Mater.* **2018**, *77*, 116.
7. Murray, K.; Kennedy, J. E.; Mcevoy, B.; Vrain, O.; Ryan, D.; Cowman, R.; Higginbotham, C. L. *Mater. Sci. Eng. C.* **2014**, *39*, 380.
8. Dânmark, S.; Finne-Wistrand, A.; Schander, K.; Hakkarainen, M.; Arvidson, K.; Mustafa, K.; Albertsson, A.-C. C. *Acta Biomater.* **2011**, *7*, 2035.
9. Kozanoğlu, S. Polymerization and Characterization of N-Vinylcaprolactam; Middle East Technical University: Ankara, Turkey, **2008**.
10. Lee, B.; Jiao, A.; Yu, S.; You, J. B.; Kim, D.-H.; Im, S. G. *Acta Biomater.* **2013**, *9*, 7691.

11. de Matos Fonseca, J.; de Fátima Medeiros, S.; Alves, G. M.; dos Santos, D. M.; Campana-Filho, S. P.; dos Santos, A. M. *Colloids Surf., B.* **2019**, *175*, 73.
12. Madhusudana Rao, K.; Mallikarjuna, B.; Krishna Rao, K. S. V.; Siraj, S.; Chowdoji Rao, K.; Subha, M. C. S. *Colloids Surf., B.* **2013**, *102*, 891.
13. Kumar, K. V. A.; Ningaraju, S.; Munirathnamma, L. M.; Ravikumar, H. B.; Ranganathaiah, C. *J. Phys.: Conf. Ser.* **2015**, *618*, 12032.
14. Allen, N. S.; Edge, M.; Rodriguez, M.; Liauw, C. M.; Fontan, E. *Polym. Degrad. Stab.* **2000**, *68*, 363.
15. Sabet, M.; Hassan, A.; Wahit, M. U.; Ratnam, C. T. *Polym.-Plast. Technol. Eng.* **2010**, *49*, 589.
16. Zavala-lagunes, E.; Ruiz, J.; Varca, G. H. C.; Bucio, E. *Mater Sci Eng C Mater Biol Appl.* **2016**, *67*, 353.
17. Sharma, K.; Kaith, B. S.; Kumar, V. V.; Kalia, S.; Kumar, V. V.; Swart, H. C. *Polym. Degrad. Stab.* **2014**, *107*, 166.
18. Cairns, M.-L.; Dickson, G. R.; Orr, J. F.; Farrar, D.; Hawkins, K.; Buchanan, F. J. *Polym. Degrad. Stab.* **2011**, *96*, 76.
19. Saba, N.; Jawaid, M.; Alothman, O. Y.; Paridah, M. T. *Construct. Build Mater.* **2016**, *106*, 149.
20. Mansouri, M.; Berrayah, A.; Beyens, C.; Rosenauer, C.; Jama, C.; Maschke, U. *Polym. Degrad. Stab.* **2016**, *133*, 293.
21. Shi, H.-Y.; Zhang, L.-M. *Carbohydr. Res.* **2006**, *341*, 2414.
22. Liu, J.; Debuigne, A.; Detrembleur, C.; Jérôme, C. *Adv. Healthc. Mater.* **2014**, *3*, 1941.
23. Sedlacek, O.; Cernoch, P.; Kucka, J.; Konefał, R.; Stepanek, P.; Vetrik, M.; P. Lodge, T.; Hruby, M. *Langmuir.* **2016**, 6115, 32.
24. Lim, Y. M.; Jeun, J. P.; Lee, J. H.; Lee, Y. M.; Nho, Y. C. *Young.* **2007**, *13*, 21.
25. Cortez-Lemus, N. A.; Licea-Claverie, A. *Prog. Polym. Sci.* **2016**, *53*, 1.
26. Oka, T.; Kanbe, H.; Yatagai, F.; Hama, Y. *Nucl. Instruments Methods Phys. Res. Sect. B Beam Interact. with Mater. Atoms.* **2003**, *208*, 181.
27. Oral, E.; Godleski-beckos, C.; Ghali, B. W.; Lozynsky, A. J.; Muratoglu, O. K. *J. Biomed. Mater. Res. B. Appl. Biomater.* **2009**, *90*, 720.
28. Meeussen, F.; Nies, E.; Berghmans, H.; Verbrugghe, S.; Goethals, E.; Prez, F. Du. *Polymer.* **2000**, 41, 8597.
29. Lebedev, V. T.; Török, G.; Cser, L.; Kálí, G.; Sibilev, A. I. *Appl. Phys. A.* **2002**, *74*, s478.
30. Yoo, S. H.; Park, S.; Park, Y.; Lee, D.; Joh, H.-I.; Shin, I.; Lee, S. *Carbon.* **2017**, *118*, 106.
31. Siepmann, J.; Peppas, N. a. A. *Adv. Drug Deliv. Rev.* **2012**, *64*, 163.
32. Wang, Y.; Chen, D. *J. Colloid Interface Sci.* **2012**, *372*, 245.
33. Guglielmi, P. O.; Herbert, E. G.; Tartivel, L.; Behl, M.; Lendlein, A.; Huber, N.; Lilleodden, E. T. *J. Mech. Behav. Biomed. Mater.* **2015**, *46*, 1.
34. Silva, P.; Ichazo, M. *Polym. Degrad. Stab.* **2004**, *85*, 85.
35. Medeiros, S. F.; Santos, A. M.; Fessi, H.; Elaissari, A. *Int. J. Pharm.* **2011**, *403*, 139.
36. Schwarz, S.; Ponce-Vargas, S. M.; Licea-Claverie, A.; Steinbach, C. *Colloids Surf., A.* **2012**, *413*, 7.
37. Wu, Q.; Wang, L.; Fu, X.; Song, X.; Yang, Q.; Zhang, G. *J. Polym. Res.* **2014**, *71*, 1.
38. Ferraz, C. C.; Varca, G. H. C. C.; Ruiz, J.; Lopes, P. S.; Mathor, M. B.; Lugão, A. B.; Bucio, E. *Radiat. Phys. Chem.* **2014**, *97*, 298.
39. Chen, S.; Zhong, H.; Gu, B.; Wang, Y.; Li, X.; Cheng, Z.; Zhang, L.; Yao, C. *Mater. Sci. Eng. C.* **2012**, *32*, 2199.

Available online at www.sciencedirect.com

ScienceDirect

Materials Today: Proceedings 10 (2019) 430–435

materialstoday: PROCEEDINGS

www.materialstoday.com/proceedings

AEM2017

Controlling the Thermosensitivity of Poly(N-vinylcaprolactam) for Smart Glass Applications via Electron Beam Irradiation

Shane C. Halligan [a], Kieran A. Murray [b], Olivier Vrain[c], John G. Lyons [a], Luke M. Geever [a],* *

[a] *Applied Polymer Technologies Gateway, Materials Research Institute, Athlone Institute of Technology, Ireland .*
[b] *CelgenTek part of the Zimmer Biomet Group, Ireland.*
[c] *STERIS Applied Sterilization Technologies, Ireland.*

Abstract

Stimuli-responsive polymers are classified as materials that can experience moderately large and abrupt, physical or chemical changes in response to small external changes in environmental conditions. When exposed to ionizing radiation such as electron beam, radiation induced free radical reactions can take place such as chain branching or crosslinking, therefore; enhancing the physicochemical characteristics of these responsive polymers. In this study, Poly (N-vinylcaprolactam) (PNVCL) was prepared by photopolymerisation and the lower critical solution temperature of the physically crosslinked PNVCL copolymers was tailored by controlling the contents of the material concentration and the electron beam irradiation dose, i.e. 0, 5, and 50 kGy. The lower critical solution temperature of the polymers was established by UV-spectroscopy. By altering the radiation dose, this allowed the key attributes of the PNVCL to be tailored in order to suit a number of applications, for example, smart glass technology.

Selection and/or Peer-review under responsibility of AEM2017.
Keywords: Smart Glass; Glazing materials; Stimuli-responsive polymers; Poly(N-vinylcaprolactam);

1. Introduction

It is expected that 70% of the world population will be urban by 2050 [1]. This, increase in population will contribute to urban heat islands which is an overheating of the urban area compared to its surrounding countryside [2]. The increase in temperature can lead to disimprovement in thermal comfort conditions, therefore; causing

* Corresponding author. Tel.: +353 (0) 90 6468054.
E-mail address: lgeever@ait.ie

Selection and/or Peer-review under responsibility of AEM2017.

harmful and serious health diseases. Due to increasing temperatures, this is leading to more energy consumption globally. As a result more extensive demands for cooling technologies [1–3]. One effective method to lower energy consumption are smart windows [4]. Although windows play a significant role in providing a source of light for buildings, they are also an important factor with regards to energy conservation as thermal energy can be efficiently dissipated through the transparent glass surface. Smart glass has the ability to adjust its transparency which can efficiently shield incident light and lower room temperature. This method is attractive in overcoming energy conservation problems. Complex engineered materials that contain photochromic and thermochromic characteristics are attractive in the development of smart glass technology due to their ability to respond automatically to change in light or temperature [5].

Poly (N-isopropylacrylamide) (PNIPAM) is one of the most studied temperature sensitive polymers as its lower critical solution temperature (LCST) can be altered to suit numerous applications such as drug delivery and chemical sensing [6]. In addition, it is a strong candidate material for smart glass technology as a result of its excellent thermotropic capabilities [1]. Ye et al. (2012) developed a thermotropic material based on poly (N-isopropylacrylamide) (PNIPAM) designed for energy saving purposes. Based on the work from the aforementioned study, it was found that when the temperature raised above the LCST of PNIPAM, a maximum reflection ratio of 33% was observed which led to a decrease in cell temperature by 6.0 °C in contrast to the cells without PNIPAM contained in the composition [2]. Long et al. (2015) was the first to report thermochromic double glazing in a full-scale room. From the results, they revealed that a low-mass room with a vanadium dioxide (VO_2) double window consumes approximately 11.1% less cooling energy than that with an ordinary double window [7]. PNIPAM polymers have been extensively studied for smart glass technology, however; another popular temperature-responsive polymer called Poly (N-vinylcaprolactam) (PNVCL) has a similar LCST to PNIPAM. Both PNVCL and PNIPAM hydrogels have reversible LCST's and exhibit similar characteristics for the swelling to collapsing transition in water that occurs at the same temperature as the LCST [6,8]. Other benefits of PNVCL in contrast to PNIPAM is that it is biocompatible and has excellent stability characteristics against hydrolysis [9,10].

Most often, improvements in physical and mechanical properties can be imparted more rapidly and cost-effectively by using current processing methods rather than developing new chemistry [11]. Currently, electron beam irradiation can impact the characteristics of polymers by undergoing simultaneous crosslinking and chain scission, however; in most cases one process dominates over the other. Crosslinking is widely used to enhance the physicochemical properties of polymeric materials, thus improving the resistance against extreme environmental conditions. Electron beam is an attractive method for altering the aforementioned properties and in particular has the potential to enhance the LCST of PNVCL [12, [12].

In this study, the key attributes of Poly (N-vinylcaprolactam) will be tailored by using various doses of electron beam irradiation.
This is hoped to improve properties of PNVCL and reduce cost. There is no such literature to our knowledge taking advantage of PNVCL LCST for smart glass technology. Physically crosslinked PNVCL samples were developed as a material with reversible LCST. Electron beam technology was used to alter the LCST for applications in smart glass technology. To the best of our knowledge, very few articles developed temperature sensitive PNVCL for the use as smart glass *via* electron beam technology.

2. Materials and Methods

2.1. Materials

N-Vinylcaprolactam (NVCL) was obtained from Sigma-Aldrich Ireland with a molecular weight of 139.19 g mol-1 and storage temperature of 2-8 °C. 1-hydroxycyclohexyl phenyl ketone (Irgacure® 184) was used to initiate the reaction of free-radical polymerisation.

2.1.1. Polymer Synthesis

The polymers investigated in this study were prepared by free-radical polymerisation using ultraviolet (UV) light. These polymers were synthesised via physical crosslinking using a UV curing system (Dr. Gröbel UV-Electronik GmbH). This chamber has a controlled radiation source with 20 UV-tubes that provide a spectral range of between 315-400 nm at an average intensity of 10-13.5 mW/cm^2. The pre-polymerised mixtures were prepared by combining desired amounts of the monomer NVCL with 0.1 wt% photoinitiator. The batches were placed in a 50 ml beaker and mixed using a magnetic stirrer for 20 minutes until a homogeneous mixture was obtained. The solutions were pipetted into silicone moulds that contained disc impressions (23 mm diameter, 2.2 mm thickness). Photopolymerisation was carried out for 30 minutes, at which time gelation occurred. All samples were cured in a silicone mould and, before use, dried for 24 h in a vacuum oven at 40 °C.

2.1.2. Electron beam irradiation

Vacuum packing was conducted on virgin PNVCL. Vacuum packing was performed to ensure the samples were contained in a controlled environment. The sample size, weight and orientation remained the same for all samples to facilitate consistency during the electron beam irradiation process. A MEVEX high energy electron beam irradiator was used to irradiate PNVCL testing specimens and granules at doses of 5 and 50 kGy. The dose rate was approximately 2.5 kGy and 25kGy per pass on each side to accomplish a uniform irradiation dose for 5 and 50 kGy samples respectively. All samples were irradiated at room temperature in the presence of air at the STERIS facility (Tullamore, Ireland). The non-irradiated samples served as the baseline for each of the results.

2.1.3 *Preparation of aqueous solutions*

Homogeneous solutions of each sample were prepared by weighing appropriate amounts of the xerogel and distilled water, leaving these mixtures at room temperature until completely dissolved. These aqueous solutions were produced for subsequent use in LCST measurements.

2.2. Characterisation methods

2.2.1. Shore D hardness

A type D shore durometer was employed to test 6 disc samples of equal thickness from each batch on a flat anti-vibration bench. Each of the samples were stored at room temperature for 24 h before testing while the experiment was performed at room temperature conditions also. This experimental procedure involved raising the stage that contained the sample up to the indenter for a period of 30 s. After this time elapsed the result from the digital readout was recorded. Each result was noted (D scale) and the average was calculated for each batch. The results provided information on the hardness of the samples before and after irradiation

2.2.2. Phase transition determination

The LCST behaviour of samples were investigated using a UV-spectroscopy synergy HT BioTek plate reader. The transmittance of samples in aqueous polymer solutions was measured at 500 nm at intervals of 1 ºC in the range of 22-44 ºC. The solution was allowed to equilibrate at each temperature for 20 minutes before the transmittance was measured.

3. Results and discussion

3.1. Shore D Hardness

Figure 1 illustrates the results obtained from the Shore D hardness test of the non-irradiated and irradiated PNVCL samples. All samples were tested for a period of 30 s at room temperature.

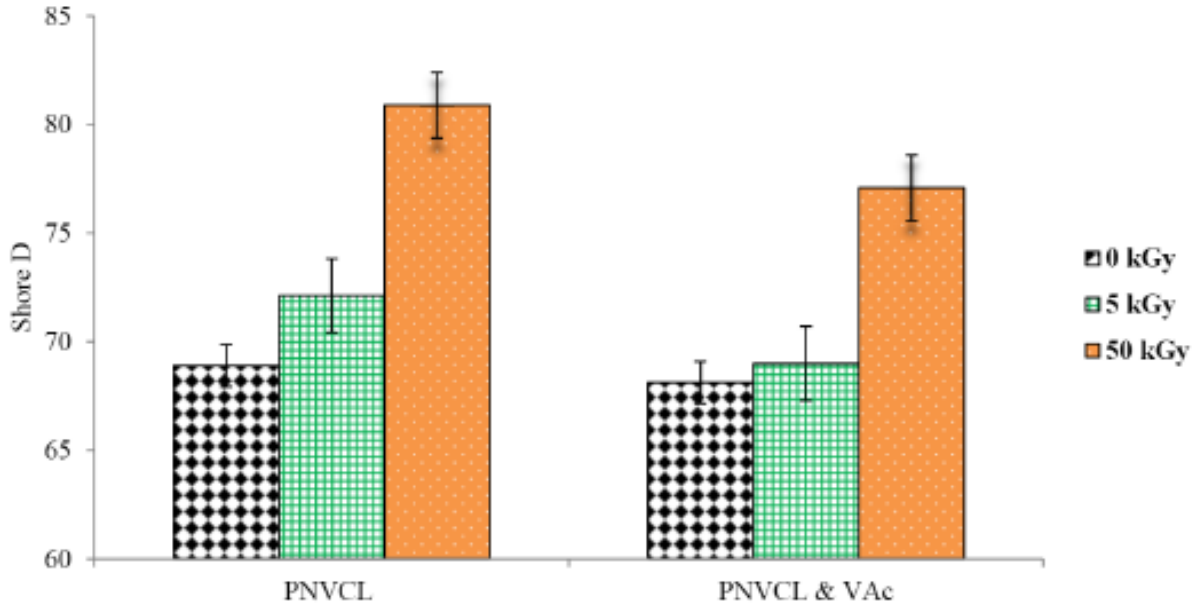

Figure 1: Shore D Hardness of PNVCL before and after irradiation

The penetration depth averaged between 68.9 and 97.2 D scale. Overall, there were statistically significant differences between sample means at 50 kGy, however; with regards to the 5 kGy samples, there were no significant differences between sample means ($P>0.05$) to report. Based on these results it was evident that an improvement in the hardness of the material was related to the formation of crosslinking.

3.2. UV-spectroscopy

The phase transition of PNVCL plays a crucial role in designing a smart glass window, as the phase transition temperature is the point at which blocks unwanted solar radiation [9,13]. PNVCL phase transition can be altered by its molecular weight, copolymer composition and finally its concentration in aqueous media. Exposing PNVCL to electron beam has the potential to modify the molecular weight of the polymer due to chain branching or crosslinking. Increasing PNVCL molecular weight is expected to decrease the phase transition based on changes in the polymer-solvent interaction. In this study, UV–spectroscopy measurement was used to observe the influence of electron beam irradiation on the optical characteristics with regards to the PNVCL phase transition.

Displayed in Figure 2 is the transmittance of PNVCL based samples as a function of temperature. Within the temperature range of 24 and 28 °C, minimum changes of transmittance were observed. However; a notable decrease was exhibited in transmittance between 28 and 34 °C due to the phase transition of the PNVCL material. These results suggest that increasing the irradiation dose from 5 to 50kGy provided an increase in the molecular weight distribution due to the formation of chain branching or crosslinking.

This study manipulated the phase transition of PNVCL via electron beam irradiation by changing the irradiation dose rate. PNVCL phase transition is affected by the molecular weight as it can change in the polymer-solvent interactions, which is illustrated in Figure 2. In this study, the phase transition decreased as the molecular weight of the polymer increased. It was found that the phase transition of PNVCL is dependent on the irradiation dose. Increases in the electron beam irradiation dose led to a decrease in the phase transition. For PNVCL 50 kGy, the initial transmittance was lower than previous samples. This lower transmittance is considered to be the effect of the high radiation dose that the material experienced during processing.

Chou *et al.* (2017) studied, the effect of graphene oxide (GO), a photothermal conversion material, and, introduced it within PNIAPM matrix of a thermotropic hydrogel. This material was utilised in smart glass and had the capabilities of auto-adjust transparency [14].

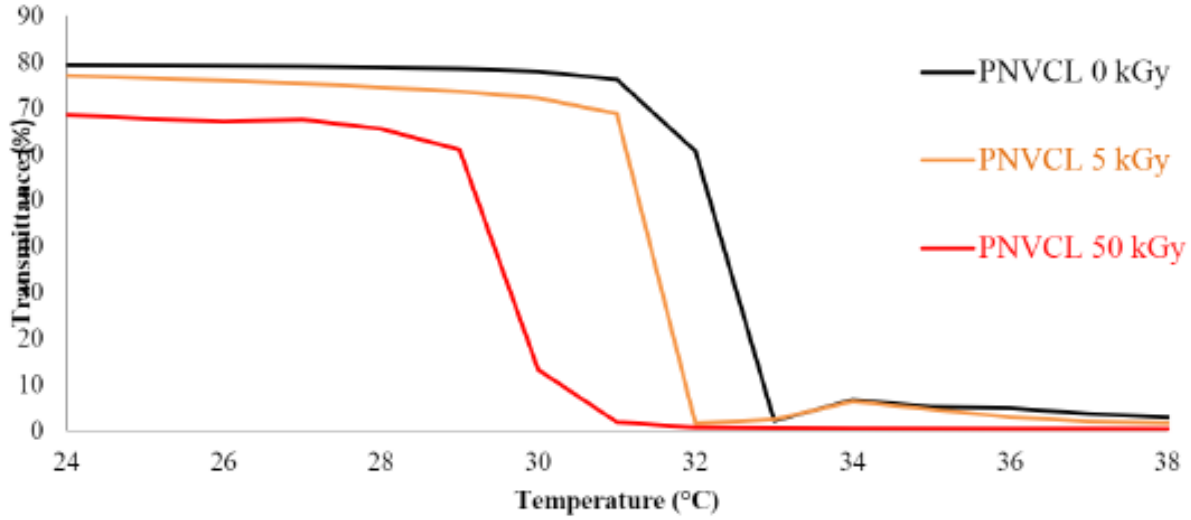

Figure 2: UV-Spectrometry illustrating the phase transition of PNVCL (3 wt %) homopolymer at different radiation dose

4. Conclusions

Overall, this study confirmed that controlling the phase transition and mechanical properties of novel PNVCL materials can be achieved by alternating the electron beam dose. The material that was developed in this study has the potential to be used as smart glass in green buildings and greenhouses. Increasing the electron beam dose can have lower the LCST of PNVCL to alter the transition to suit smart glass applications. The findings from this study demonstrate that PNVCL samples are an excellent candidate for smart glass technology.

Acknowledgments

The authors would like to thank STERIS Applied Sterilisation for their support throughout this project.

5. References

[1] E. Vardoulakis, D. Karamanis, A. Fotiadi, G. Mihalakakou, The urban heat island effect in a small Mediterranean city of high summer temperatures and cooling energy demands, Sol. Energy. 94 (2013) 128–144.

[2] X. Ye, Y. Luo, X. Gao, S. Zhu, Design and evaluation of a thermochromic roof system for energy saving based on poly (N-isopropylacrylamide) aqueous solution, Energy Build. 48 (2012) 175–179. doi:10.1016/j.enbuild.2012.01.024.

[3] M. Santamouris, On the energy impact of urban heat island and global warming on buildings, Energy Build. 82 (2014) 100–113.

[4] Y. Zhao, R. Xu, X. Zhang, X. Hu, R.J. Knize, Y. Lu, Simulation of smart windows in the ZnO / VO 2 / ZnS sandwiched structure with improved thermochromic properties, Energy Build. 66 (2013) 545–552.

[5] R. Baetens, B. Petter, A. Gustavsen, Solar Energy Materials & Solar Cells Properties , requirements and possibilities of smart windows for dynamic daylight and solar energy control in buildings : A state-of-the-art review, Sol. Energy Mater. Sol. Cells. 94 (2010) 87–105. doi:10.1016/j.solmat.2009.08.021.

[6] M.B. Dalton, S.C. Halligan, The effect acetic acid has on poly (N -vinylcaprolactam) LCST for biomedical applications, Polym. Technol. Eng. (2017). doi:10.1080/03602559.2017.1373400.

[7] L. Long, H. Ye, H. Zhang, Y. Gao, Performance demonstration and simulation of thermochromic double glazing in building applications, Sol. Energy. 120 (2015) 55–64.

[8] N.A. Cortez-lemus, A. Licea-claverie, Poly (N -vinylcaprolactam), a comprehensive review on a thermoresponsive polymer becoming popular, Prog. Polym. Sci. 53 (2016) 1–51.

[9] S.C. Halligan, M.B. Dalton, K.A. Murray, Y. Dong, W. Wang, J.G. Lyons, L.M. Geever, Synthesis, characterisation and phase transition behaviour of temperature-responsive physically crosslinked poly (N-vinylcaprolactam) based polymers for biomedical applications, Mater. Sci. Eng. C. 79 (2017) 130–139. doi:10.1016/j.msec.2017.03.241.

[10] P. Chem, P. Brian, V. Currently, Temperature-sensitive nanogels: poly(N-vinylcaprolactam) versus poly(N-isopropylacrylamide), Polym. Chem. (2012). doi:10.1039/c2py00485b.

[11] P.F. Mcdonald, L.M. Geever, J.G. Lyons, C.L. Higginbotham, Physical and mechanical properties of blends based on poly (dl-lactide), poly (l-lactide-glycolide) and poly (??-caprolactone), Polym. - Plast. Technol. Eng. 49 (2010) 678–687. doi:10.1080/03602551003681846.

[12] K. a. Murray, J.E. Kennedy, B. McEvoy, O. Vrain, D. Ryan, R. Cowman, C.L. Higginbotham, Effects of temperature, packaging and electron beam irradiation processing conditions on the property behaviour of Poly (ether-block-amide) blends, Mater. Sci. Eng. C. 39 (2014) 380–394. doi:10.1016/j.msec.2014.03.021.

[13] M. Kamalisarvestani, R. Saidur, S. Mekhilef, F.S. Javadi, Performance , materials and coating technologies of thermochromic thin fi lms on smart windows, Renew. Sustain. Energy Rev. 26 (2013) 353–364.

[14] H. Chou, Y. Chen, C. Lee, Switchable transparency of dual-controlled smart glass prepared with hydrogel-containing graphene oxide for energy efficiency, Sol. Energy Mater. Sol. Cells. 166 (2017) 45–51. doi:10.1016/j.solmat.2017.01.025.